2007

Laboratory testing of precast bridge elements, verification of post-tensioning forces and construction documentation of the Boone County IBRC accelerated bridge replacement project

Samantha Jo Hockerman
Iowa State University

Laboratory testing of precast bridge elements, verification of post-tensioning forces and construction documentation of the Boone County IBRC accelerated bridge replacement project

by

Samantha Jo Hockerman

A thesis submitted to the graduate faculty

in partial fulfillment of the requirements for the degree of

MASTER OF SCIENCE

Major: Civil Engineering (Structural Engineering)

Program of Study Committee:
F. Wayne Klaiber, Co-major Professor
Terry J. Wipf, Co-major Professor
Vernon R. Schaefer
Loren Zachary

Iowa State University

Ames, Iowa

2007

TABLE OF CONTENTS

LIST OF FIGURES

LIST OF TABLES

ACKNOWLEDGMENTS

The research presented in this thesis was possible through the cooperation of the Iowa DOT Office of Bridges and Structures, the Iowa High Research Board, the FHWA, and the Boone County Engineer's Office. I would like to thank the aforementioned entities for the opportunity to work on this project.

I would like to recognize several people who have been instrumental to me in earning this degree. First, I would like to thank my POS committee members, particularly my co-major professors, Dr. F. Wayne Klaiber and Dr. Terry J. Wipf for their knowledge and guidance throughout this project, which has proved to be invaluable. I also want to thank the ISU Structures Laboratory manager, Doug Wood, for all of his assistance and expertise related to the laboratory and field testing which I was responsible for.

I need to thank my fellow graduate students, Vernon Wineland, Ryan Bowers, Jeremy Koskie, Justin Dahlberg, and Mark Currie for their assistance in the laboratory and in the field. I also want to thank the undergraduate research assistants who helped on this project, too numerous to name.

ABSTRACT

In July 2006, construction began on an accelerated bridge project in Boone County, Iowa that was composed of precast substructure elements and an innovative, precast deck panel system. The superstructure system consisted of full-depth deck panels that were prestressed in the transverse direction, and after installation on the prestressed concrete girders, post-tensioned in the longitudinal direction.

Prior to construction, laboratory tests were completed on the precast abutment and pier cap elements. The substructure testing was to determine the punching shear strength of the elements.

Post-tensioning testing and verification of the precast deck system was performed in the field. The forces in the tendons provided by the contractor were verified and losses due to the post-tensioning operation were measured. The stress (strain) distribution in the deck panels due to the post-tensioning was also measured and analyzed.

The entire construction process for this bridge system was documented. Representatives from the Boone County Engineers Office, the prime contractor, precast fabricator, and researchers from Iowa State University provided feedback and suggestions for improving the constructability of this design.

CHAPTER 1. INTRODUCTION

1.1 Background

Constructing and rehabilitating bridges with minimal impact to traffic has become a transportation priority as traffic volumes nationwide increase. Renewal of the infrastructure in the United States (U.S.) is necessary for several reasons, including increases in population, projected increase in vehicle miles traveled, obsolete or deficient structures, impact of road construction, and injuries and fatalities related to work zones (NCHRP, 2003).

Rapid construction has several advantages over traditional construction methods. The six main goals of rapid construction technology include:

- Minimize traffic disruption
- Improve work zone safety
- Minimize environmental impact
- Improve constructability
- Increase quality
- Lower life-cycle cost (NCHRP, 2003)

There are several different types of rapid construction technologies currently used in the U.S. One technology uses precast concrete bridge components. The precast components are fabricated off-site, allowed to cure, and then transported to the construction site for installation. This technology allows bridges to be constructed faster than traditional construction methods, reducing the amount of time the bridge and/or associated roads are closed to the public, and reducing the total construction time. Since construction time above

waterways can be reduced, the amount of debris that falls from the construction site is reduced, therefore reducing the environmental impact.

The importance of rapid construction technologies has been recognized by the Federal Highway Administration (FHWA) and the Iowa Department of Transportation (DOT) Office of Bridges and Structures. This report is based on the construction of a new accelerated construction precast bridge system located in Boone County, Iowa and evaluation of bridge components tested in the laboratory. Funding for the design, construction, and evaluation of this project was provided by the FHWA-sponsored Innovative Bridge Research and Construction (IBRC) Program. Funding for the laboratory testing was provided by the Iowa DOT and the Iowa Highway Research Board; funding for the documentation and the post-tensioning monitoring and verification was provided by the FHWA and Boone County.

This research focused on the bridge constructed on 120th Street in Boone County over Squaw Creek; the bridge replaced an existing Marsh Arch bridge at the site, which can be seen in Figure 1. The new bridge is a continuous, four-girder, three-span bridge with a full-depth, precast deck and can be seen in Figure 2. Bridge dimensions are 151 feet and 4 inches long and 33 feet and 2 inches wide. Deck panels were 8-inches thick, half the width of the bridge, and prestressed in the transverse direction. Each panel had two full-depth channels, located over the prestressed girders, for post-tensioning. Once the panels were erected, the entire bridge deck was post-tensioned in the longitudinal direction, after which the post-tensioning channels were grouted. Precast pier caps and precast abutments were also used in the bridge substructure. Although this exact design had not been previously constructed, a similar partial-depth deck system has been constructed and tested in Nebraska (Badie *et al.*, 1998).

Figure 1. Marsh Arch bridge previously on 120th Street.

Figure 2. Completed replacement bridge on 120th Street.

1.2 Research Objectives

The objectives of this project were determined based on input from the Iowa DOT, the Boone County engineer, the Federal Highway Administration (FHWA), and the faculty at Iowa State University (ISU) involved with the project. This research project focused on the following objectives:

- Determine the actual strength of the connection between the precast abutment cap and the piles

- Document the construction process, particularly any problems or difficulties that occurred
- Install instrumentation to allow for long-term monitoring of the bridge deck
- Monitor and evaluate the deck panels and post-tensioning strand forces during the post-tensioning operation

These objectives were met through various tests performed on test specimens in the laboratory and through field testing during the post-tensioning operation. Additional laboratory testing was performed under the same project funding, but was not the responsibility of the author and thus not reported in this thesis.

1.3 Scope of Research

The first task for this project was to complete a literature review related to the project. First, literature on accelerated bridge technologies, along with precast, prestressed, and post-tensioned concrete bridge components was reviewed. Since the bridge deck system and substructure had never been constructed in the state of Iowa, the focus of the literature review was on full-depth, precast concrete deck panels, partial-depth precast concrete deck panels, hybrid deck panels such as NUDECK (Badie *et al.*, 1998) and on precast substructures. Several papers on the shear strength of deep beams were also reviewed because of concerns regarding the shear capacity of the abutment caps and pier caps. A summary of the literature reviewed for this project is presented in Chapter 2.

After completion of the literature review, the next task in the project was the laboratory testing. Three different laboratory tests were performed: a single pile abutment

cap test, a double pile abutment cap test, and a single pile pier cap test. Each of these tests and the fabrication of the test specimens are further described in Chapter 3.

In Chapter 4, results of the laboratory tests as well as a complete discussion of the results are presented. The connection between the pile and the abutment was analyzed and compared to the laboratory results and the design strength as calculated by the Iowa DOT.

The next task included the post-tensioning testing and verification. During the post-tensioning operation, field measurements were recorded and later analyzed. A description of the field testing associated with the post-tensioning operation, a summary of the tests results from the field verification, and a comparison of the results obtained by the contractor and those of the research team are presented in Chapter 5.

The final task for this project was documentation of the construction process. This task involved taking pictures in the field as construction progressed and getting feedback from the contractor, subcontractor and the construction inspector. Documentation of the construction process was performed to evaluate the time savings of the precast system and to determine where improvements could be made. Representatives from the Boone County Engineer's Office, from the prime contractor, from the precast fabricator, and researchers from Iowa State University submitted feedback on the project. Construction documentation is described in Chapter 6.

Chapter 7 contains a summary and conclusions based on the completed research and documentation, and in Chapter 8 recommendations for additional research are presented.

CHAPTER 2. LITERATURE REVIEW

2.1 General

Constructing and rehabilitating bridges with minimal impact to traffic has become a priority with the increase in traffic volume. In April 2004, an 11-person team from the U.S. took a tour of Japan, the Netherlands, Belgium, Germany, and France to observe rapid construction bridge technologies being used in these countries and to identify technologies that may be implemented in the U.S. (Russell *et al.,* 2005). Renewal of the infrastructure in the U.S. is necessary for several reasons, including increases in population, projected increase in vehicle miles traveled, obsolete or deficient structures, impact of road construction, and injuries and fatalities related to work zones (NCHRP, 2003).

Rapid construction has several advantages over traditional construction methods. The six main goals of rapid construction technology include: minimize traffic disruption, improve work zone safety, minimize environmental impact, improve constructability, increase quality, and lower life-cycle cost (NCHRP, 2003).

The disadvantages of rapid construction include an increase in construction cost, size and weight limitations of precast members, availability, and contractor familiarity (Russell *et al.*, 2005). These disadvantages need to be considered when determining if using rapid construction technologies are appropriate for a given project.

2.1.1 Precast Concrete

There are many advantages for using precast concrete elements in a bridge project. Elements can be fabricated off-site and stock piled before construction begins. Once construction has progressed, the precast elements can be transported to the bridge site and set

in place immediately. At a precast plant, formwork is reused for standardized elements, and no formwork is required in the field, which reduces material costs and results in time and labor savings (VanGeem, 2006).

Most rapid construction technologies are focused around using precast elements in the super- and sub-structure. Disadvantages in using precast elements include increased cost, finding a qualified fabricator, and also stock piling and transportation issues. Fortunately, many of the costs associated with these disadvantages can be reduced by standardization of the precast elements used. For low- to moderate-volume bridges, transportation and storage of the elements does not pose a problem. To reduce quality control problems or issues with an inexperienced contractor, the Precast/Prestressed Concrete Institute (PCI) certifies precast manufacturers (Arditi *et al.*, 2000).

Precast concrete also has the advantage of being prestressed or post-tensioned. The concept behind prestressing and post-tensioning is to put the concrete element under permanent compression, which increases the performance and durability of the member since concrete performs well under compression but has low tensile strength. The permanent compressive forces are designed to offset the forces induced by the self weight of the member and external loading (Naaman, 2004).

There are several different methods of prestressing and post-tensioning, however the most common technique is to use high strength steel bars or strands to apply compressive force to the concrete element. Typically, a hydraulic jack is used to tension the bar or strand to a pre-determined stress before it is anchored. The force in the steel is usually measured by hydraulic pump pressure and checked by measuring the elongation of the bar or strand. When the pump pressure and required minimum elongation has been met, the desired force

has been obtained in the bar (Naaman, 2004). There are additional methods of prestressing, such as electrothermal methods or self-expanding cement, but these are not typically used in the United States and therefore will not be discussed.

The main difference between prestressing and post-tensioning is the time when the compressive force is applied to the concrete. For prestressing, the tendons are stressed before the concrete is cast. Bonds between the tendons and the concrete resist the force from the strands trying to shorten, putting a compressive force on the concrete (Naaman, 2004).

In contrast, post-tensioning is performed after the concrete element has reached strength and typically after it has been cast or erected at the construction site. Before the concrete is cast, post-tensioning ducts are installed in the forms; after the precast element has been placed in the field, post-tensioning tendons or bars are threaded through the element. After the post-tensioning has been completed, the ducts may be grouted or other measures taken to prevent corrosion (Naaman, 2004).

2.1.2 Prestressed Concrete

There are many benefits to using precast, prestressed elements, especially in low-volume bridge replacements such as the bridge replacement in Boone County. Low-volume roads are good candidates for precast, prestressed bridges because of the typical simple layout and the requirement for short- to medium-span lengths of the bridges. The use of standard precast elements, along with the elimination of falsework, forms, tying steel and finishing concrete in the field, can reduce cost, which is always a factor in construction projects (Tokerud, 1979).

Prestressed concrete beams and slab elements are typically cast in long beds, allowing more than one element to be cast at a time. Before the concrete is placed, the wires or stands

are threaded through the formwork and then stressed. The stressed tendons are anchored to bulkheads located outside the concrete forms. After the concrete is cast and has reached an appropriate strength, the wires or strands are cut, compressing the concrete. A bulkhead located on a precasting bed can be seen in Figure 3.

One of the most significant benefits of prestressed concrete is the quality control during fabrication and regulation of the design and construction processes. There are several different regulatory manuals including *AASHTO LRFD Bridge Design Specifications (1998)*, the *ACI 318-05 Building Code (2005)*, and *PCI Design Handbook (2004)* which provide guidelines for strength, serviceability, and durability of precast concrete products. The aforementioned manuals also provide guidelines for estimating short- and long-term losses in prestressed elements. Calculating exact values for prestressing losses can be difficult since there are different factors that attribute to losses such as: elastic shortening of concrete, creep of concrete, shrinkage of concrete, relaxation of the tendons, and seating losses (ACI 318-05, 2005).

Figure 3. Bulkhead in a prestressed concrete casting bed.

Durability of a prestressed element is directly related to the quality of fabrication. High strength concrete is used to decrease the permeability of the concrete and to decrease the time required for the concrete to reach the desired strength. The prestressing tendons may not be released and the concrete element may not be moved until the concrete has reached the strength specified by the designer. After the concrete has reached strength, the tendons can be released and the element can be moved without risk of cracking the concrete. Stress guidelines provided by bridge specifications and/or building codes ensure precast concrete does not crack under self weight or service loads (Hale and Russell, 2006).

2.1.3 Post-tensioned Concrete

The process of post-tensioning concrete is similar to prestressing concrete and applies the same design principles. One advantage of post-tensioning concrete is several concrete elements may be post-tensioned together to act continuously. Primarily, there are two post-tensioning schemes: one uses bonded tendons and the other uses unbonded tendons. For bonded tendons, the post-tensioning ducts are filled with grout after the tendons are stressed and anchored; after the grout cures, the force along the length of the tendon is distributed to the adjacent concrete. In contrast, unbonded tendons are coated with grease or bitumen, covered with waterproof material, and threaded through the ducts. Since no grout is used, the force in the tendons essentially applied at the anchorage zones (Naaman, 2004).

There are several different types of proprietary post-tensioning anchors that can be used, depending on the strand or bar being post-tensioned. The type of anchorage used also depends on the size and strength of the concrete element, the number of strands used, and other design constraints. Several common post-tensioning anchors are shown in Figure 4.

a) DSI bonded multi-strand anchorage

b) DSI bonded multi-strand flat anchorage

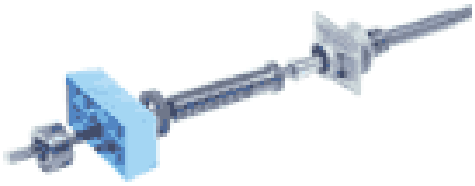

c) VSL mono-strand anchorage

d) VSL threaded bar anchorage

Figure 4. Common post-tensioning anchorages (Bonded Strand Post-Tensioning System, 2007) (VSL Post-Tensioning Systems, 2007).

Anchorage zones in post-tensioned concrete are an area of concrete subjected to high levels of stress. Anchorage zones can be congested and difficult to design and construct due to the size of the anchorages and the amount of mild reinforcing required. To prevent cracking and bursting of concrete in the anchorage zone, secondary reinforcement such as spirals and closed stirrups can be used, and recently fiber-reinforced concrete has been used to reduce congestion (Haroon *et al.*, 2006). The Boone County project did not require abnormally high amounts of post-tensioning strand, but the end panels with the anchorage plates were still congested. Fabrication of one of the end panels is shown in Figure 5a while one of the completed end panels is shown in Figure 5b.

a) end panel reinforcement

b) complete end panel in the field

Figure 5. Boone County anchorage zone reinforcement.

The durability of post-tensioned bridges relies on one key factor – preventing corrosion of the post-tensioning tendons. Corrosion occurs when the tendons are exposed to moisture and air, and can be accelerated by several different factors. Bridges that are located in marine environments or exposed to highway deicing salts are at a higher risk or are more susceptible to corrosion because of the chlorides present. A common factor causing corrosion of post-tensioning tendons is the presence of air voids in the grout ducts which allows moisture to come into direct contact with the tendons (Cooper and Pearson-Kirk, 2006).

One material commonly used for post-tensioning ducts is galvanized steel. This material is highly susceptible to corrosion and research has shown that tendons corrode at a faster rate if the galvanized duct is also corroded (Salas *et al.*, 2004). Plastic ducts are now being used to prevent early onset of corrosion, but even with plastic ducts, there are areas where tendons are still susceptible to corrosion. Joints between concrete elements and high- and low-profile points in the tendons are at the highest risk (Cooper and Pearson-Kirk, 2006).

Issues with corrosion have forced improvements in grouting practices for post-tensioned bridges. One way to ensure the ducts are completely grouted is by using high-pressure grouting. In this method, the duct is typically grouted from one location, either the center or from one end. The high pressure forces the grout through the ducts, until grout can be seen at the farthest end of the duct (Schokker *et al.*, 1999). Even if the duct is completely filled with grout, this does not guarantee corrosion protection. If the grout cracks, moisture can still reach the tendons. For the best corrosion protection, high performance, low-shrinkage grouts are recommended (Hamilton *et al.*, 2000). High performance grouts with the use of silica fume have low permeability which slows chloride penetration and corrosion (Khayat *et al.*, 1999).

Post-tensioning channels used in the Boone County project avoided the corrosion protection issues related to the type of post-tensioning ducts and the presence of air voids in the ducts by eliminating the ducts all together. Open channels allowed the strands to be inspected as grout was placed and prevented the formation of air voids around the tendons. The channels in one of the deck panels can be seen in Figure 6.

Figure 6. Boone County replacement bridge deck panel.

A specialty concrete, designed to have low-permeability and low shrinkage to further prevent cracks near the tendons, was used in the channels. Details of the specialty concrete mix can be found in Chapter 3.

2.2 Bridge Deck Systems

The most common bridge superstructure in the U.S. consists of erecting steel, reinforced concrete, or prestressed concrete girders, and using formwork to place a cast-in-place (CIP) concrete deck. Eliminating the deck formwork reduces construction time and lane closure time, and improves worker safety (Russell *et al.*, 2005). There are several different types of deck systems that are used in rapid construction projects. In the following section, three different types of bridge deck systems are discussed: full-depth precast deck panels, partial-depth precast deck panels, and hybrid deck panels.

2.2.1 Full-Depth Concrete Deck Panels

A typical precast deck panel system consists of precast concrete panels, placed adjacent to each other, perpendicular to the bridge girders. Most recent systems use prestressing as reinforcement in the transverse direction. Longitudinal post-tensioning is used to place the joints between panels in compression, which promotes monolithic behavior and improves durability. Grouted shear keys are used at the transverse joints. The panels are connected to the bridge girders using shear pocket connectors which ensure composite action between the deck and girders (Hieber *et al.*, 2005).

Typically, the panels are approximately eight inches thick, span the width of the bridge, and are approximately ten feet long. A wearing course is not required, but is often included to improve the riding surface of the finished panels.

There are several key issues to consider with a full-depth deck system. The first is the bearing between the panels and the girders. Differential camber and fabrication variations can affect the bearing between the deck and the girders. An uneven bearing surface can cause spalling at the transverse joints and an uneven riding surface. One solution to this potential problem is to grout between the panel and the girder, thus creating a continuous bearing surface. However, often times the gap between the panel and girder is too small to grout. Another solution is to temporarily support the panels above the girders to create a haunch region. The haunch can be grouted and the supports removed after the grout cures. Leveling bolts and shims are typically used in this application (Hieber *et al.*, 2005).

Another key issue to consider is the connection of the panels to the bridge girders. Proper connection ensures a composite action between the panels and girders. Insufficient connections can allow the panels to lift off the bridge, which causes fatigue and vibration problems. Insufficient connections may also cause cracking in the panels and at the joints. There are several different types of connections, all of which included a mechanical connection and a grouted region (Hieber *et al.*, 2005).

Typically, full-depth concrete deck panels are post-tensioned together. The amount of post-tensioning force required for the bridge deck is a critical issue. If insufficient force is applied, the connection between the panels may crack, which can cause maintenance issues and shorten the lifespan of the bridge. The amount of post-tensioning force required varies depending on the bridge properties and the type of support. Continuously-supported bridges require higher post-tensioning force to prevent joint cracking than simply-supported bridges (Issa *et al.*, 1998). There are two options for post-tensioning the deck panels together: full bridge post-tensioning and staged post-tensioning. For full bridge post-tensioning, the deck

panels are all stressed after every panel is in place. In staged post-tensioning, each panel is post-tensioned once in place next to the previously placed panel. This may be temporary or permanent, but the design details for staged post-tensioning are more involved than full bridge post-tensioning because of the multiple post-tensioning operations required (Yamane *et al.*, 1998).

A third issue to consider is the joints between the panels. These joints must be able to transfer shear and axial forces between adjacent panels, and prevent leakage through the deck. Often, water that leaks through the deck contains chlorides, which accelerates deck, girder, and reinforcement deterioration. Typically, 'female-to-female' shear keys have been used because of superior performance over 'female-to-male' shear keys. Problems with joints usually arise because of low-quality joint material, poor joint details, inconsistent/inadequate construction procedures, or the lack of routine maintenance. Joints that have a larger area and easy flow path often perform better because there is more room for the grout to flow. Grout with high-early strength is the most commonly recommended material. This allows post-tensioning to be completed shortly after the joint has been grouted, so construction can proceed (Harrison and LeBlanc, 2005).

Another issue with full-depth deck panels is the transverse prestressing in each panel. Prestressing allows thinner panels, provides better crack controls, and helps with the durability of the panel during transportation and erection. One drawback to prestressed panels is the development of the strands in the section of the panels that overhangs the exterior girder. This problem can be solved by adding mild reinforcing steel to that area (Hieber *et al.*, 2005).

The last key issue to consider is the wearing surface of the deck. Full-depth panels typically have a rough surface due to the grouted joints and shear pockets. Typically, a wearing surface is added for rider satisfaction and safety, and improved durability (Hieber *et al.*, 2005). Another option is to fabricate the panels one quarter inch thicker and then grind the surface of the deck when construction is finished.

2.2.2 Partial-Depth Concrete Deck Panel

Partial depth precast panels are thin reinforced/prestressed concrete deck panels that are used to span in between girders and serve as stay-in-place formwork for the CIP deck. Panels are designed to span between each girder, are typically about eight feet in the longitudinal direction and about 3.5-inches thick. The panels are typically prestressed in the transverse direction and the prestressing strands serve as the reinforcement in the bottom of the bridge deck. Panels are then placed adjacent to each to each other, but not connected at the adjacent transverse joints. Deck overhangs have to be formed with removable formwork. A layer of reinforcing steel is placed on top of the panels, and then the CIP deck is placed (Hieber *et al.*, 2005).

The biggest advantage to partial depth precast panels is the elimination of deck formwork. However, since CIP concrete is still used for the deck and formwork is still required for the deck overhangs, the time-savings for partial deck panels is not as great as the time-savings for full-depth concrete panels. Reflective cracking over the transverse joints can be a problem. This is attributed to the discontinuity between precast panels which leads to a decrease in deck stiffness (Badie *et al.*, 1998).

There are several key issues to consider when using partial-depth precast panels. First is issue of panel thickness; because the panels are so thin, they are susceptible to

damaged during handling and construction. Damage to the panels can be avoided by limiting the number of times the panels must be moved and placing the lifting hardware at locations in the panels to minimize stresses (Hieber *et al.*, 2005).

Another issue of concern is the bearing of the panels on the supporting girders. Cracks can form in the concrete deck if a solid, uniform bearing region is not provided. Cracked concrete can prevent the deck from acting continuously over the girders. As a result, the CIP deck may delaminate from the panels at the joints. Current practices use grout or concrete to fill the bearing area which provides proper bearing (Hieber *et al.*, 2005).

The third issue with partial-depth deck panels is the development of prestressing within the panels. Because the partial-depth panels span in between the girders, there is a short distance to develop the prestressing strands in the panels. It is important to make sure other factors, such as dirty prestressing strands or sudden de-tensioning by the fabricator, don't increase the required development length. However, decreasing the development length too much can create problems as well. Panels with small development lengths have a greater potential for splitting (Hieber *et al.*, 2005).

The last issue of concern with partial-depth is ensuring composite action between the CIP deck and the precast panels. A common way to increase the composite action is to roughen the surface of the precast panels during fabrication. Precast panels should also be clean and free of debris and contaminants to ensure complete bond is achieved between the CIP deck and precast panels.

There are limitations on the size of partial-depth panels. According to AASHTO LRFD Section 9.7.4.3.1 (1998) the precast panels should not be greater than 55 percent of the

total deck depth nor less than 3.5 inches. These limitations help to reduce cracks in the CIP deck over the panel joints and also to help develop composite action.

2.2.3 Hybrid Deck Systems

The NUDECK system is a stay-in-place precast, prestressed system developed to solve the problems in the existing stay-in-place (SIP) systems. This system uses partial-depth panels with a CIP composite deck. NUDECK can be constructed significantly faster than CIP systems and slightly faster than other SIP systems. Shown in Figure 7 is a section view of a typical NUDECK panel; the panel is symmetric about the bridge's longitudinal centerline (Badie *et al.*, 1998).

Several changes were made to previous SIP systems in the development of the NUDECK system. The first problem addressed was reducing the number of panels needed; the NUDECK system spans the entire width of the bridge, thus reducing the required number of panels needed by two. Eliminating the need for forming the overhangs was the second issue. To accomplish this, the NUDECK panels extend over the outside girders providing SIP formwork for the overhangs. Third, the issue of the transverse prestressing being not fully developed in the panels was addressed. In the NUDECK system, the prestressing is continuous over the girders, allowing the prestressing to fully develop (Fallaha *et al.*, 2004).

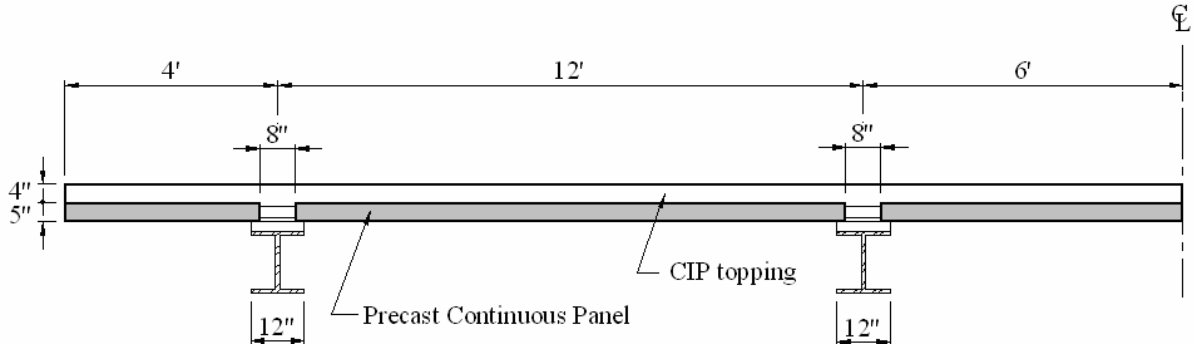

Figure 7. Typical cross-section of the NUDECK panel.

Another issue was transverse cracking. In the NUDECK system, the entire bridge is post-tensioned, providing continuous longitudinal support. Next, the issue of supporting finishing machines without the need for additional brackets was addresses. NUDECK panels were designed to support the weight of the finishing machines, the CIP concrete surface, and the panel self-weight without additional support. The last issue was longitudinal cracking over girder lines caused by creep in the individual SIP panels. In the NUDECK system, the panels are continuous over the girder lines, thus eliminating creep issues (Badie *et al.*, 1998).

There are several block outs in each panel, located longitudinally over the each beam line. Block outs serve as post-tensioning channels, are positioned to avoid interference with the shear studs, and also simplify the post-tensioning process (Fallaha *et al.*, 2004).

In order to provide adequate shear connection between precast panels in the longitudinal directions, shear keys and reinforced pockets were used. A simple leveling device was used to level the panels on the girders. After post tensioning, the block outs in the panels were grouted using a flowable mortar to connect the panels to the girders. The CIP surface was placed once the mortar reached a specified compressive strength (Badie *et al.*, 2005).

All of the precast deck panel systems discussed use grouted joints to connect the panels. However, grouted joints are a major issue of concern because of difficulty in achieving high-strength grout in the field. Panels are typically grouted together using a variety of different grouting materials such as cememtitious grout, epoxy mortar, or polymer concrete. Because the transverse joint acts as a structural member, it must resist vertical shear and bending caused by vehicle loading. Effects of shrinkage of the grout and vertical shortening of the panels induce direct tension on the joint as well (Issa *et al.*, 2003).

Strength and quality of joint material is very important to the durability of the bridge. If the grouting material is not strong enough to resist the service loads, the joint will crack, resulting in leakage. Cracked joints can be expensive to repair and maintain (Issa *et al.*, 2003).

2.3 Bridge Substructure Systems

2.3.1 Precast Abutments

Precast abutments can be beneficial to rapid construction projects. One drawback to using precast abutments is connecting the abutment to the deck. If the abutment is entirely precast, an expansion joint has to be placed between the deck and the abutment. Expansion joints tend to reduce the lifespan of bridges, and integral abutments are typically preferred. Even if an integral abutment is used, precast elements can still be used for the wingwalls to reduce the amount of formwork and CIP concrete (Tokerud, 1979). A closure pour between the precast elements and the abutment will be required to achieve an integral abutment.

2.3.2 Precast Concrete Piers

Precast concrete pier systems use precast piles and a precast pier cap to create a pier. Precast piers are compatible with a number of different foundation and substructure types. For larger bridges, precast pier caps, also called bent caps or cap-beams, may be necessary. A picture of a bridge in Nebraska using precast girders and precast pier caps is shown in Figure 8. Pier caps allow twin-span bridges to use the same piers for foundations. Precast, prestressed or post-tensioned caps can significantly reduce the cap size, which reduces the weight of the substructure. For extremely large bridges, pier caps may be fabricated and transported in two pieces and post-tensioned together on site (Billington *et al.*, 1999).

Figure 8. Bridge pier cap located Lincoln, Nebraska.

Individual components of the pier are connected with mild reinforcing steel splices or post-tensioning. Two types of connections are typically used: grouted joints and match-cast joints. Match-casting uses the joint face of a previously cast component as part of the formwork for the adjacent component. This results in a "perfect" fit between the two components and reduced on-site construction time, when the elements are delivered in the correct order. The drawback to this procedure is that the fabrication process is often more time and labor intensive, which can be more expensive and if the elements are placed in a different order than which they were fabricated, the segments may not fit (Hieber *et al.*, 2005).

There are several advantage to using precast concrete piers besides the time and labor savings in the field. As with all precast elements, fabrication of all the elements is done off-site, which allows the precast elements to be fabricated before construction at the bridge site begins. Elements can then be stockpiled until they are needed in the field. Because precast elements are typically fabricated in a climate-controlled environment, the quality control for

the material and construction of precast elements is higher than the quality control that can be maintained though all kinds of weather in the field. This results in higher durability of the precast elements (Billington *et al.*, 2001).

Precast elements also have the advantage of using high performance concrete, which typically increases the strength and durability of precast elements. The use of high-performance concrete also results in more slender substructure designs, as can be seen in Figure 9, which also results in significant material savings for a project (Billington *et al.*, 2001).

There are several key issues to consider with precast concrete piers. The first issue is the connection between the footing and the column, which will depend on the type of footing, precast or cast-in-place. There are several different types of connections available, however, the most appropriate connection will depend on project-specific conditions (Hieber *et al.*, 2005).

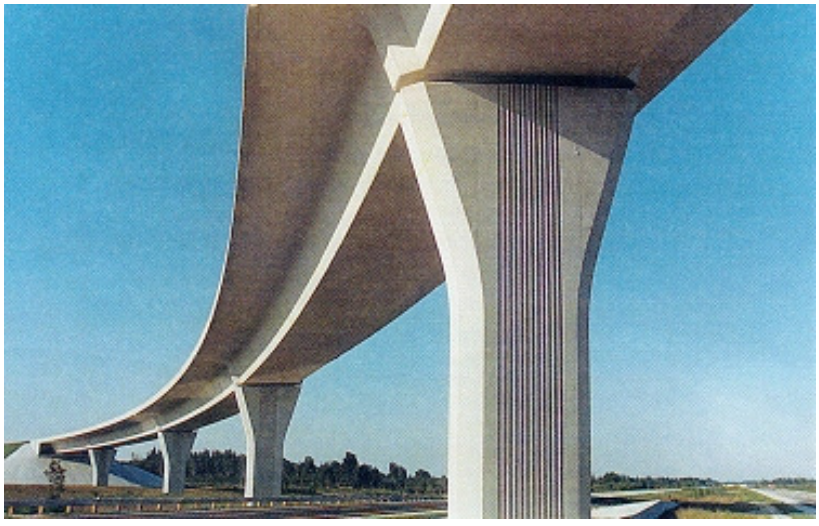

Figure 9. Slender pier design of the Florida Turnpike in Miami, Florida.

The next issue is the connection between the column elements. Match-cast joints are typically preferred because of problems that may occur with grouted joints. Grouted joints may lack a uniform bearing surface, which can cause edge crushing. Poor grout placement or grout quality may result in partially filled joints, stress concentrations, cracking, and corrosion of the reinforcing steel. Shear keys can be added to increase the shear capacity of the joint. The epoxy used in the joint may also provide extra shear capacity, but typically is not designed to do so (Hieber *et al.*, 2005).

Another issue to consider with precast pier systems is the connection between the column and pier cap or abutment. There are two types of connections used: post-tensioning bars or strands, or mild reinforcing bars in grouted ducts. A drawback to the grouted duct connection is the ducts takes up twice as much room as a normal reinforcing bar. The connection region in the column and pier cap is already congested, so fitting the ducts in can be a problem (Hieber *et al.*, 2005).

A fourth issue to consider is the connection between the pier cap elements. If the pier cap has to be fabricated and transported in several segments, the segments will have to be connected with grouted, cast-in-place concrete or match-cast connections. The last issue to consider in precast pier systems is the weight and size that can be transported, either of which can govern the size of the precast segment. Local limitations should be researched and considered during design (Hieber *et al.*, 2005).

As with most accelerated construction technologies, there is an increased cost to precast substructures. Part of the cost is related to the experience of the contractor and precast concrete fabricator. Some of the cost of precast substructures will reduce as

standardized substructures are developed and the contractors involved gain experience (Billington *et al.*, 2005).

Another precast pier system currently under investigation for use in the United States is the Sumitomo system. The Sumitomo precast structure for resisting earthquakes and for rapid construction (SPER) system uses stay-in-place precast concrete panels as formwork and as structural elements. For shorter piers, the segments are stacked on top of each other, epoxied together, and then filled with CIP concrete, creating a solid pier. For taller piers, inner and outer panels are used to create a hollow pier. For both types of piers, cross ties and couplers are used to provide transverse reinforcement. High strength bars are typically used for the transverse reinforcement to reduce congestion between the panels. CIP concrete is typically used to connect the piers to the superstructure (*Russell et al.*, 2005).

CHAPTER 3. LABORATORY CONSTRUCTION AND TESTING

3.1 Laboratory Specimen Fabrication

The substructure specimens tested in the laboratory were designed and fabricated based on the project plans for these elements in the Boone County bridge replacement project. In other words, the laboratory specimen were built to replicate the actual bridge elements. A total of nine full-scale specimens were fabricated in the laboratory, seven abutment specimens and two pier cap specimens. A description of the various test elements and their designations are presented in Table 1.

Table 1. Laboratory specimens and designations.

Specimen	Description
Abutment 1	ASC1
Abutment 2	ASC2
Abutment 3	ASO1
Abutment 4	ASC3
Abutment 5	ASO2
Abutment 6	ADC1
Abutment 7	ADC2
Pier Cap 1	PSC1
Pier Cap 2	PSC2

Where: A = Abutment specimen
P = Pier cap specimen
S = Single pile
D = Double pile
C = Centered pile
O = Offset pile

Specimens were fabricated and tested three at a time to optimize the space required in the laboratory for storing materials, building formwork, and casting concrete.

3.1.1 Single Pile Abutment Cap Construction

The abutment system consisted of a precast abutment cap that used corrugated metal pipe (CMP) as a 'block out' for the piles. During construction, the abutment cap was placed over H-piles already driven in the field after which a special concrete mix was used to fill the void and thus connect the piles and the abutment. Specimens were designed to represent the worst-case load condition on the actual abutments. Tests were performed using the prestressed girder spacing around the center pile; this provided the maximum moment to which the abutment would be subjected. The side view of the entire abutment, along with the sections of the abutment used in the various test specimens, can be seen in Figure 10. In this figure, the four precast girders and five piles can be seen.

During fabrication and testing, the abutment specimens were inverted. This provided the safest, most stable configuration for testing, and also made grouting the piles in place easier. The external details of the abutment test specimen are presented in Figure 11. There were two different single pile abutment tests specimen fabricated: one test with the pile centered in the CMP (i.e. the "C" designation in Table 1) and one with the pile offset the maximum distance in the CMP (i.e. the "O" designation in Table 1), designated by dimension "A" in Figure 11. Actual values for "A" and a top view of the centered and offset pile are shown in Figure 12.

Test specimens replicated the actual abutment cross-section used in the field, including the dimensions and reinforcement. Both test specimens were ten feet in length, with the CMP centered in the specimen. The reinforcement (size and spacing) in the test

specimens was taken from the project plans and adapted for a ten-foot long section of the abutment. In the abutment, the No. 8 longitudinal bars were continuous; bars were lap spliced where necessary. In the test specimens, the longitudinal bars were limited to nine-feet and ten-inches in length, to provide one inch cover at the end of the bars; this provided sufficient bar length to ensure full development. A top view of the specimen, as well as an end view, showing the reinforcement is presented in Figure 13.

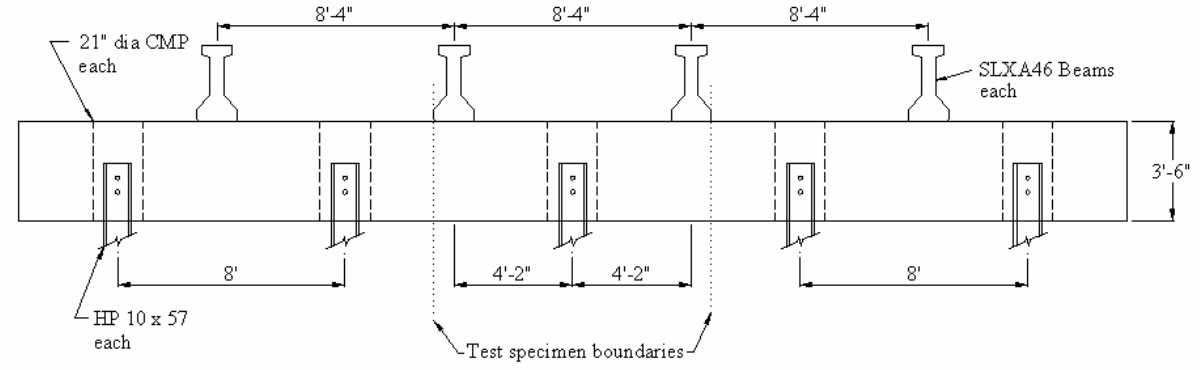

Figure 10. Side view of the Boone County replacement bridge abutment.

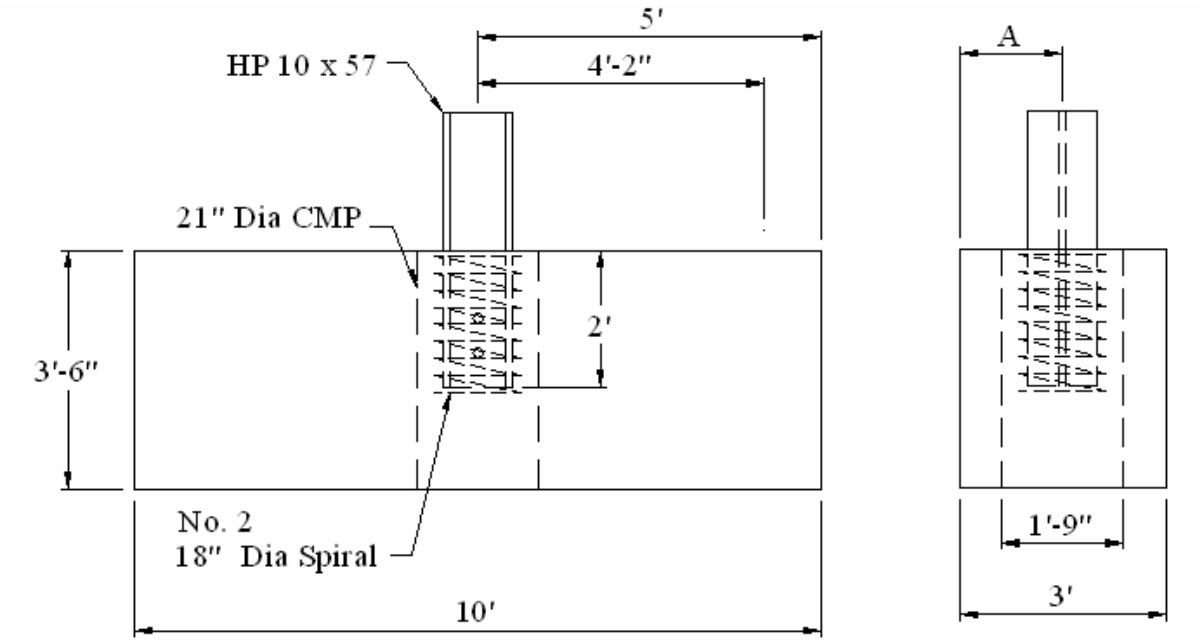

Figure 11. Single pile abutment test specimen.

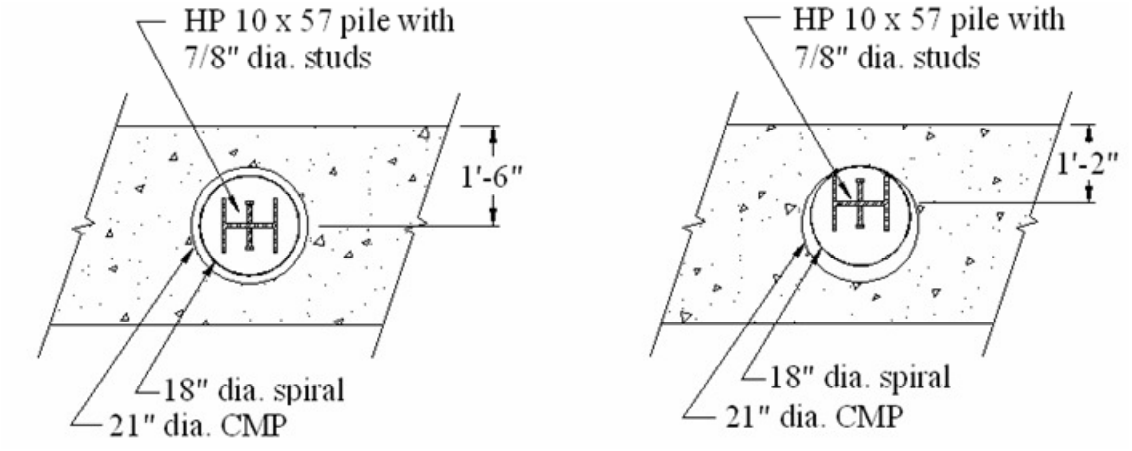

a) centered pile location **b) offset pile location**

Figure 12. Abutment pile locations.

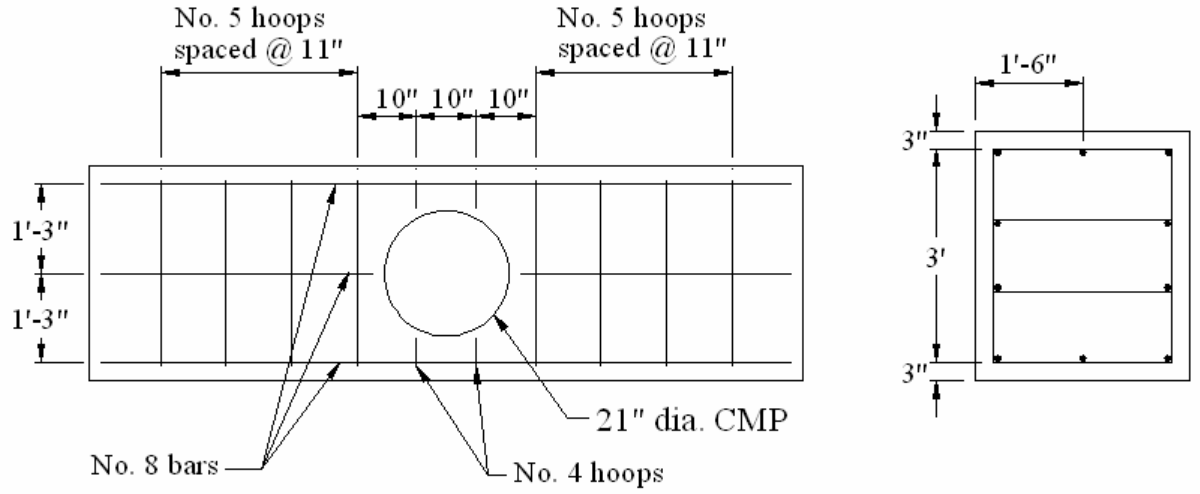

a) top view **b) end view**

Figure 13. Single pile abutment reinforcement.

Each H-pile in the abutment specimens had four 7/8-inch diameter studs, five inches in length, welded to the pile web six inches apart, two of which can be seen in Figure 14. A No. 2 bar, bent in an 18-inch diameter spiral with a 3-inch pitch was designated in the bridge plans to complete the connection between the abutment and the pile. A portion of the CMP, spiral, and pile section with the studs is shown in Figure 15.

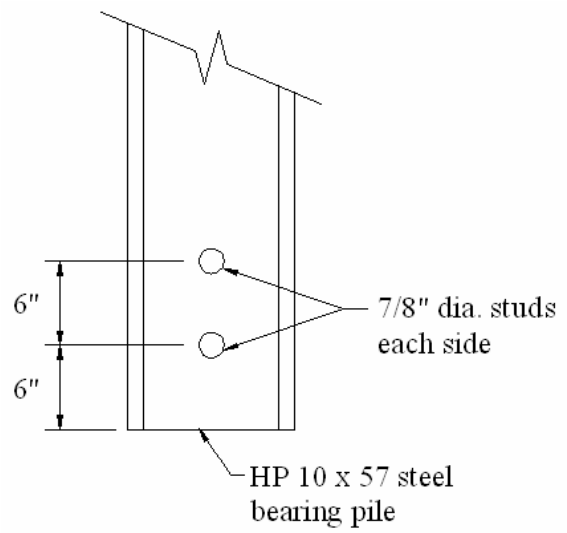

Figure 14. H-pile stud connection detail.

Figure 15. H-pile connection in test specimen before concrete was placed.

All of the reinforcing steel used was ordered through a local contractor's supply store and was pre-cut and bent to the appropriate dimensions except for the No. 4 ties, which were cut and bent in the laboratory. The reinforcement was assembled in the laboratory and placed in the partially assembled formwork, which had been previously coated with a release agent. One of the reinforcement cages in the formwork before the last side of the forms was attached is shown in Figure 16.

Figure 16. Single pile abutment specimen reinforcement placed in the formwork.

Metal chairs were used under the cages to ensure proper cover for the reinforcement. When required, wooden blocks were used between the ends of the formwork and the reinforcement cages to obtain the desired cover. The blocks were removed during concrete placement, after enough concrete was placed to keep the reinforcement from moving.

After the formwork was partially assembled, the CMP was placed in the reinforcement cage and secured with wire ties, after which the formwork was completed. To give the forms more stability during concrete placement, internal and external steel straps were used. Internal straps were placed at three of the joints in the formwork, one foot from the bottom of the forms. Two external straps were used on top of the formwork. The CMP, external straps, and the completed formwork for one test specimen are shown in Figure 17.

The estimated weight of each individual specimen was 7.8 ton. To facilitate lifting and moving the specimens, four lifting hooks were embedded in each specimen. Lifting hooks were attached to wooden “two-by-fours” with bolts and positioned to provide at least two inches of concrete cover for the top of the hooks. Each bolt was greased before the

Figure 17. Completed formwork with the CMP for the first abutment test specimen.

concrete was placed so after the concrete had cured, the bolts and two-by-fours could be easily removed. Styrofoam was used to cover each CMP to keep concrete out during the casting of the abutment specimens. A view of the lifting hooks attached to the formwork and the styrofoam is presented in Figure 18.

After all of the formwork for the first three specimen was completed, as specified in the Iowa DOT bridge replacement plans, a C4 precast concrete bridge mix in compliance with AASHTO Standard Specification for Highway Bridges (1996) with a four-inch slump and a minimum 28-day compressive strength of 5,000 psi was ordered from Iowa State Ready Mix and placed. This was the same concrete mix specified in the Boone County plans for the precast substructure elements.

Before concrete was actually placed, slump tests were performed to ensure the concrete had the minimum desired slump of three inches. If the concrete slump was less than three inches, water was added until the desired slump was obtained. Slump tests were performed whenever concrete was placed. The laboratory concrete bucket and overhead

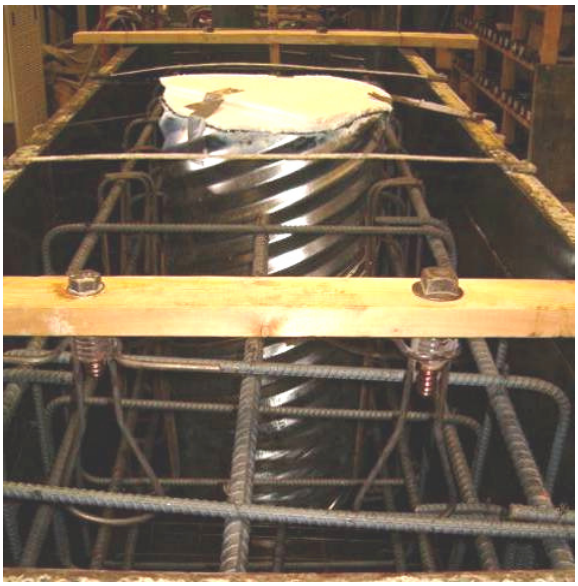

Figure 18. Lifting hooks and styrofoam cover before placing concrete.

crane were used for placing the concrete. Several electric concrete vibrators were used throughout the pour to consolidate the concrete, especially in the area surrounding the CMP. Concrete was placed in approximately four lifts and vibrated between each lift; placement in one of the specimen is shown in Figure 19. While the concrete was being placed, twelve control cylinders were made using the concrete from a particular truck.

A screed was used to strike off the concrete even with the formwork, after which trowels were used to hand-float the surface. The first finished series of test specimens can be seen in Figure 20. In total, thirteen cubic yards of concrete were required to fabricate the three specimen and control cylinders. Once the concrete reached initial set, the surface was covered with wet burlap and plastic sheets for curing. Each specimen remained covered with the plastic and wet burlap, which was removed after seven days and the formwork was 'stripped'.

The H-piles were grouted into place one week after the concrete in the precast portion of the abutment specimen was placed. For grouting the piles into place, the plans called for a

special high-strength concrete mix (minimum compressive strength of 6,000 psi) with 1/2-inch aggregate and a high-range water reducer (HRWR) to improve the long- term workability of the concrete. In the laboratory, the concrete mix did not have the HRWR, but was otherwise the same mix specified in the bridge plans. Since the quantity placed in the laboratory was less than two cubic yards, the long-term workability was not an issue.

Figure 19. Concrete being placed in the first series of abutment specimen.

Figure 20. Hand-finished specimen before initial set.

Each H-pile was to be placed in the CMP with a minimum two foot embedment length, as specified on the bridge plans. As previously described, the test specimens were inverted from the field orientation; therefore, the piles were grouted in at the top of the

specimens. To obtain the desired embedment length, the piles were attached to steel angles using C-clamps, which in turn were supported by the CMP. One of the piles offset in the CMP, before the special concrete mix was placed, is shown in Figure 21.

Placing concrete in the CMP was challenging. The opening was too small to use the concrete bucket without wasting large amounts of concrete. Thus the concrete was placed by hand using shovels and buckets; a student can be seen placing concrete around the H-pile in Figure 22. Vibrators were again used to ensure adequate compaction, and to eliminate voids under the ends of the piles and around the shear studs. Fifteen control cylinder were made using the grout concrete mix.

Figure 21. H-pile in place before placing grout.

Grouted concrete was finished by hand, however, because of the small space between the CMP and piles, a straight edge or trowel could not be used. A pile grouted in place can be seen in Figure 23. After the grouted concrete reached initial set, since each CMP was approximately one half inch longer than the depth of the added grout, water was ponded on top of the grout for curing. After 24 hours, the C-clamps and angles previously described were removed. Water was kept on the surface of the grouted concrete for seven days.

Figure 22. Concrete being placed in the CMP around the H-pile.

Figure 23. H-pile after being grouted in place.

3.1.2 Single Pile Pier Cap Construction

The pier cap design was similar to the precast abutment cap design. Instead of using H-piles, the piers were supported by concrete-filled pipe piles. During construction, the pier caps were supported by falsework until the concrete connecting the piles to the pier had

reached sufficient strength. In the single pier cap test specimen, the pipe pile was centered in the CMP. Each test specimen replicated the pier cap used in the field, including the dimensions and reinforcement. Similar to the abutment specimens, the pier cap specimens were inverted during fabrication and testing. External details of the pier cap specimens are shown in Figure 24.

The reinforcement in the specimens was the same as that specified the project plans (size and spacing), which was adapted for a ten-foot long section of the pier cap. As previously described for the abutment, the pier cap longitudinal bars were continuous, lap spliced where needed and cut to provide one inch of cover for the ends of the No. 8 bars. A top view and cross-section of the pier cap reinforcement can be seen in Figure 25.

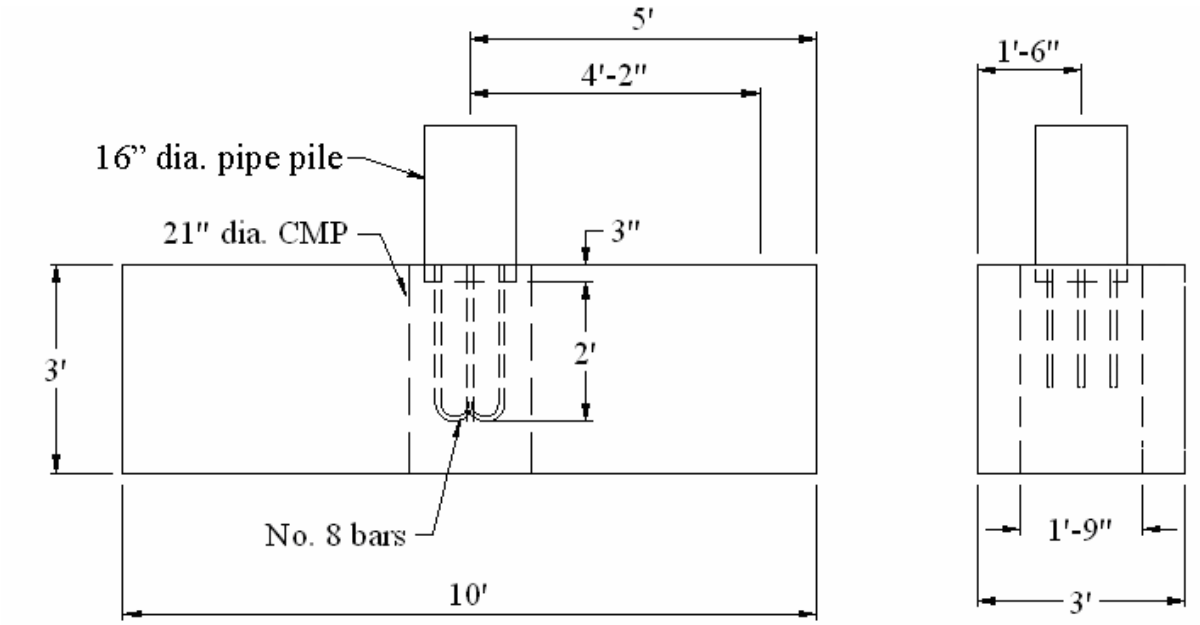

a) side view **b) end view**

Figure 24. Single pile pier cap test specimen.

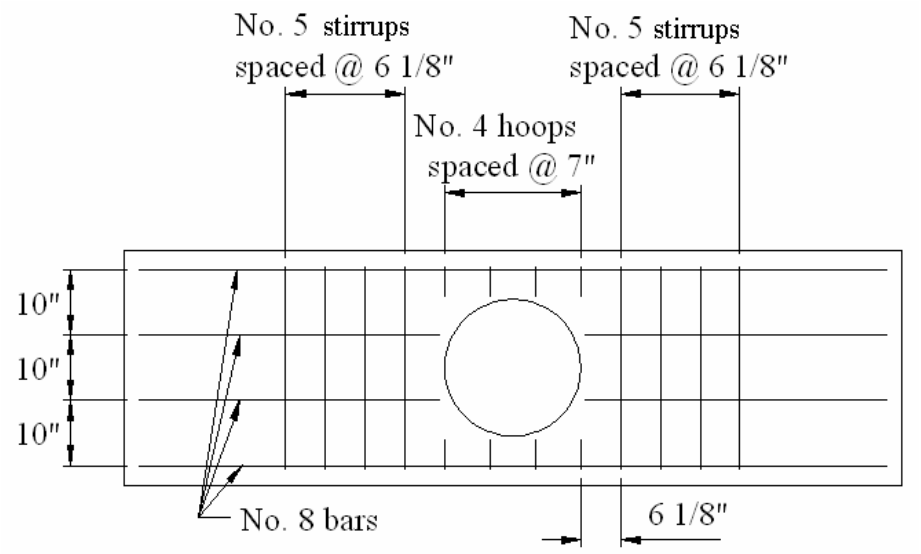

a) top view of pier cap reinforcement

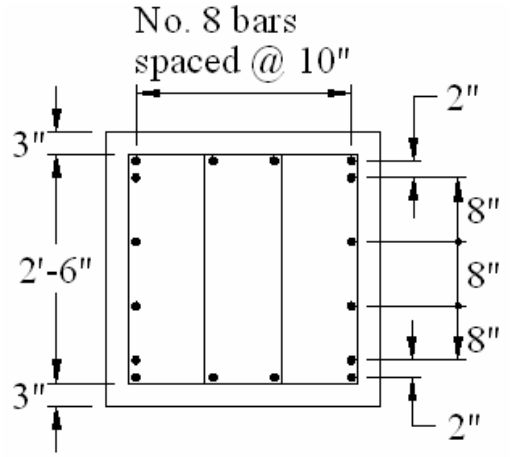

b) cross-section view of pier cap reinforcement

Figure 25. Pier cap reinforcement.

The reinforcement connection between the pipe pile and the pier cap consisted of four No. 8 bars, two straight bars and two bars with 180° hooks, shown in Figure 26. Additional No. 4 hoops, 10-inches in diameter, were also used in the connection. As the concrete in the pipe piles was placed, the reinforcement connection was embedded in the fresh concrete.

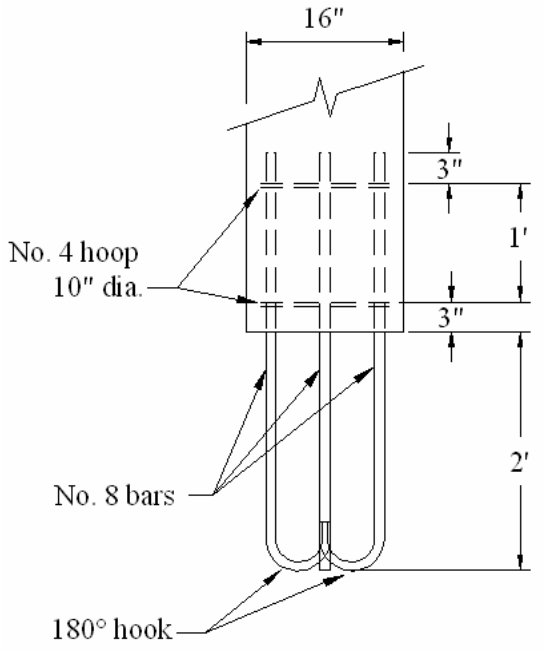

Figure 26. Pipe pile connection detail.

The same formwork used for casting the abutment specimens were used in the pier cap specimens. After the formwork was partially assembled and a release agent applied, the reinforcement cages were placed in the formwork on metal chairs, and the CMP was placed in the reinforcement and secured. Since the abutment specimens and pier cap specimens were the same size, the same lifting hooks and internal and external strap arrangements were used. One of the finished pier cap forms, with the CMP, reinforcement, and external straps is shown in Figure 27.

The pipe pile connection before and after placing concrete is shown in Figure 28. A wooden shim was used to hold the reinforcing steel in place at the correct embedment length. Another wooden shim was used inside the pipe to obtain the desired cover for the No. 4 hoop. Shims were removed after sufficient concrete was placed to keep the reinforcement stable.

Figure 27. Pier cap reinforcement.

Pier cap specimen PSC1 was constructed with the second set of single pile specimens, (ASC3 and ASO2); PSC2 was fabricated and placed with the third series of specimens. The last two series were fabricated, finished, and cured in the same manner as the first series, which has been previously described in some detail. Twelve control cylinders for each truck were also placed for each series of specimens. Concrete on the inside of the pipe piles was placed at the same time as the corresponding series of specimen, and thus had the same strength. Concrete in the pipe was also cured with wet burlap and plastic, in the same manner as the concrete in the test specimen.

Pipe piles were grouted into place seven days after the specimen and pipe pile concrete was placed. The pipe pile was grouted in using the same method as was described for grouting the H-piles into place. Steel angles were bolted to the side of the pipe pile, which in turn was supported by the CMP to provide the desired embedment length for the pile; a pipe pile grouted in place can be seen in Figure 29.

a) pipe pile before placing concrete **b) pipe pile after placing concrete**

Figure 28. Pipe pile connection before and after placing concrete.

Figure 29. Pipe pile after being grouted in place in PSC1.

3.1.3 Double Pile Abutment Specimen Construction

For the abutment section, a double pile test was also performed. Connection details in the double pile test varied slightly from the single pile tests due to changes made in the actual field connection. The single pile test specimens were constructed according to the project plans and tested before construction of the substructure in the field. However, during

field construction, the spiral reinforcement was omitted. Thus, the spiral reinforcing was eliminated in the double pile test to better represent field conditions.

Another change was made to the double pile connection detail. Based on the results from the single pile tests, the depth of concrete inside the CMP was decreased to reduce the capacity of the connection, which should lead to failure at a lower applied force. In order to decrease the depth of concrete in the pipe while keeping the pile connection intact, 12 inches of insulation board was placed in the bottom of the CMP, resulting in a concrete depth of two and a half feet. As with the single pile abutment specimens and pier cap specimens, the double pile abutment specimens were inverted during fabrication and testing. The external details of the double pile specimens are presented in Figure 30.

Specimen size was limited to twelve feet for handling and constructability purposes. The reinforcing cages used in the double pile specimens were adapted from the bridge plans and thus had reinforcement similar to that used in the single pile abutment specimens. However, the reinforcement was designed and constructed to fit two CMP in the formwork; all other construction details remained the same. The top view as well as the end view of the reinforcement are presented in Figure 31.

H-piles used in the double pile specimen had the same welded studs on the pile web as shown in Figure 14. Internal straps were increased from three straps for the single pile specimens to four straps for the double pile specimens; external straps were also increased from two straps for the single pile specimens to three straps for the double pile specimens. Lifting hooks used in the double pile specimens were the same number and layout as were used in the single pile specimens. The reinforcement in the formwork for a double pile test specimen, along with the external straps and lifting hooks, can be seen in Figure 32.

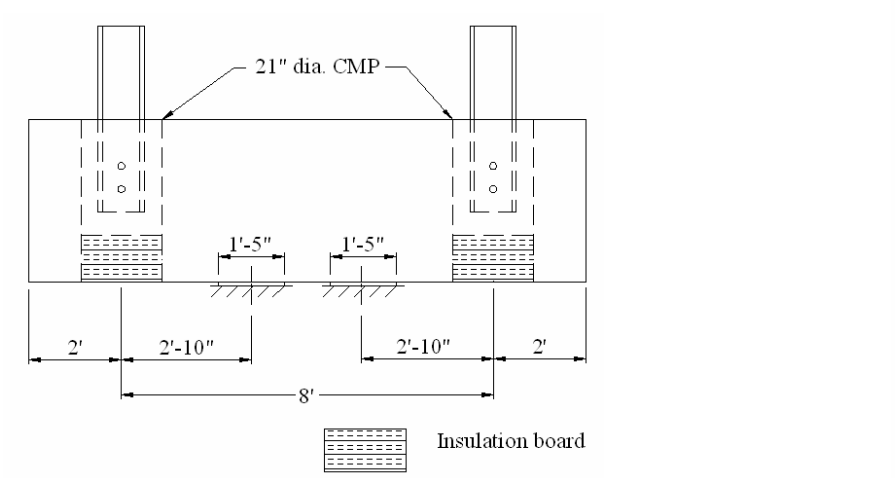

a) top view

b) end view

Figure 30. Double pile abutment test specimen.

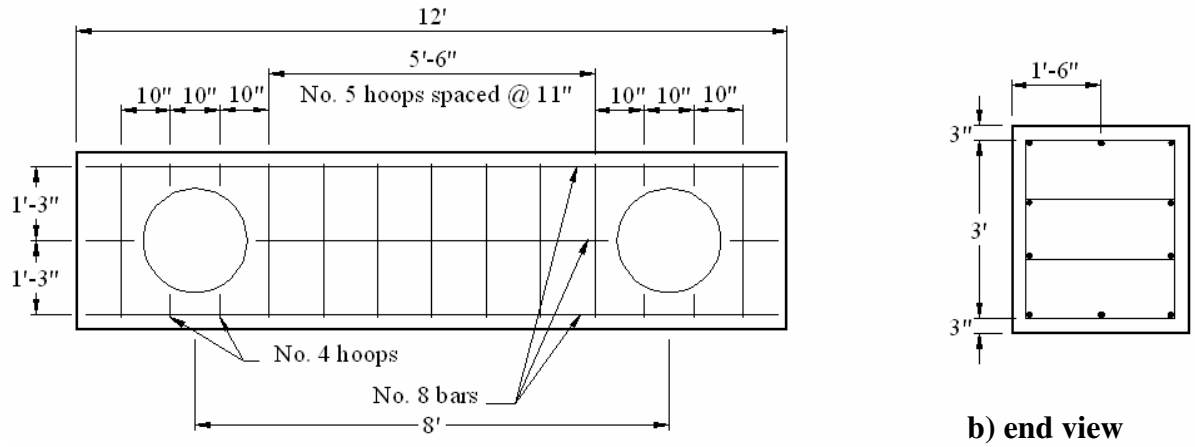

a) top view

b) end view

Figure 31. Double pile abutment specimen reinforcement.

Concrete used in the double pile abutment specimens was the same mix used in the single pile abutment and pier cap specimens. As with the previous specimens, styrofoam was used to cover the CMP to keep concrete out of the void. Concrete was placed using the overhead crane and concrete bucket, vibrated, and finished by hand. A finished double pile specimen before initial set was reached is shown in Figure 33.

Figure 32. Finished reinforcement and formwork for ADC1.

Figure 33. Abutment 6 after hand-finishing.

While the concrete was being placed, twelve control cylinders from the concrete in each truck were made. Once the concrete reached initial set, the surface was covered with wet burlap and plastic sheets for curing. The specimen remained covered for seven days, after which the covering was removed and the formwork 'stripped'.

Before the H-piles were grouted into place, as previously noted, twelve inches of insulation board were placed at the bottom of the CMP, leaving six inches of concrete cover below the tip of the H-piles. Steel angles and C-clamps were used to support the H-piles, which in turn were supported by the CMP during concrete placement. One of the H-piles being held in the desired position before placing concrete was complete is shown in Figure 34. Note the absence of the spiral reinforcement in the CMP.

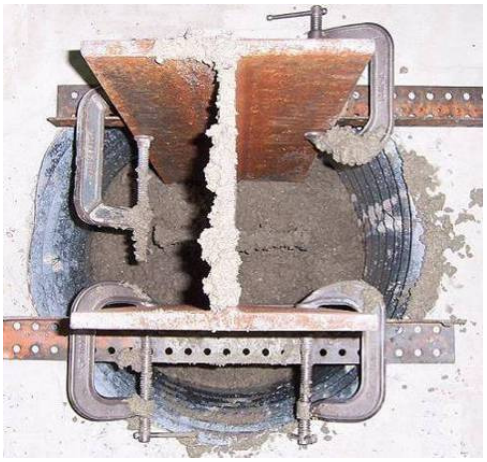

Figure 34. Double pile abutment specimen H-pile before being fully grouted.

The concrete inside the CMP was hand finished because of previously described space constraints. After the grout concrete reached initial set, the height of the CMP allowed water to be ponded on top of the grout concrete for curing. After twenty-four hours, the C-clamps and steel angles were removed, however, water was kept on the surface of the grouted concrete for seven days. As before, a total of twelve control cylinders were made for the grout concrete mix.

The last construction task was to use a grinder to smooth and level the surface of the pile. This was to ensure even loading during testing and to prevent localized failure in one of the pile flanges.

3.2 Laboratory Testing

The main concern with the substructure elements was the possibility of the grouted concrete shearing from the CMP and 'punching' through the precast section of the abutment and pier caps. For the abutment sections, there also was a concern that the pile may punch through the concrete in the CMP; this was not a concern for the pier cap due to the large surface area of the concrete-filled pipe pile.

Test were performed on three different substructure specimens: single pile abutment and pier cap tests were performed to determine the capacity of the specimen when subjected to a combination of shear and negative moment; double pile abutment tests were performed to determine the positive moment capacity of the abutment section. After the double pile specimens were tested, punching shear tests were performed on each individual pile to determine the punching shear capacity of the H-pile connection.

3.2.1 Single Pile Test – Abutments and Pier Cap

The single pile abutment and pier cap tests had two simulated beams spaced on eight-feet, four-inch centers, according to the bridge plans. This beam spacing provided the maximum negative moment in the substructure sections at the pile location. Beam spacing and support dimensions are presented in Figure 35.

The pier cap specimens were tested using the same arrangement as the abutment test shown. Each specimen was instrumented with linear variable deflection transducers (LVDT) and strain gages. Transducers were placed on the top and bottom faces of the specimen to measure differential deflection between the precast concrete and the grouted concrete in the CMP, and total deflections during testing. A total of nine deflection transducers were used: four on the top surface of the specimen and five on the bottom surface. On the bottom

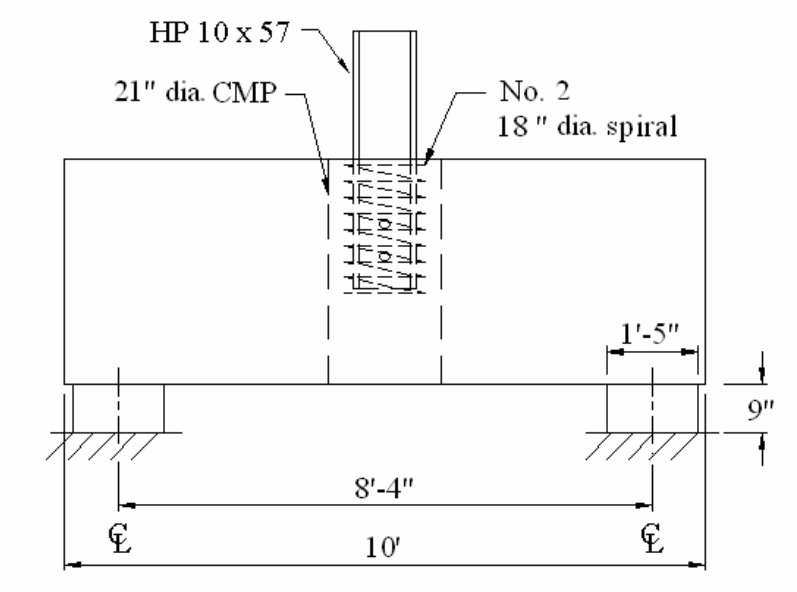

Figure 35. Single pile abutment test support details.

surface of the specimen, one deflection transducer was placed adjacent to the support to measure the deflection due to the compression of the neoprene pads so that the actual deflection of the test specimen could be determined.

Strain gages were used on the pile flanges to determine if there was uniform loading. Each H-pile was instrumented with four strain gages, one gage on each flange of the pile; each pipe pile had two gages placed opposite each other. The concrete was also instrumented with four strain gages. Each of the transverse sides of the specimen had two strain gages attached, one at the top and one at the bottom. Placement of the gages varied slightly for each specimen, depending on the quality of the concrete surface. The instrumentation plan for the single pile specimens is presented in Figure 36 (spirals and pipe pile steel not shown for clarity); instrumentation used on the pier cap specimens was the same as that was used on the single pile abutment specimens, with the exception that only two strain gages were used on the pipe piles.

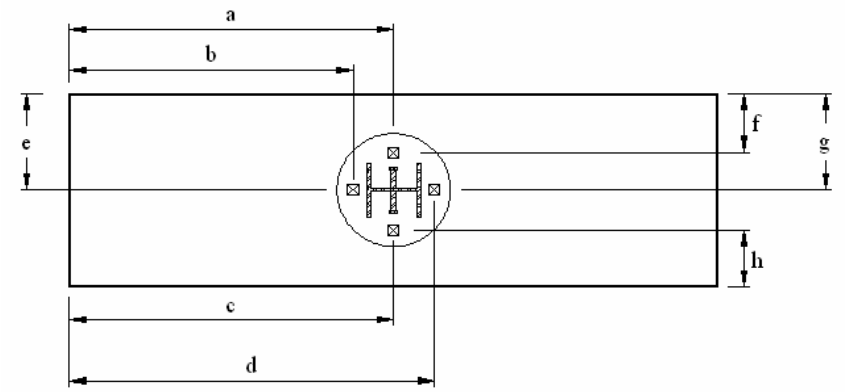

a) location of the deflection transducers used in the single H-pile and pipe pile tests, top view

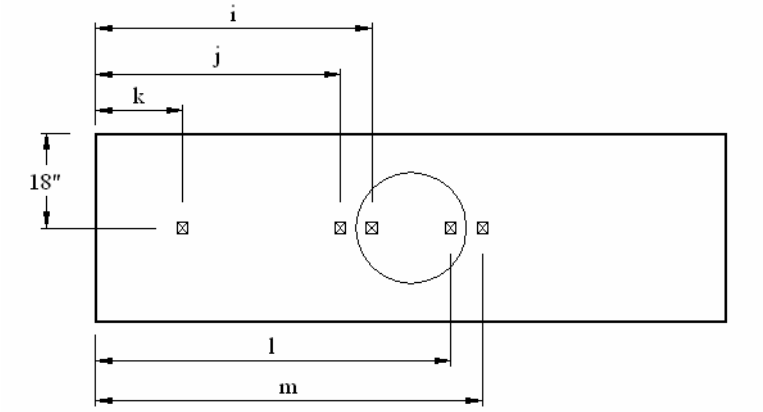

b) location of the deflection transducers used in the single H-pile and pipe pile tests, bottom view

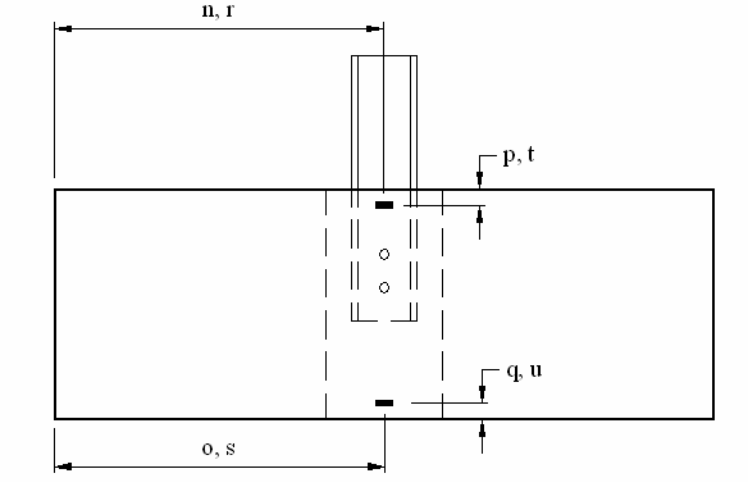

c) location of the strain gages used in the single pile tests (north face, south face)

Figure 36. Single pile abutment test instrumentation plan.

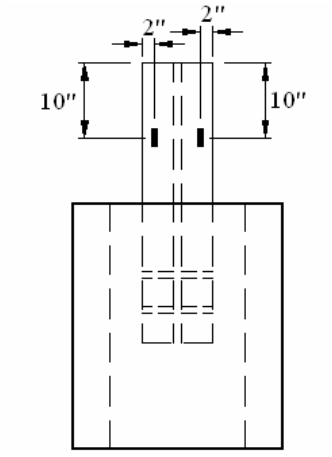

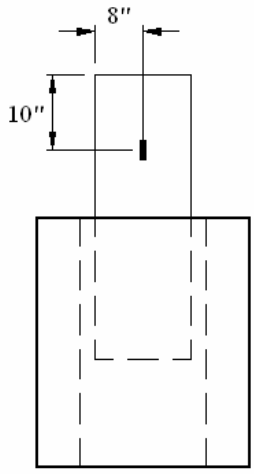

d) location of H-pile strain gages **e) location of pipe pile strain gages**

Figure 36. (continued).

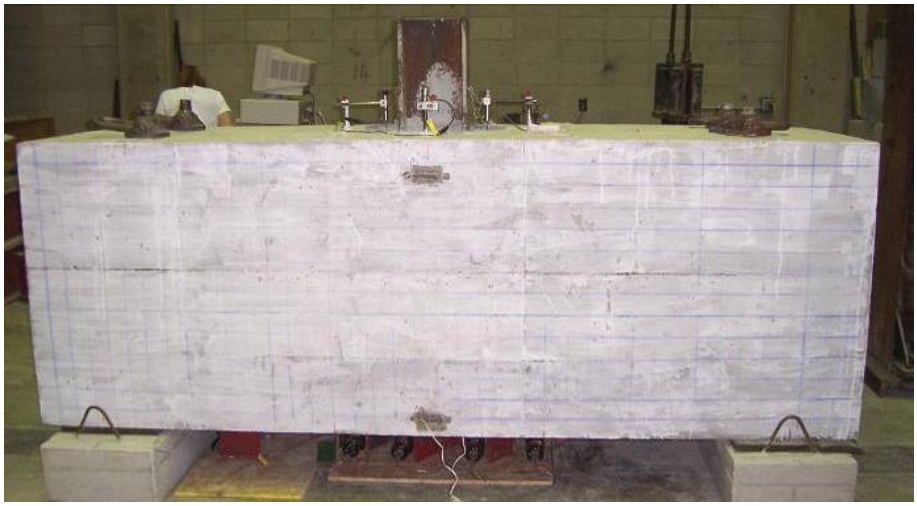

Figure 37. Instrumentation on ASC1 prior to testing.

The variable dimensions for the deflection transducers and strain gages are labeled with letters in Figure 36; deflection instrumentation dimensions for each specimen are given in Table 2 and strain gage location dimensions are given in Table 3. Some of the instrumentation on ASC1 can be seen in Figure 37.

Table 2. Location of deflection instrumentation on the single pile specimens.

Specimen	Top Deflection Dimensions (in.)								Bottom Deflection Dimensions (in.)				
	a	b	c	d	e	f	g	h	i	j	k	l	m
ASC1	58	50.5	57.5	66.5	19	10.5	16	26	54	45	24	66	75
ASC2	59.75	51.5	59.75	67.75	17.5	9.5	18	10.75	53.5	45.75	22	65.5	75.25
ASC3	62	62.5	60	67.5	18.5	10	20	10	54.5	43.5	20	65	74
ASO1	61.5	52.25	59.25	68	17.25	10.75	15.75	10	54	45.25	21.5	65.5	75
ASO2	60	44.5	59.75	70.5	17.5	4.75	18.25	6	55.75	47.25	21	67.75	66.25
PSC1	57.5	51	58.5	68.5	18	8.25	51.5	9	53.75	45	21.75	68	77.5

Table 3. Location of strain gage instrumentation on the single pile specimens.

Specimen	North Face Dimensions (in.)				South Face Dimensions (in.)			
	n	o	p	q	r	s	t	u
ASC1	59	59	4.5	2.75	58.25	58.5	1.5	4
ASC2	60	60	3.25	2.25	60	60	5.25	2
ASC3	57.5	60	2.25	3.5	60.25	58.25	2.5	1
ASO1	60.5	60.5	3.75	2.25	60.25	60.25	3.25	7
ASO2	62.5	62	4	1	63.5	62.75	3	2
PSC1	59	59	1	0.75	57.5	59.5	3	2.5

As previously noted, the specimens were inverted for testing due to stability concerns. The simulated beams rested on the floor, the specimens were placed on neoprene pads on top of the beams, and the protruding pile was then loaded. An actual test arrangement for one of the abutment specimen is shown in Figure 38.

Abutment and pier cap specimens were tested seven days after the grouted concrete was placed, or as soon as the grouted concrete reached the appropriate strength, if strength was not met in seven days. Specimens were initially loaded to a proof load of 160 kip, twice the unfactored design load. This proof load was held for 15 minutes before loading continued. The load cell used for testing had a maximum capacity of 300 kips (±10 pounds) while the hydraulic pump and Load Frame 1 each had capacities of 400 kips. Therefore, each specimen was loaded to 300 kips after which the load cell was removed, and loading continued to the maximum capacity of the test specimen. While the load cell was in use, strain and deflection measurements were taken at approximately 10 kip increments.

Figure 38. Laboratory test arrangement for ASC1.

After the load cell was removed, loading continued and measurements were taken at approximately eight kip increments, as measured using the gage reading of the hydraulic pump. Each specimen was loaded until failure or until the safety of the load frame became a concern. Periodically during testing, loading was paused to mark the crack pattern on the specimen; the crack pattern was also marked at the final load.

3.2.2 Double Pile Positive Moment Test

Double pile abutment specimens were tested to measure the effects of the combination of shear and positive moment on the abutment and to determine if this loading condition could produce a punching shear failure between the precast concrete and the concrete in the CMP. Support conditions were adjusted from the plans to produce a maximum positive moment in the abutment section between the piles. In the field, the abutment section can never be subjected to the same loads as in the laboratory tests because of the support conditions (i.e. continuous spans); the loads in the laboratory (i.e. simple spans) were more severe than actual field conditions. Double pile specimens were inverted and tested in the same manner as the single pile specimens; the support conditions for the double pile specimens are presented in Figure 39.

Each test specimen was instrumented using twelve strain gages on the concrete, eight strain gages on the H-pile, four deflection transducers at each pile connection (eight LVDTs total), and six deflection transducers along the bottom of the specimen. Deflection transducers were placed on the top and bottom faces of the specimen to measure total deflection and differential deflection during testing; the eight LVDTs on the top surface of the specimen were used for differential deflection measurements while the six transducers on the sides of the specimen were used for measuring total deflections.

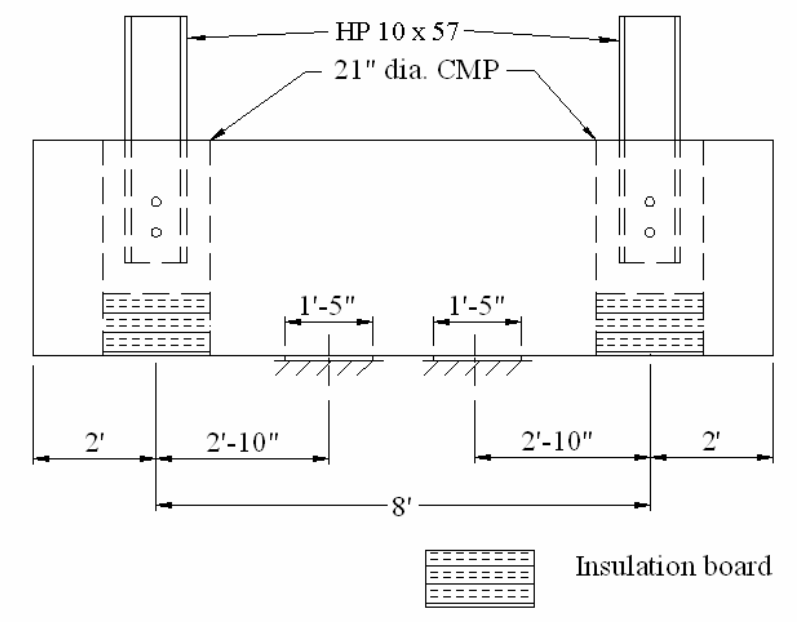

Figure 39. Double pile abutment test support details.

Strain gages were used on the H-piles to ensure even loading. Each H-pile was instrumented with four strain gages, one on each flange of the pile. The concrete section was also instrumented with a total of twelve strain gages. Strain gages were placed at the top and bottom of the transverse sides at both pile locations and at the center of each specimen; the exact location of the strain gages varied slightly for each specimen depending on the surface of the concrete.

The instrumentation plan for the double pile specimens is presented in Figure 40 (the insulation board is not shown for clarity). Variable dimensions for the location of the top deflection transducers, the bottom deflection transducers, the strain gages on the north face of the specimens, and the strain gages on the south face of the specimens are presented in Table 4, Table 5, Table 6, and Table 7, respectively.

Complete instrumentation on the north face of ADC1 can be seen in Figure 41 prior to testing. Laboratory testing arrangements were similar to that used in the single pile

specimen tests, however, the double pile test required two load frames so that both piles could be loaded simultaneously; Load Frame 2 had a capacity of 150 kips. The laboratory testing arrangement for ADC2 is shown in Figure 42.

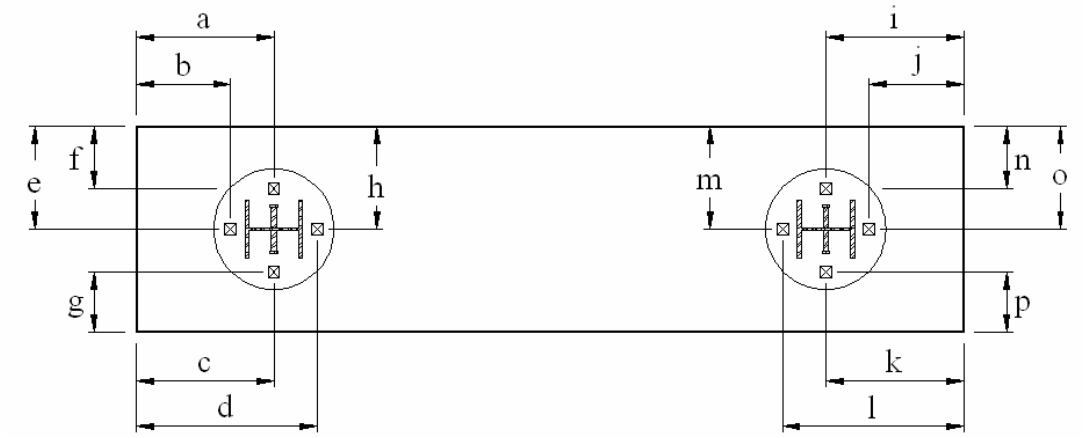

a) location of deflection transducers, top view

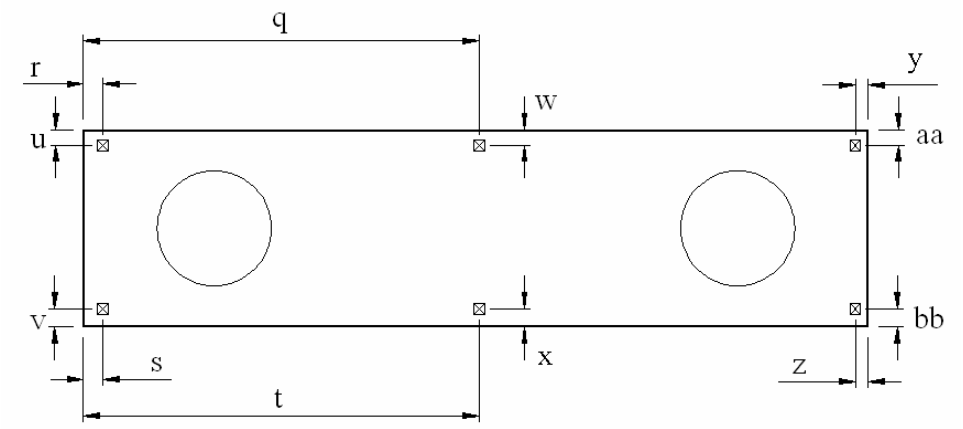

b) location of deflection transducers, bottom view

Figure 40. Double pile abutment test instrumentation plan.

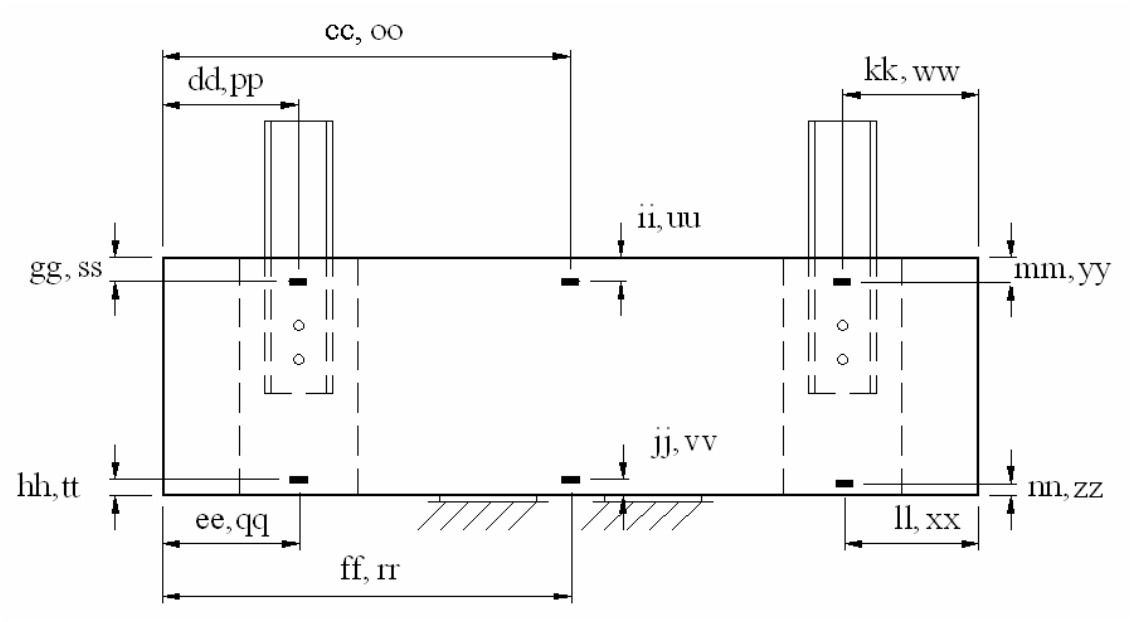

c) locations of the strain gages (north face, south face)

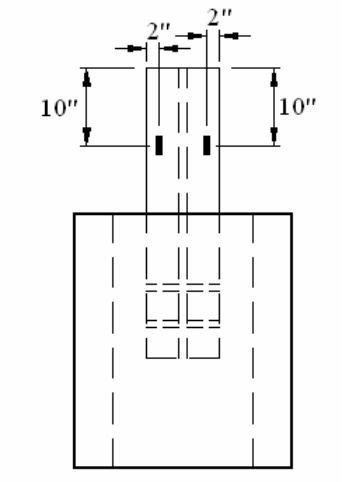

d) location of the strain gages on the H-piles

Figure 40. (continued).

Table 4. Double pile specimens: location of top deflection instrumentation.

Specimen	Top Deflection Dimensions (in.)															
	a	b	c	d	e	f	g	h	i	j	k	l	m	n	o	p
ADC1	21.5	15.3	23	35.5	19	11.5	11.3	17.8	21	13.5	19.5	29	21	13.5	17.8	11.5
ADC2	22.5	17.5	23.3	38	18.5	9.5	13.3	18.8	21.3	11.3	21	35.5	17.8	10.5	18	11.5

Table 5. Double pile specimens: locations of bottom deflection instrumentation.

Specimen	Bottom Deflection Dimensions (in.)											
	q	r	s	t	u	v	w	x	y	z	aa	bb
ADC1	72.75	0.5	0.5	78	0.5	0.5	0.5	0.5	0.5	0.5	0.5	0.5
ADC2	72.5	0.5	0.5	76.5	0.5	0.5	0.5	0.5	0.5	0.5	0.5	0.5

Table 6. Double pile specimens: locations of strain gages, north face.

Specimen	North Face Strain Dimensions (in.)											
	cc	dd	ee	ff	gg	hh	ii	jj	kk	ll	mm	nn
ADC1	68	21.25	20.25	69.25	2.5	3.25	3	3.25	19.25	18.5	2.75	4
ADC2	68.5	21.5	24.3	67.5	2	2.5	2.75	3	20.5	20.75	1.75	2.75

Table 7. Double pile specimens: location of strain gages, south face.

Specimen	South Face Strain Dimensions (in.)											
	oo	pp	qq	rr	ss	tt	uu	vv	ww	xx	yy	zz
ADC1	66.5	19.5	20	75.5	2.75	3	2	2.5	21	21.25	3.25	1.75
ADC2	75.5	20.5	21.25	74	2.25	2.5	2	1.75	21.5	23	2.5	1.75

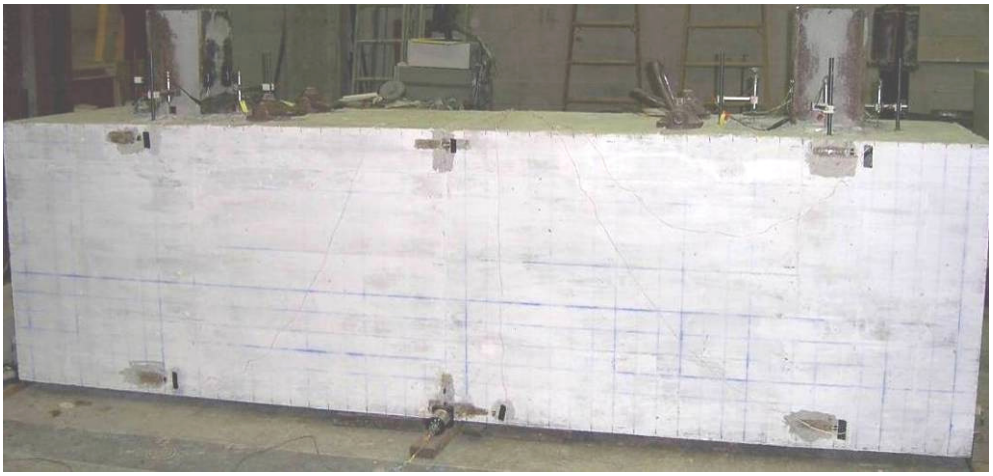

Figure 41. Instrumentation on a ADC1 prior to testing.

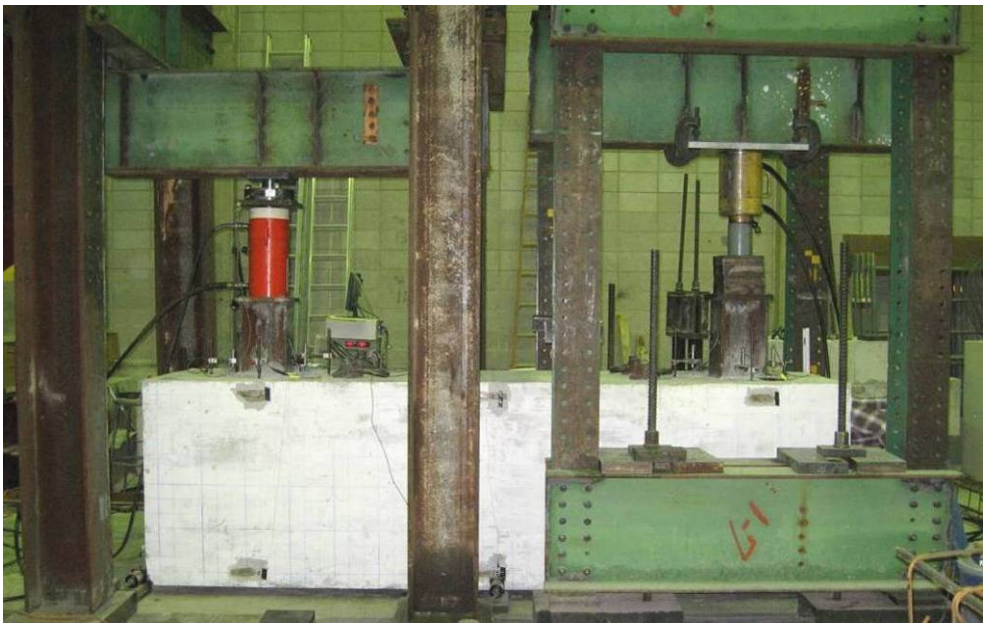

Figure 42. Laboratory test arrangement for ADC2.

The double pile abutment specimen were tested seven days after the grouted concrete was placed, or as soon as the grouted concrete reached the appropriate strength, if strength was not met in seven days. Specimen were tested by simultaneously loading both of the H-piles at approximately the same rate up to 140 kips (ADC1) or 150 kips (ADC2). Deflection and strain measurements were taken at approximately 10 kip intervals. Loading was stopped

at 140 or 150 kips due to concerns with the safety of the load frames. Periodically during testing and at the final load, loading was paused to mark the crack pattern on the sides and top surface of the specimen.

3.2.3 Shear Test

After the combination shear and positive moment tests were complete, the double pile abutment specimen had not completely failed. The area of concrete around the CMP had not cracked, so additional tests were performed on the specimen. Each abutment was adjusted to center one of the piles under the larger load frame. Support conditions were moved so there were two supports located adjacent to the CMP around the pile being tested. A third support was placed under the opposite end of the abutment for stability. The load frame and test arrangement for one of the pile shear test can be seen in Figure 43.

Since the abutments were already instrumented, the same instrumentation was used in the shear test. The bottom deflection gages were omitted since the bottom of the concrete in the CMP could not be instrumented for comparison; also the four strain gages on the concrete located at the center of the specimen were omitted since the center gages were beyond the area of interest. Thus in the shear tests, data measured by the four strain gages on the concrete at the pile location, the four strain gages on the H-pile being tested, and the four LVDTs located adjacent to the pile were recorded.

Each pile was loaded to 400 kips, measurements being recorded approximately every 10 kips with the load cell in place (up to 300 kips), and every eight kips after the load cell was removed. The differential deflections were monitored and the specimen was checked for cracks throughout the loading. Since there were no cracks on the specimens visible to the naked eye, none were marked.

Figure 43. Double pile abutment shear Test 1.

CHAPTER 4. LABORATORY TEST RESULTS

4.1 Single Pile Abutment Test Results

The results from the abutment and pier cap tests described in Chapter 3 are presented in this chapter. During the test of PSC2 there was a premature localized failure over one of the supports. Since the failure that occurred was independent of the CMP and pile connection, the results for PSC2 are not presented. Each pile in the actual abutment in the field was designed by the Iowa DOT to support a service load of 80 kip; the piles in the pier cap were designed to support a service load of 72 kip each.

To simplify the comparison of results, the instrumentation numbering for the single pile specimens was kept consistent. The following instrumentation labels and locations apply to all of the single pile tests. Labels and locations for the strain gages applied to the concrete are shown in Figure 44. As previously noted, the location dimensions for all of the gages which vary on each specimen can be found in Table 2 and Table 3.

The only difference in instrumentation labeling for all of the single pile specimens was for the pier cap test; only two strain gages were used, G5 and G7, which were directly

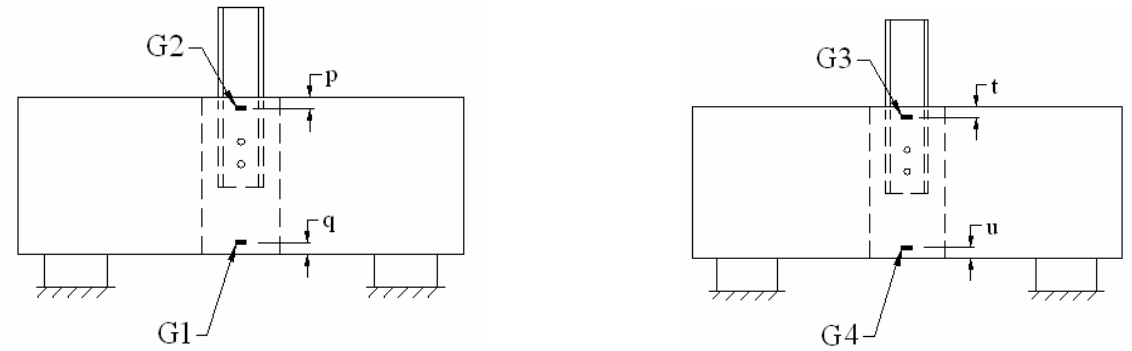

a) strain gage locations on the north face **b) strain gage locations on the south face**

Figure 44. Single pile specimens: locations of strain gages on concrete.

each other on the pipe pile. Locations of the strain gages on the H-pile for the abutments are shown in Figure 45a, the locations for the top deflection transducers are shown in Figure 45b, locations of the strain gages on the pipe pile are shown in Figure 45c and the locations for the bottom deflection transducers are shown in Figure 45d. This instrumentation labeling will be used throughout the results section.

Control cylinders for the precast concrete and the grouted concrete were broken at seven days and twenty-eight days, corresponding to when the concrete was placed. Separate cylinders were also made from the precast concrete and the grouted concrete for each specimen and were broken on the day each respective test was performed. All of the

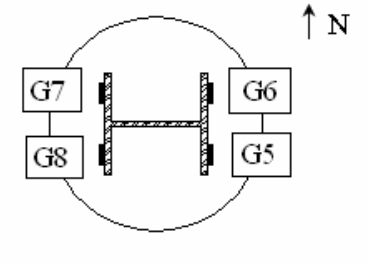

a) strain gage locations on H-pile

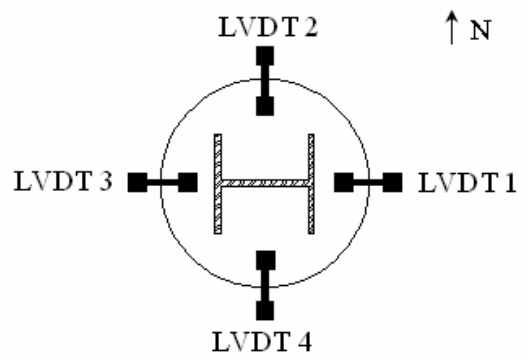

b) location of top deflection transducers

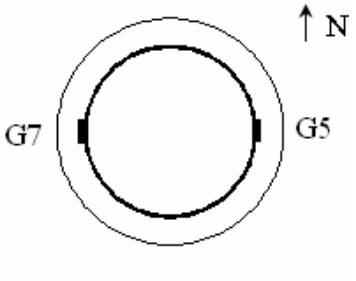

c) strain gage locations on pipe pile

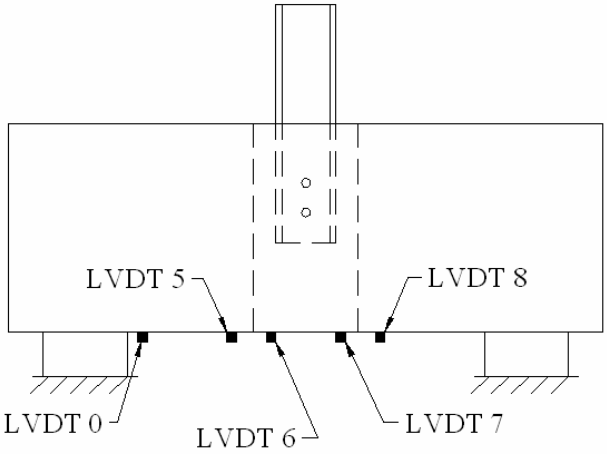

d) location of bottom deflection transducers

Figure 45. Single pile specimen instrumentation locations.

concrete cylinders were broken according to ASTM C39; concrete strengths on test day and at 28-days are listed in Table 8.

Results from the slump tests were also recorded. All of the concrete met the minimum slump requirement of three inches before the concrete was placed. The maximum slump recorded was 4.5 inches; complete results from the slump test can be found in Appendix I.

Table 8 Test day and 28-day concrete strengths for each test.

Specimen	Precast Concrete Strength (psi)		Grouted Concrete Strength (psi)	
	Test Day	28-Day	Test Day	28-Day
ASC1	5020	6230	5220	6955
ASC2	4945	6230	5300	6955
ASO1	4340	5505	5520	6955
ASC3	5185	5315	4000	4280
ASO2	5685	5855	3115	4280
ADC1	6490*	5745	5540	5975
ADC2	6515*	5650	4010	5525
PSC1	5270	5315	3500	4280

* Test was performed after the precast concrete 28-day strength was measured.

4.1.1 Centered Pile Results

There were three single pile abutment specimens tested with centered piles, all of which displayed similar strain and deflection behavior, and had similar crack patterns under the applied load. The results for ASC3 are presented and discussed in the following pages; complete results for ASC1 and ASC2 are presented in Appendix I.

During testing, four parameters were measured: strains in the steel pile, concrete strains, differential movement between the concrete in the CMP and the precast concrete, and the total deflection of the specimen (see Figure 36 for location of instrumentation). Strains in the steel pile were examined first to ensure the pile was loaded uniformly. Steel

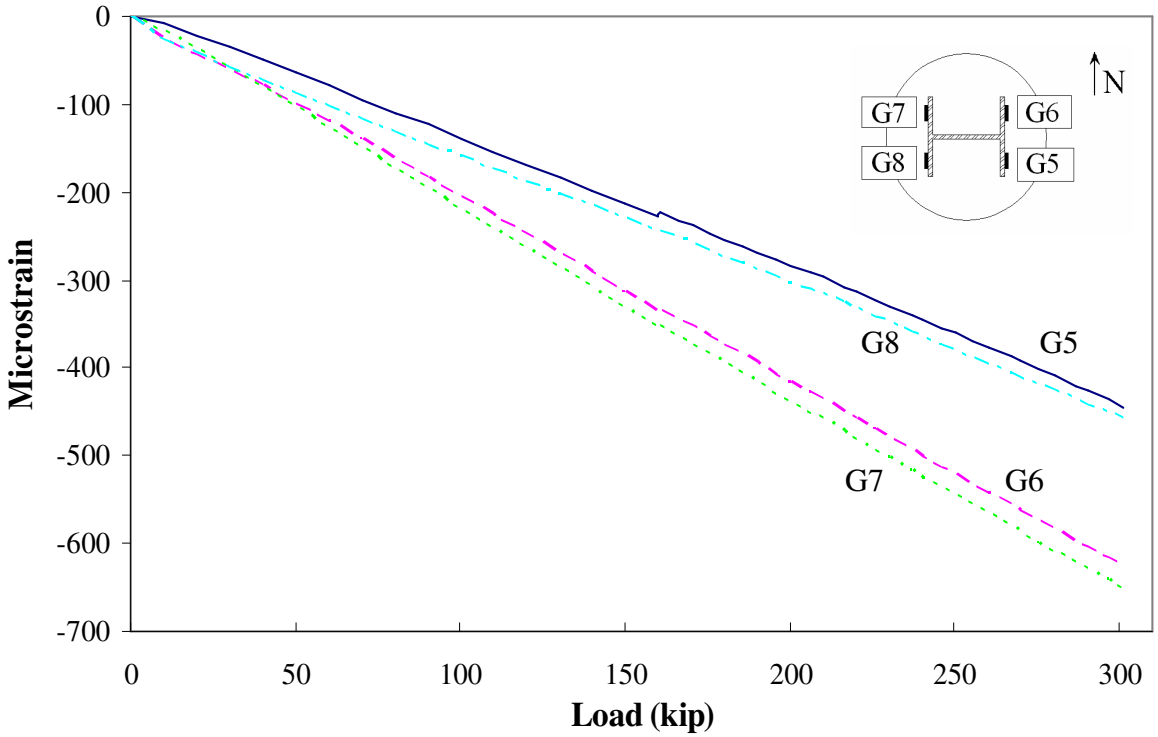

Figure 46. Steel strains for ASC3.

pile strains measured during the testing of ASC3 are presented in Figure 46. The behavior of the H-piles is represented by the measured strain data. Stress data for the pile will not be presented since the stress-strain relationship remains linear throughout testing (i.e. the piles did not yield). For this report, compressive strains and stresses are negative, tensile strains and stresses are positive.

As may be seen in the figure, the strains measured in the flanges of the pile were not equal, however, the strains in the two flanges did increase at approximately the same rate; this indicates an eccentricity of the applied load. For example, during the ASC3 test, for an applied load of 276 kip, the difference between the north strains and south strains was approximately 175 μ-strain; actual strains and stresses in the four gages are listed in Table 9 (stresses were calculated using Hooke's Law and 29,000 ksi for the modulus of elasticity for the pile). Strains measured are due to the axial load applied to the pile and the load

Table 9. Strains and stresses in ASC3 at applied load of 276 kip.

Gage	Strain (10^{-6})	Stress (ksi)	Stress Difference (%)
G5	401	11.6	-
G6	574	16.6	43
G7	598	17.4	49
G8	418	12.1	4

eccentricity. A system of equations, using the known strains, gage locations, and pile properties, was used to calculate the load eccentricity. Based on the strains given in Table 9, the axial load on the pile was offset 0.35 inches to the north and 0.07 inches to the west, which caused a stress difference of approximately 50% in the pile at this load.

The maximum strain difference measured in all of the piles was approximately 180 μ-strain in ADC2, which corresponds to a maximum eccentricity of 0.14 inches to the south and 0.86 inches to the west. Inadvertent eccentricity of the applied load was noted in all of the tests, the largest eccentricity calculated was less than one inch. Concrete stresses were examined to see if the eccentricity affected the specimen behavior, however, no clear trend relating the eccentricities to the stresses emerged.

All of the specimens tested were classified as deep beams based on the ACI Building Code (2005) criteria stating a deep beam is a beam under point load where the clear span is less than four times the beam depth. Since the clear span in all tests was eight-feet, four-inches and the depth was three-feet, six-inches the specimens met the deep beam criteria.

Strains in the concrete were examined to see how the pile connection affected the specimen behavior. Concrete strains were converted to estimated stresses using the modulus of elasticity of the concrete and Hooke's Law. The modulus of elasticity was calculated according to Section 5.4.2.4 of the AASHTO LRFD Bridge Design Specifications (1996).

Concrete tensile strength was estimated based on the assumption that tensile strength is approximately 8-10% of the compressive strength. Concrete compressive strength, a range of the tensile strength, and the modulus of elasticity for each centered single pile abutment specimen are presented in Table 10. Concrete stresses in ASC3 are presented in Figure 47. Locations of the stresses (strains) in the figure were presented in Figure 44.

There are two distinct trends in the top and bottom specimen stresses that can be seen in Figure 47. At the bottom of the specimen, G1 and G4 indicate only tensile forces in the

Table 10. Strength properties for centered, single pile abutment specimens.

Test	Concrete Compressive Strength (psi)	Concrete Tensile Strength (psi)	Modulus of Elasticity (ksi)
ASC1	5020	400-500	4295
ASC2	4945	395-495	4265
ASC3	5180	415-520	4365

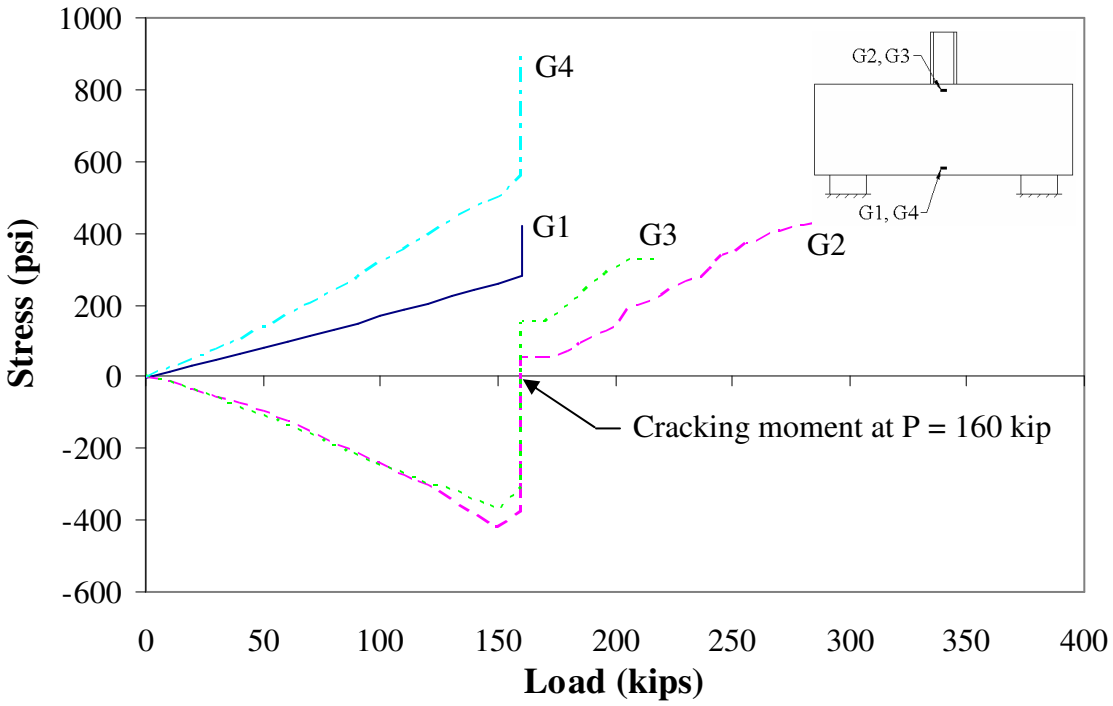

Figure 47. Concrete stresses in ASC3.

concrete at that location for all loads applied. The gages at the top of the specimen, G2 and G3, indicate the concrete is initially in compression, which agrees with simple beam theory. At a load of approximately 160 kip, ASC3 reached the cracking moment capacity of the section and the initial cracks in the sides of the specimen were noticed.

As presented in Table 10, the tensile capacity of ASC3 was between 415 psi and 520 psi. Before the cracking moment was reached, the tensile stresses at the bottom of the concrete were less than 520 psi. During testing, cracks in the concrete propagated through several of the strain gages, which made them inoperable.

Stresses in the concrete at the top of the specimen changed when the cracking moment was reached; stresses changed from compressive to tensile. However, the concrete at the top of the specimen did not crack since the tensile stresses were less than 520 psi. The expected behavior of the section was the uncracked concrete at the top of the specimen should have been in compression. Since the concrete at the top of the specimen had tensile stresses immediately after the cracking moment was reached, it is apparent the pile connection and CMP affected the behavior of the specimen. This will be discussed in some detail in Section 4.4 of this chapter.

The ultimate goal of the laboratory testing was to determine if a pile would shear through the concrete, or cause the concrete in the CMP to ‘punch’ through the specimen. During testing, none of the H-piles punched through the concrete and none of the connections failed in shear. To determine if there was any differential movement between the precast concrete and the concrete in the CMP, the differential deflection measurements taken from the top of the specimen were analyzed. The transducers did measure small amounts of movement between the concrete in the CMP and the precast abutment (LVDT

precision was 0.0005 inches); differential deflections measured during the testing of ASC3 are presented in Figure 48. Note for the LVDTs, negative movement was downward movement. The maximum differential deflection measured on top of ASC3 was -0.0033 inches at the east transducer and slightly less at the north transducer. The transducers at the west and south locations measured -0.001 inches or less.

Deflections on the bottom of the specimen were found by subtracting the compression of the neoprene bearing pads, measured by the transducer located adjacent to the support (LVDT 0) from the four deflections measured near the center of the specimen. As shown in Figure 49, the largest deflections measured during testing were from LVDT 6 and LVDT 7, the two transducers located closest to the center of the specimen. Deflections measured by LVDT 5 and 8 were further from the center of the specimen and as would be expected, were also smaller than the deflections measured LVDT 6 and 7. As

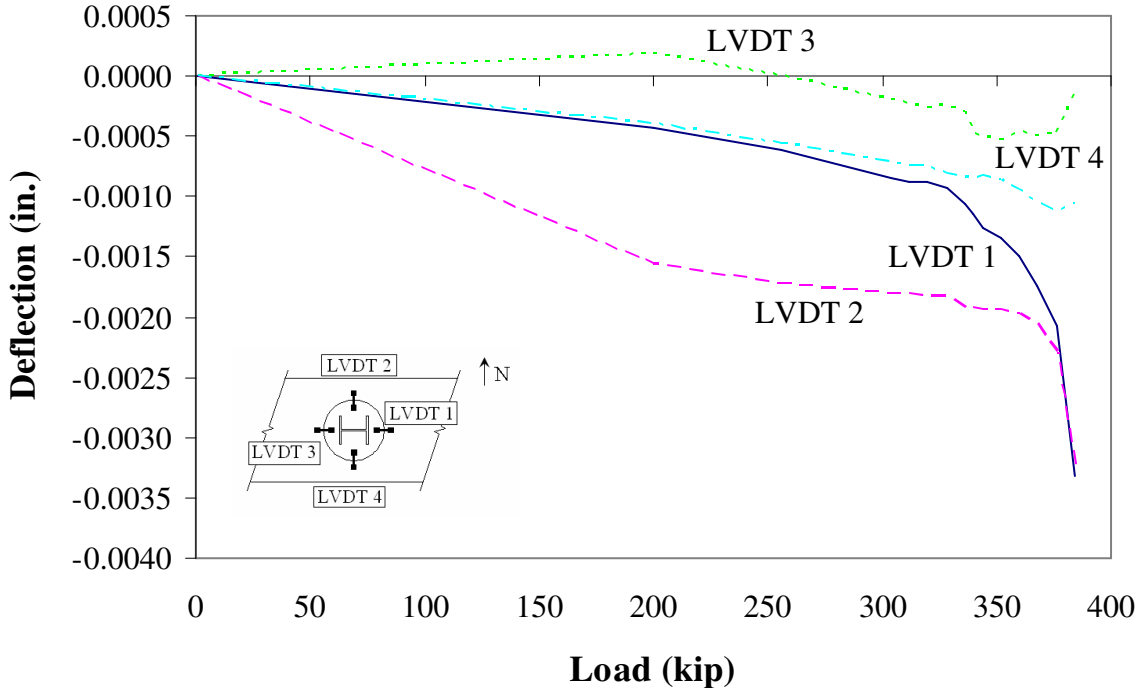

Figure 48. Differential deflection for ASC3.

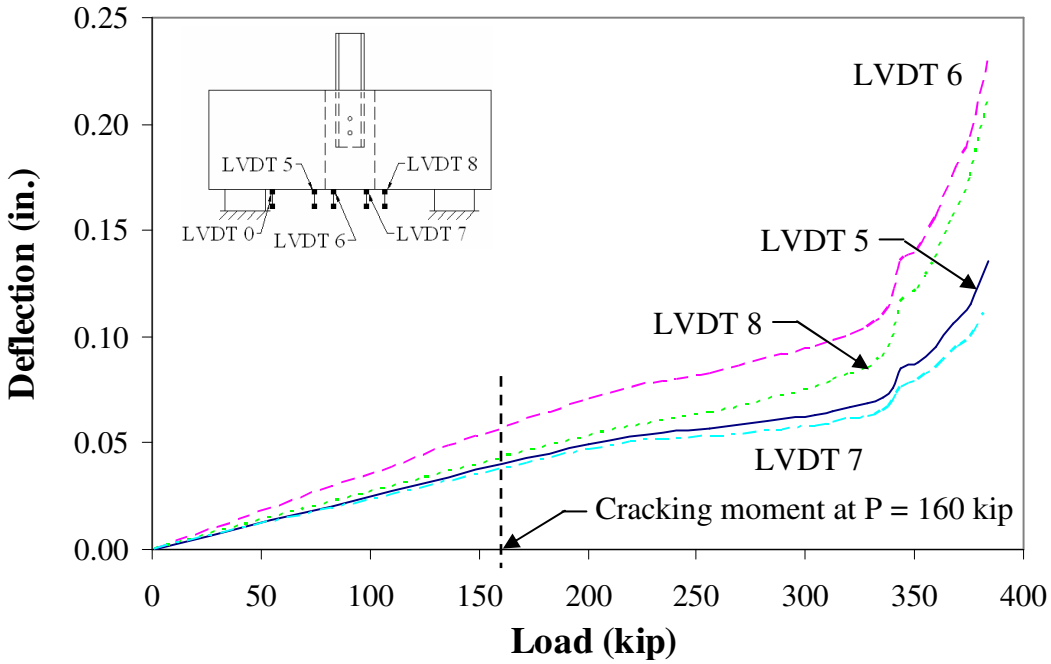

Figure 49. Bottom deflection for ASC3.

shown in the two figures, there is a large difference in the magnitude between the differential deflections (Figure 48) and the total deflections (Figure 49). Based on the small magnitude of the measured differential deflection and possible experimental error, shear failure between the precast concrete and the concrete in the CMP was not detected.

As shown in Figure 49, the total deflection was linear before the cracking moment was reached. The deflection continued to increase essentially linearly up to an applied load of 340 kip, when the deflection behavior changed. After 340 kip, deflections increased rapidly under a small change in applied load, most likely due to yielding of the tension reinforcement in the specimen. In comparison, the stiffness of the uncracked specimen was approximately 3830 kip/inch, while at failure the stiffness was approximately 400 kip/inch. Based on the criteria that failure occurs when the specimen stiffness decreases by 50% or more, ASC3 failed at the applied load of 384 kip. The specimen failed in flexure, not due to

punching shear at the pile connection, which was expected. However, since the specimen was a deep beam, the total deflection was caused by a combination of flexure and shear.

Each pile in the actual abutments was designed by the Iowa DOT to support an unfactored service load of 80 kip. Test specimens were loaded to at least four and a half times this magnitude before flexural-shear failure in the precast concrete occurred. The maximum applied load, the load to produce the cracking moment, and the experimental cracking moment for the centered, single-pile abutment tests are presented in Table 11.

As can be seen, laboratory testing for the centered, single pile abutment test show that the actual strength of the section is at least four and a half times the required strength of 80 kip. The minimum cracking moment for the centered, single pile specimens was reached at 250 kip-feet, or a pile load of approximately 120 kip; the average calculated cracking moment was 280 kip-feet, or when an average load of 135 kip was applied.

Table 11. Test results for centered-pile abutment tests.

Specimen	Maximum Applied Load (kip)	Applied Load at Cracking Moment (kip)	Experimental Cracking Moment (kip-feet)
ASC1	360	120	250
ASC2	396	125	260
ASC3	384	160	330

Due to the fact the laboratory specimens were simply supported and the abutments in the field are continuously supported, the loading conditions in the laboratory are more severe than actual conditions. Loading conditions (including self-weight) and moment diagrams for the laboratory specimens and the actual abutments are shown in Figure 50 and Figure 51, respectively. For comparison, the load and moment diagrams were based on a load of 80 kip and the self-weight of the abutment. As shown, the maximum moment resulting from an 80

a) load diagram **b) moment diagram**

Figure 50. Load and moment diagrams for laboratory tests.

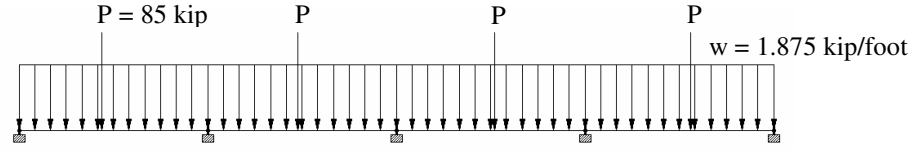

a) load diagram

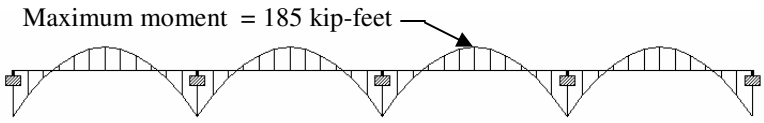

b) moment diagram

Figure 51. Load and moment diagrams for actual abutment.

kip load in the field was only eighty percent of the maximum moment induced by an 80 kip load in the laboratory. Note: moment diagrams are plotted on the compression side.

4.1.2 Offset Pile Results

Two offset, single pile abutment specimens were tested, ASO1 and ASO2. Each pile was offset approximately four inches, the maximum offset to allow the spirals to fit. Both of the specimens exhibited similar strain and deflection behavior and similar crack patterns under load. Since the offset specimens behaved in the same manner, only the results for ASO2 are presented and discussed; complete results for ASO1 are presented in Appendix I.

For the offset pile abutments, the steel strain data were analyzed first to ensure even loading; the strains in the steel pile for ASO2 are shown in Figure 52. The difference in strains was less than 100 μ-strain. As previously discussed, the difference in measured strains was due to a slight eccentricity in the axial loading applied to the pile.

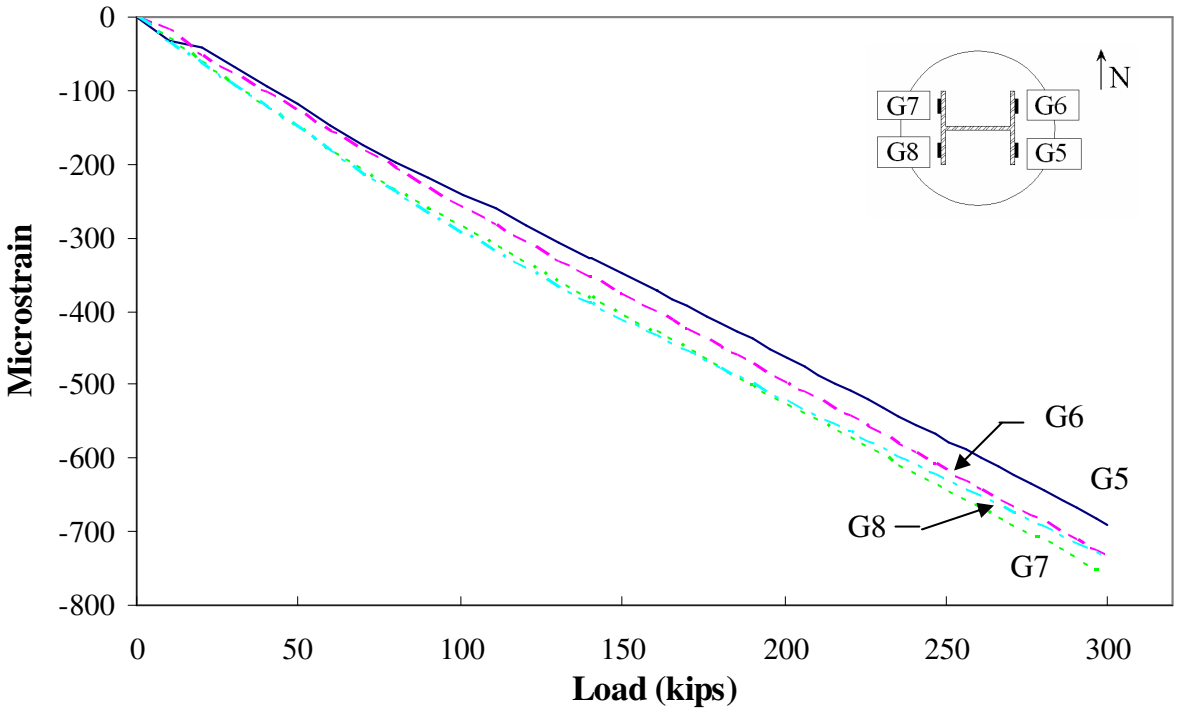

Figure 52. Steel strain for ASO2.

Hooke's Law was again used to convert concrete strains to stresses while the tensile strength of the concrete as before was assumed to be eight to ten percent of the compressive strength of the concrete. The concrete compressive strength, range of concrete tensile strength, and the calculated modulus of elasticity for each of the offset, single pile abutment tests are presented in Table 12. Concrete stresses for ASO2 are shown in Figure 53.

As can be seen in Figure 53, the stress behavior in the concrete for the offset single pile abutment is similar to the stress behavior in the centered pile specimen previously discussed. A difference in behavior can be seen between the top and the bottom of the specimen. In specimen ASO2, the cracking moment was reached at an applied load of approximately 150 kip. After the cracking moment was reached, the concrete at the top of the specimen displayed tensile stresses, the same as in the centered, single pile abutment.

Table 12. Strength properties for offset, single pile abutments.

Specimen	Concrete Compressive Strength (psi)	Concrete Tensile Strength (psi)	Modulus of Elasticity (ksi)
ASO1	4340	350-435	3995
ASO2	5685	455-570	4570

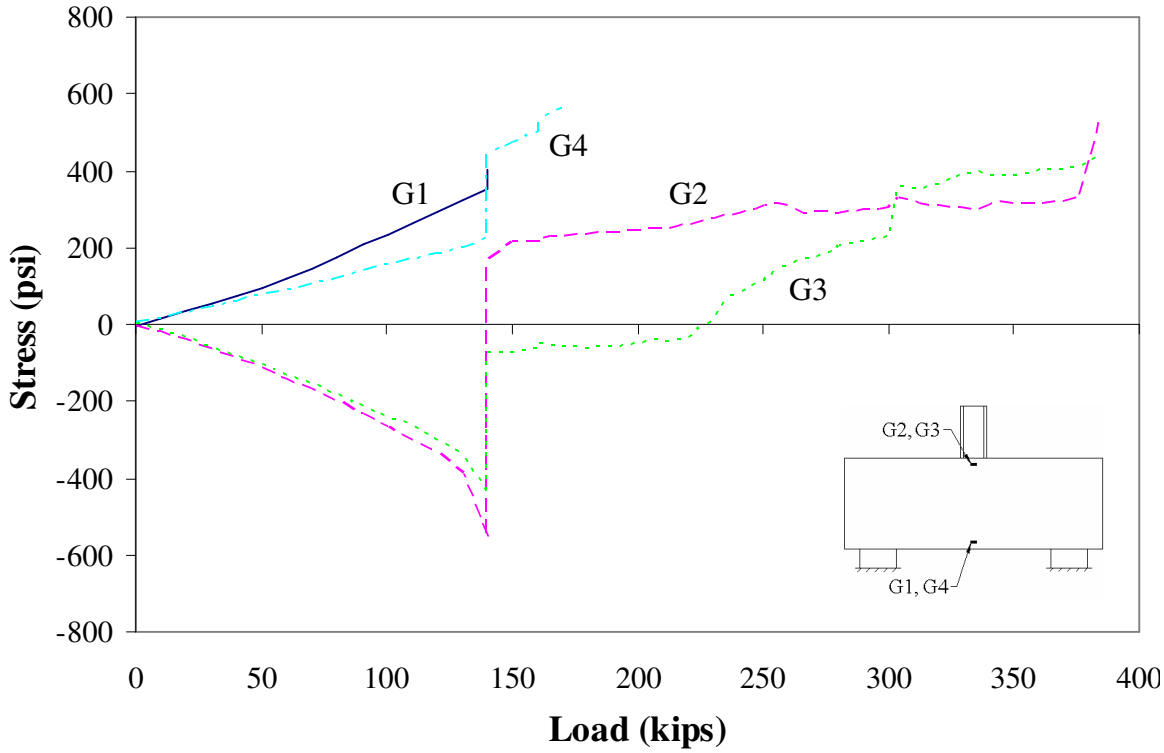

Figure 53. Concrete stresses in ASO2.

Differential movements between the precast concrete and the concrete in the CMP were measured using the top deflection transducers in ASO2 and are presented in Figure 54. The maximum differential deflection measured was -0.0018 inches at the south transducer (the concrete in the CMP moved down) and slightly less at the east transducer; the north and west transducers measured less than -0.001 inches of differential movement. The total deflections were calculated using the same procedure as was used in the centered, single pile abutment deflections and are shown in Figure 55.

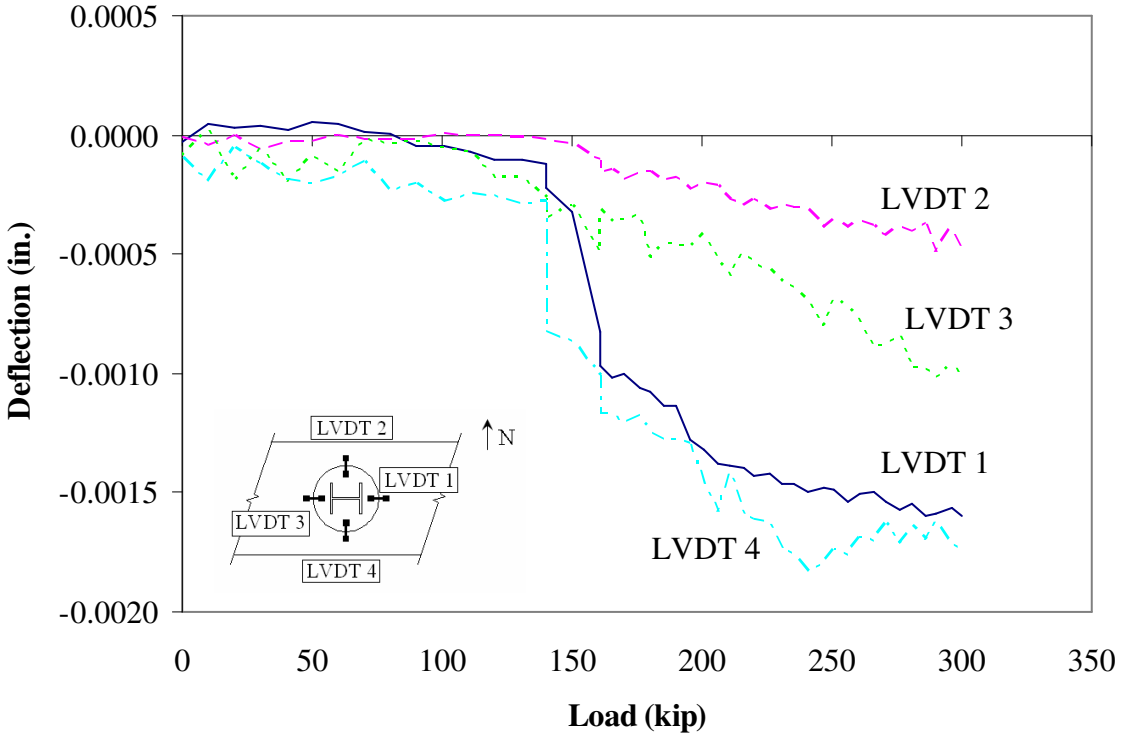

Figure 54. Differential deflection for ASO2.

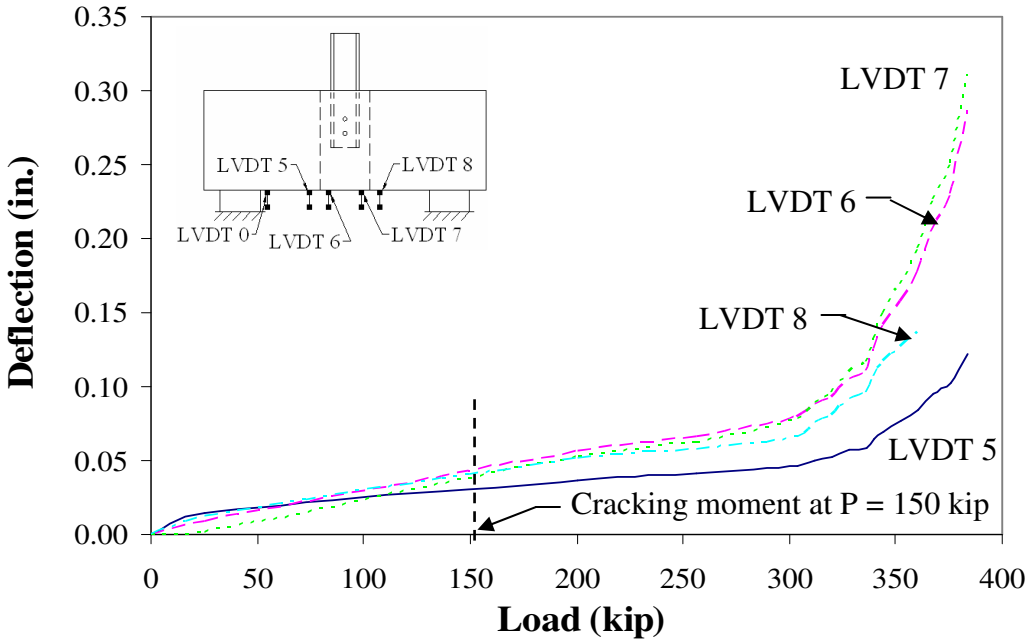

Figure 55. Total deflection for ASO2.

As shown in Figure 55, the total deflection was linear prior to the cracking moment. The linear behavior continued until the applied load approximately reached 300 kip. After

this point, the deflections increased rapidly with a slight increase in the load, similar to the deflection behavior discussed for the centered, single pile specimen. Based on the failure criteria discussed earlier, ASO2 failed at the final load of 384 kip. As with the centered pile specimen, total deflection was due to a combination of flexure and shear.

The offset, single pile abutment specimens were designed for the same load as the centered abutment specimen. Each of the offset abutments were loaded to 4.8 times the unfactored design load without significant differential movement between the precast concrete and the concrete in the CMP. Maximum load, load to produce the cracking moment, and cracking moment determined through testing are presented in Table 13.

Table 13. Test results from offset-pile abutment tests.

Specimen	Maximum Load (kip)	Applied Load at Cracking Moment (kip)	Experimental Cracking Moment (kip-feet)
ASO1	384	160	330
ASO2	384	150	315

Stress, strain and deflection behavior for the offset abutments was very similar to the behavior of the centered, single pile abutments. Laboratory testing for the offset, single pile abutment test has shown the strength of the section is at almost five times the required unfactored design load of 80 kip. At approximately 150 kip, the cracking moment for each section was reached. No significant difference in strength or behavior of the specimen was determined due to the offset locations of the piles. As previously discussed, the loading conditions for the offset pile specimens were more severe than the loading condition on the actual abutments.

4.2 Pier Cap Test Results

In addition to the abutment testing, two single pile pier caps were tested to determine if the concrete in the CMP would fail in shear and punch through the precast section of the pier cap. Because of the surface area of the concrete-filed pipe pile, there was not the same concern for the pile punching through the concrete. The cross-section of the H-pile was 16.8 square inches, compared to the 201.1 square inch cross-section of the pipe pile.

There were two pier cap sections initially tested; however, as previously mentioned, PSC2 failed prematurely due to a localized failure at one of the supports. Failure occurred over the support, however, the pile connection did not exhibit any signs of distress or failure. Therefore, the results for PSC2 will not be presented. The results for PSC1 are presented and discussed in this section.

Strain gages were applied to the pipe pile to measure strains during loading; G5 was located on the east side of the pile and G7 was located on the west side of the pile (see Figure 45c); steel strains measured during the testing of PSC1 are shown in Figure 56. Since strain gage G7 was not working properly during the test, only the results from G5 are presented in the figure. Because results from G7 were invalid, strains were recorded from only one gage, and therefore load eccentricity could not be determined.

When compared to the steel strains measured in the abutment specimen, the pipe pile strains are significantly less. This is due to the fact that in the abutment tests, the entire applied load was transferred solely through the H-pile. In contrast, for the pier cap testing the pipe pile was filled with concrete. Load was transferred through the concrete and steel, and over a much larger surface area. The larger bearing area for the same load will produce smaller stress.

Concrete strains in the pier cap were measured at the same locations as the abutment specimen, shown in Figure 44. Hooke's Law was used to convert concrete strains into stresses. Tensile strength was approximated as eight to ten percent of the compressive strength. The compressive strength, a range of the tensile strength and modulus of elasticity are presented in Table 14 and the concrete stresses are presented in Figure 57.

As with the abutment sections, the pier cap exhibited two distinctly different stress patterns in the concrete at the top of the specimen and at the bottom of the specimen. However, there is a noticeable difference in the behavior of the pier cap compared to the abutments. As with the abutments during initial loading, the stress at the top of the concrete is in compression and the bottom of the concrete is in tension. After the cracking moment is

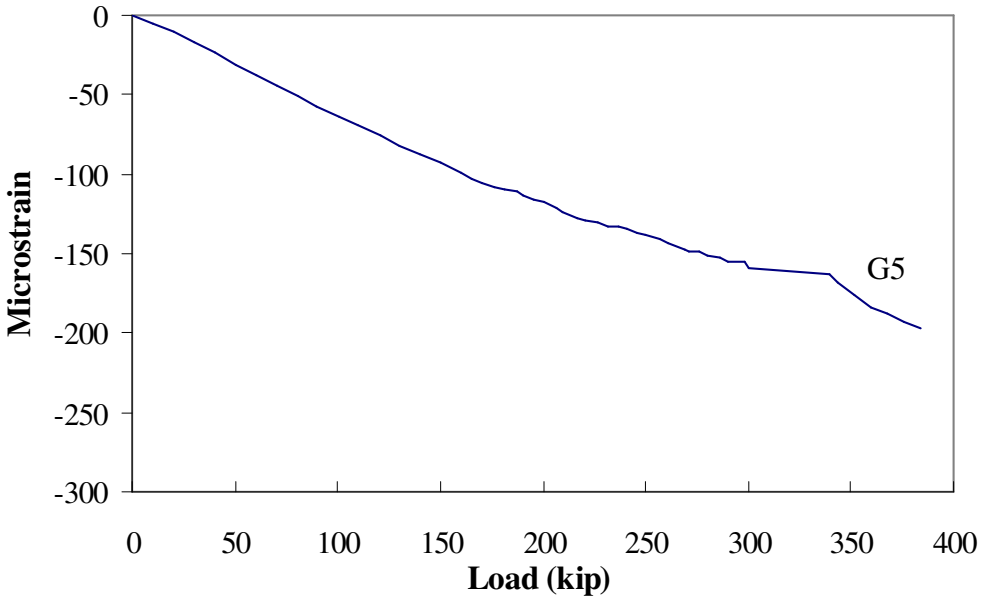

Figure 56. Steel strains for PSC1.

Table 14. Strength properties for PSC1.

Specimen	Concrete Compressive Strength (psi)	Concrete Tensile Strength (psi)	Modulus of Elasticity (ksi)
PSC1	5270	420-530	4400

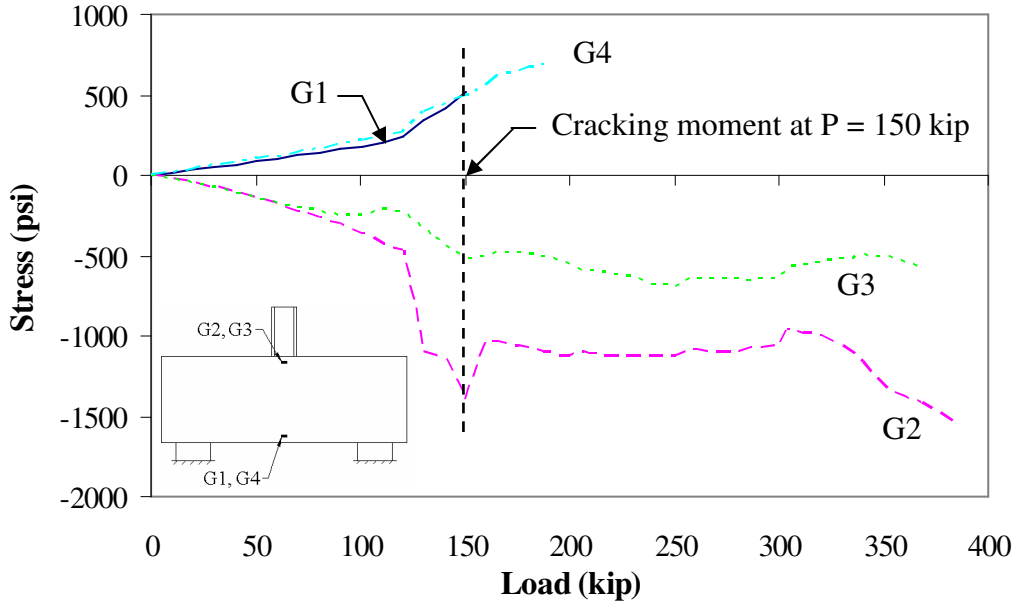

Figure 57. Concrete stresses in PSC1.

reached, the concrete at the top of the pier cap remains in compression and the concrete at the bottom remains in tension, following the expected behavior of the specimen. In comparison, the concrete at the top of the abutment specimen was subjected to tensile stresses immediately after the cracking moment was reached. This indicates the CMP and pile connection had a different effect on the behavior of the section.

During loading, the concrete in the CMP did not punch through specimen and there was no movement between the precast concrete and the concrete in the CMP that was noticeable. Deflection transducers on top of the specimen were used to measure any differential movement that may not have been visible; these differential deflections are presented in Figure 58.

The differential deflection measured in the pier cap was similar to the differential deflection measured for the abutments. A maximum deflection of -0.003 inches was measured by the west transducer and was slightly less at the north transducer; the south and

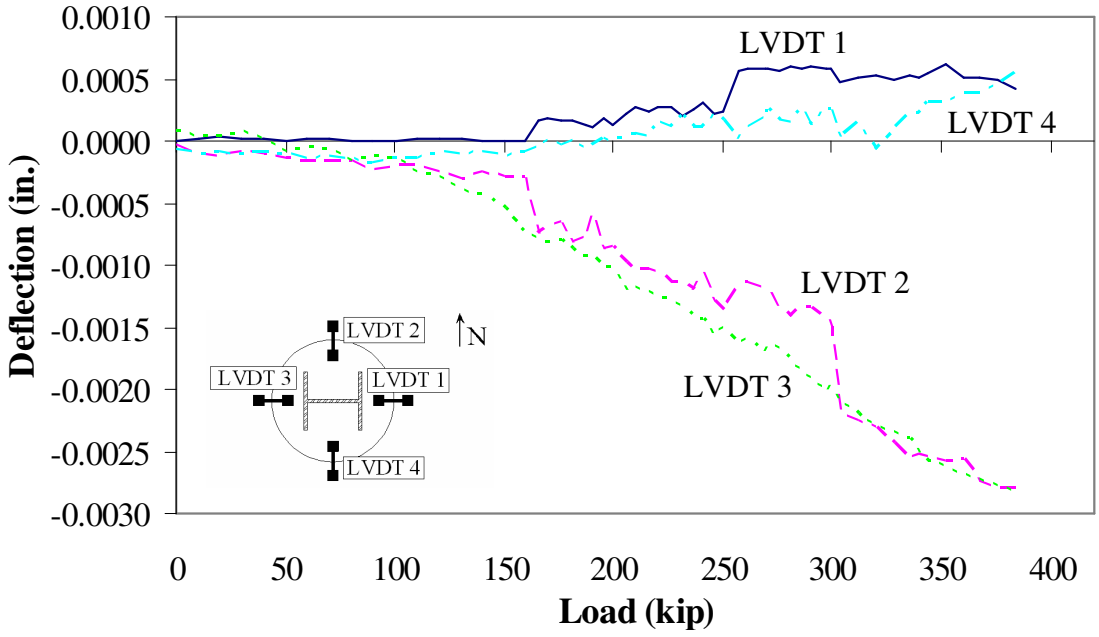

Figure 58. Differential deflection in PSC1.

east transducers measured less than 0.0005 inches of total movement, which is the LVDT precision and therefore most likely noise.

Total deflections were also measured and are presented in Figure 59. To obtain the total deflection of the specimen, the deflection of the neoprene pad was subtracted from the original deflection data taken at the center of the specimen. As Figure 58 and Figure 59 have shown, the differential movement was several orders of magnitude smaller than the total deflections measured.

As shown in Figure 59, the total deflection of PSC1 was relatively small before the cracking moment was reached. After the specimen cracked, the deflection was linear until the maximum load was applied, indicating the reinforcing bars did not yield. The difference in deflections between the abutments and the pier caps will be discussed later in this chapter.

The pier cap was designed by the Iowa DOT to support a unfactored load of 72 kip. PSC1 was loaded to 384 kip, which is close to 5.3 times the unfactored design load specified.

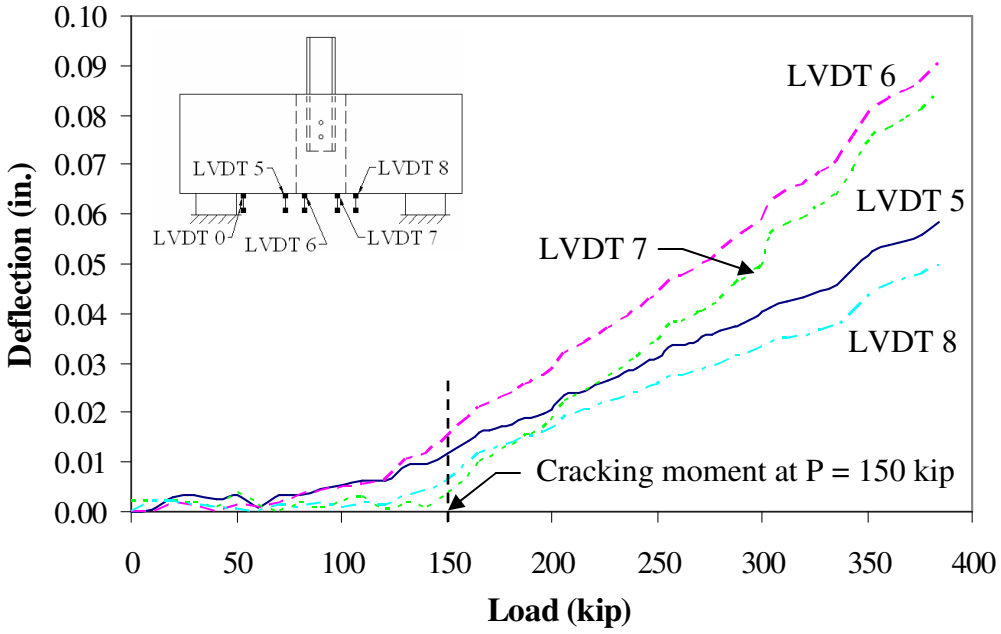

Figure 59. Total deflection in PSC1.

Under the ultimate load, no appreciable differential movement was detected between the precast concrete and the concrete in the CMP, and the reinforcement did not yield. Maximum load, the load to produce the cracking moment, and the experimental cracking moment for PSC1 are presented in Table 15.

Laboratory testing for the pier cap has shown the strength of the pier cap is over five times the required design load of 72 kip. First cracks were noticed at an applied load of approximately 150 kip, which is equivalent to a cracking moment of approximately 312 kip-feet; 2.1 times greater than the maximum load the pier cap was designed to support. As previously discussed, the loading conditions in the laboratory were more severe than the actual loading conditions.

Table 15. Pier cap test results.

Specimen	Maximum Load (kip)	Applied Load at Cracking Moment (kip)	Experimental Cracking Moment (kip-feet)
PSC1	384	150	312

4.3 Double Pile Abutment Test Results

Results from the double pile tests described in Chapter 3 are presented in this section. There were two different tests performed on the double pile specimen: combination shear and negative moment tests on the entire specimens and shear tests on t individual pile.

4.3.1 Negative Moment Test Results

Instrumentation was increased for the double pile abutment specimen, requiring a change to the labeling system previously used in the single pile tests. The labels and locations of the strain gages on the concrete are shown in Figure 60. As previously noted, the dimensions for the concrete gages varied slightly based on the quality of the surface of the concrete; those dimensions are presented in Table 6 and Table 7.

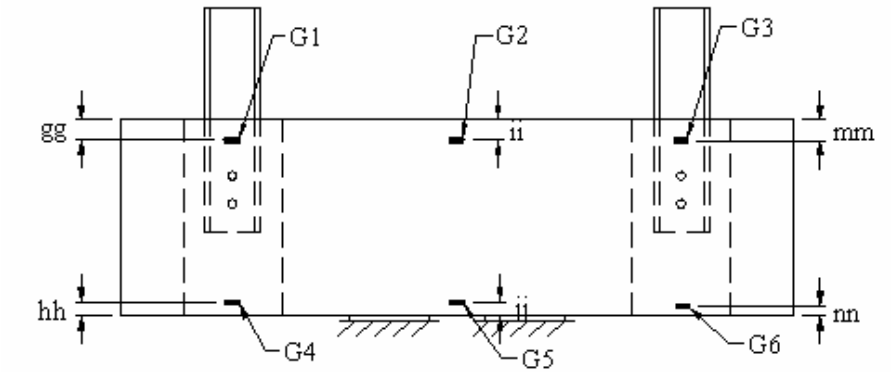

a) north face (nf) strain gage locations

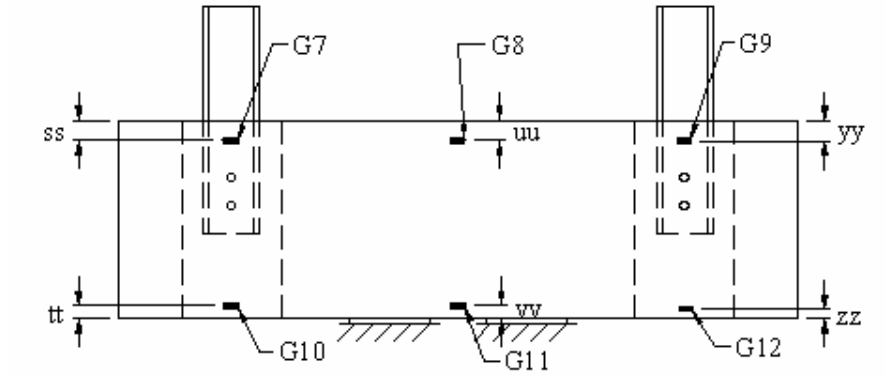

b) south face (sf) strain gage locations

Figure 60. Double pile specimen strain gage instrumentation plan.

Both piles were instrumented with strain gages, and the pile connection was instrumented with LVDTs to measure differential movement between the precast concrete and the concrete in the CMP. The labels and location of the strain gages on the H-pile and deflection transducers are shown in Figure 61 and Figure 62, respectively. Based on the testing system and support conditions, the total deflection transducers were placed on the bottom outside perimeter of the test specimens. The labels and locations of the total deflection transducers are shown in Figure 63.

The negative moment tests were performed first. Similar stress and deflection behavior, and similar crack patterns were exhibited in each specimen. For this reason, only

Figure 61. Double pile specimens: identification and location of pile strain gages.

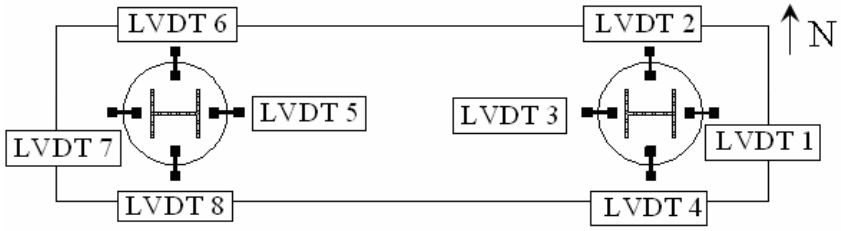

Figure 62. Double pile specimens: identification and location of top deflection transducers.

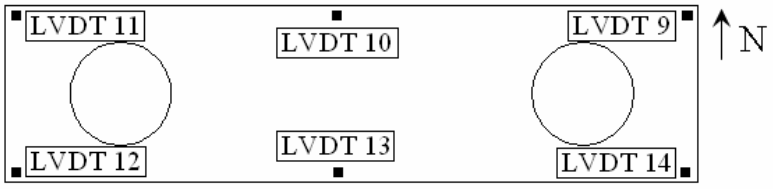

Figure 63. Double pile abutment specimens: identification and location of bottom deflection transducers.

the results from ADC1 are presented and discussed in this chapter; results for ADC2 are presented in Appendix I.

One of the difficulties encountered with the double pile test was using two different hydraulic jacks to load the piles at the same rate. The measured strains in the H-piles were analyzed first to ensure even loading between the piles and even load distribution through each pile. Results from the steel pile strain gages for ADC1 are presented in Figure 64 and Figure 65, respectively.

When compared, the magnitude of the strains in the H-piles are relatively similar. The west pile had slightly lower strains, indicating a lower load than the east pile. This agrees with the recorded loads; the east pile had a maximum load of 140 kip and the west pile had a maximum load of 138 kip. The difference in strains in each pile was also analyzed. As previously discussed, the difference in strains was caused by an eccentricity in the pile load.

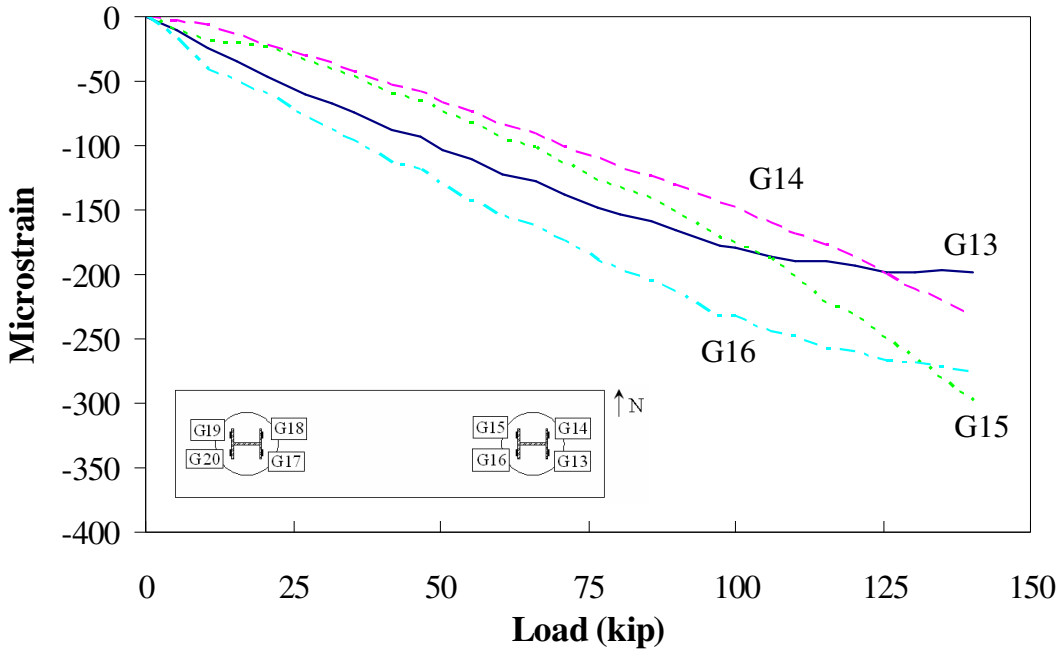

Figure 64. East pile steel strains in ADC1.

Pile load eccentricities were less than 0.9 inches, and as previously discussed, eccentricities did not correlate to concrete stress behavior. Next, strains measured at the concrete face were converted to stresses. Before the stresses were calculated, the modulus of elasticity was calculated. Concrete compressive strength, a range for the concrete tensile strength, and the calculated modulus of elasticity are presented in Table 16.

Stresses measured in the concrete were examined at three different locations: the center of the specimen, the east pile connection, and the west pile connection. Since both piles were loaded simultaneously, the maximum moment in the abutment occurred between the supports at the center of the specimen; obviously the maximum stresses occurred at this location as well. Concrete stresses at the center of the specimen are shown in Figure 66.

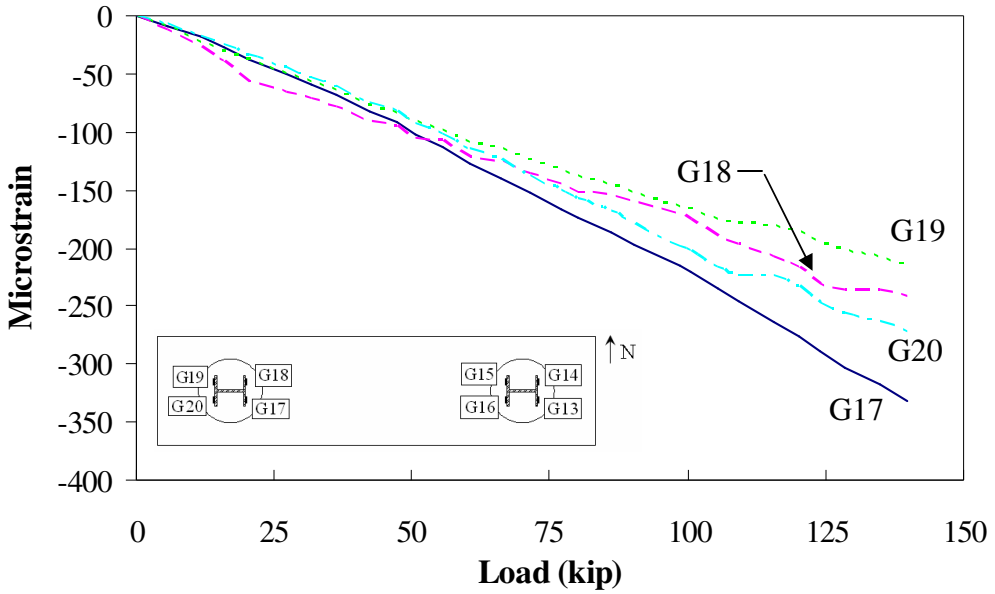

Figure 65. West pile steel strain in ADC1.

Table 16. Strength properties for double pile abutment tests.

Specimen	Concrete Compressive Strength (psi)	Concrete Tensile Strength (psi)	Modulus of Elasticity (ksi)
ADC1	6490	520-650	4885
ADC2	6515	520-650	4895

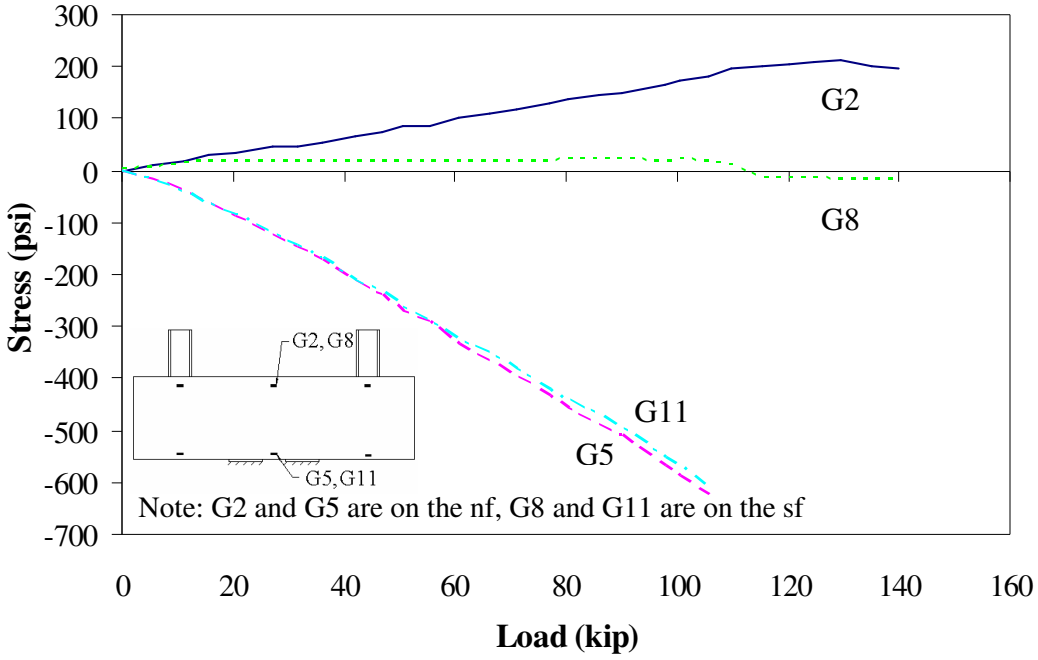

Figure 66. Concrete stresses at the center of ADC1.

As would be expected, the stress data show the concrete at the bottom of the specimen was subjected to compressive stress and the concrete at the top of the specimen was under tensile stress. However, at the center of the specimen, there was no pile connection or CMP, which was the connection and area of interest. Stresses at the east and west piles were examined next and are shown in Figure 67 and Figure 68; see Figure 60 for the strain gage locations applied to the concrete.

When comparing the stresses measured at the center of the specimen to the stresses measured at the pile locations, there is one noticeable difference. The levels of stress measured at the pile locations are at least ten times less than the stresses measured at the center of the specimen. Maximum stress measured at the pile locations was approximately 30 psi, for tension and compression. This level of stress is six percent of the tensile strength of the concrete and less than one-half of one percent of the compressive strength of the

concrete. Stress levels at the piles were small compared to the stresses at the center of the specimen and well below the tensile and compressive strengths of the concrete. This explains why no cracks or other signs of concrete distress were recorded at the pile locations, and also allowed for the additional shear tests to be performed.

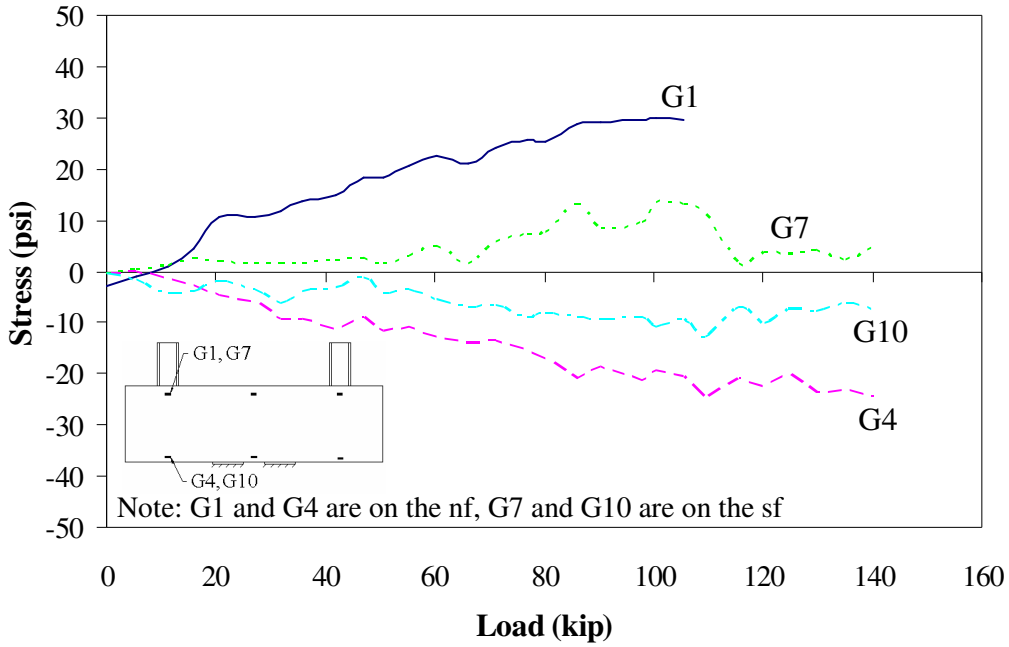

Figure 67. Concrete stresses at the east connection in ADC1.

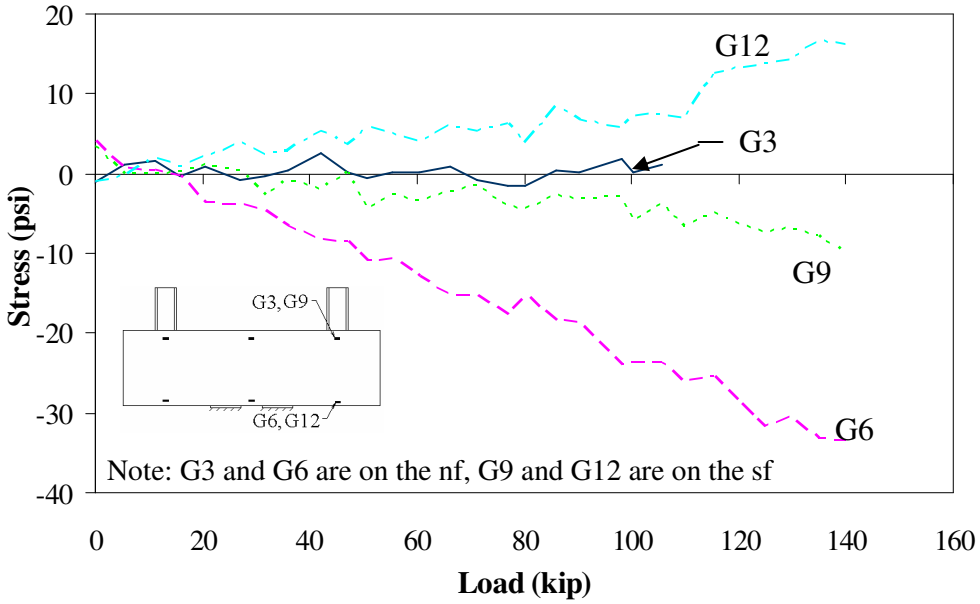

Figure 68. Concrete stresses at the west connection in ADC1.

Unlike the single pile abutments, the concrete stress behavior did not show a clear indication when the cracking moment was reached. The cracking moment for the specimens was determined using the loads that were applied and when the first cracks in the specimen were noticed during testing. For both of the double pile tests, this was when each pile was loaded to approximately 70 kip, producing a moment of 290 kip-feet.

Deflection transducers were placed near each pile to measure differential movement between the precast concrete and the concrete in the CMP (see Figure 62). Differential movements for the east and west piles are shown in Figure 69 and Figure 70, respectively. The largest movements were measured from LVDT 3 and LVDT 5, the two gages located closest to the supports. Most likely, these two gages were measuring the flexural bending of the specimen along with differential movement. Even if these transducers were measuring differential movement, the maximum deflection measured was approximately 0.001 inches. The other six gages measured less than 0.005 inches, which is the tolerance of the LVDTs and therefore most likely picking up noise.

Total deflections of the specimen were also measured and are presented in Figure 71. Total deflection measurements are as expected: at the center of the specimen the specimen deflected upward (positive deflections) and the ends of the specimen deflected downward (negative deflections). In comparison with the total deflections, the magnitude of the differential movements are very small, less than the LVDT precision in six of the transducers. As the figures have shown, the total deflection is two-hundred times greater than the differential movement.

Each pile in the double pile abutment specimens were loaded to at least 140 kip. Specimens were loaded to approximately 1.75 times the required design load of 80 kip for

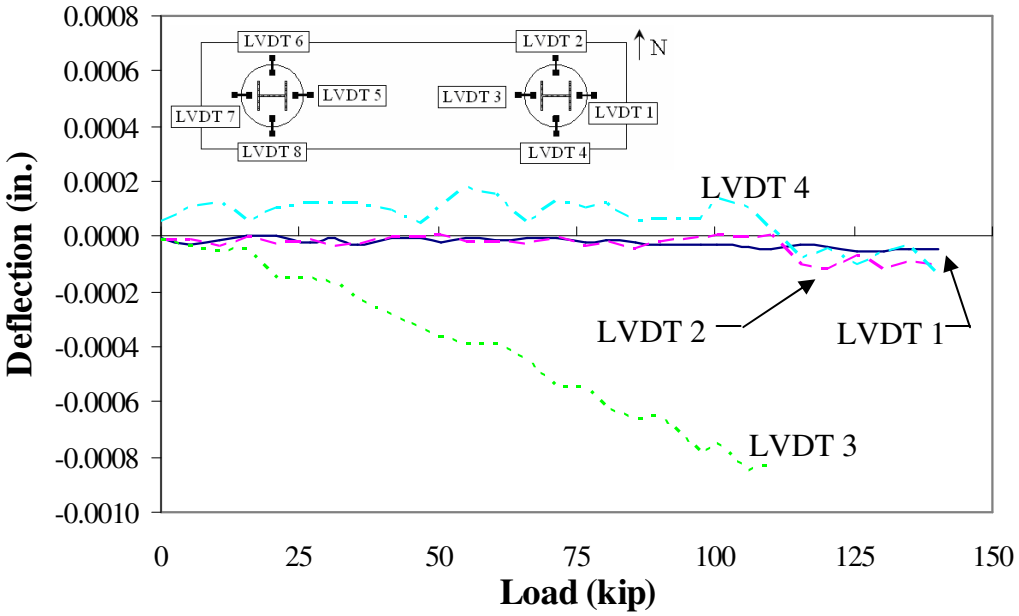

Figure 69. East pile differential deflections for ADC1.

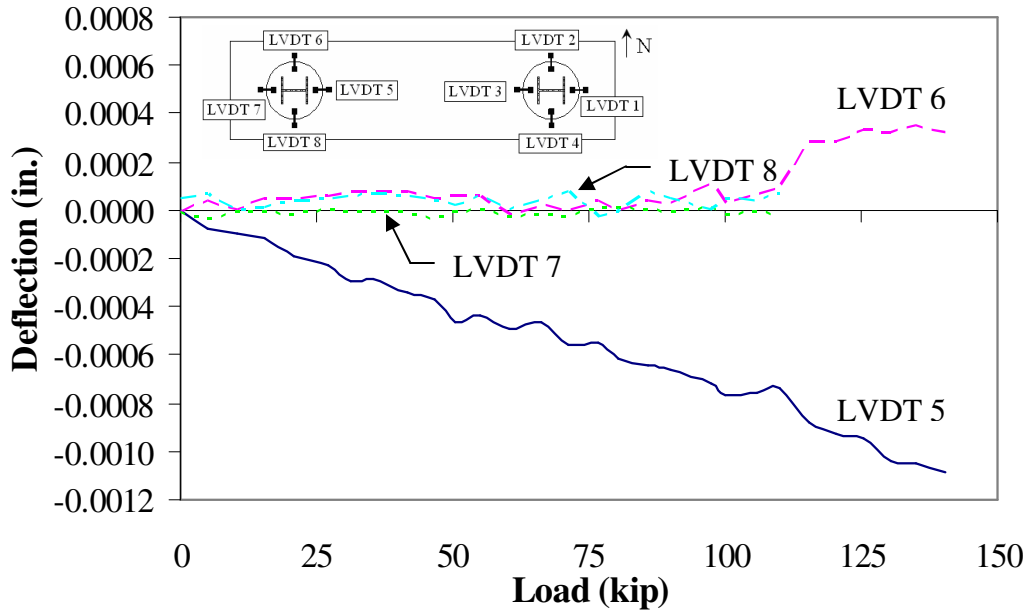

Figure 70. West pile differential deflections for ADC1.

each pile, under more severe support conditions than the abutment would be subjected to in the field. The maximum applied load, the load producing the cracking moment, and the cracking moment determined through testing are presented in Table 17.

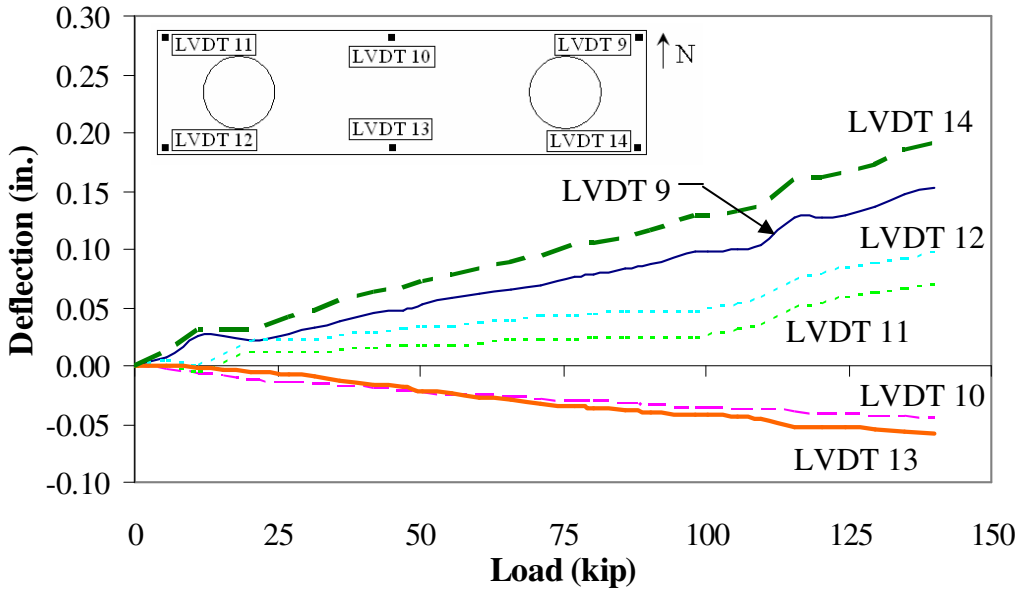

Figure 71. Total deflection of ADC1.

Table 17. Double pile abutment tests results.

Specimen	Maximum Applied Load (kip)	Applied Load at Cracking Moment (kip)	Cracking Moment (kip-feet)
ADC1	140	70	290
ADC2	150	70	290

In the double pile abutment tests, it was determined that the negative moment capacity for this loading was almost twice the design load of the abutment, under more severe conditions. The cracking moment was reached when each pile in the test was subjected to 70 kip. Note that the testing system and support conditions were not completely representative of the abutment field conditions. Also, for the double pile testing, the CMP in the specimens were only 70% full of concrete. Based on the beam spacing in the field, the abutment will never be subjected to this type of load and all of the CMPs are completely filled with concrete, so cracking under service loads should not occur.

4.3.2 Shear Test Results

After the negative moment tests were completed, no cracks were noticed near the H-piles, so each pile was tested individually. The support conditions were adjusted to provide minimal flexural bending and maximum shear in the piles and adjacent concrete. All four of the piles from the two double pile specimens were tested in this manner. In the shear tests, the same gage labeling and locations were used as were used in the single pile tests; the only difference being no bottom deflection transducers were used. Refer to Figure 44 and Figure 45 for instrumentation labels and locations.

Each pile was loaded to 400 kip - the maximum capacity of the hydraulic jack and load frame. Even at the maximum applied load, no differential movement was noticed and no cracks formed in the specimen. As previously noted, the CMP in these specimen were filled 70% with concrete, therefore, the connections in the field will have an even greater capacity since they are filled 100% with concrete. Because all the piles behaved in a similar manner, only the results from the shear Test 1 are presented and discussed in the following paragraphs; the complete results for Test 2 through Test 4 are presented in Appendix I.

Steel pile strains were first analyzed; strains for Test 1 are relatively linear as can be seen in Figure 72. There was a slight anomaly that occurred around 300 kip in two gages, which was likely due to unloading and reloading required since the load cell only had a capacity of 300 kip. Shortly after the load was reapplied, the strains stabilized and continued with the previous trend. There was a slight difference in the strains measured; the greatest difference was less than 150 μ-strain between gages G5 and G6. This was due to an eccentricity in the pile load, which has been previously discussed.

The strain gages on the concrete used in the double pile testing were reused for the shear testing. Strain data were converted into stresses using Hooke's law; ADC1 strength parameters and modulus of elasticity were used for shear Tests 1 and 2 and ADC2 strength parameters and modulus of elasticity were used for shear Tests 3 and 4. Concrete stresses occurring in shear Test 1 are shown in Figure 73.

Concrete located at the top of the specimen experienced low levels of compressive stresses - less than one-tenth of the compressive strength of the concrete. At the bottom of the specimen, the concrete was subjected to tensile stresses less than the tensile strength of the concrete (650 psi), thus the concrete did not crack. This is consistent with the fact no cracks were observed during the shear test in any of the connections. Even though no visible sign of differential movement were noticed during testing, the differential movements measured by the top deflection transducers, presented in Figure 74, were analyzed.

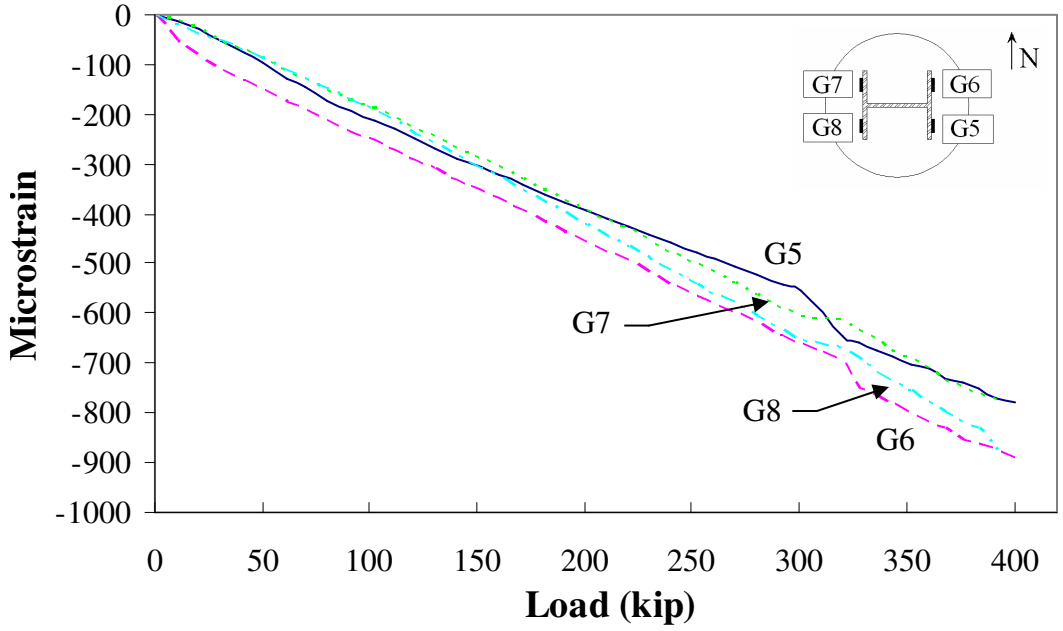

Figure 72. H-pile steel strains for Test 1, specimen ADC1.

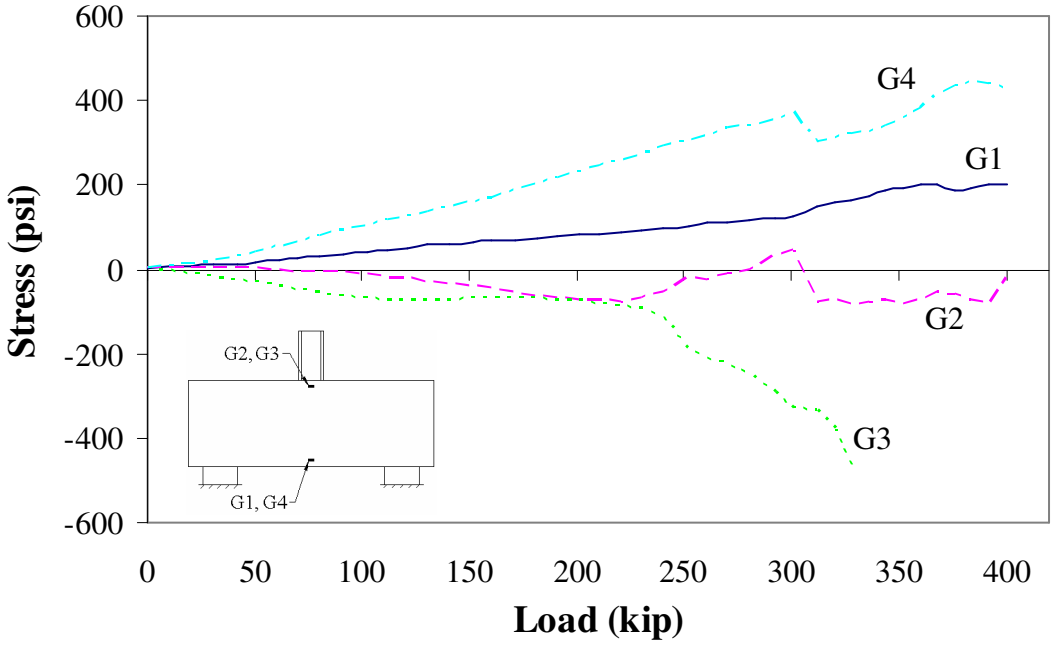

Figure 73. Concrete stresses for Test 1, specimen ADC1.

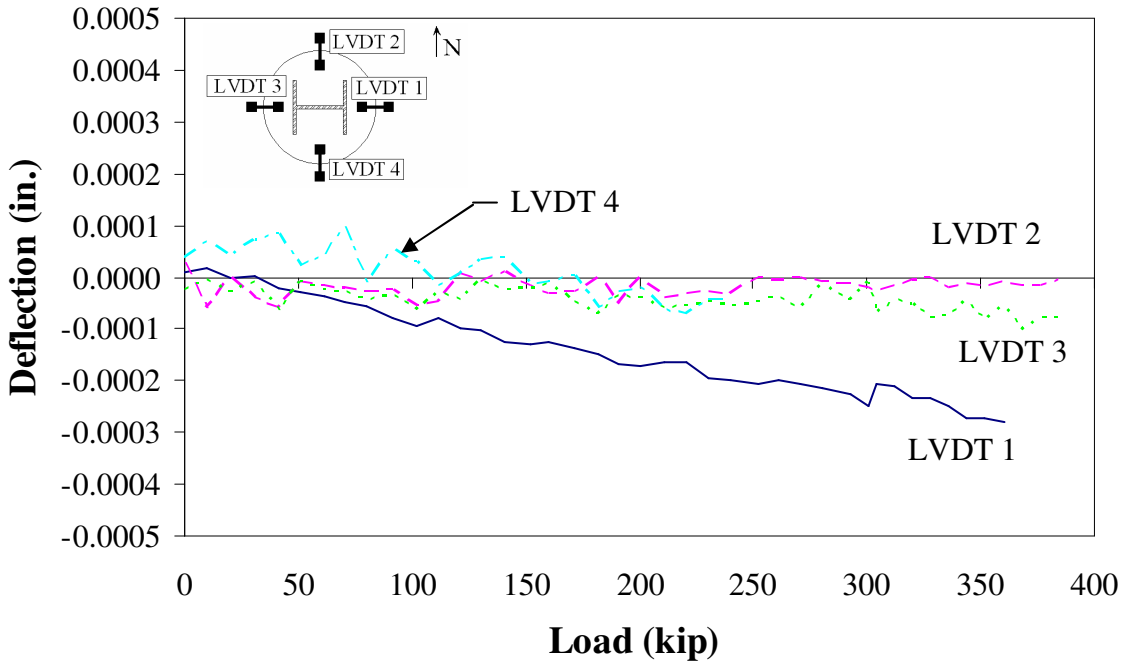

Figure 74. Top deflection for Shear Test 1, specimen ADC1.

Differential deflections measured during Test 1 were less than 0.0003 inches for all transducers, which were less than the precision of the LVDT (0.0005 inches). Since the differential deflections measured were less than the transducer precision, the measurements

were likely noise. Based on the low concrete stresses, the absence of cracks in the specimen, and the insignificant amount of differential movement, the shear capacity of the pile connection (filled only 70% with concrete) can safely be assumed greater than the maximum load of 400 kip. Under loads in the field, shear failure between the pile and the concrete, or shear failure between the precast concrete and the concrete in the CMP should not occur.

4.4 Abutment and Pier Cap Section Behavior Analysis

Substructure testing was successful in determining that shear failures would not be an issue for the actual abutments or pier caps. The piles in the abutments were designed to support a load of 80 kip each and the piles in the pier caps were designed to support a load of 72 kip each. All of the test specimen were load to at least 4.5 times the unfactored design load. The maximum load applied in the single pile tests are presented in Table 18.

While the pier cap specimen and the abutment specimens were loaded to approximately the same load, the stresses in the concrete and the crack patterns in the tested specimens indicate different behaviors. The crack pattern for ASC3 is shown in Figure 75 while the crack pattern for the PSC1 is presented in Figure 76. Note the cracks were scaled off the actual specimens using a three inch by three inch grid; thus the crack patterns shown are to scale.

Table 18. Maximum load for single pile tests.

Specimen	Maximum Load (kip)
ASC1	360
ASC2	396
ASC3	384
ASO1	384
ASO2	384
PSC1	384

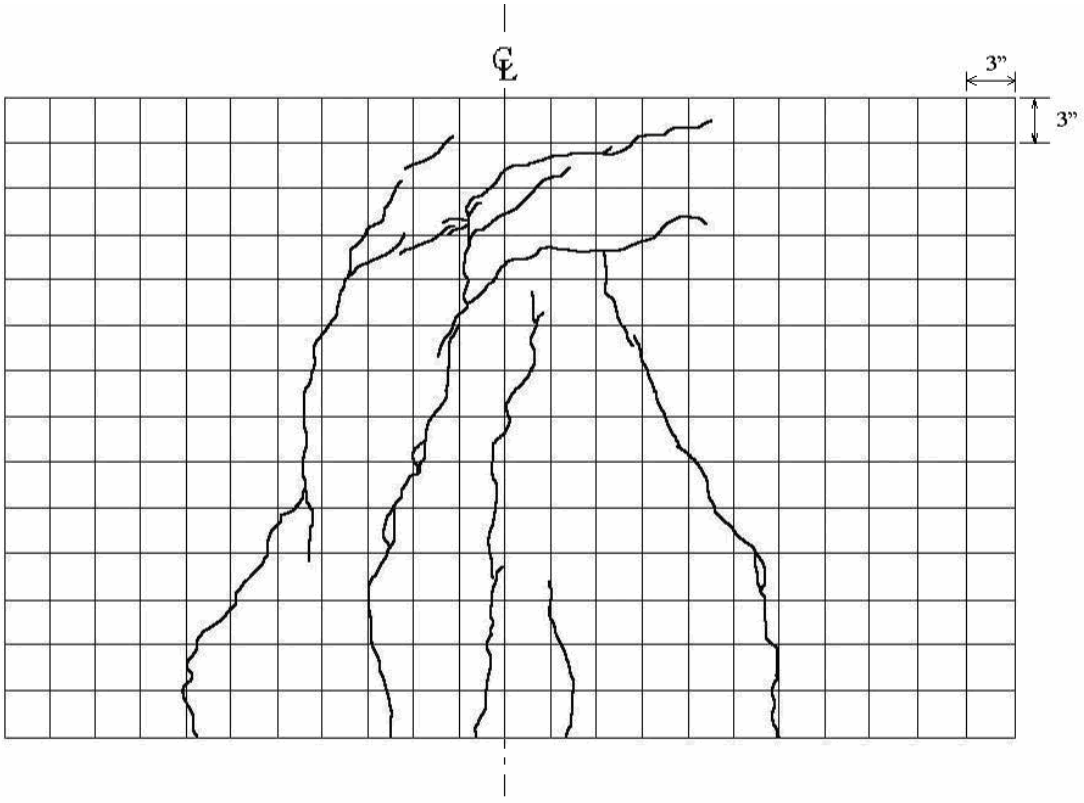

Figure 75. ASC3 crack pattern, north face.

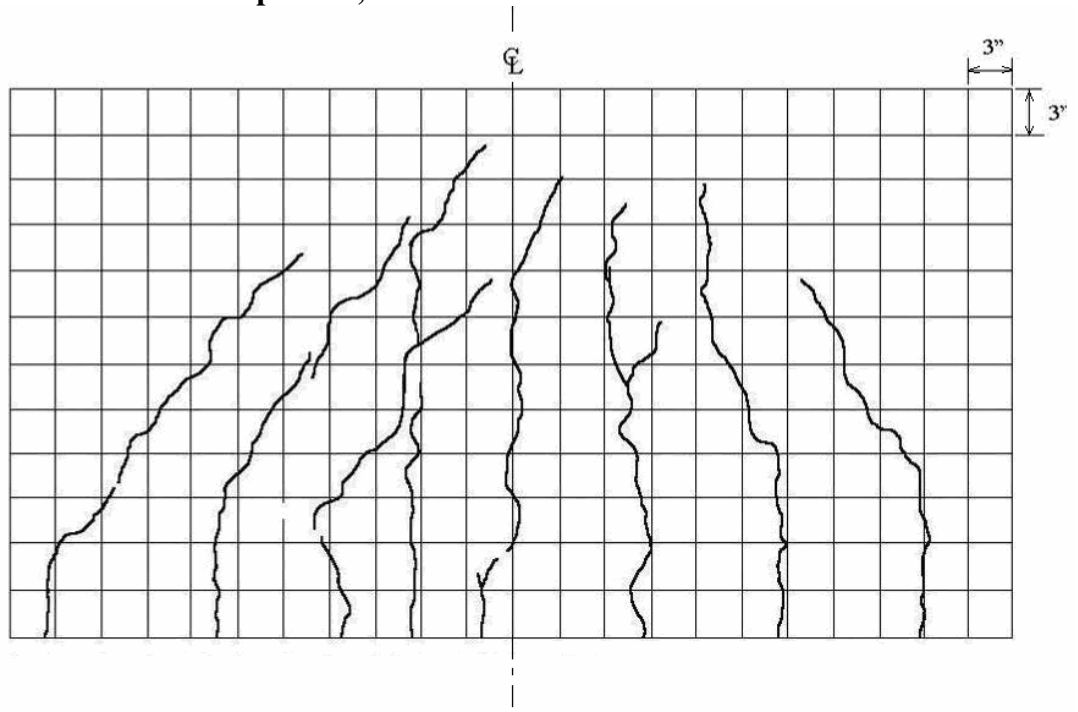

Figure 76. PSC1 crack pattern, north face.

When comparing the two crack patterns, one sees two main differences in the way each specimen cracked under load. Cracks in the abutment (shown in Figure 75) started as flexural cracks, but as the cracks progresses to the top twelve inches of the concrete, the cracks changes direction. Instead of pure flexural cracks, the cracks become almost horizontal, and appear to follow the same slope as the CMP cast in the concrete. The angle of incline of the CMP was measured to be approximately twenty-five degrees; the abutment crack pattern is compared to the angle of incline of the CMP in Figure 77.

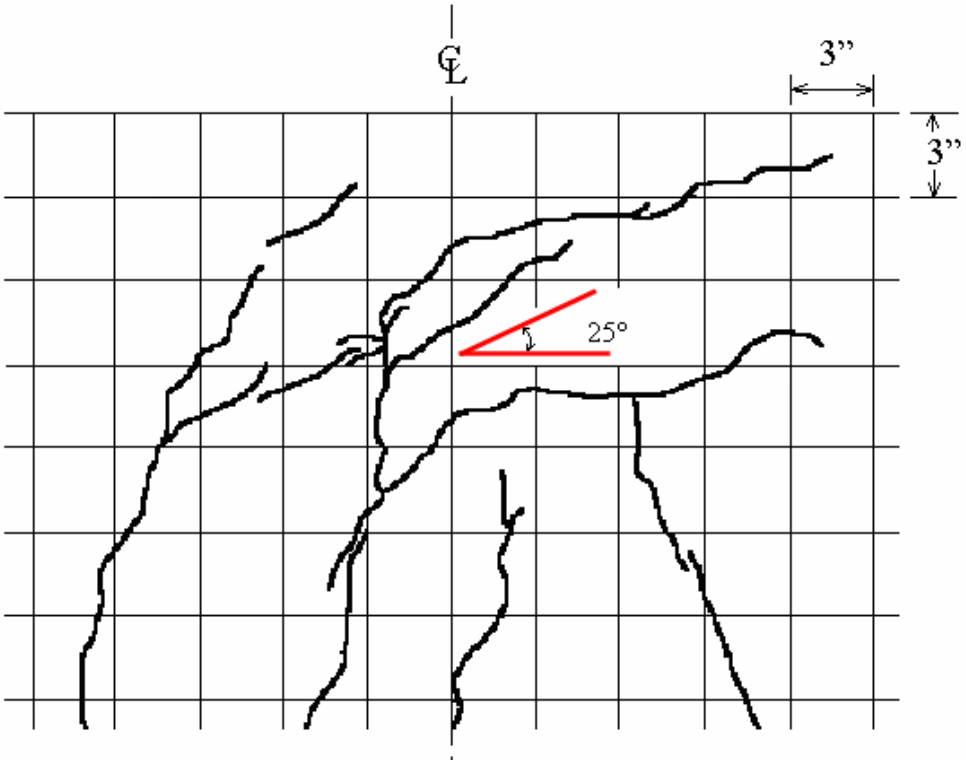

Figure 77. Abutment crack pattern compared with the CMP angle of incline.

The presence of the angled cracks indicate that the specimen was reacting to more than pure flexural bending. Strains measured in all of the abutment specimens reinforce this observation. After the cracking moment was reached, the external concrete at the top of the specimen was subject to tensile stresses, as shown in Figure 47. Based on the crack patterns

and the stress data from all of the abutments, the presence of the CMP caused localized tensile stresses in the concrete at the top of the specimen.

In the pier cap, there are no cracks that followed this angled behavior. The pier cap crack pattern reflects flexural bending, which agrees with the stresses measured in the concrete. As shown in Figure 57, the concrete at the top of the specimen was subjected to compressive stresses while the concrete at the bottom of the specimen was subjected to compressive stresses, which correlate with flexural bending.

The abutment specimens and pier caps were close in size and were loaded to approximately the same maximum load. To determine the reason for the differences in the behaviors of the abutment and pier cap, the reinforcement used in each specimen (shown in Figure 78) was compared.

As shown in Figure 78, the pier cap has a slightly smaller gross area of concrete (1,368 in^2 versus 1,512 in^2) than the abutment, but it has six additional No. 8 longitudinal bars. Spacing for the transverse reinforcement in the pier cap was almost half that in the abutment transverse reinforcement. To better compare the reinforcement in each section,

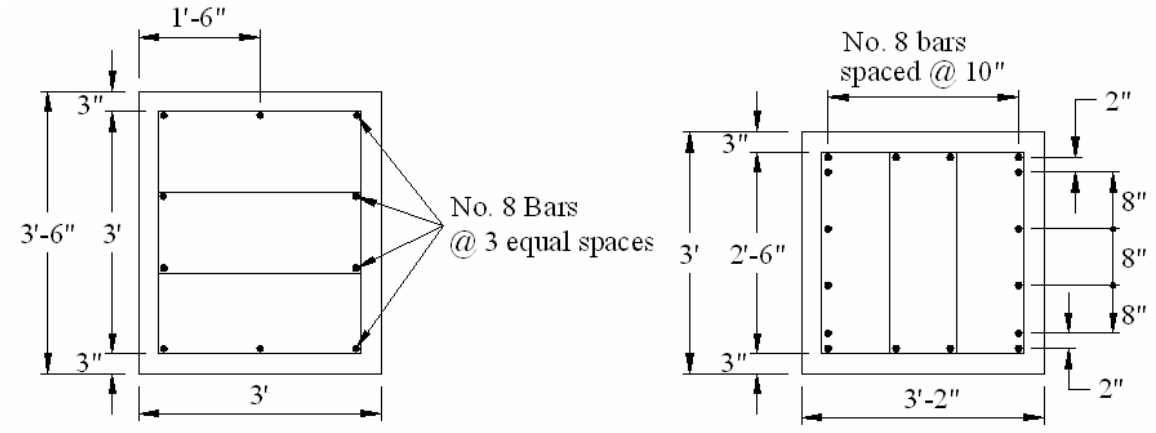

a) abutment reinforcement **b) pier cap reinforcement**

Figure 78. Comparison of the reinforcement used in the abutments and the pier caps.

the ratio of the area of longitudinal tensile reinforcing steel to the area of concrete, effective depth times the width (ρ), and the ratio of transverse steel to the area of concrete (ρ_t) were calculated using the definitions in the ACI Building Code (2005). The gross moment of inertia for each section was calculated, using a transformed section to account for the presence of the steel. All of these properties are presented in Table 19.

Table 19. Abutment and pier cap reinforcement ratios and moment of inertias.

Section	ρ	ρ_t	I_{gross} (in^4)
Abutment	0.0016	0.002	234,140
Pier Cap	0.0036	0.005	161,979

Based on percentages, the pier cap has almost twice the amount of longitudinal reinforcement as the abutment and 2.5 times the transverse reinforcement. The gross moment of inertia for the pier cap is lower than the abutment, but the contribution from the reinforcing steel is higher. As the concrete cracks, the specimen's moment of inertia decreases due to the cracking of the concrete, but the contribution from the reinforcement remains constant.

In the abutment testing, the CMP affected the behavior of the specimen as shown by the stresses measured and the crack patterns recorded. The reason the pier cap was not affected in the same manner is due to the larger area of longitudinal and transverse steel and a smaller cross-section, compared to the abutment. This also explains why the total deflection measured in the pier cap specimen was less than the total deflections measured in the abutment specimens. The behavior of the abutment was affected by the CMP connection, but in comparison to the pier caps, the combination of flexural and shear capacity of the specimen was not reduced.

4.5 Laboratory Testing Summary

4.5.1 Abutment Testing Summary

The single and double pile abutment tests have shown that there is no concern for a shear failure between the H-pile and the concrete, or between the precast concrete and the concrete in the CMP. For the single pile tests, the piles were loaded to at least 4.5 times the unfactored design load. For the double pile tests, which produced a more severe loading condition than actual field conditions, the specimens were loaded to approximately twice the unfactored design load. Shear failure was not detected in any of the tests; shear testing has shown the shear capacity of the pile and CMP connection to be greater than 400 kip.

Abutment testing has shown that even though the strength of the abutments was not compromised, the pile connection in the CMP did affect the stress behavior of the section. The presence of the CMP caused localized tensile stresses on the side of the abutment. The experimental cracking moment determined by the single pile tests was in agreement with the experimental cracking moment determined by the double pile tests. Since the cross-section is symmetrical, the cracking moment for positive bending and negative bending were approximately the same. Experimental cracking moments for each of the abutment tests are presented in Table 20.

The cracking moment in a concrete section is dependent on the concrete strength at the time of testing. Based on an average concrete strength of 5450 psi, the average cracking moment in the abutment specimens was 295 kip-feet (an average single pile load of 142 kip with a clear distance of eight feet, four inches), which is much greater than the expected loads for the actual bridge abutments. The possibility of the abutments experiencing loads of this magnitude in the field is very small.

Table 20. Cracking moments for abutment specimens.

Specimen	Cracking Moment (kip-feet)
ASC1	250
ASC2	260
ASO1	330
ASC3	330
ASO2	315
ADC1	290
ASC2	290

4.5.2 Pier Cap Testing Summary

Results from the pier cap tests have shown that the pier cap has approximately the same capacity as the abutment, even though the piles in the abutment are designed for an unfactored service load of 80 kip each and the piles in the pier cap are designed for an unfactored service load of 72 kip each. The pier cap specimen was subjected to a maximum load of 384 kip, more than five times the design load. During testing, no significant differential movement was detected between the precast concrete and the concrete in the CMP. The cracking moment was determined to be 312 kip-feet for the pier cap tested. Based on the tests performed, shear failure between the precast concrete and the concrete in the CMP is not a concern.

CHAPTER 5. POST-TENSIONING TESTING AND VERIFICATION

5.1 Post-Tensioning Field Testing

The Boone County replacement bridge was the first post-tensioned bridge deck in the state of Iowa. One of the tasks in the proposed research included monitoring the post-tensioning process and verifying the forces in the strands reported by the contractor. Instrumentation was embedded in four deck panels and attached to four post-tensioning strands to monitor and verify the post-tensioning process, and to allow long-term monitoring of the deck. The instrumentation will also be used in the field service test associated with the project (not included in this report). This chapter presents the instrumentation layout, the post-tensioning monitoring process and the results obtained from the instrumentation.

Post-tensioning took place after all the interior and exterior deck panels were installed, leveled, and the transverse joints between panels were cast and had reached strength. The bridge was post-tensioned using a hydraulic, mono-strand jack system. Friction losses in the strands were essentially non-existent due to the strand layout and an average strand length of 144 feet and 9 inches. This allowed the entire post-tensioning operation to be performed from the west end of the bridge. Greg Gear P.E., a technical expert from Des Moines, was hired by the prime contractor to supervise the post-tensioning operation. Mr. Gear certified the jack calibrations prior to post-tensioning, and certified that the final forces in the strands met the limits set by the Iowa DOT after post-tensioning was complete; the certification from Mr. Gear is included in Appendix II.

The strand used was 0.6 inch diameter, 270 ksi post-tensioning strand with an area of 0.217 square inches. The bridge plans required each strand be tensioned to 41 kip; since

there were 12 strands in each of the post-tensioning channels, this resulted in 984 kips of post-tensioning in each half of the bridge deck. The purpose of the post-tensioning testing was to verify the force in the strands as reported by the contractor, to measure losses between initial stressing and after the strands had been stressed, and to determine how the force in the strands was distributed through the deck panels.

Before the deck panels were cast, a total of twelve vibrating wire gages (VWG) were embedded in four of the deck panels so that strains in each of the panels could be measured during the post-tensioning operation. The strain data were then converted to deck panel stresses using Hooke's law. Location of the instrumented panels (Panels A, B, C, and D) and the number of gages in each panel are shown in Figure 79.

The instrumentation was concentrated around the southern-most post-tensioning channel. Gage identification and location is presented in Figure 80; the number of gages in each deck panel varied with the location of the panel. To simplify the comparison of the deck results, the numbering system for the deck panel gages was kept consistent between the panels. For example, gages A1, B1, C1and D1 were all located at Position 1. Number and location of the gages embedded in each of the four panels are presented in Table 21; the gage number corresponds to the positions shown in Figure 80.

The lead wires for the gages were threaded through the panel formwork and secured in the post-tensioning channel during casting and transportation of the panels. This allowed access to the wires from the deck for testing. Two of the VWGs attached to the panel reinforcement are shown in Figure 81 before the panel was cast. The gage lead wires can also be seen threaded through the formwork and secured in a channel in this figure as well.

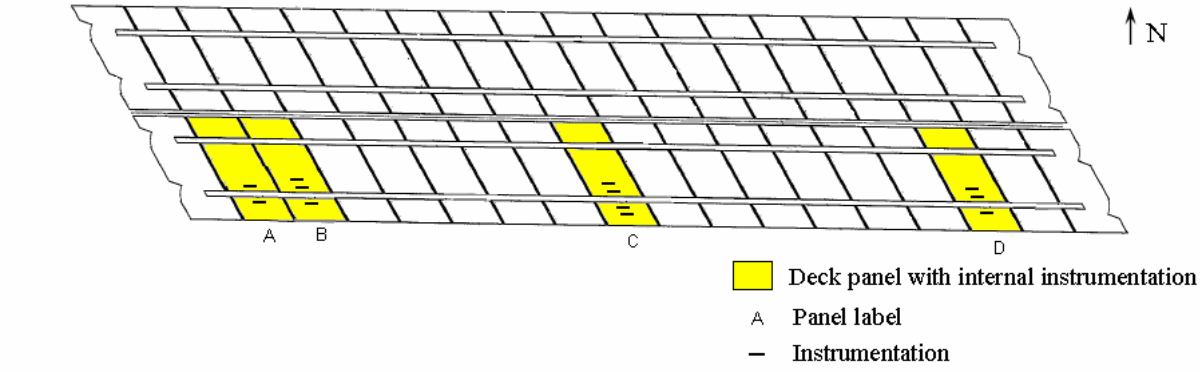

Figure 79. Location of instrumented panels.

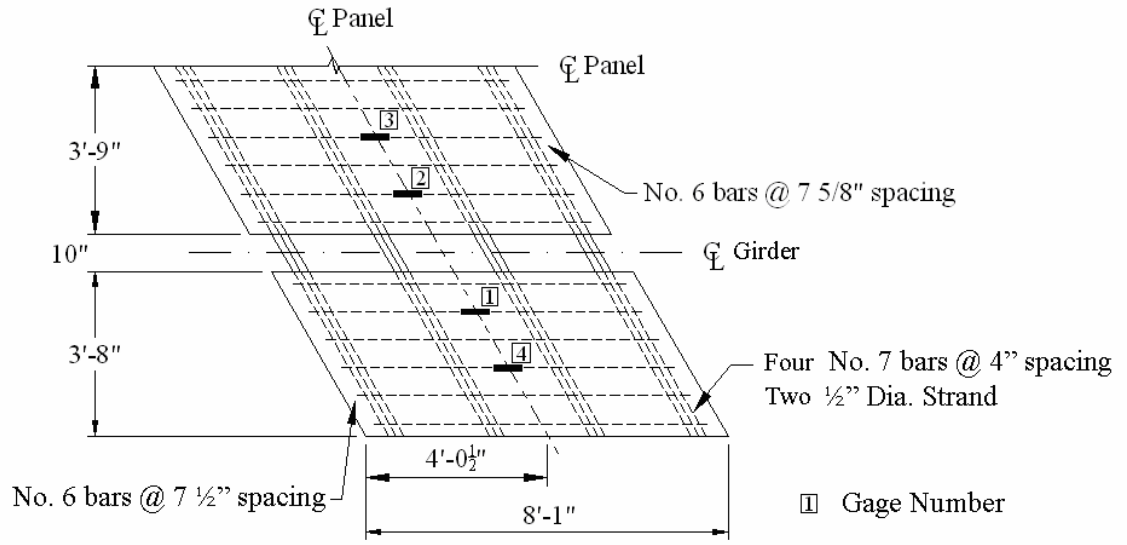

Figure 80. Deck panel internal instrumentation.

Table 21. Number of gages and locations in each deck panel.

Deck Panel	Number of Gages	Gage Location
A	2	A1, A2
B	3	B1, B2, B3
C	4	C1, C2, C3, C4
D	3	D1, D2, D3

As shown in Figure 82, seven VWGs were used on the post-tensioning strand. Gages (No. 3, 5, 6, and 7) were placed on the top center strand in each of the post-tensioning channels at the center of the bridge, approximately three and one half inches below the

surface of the deck panel. Three additional gages (No. 1, 2, and 4) were placed along the strand previously instrumented in Channel 1. A VWG was placed one foot from the exterior edge of the first interior panel at both ends of the bridge. Another VWG was placed directly over the west pier, closest to the 'live' end of the jacking operation.

As previously noted, the gages were placed on the top interior strand in the channels; this was done to allow sufficient room for protection of the four gages to be embedded in the channels after post-tensioning and to allow for easy access for installation and removal of the gages. The strands instrumented were the first strand in each channel to be post-tensioned, according to the stressing sequence submitted by the contractor; the post-tensioning sequence

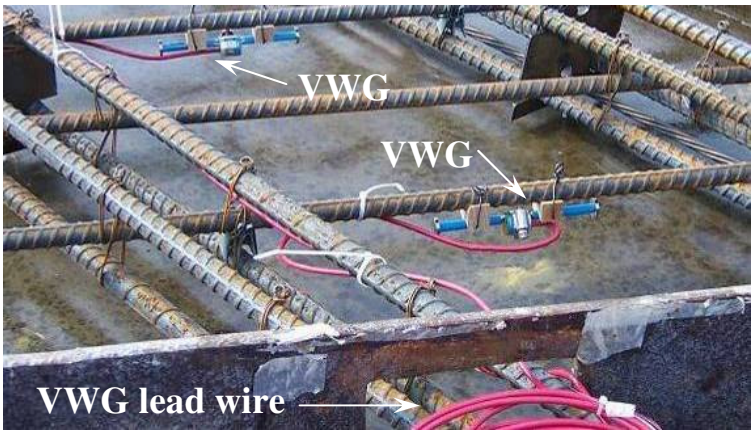

Figure 81. Deck panel vibrating wire gages.

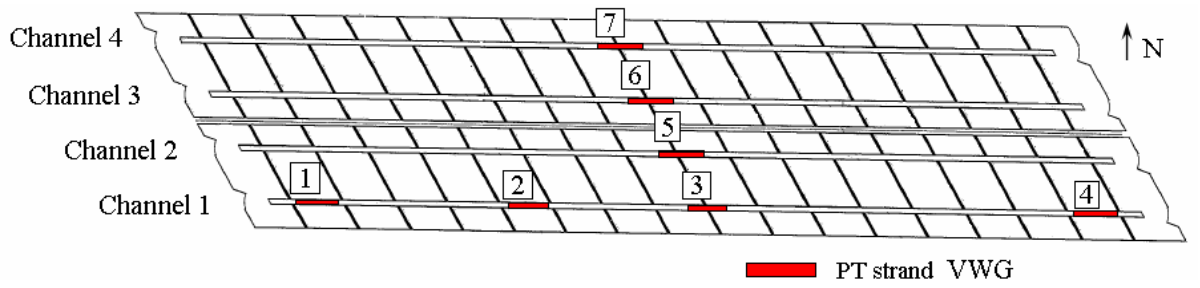

Figure 82. Post-tensioning VBG locations.

for the south half of the bridge deck is presented in Figure 83. Instrumenting the initial strand stressed provides post-tensioning loss data throughout the entire stressing sequence.

The south half of the bridge (Channel 1 and Channel 2), which contained the majority of the panel and strand instrumentation, was stressed first. Since a single jack was used for all of the stressing, the contractor had to alternate between channels while post-tensioning (i.e. T1 and T2 in Channel 1, T3 through T6 in Channel 2, etc.). One of the VWGs attached to the post-tensioning strand is shown in Figure 84.

The entire post-tensioning process took approximately four hours. The mono-strand jack used for post-tensioning can be seen in Figure 85. The two halves of the bridge, which were post-tensioned separately, acted independently since the longitudinal joint connecting

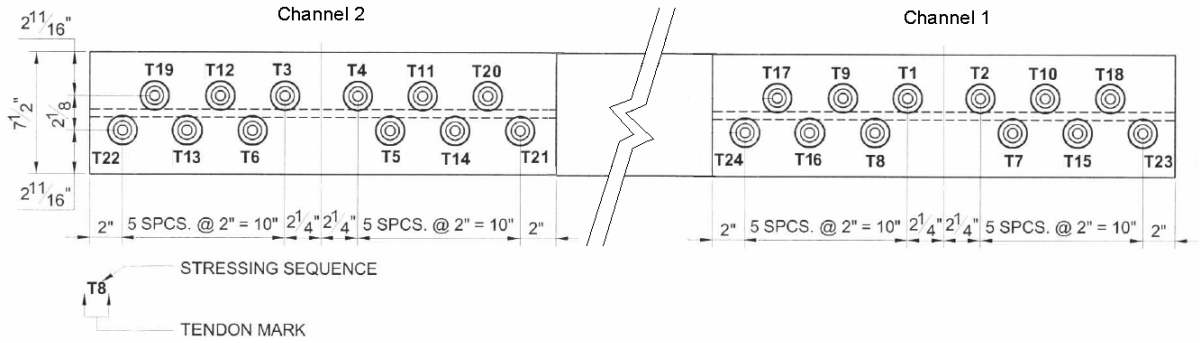

Figure 83. Post-tensioning stressing sequence (looking east).

Figure 84. PT strand vibrating wire gage.

the two halves was not cast until the post-tensioning was completed. The initial gage readings for the deck and tendon gages were recorded before the post-tensioning operation started.

The stressing sequence was not followed exactly on the south half of the bridge due to an obstruction in one of the channels. After sixteen of the twenty-four strands were stressed, it was noticed that the concrete at one of the transverse joints (see Figure 86) was projecting into the post-tensioning channel and was creating a friction point for two strands. The stressing sequence on that half of the bridge was stopped and the obstruction was

a) Mono-strand jack and hydraulic pump

b) Mono-strand jack in use

Figure 85. Mono-strand jack used for post-tensioning.

Figure 86. Concrete obstruction in Channel 1.

removed without disturbing the strands that had been previously stressed. While the excess concrete was being removed, the north half of the bridge deck, Channels 3 and 4, was stressed in its entirety, after which the remaining strands in the south half of the bridge were stressed without incident.

The VWGs used were not capable of providing continuous data readings and had to be read using a hand-held data collector. Data were recorded while the jacking hardware was moved from one channel to the next; stressing continued after the readings were taken. Since a data acquisition system was unavailable, all of the deck panel and strand gages were connected to two switch-and-balance units to make the data reading process faster. This allowed for sufficient data collection without slowing down the jacking operation.

On the day the bridge was post-tensioned, there was concern about inclement weather, thus in order to complete the jacking operation before the weather conditions worsened, data readings were only taken eight times. Table 22 presents the eight stages of post-tensioning after which readings were taken.

Table 22. Description of post-tensioning stages.

Stage	South Half of Deck				North Half of Deck			
	Channel 1		Channel 2		Channel 3		Channel 4	
	Tendons Stressed	Force (kip)	Tendons Stressed	Force (kip)	Tendons Stressed	Force (kip)	Tendons Stressed	Force (kip)
1	2	82	0	0	0	0	0	0
2	2	82	4	164	0	0	0	0
3	6	246	8	328	0	0	0	0
4	8	328	8	328	2	82	0	0
5	8	328	8	328	2	82	4	164
6	8	328	8	328	6	246	4	164
7	8	328	8	328	12	492	12	492
8	12	492	12	492	12	492	12	492

The first reading was taken after the first two strands in Channel 1 were stressed. Next, a second set of readings was taken after the six of the tendons in the south half of the bridge were stressed; two strands in the first channel and four strand in Channel 2. A third set of readings were taken after fourteen of the strands in the south half of the bridge had been stressed. Two additional strands were stressed in Channel 1 before the previously described obstruction in the channel was noticed. As previously noted, post-tensioning was then moved to the north half of the bridge while the obstruction was removed.

While stressing the north half of the bridge, a construction error was noticed. The anchor plates shown in Figure 83 were inverted during fabrication at the precast plant in Channel 3 and Channel 4. Thus, instead of post-tensioning the top interior strands first, the bottom interior strands were initially stressed; the stressing sequence used for the north half of the bridge is shown in Figure 87.

The fourth set of readings were taken after the first two strands, which were not instrumented, in the north half of the bridge were stressed. Since the instrumented strands were not initially stressed, the VWGs in the north half of the bridge did not provide force data during this reading. However, since two non-instrumented strands were stressed, the

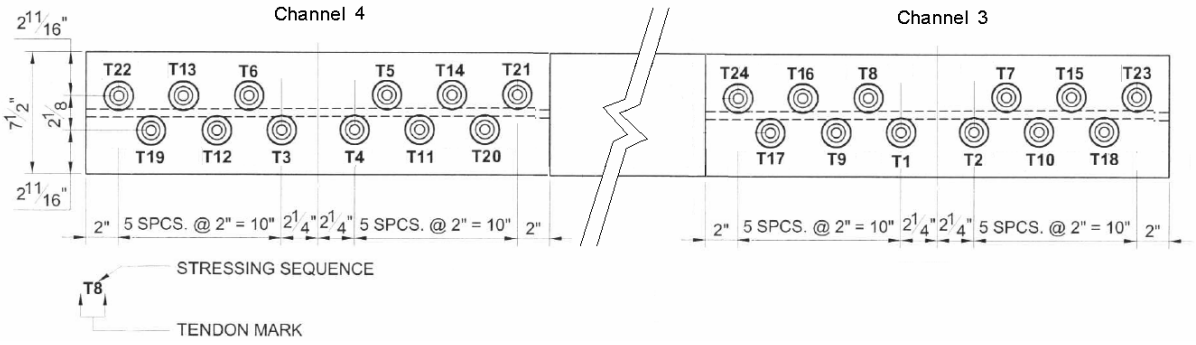

Figure 87. Post-tensioning sequence for the north half of the bridge (looking east).

effects of elastic shortening in the deck were noticeable in VWGs on the unstressed strands in the north half of the deck; these results are presented later in this chapter.

Additional readings were taken after the first six tendons, and after fourteen tendons in the north half of the bridge were stressed. Last, two sets of readings were taken: after the north half of the bridge was stressed and after the south half of the bridge was stressed, respectively. After the post-tensioning operation was complete, final readings were taken from the embedded gages to use as initial values for long-term monitoring.

The four strand gages located along the centerline (No. 3, 5, 6, and 7) of the bridge were embedded in the post-tensioning channels when the longitudinal joints were cast and the other three gages were removed. Before the channels was grouted, each of the gages that were to be embedded were protected with pre-cut PVC pipe, shown in Figure 88, that were sealed with a waterproof material and secured in place with two hose clamps.

The four embedded strand gages and the twelve internal deck panel gages will be used during the service load testing of the bridge and will make it possible for long-term monitoring of the deck system. All of the lead wires for the four gages were labeled, threaded through the formwork under the bridge deck and secured for future use.

Figure 88. Vibrating wire gage with PVC pipe cover.

5.2 Post-Tensioning Test Results

5.2.1 Post-Tensioning Strand Results

The first task of the post-tensioning testing was to verify the force measured by the contractor in each of the post-tensioning strands. According to the plans, each strands was to be stressed to 41 kip, with a tolerance of ±5 percent (± 2.05kip). For the tendon gages, all of the data was output in Digits, a unit used by the manufacturer, that can be converted into a change in length. The Digits reading is corrected for temperature effects and for the calibration of the individual gage. Data were converted from Digits to a corrected change in length using the following equation provided by the manufacturer, Geokon.

$$D_{corrected} = [(R_1 - R_0) \times C] + [(T_1 - T_0) \times K]$$

Where $D_{corrected}$ = the corrected change in length

R_1 = the current reading in Digits

R_0 = the initial reading in Digits

C = the calibration factor for each gage (provided by Geokon)

T_1 = the current temperature

T_0 = the initial temperature

K = the thermal coefficient for each gage

The thermal coefficient for each gage was determined based on the calibration factor and the current reading, using the following equation provided by the manufacturer:

$$K = [(R_1 \times 0.000295) + 1.724] \times C$$

All of the original test data, including the calibration factor for each gage, the initial and subsequent gage readings in Digits, the temperature readings, and the thermal coefficient of each gage for each reading are presented in Appendix I. The final reading to be used for

long-term monitoring, taken to get the correct temperature and final readings in Digits, are also presented in Appendix I.

The corrected change in length was calculated and then converted into strain based on a gage length of 7 ½ inches; strains were converted in stresses using an elastic modulus of 28,500 ksi, based on the PCI Design Handbook (2004) elastic modulus for 0.6-inch diameter strand with a yield stress of 270 ksi. Finally, the stress was converted into force using the area of the 0.6-inch diameter strand (0.217 in^2). The corrected change in length, strain, stress and force in each strand for each of the gages (Gage 1 – Gage 7) are presented in Table 23 through Table 29. Recall the location of the strand gages were identified in Figure 82.

There were difficulties in obtaining readings from Gage 4, as can be seen in Table 26, which were most likely the result of the rainy weather the day of the post-tensioning; this was the only strand gage that did not work properly during the post-tensioning operation. The percent of force lost during the post-tensioning operation was determined by using the force measured after each strand was initially stressed and comparing it to the force measured after post-tensioning was complete. The initial force, final force, force lost and percent of force lost are presented in Table 30.

Table 23. Post-tensioning results for Gage 1.

Stage	$D_{corrected}$ (in.)	Strain (μ)	Stress (ksi)	Force (kip)
1	0.000503	0.00675	192.2	41.7
2	0.050269	0.00674	192.0	41.7
3	0.050023	0.00667	190.1	41.3
4	0.049979	0.00666	189.7	41.2
5	0.049827	0.00665	189.6	41.1
6	0.049820	0.00665	189.6	41.1
7	0.049820	0.00665	189.5	41.1
8	0.049505	0.00661	188.3	40.9

Table 24. Post-tensioning results for Gage 2.

Stage	$D_{corrected}$ (in.)	Strain (μ)	Stress (ksi)	Force (kip)
1	0.050110	0.00668	190.4	41.3
2	0.049931	0.00666	189.7	41.2
3	0.049407	0.00659	187.7	40.7
4	0.049267	0.00657	187.2	40.6
5	0.049251	0.00657	187.2	40.6
6	0.049251	0.00657	187.2	40.6
7	0.049207	0.00656	187.0	40.6
8	0.048877	0.00652	185.7	40.3

Table 25. Post-tensioning results for Gage 3.

Stage	$D_{corrected}$ (in.)	Strain (μ)	Stress (ksi)	Force (kip)
1	0.050535	0.00674	192.0	41.7
2	0.050340	0.00671	191.3	41.5
3	0.049380	0.00658	187.6	40.7
4	0.049194	0.00656	186.9	40.6
5	0.049177	0.00656	186.9	40.6
6	0.049177	0.00656	186.9	40.6
7	0.049118	0.00655	186.6	40.5
8	0.048544	0.00647	184.5	40.0

Table 26. Post-tensioning results for Gage 4.

Stage	$D_{corrected}$ (in.)	Strain (μ)	Stress (ksi)	Force (kip)
1	0.050208	0.00669	190.8	41.4
2	NR*	-	-	-
3	0.049564	0.00661	188.3	40.9
4	NR	-	-	-
5	NR	-	-	-
6	0.049278	0.00657	187.3	40.6
7	0.049242	0.00657	187.1	40.6
8	NR	-	-	-

* NR = data collector could not get a reading

Table 27. Post-tensioning results for Gage 5.

Stage	$D_{corrected}$ (in.)	Strain (μ)	Stress (ksi)	Force (kip)
1	0.000503	0.00007	1.9	0.4
2	0.050269	0.00670	191.0	41.5
3	0.050023	0.00667	190.1	41.2
4	0.049979	0.00666	189.9	41.2
5	0.049827	0.00664	189.3	41.1
6	0.049820	0.00664	189.3	41.1
7	0.049820	0.00664	189.3	41.1
8	0.049505	0.00660	188.1	40.8

Table 28. Post-tensioning results for Gage 6.

Stage	$D_{corrected}$ (in.)	Strain (μ)	Stress (ksi)	Force (kip)
1	0.000629	0.00008	2.4	0.5
2	0.001250	0.00017	4.8	1.0
3	0.001288	0.00017	4.9	1.1
4	-0.000745**	-0.00010	-2.8	-0.6
5	-0.000651**	-0.00009	-2.5	-0.5
6	0.050243	0.00670	190.9	41.4
7	0.050214	0.00670	190.8	41.4
8	0.050170	0.00669	190.6	41.4

** indicates compressive values were measured due to post-tensioning in adjacent channel.

Table 29. Post-tensioning results for Gage 7.

Stage	$D_{corrected}$ (in.)	Strain (μ)	Stress (ksi)	Force (kip)
1	0.001373	0.00018	5.2	1.1
2	0.001402	0.00019	5.3	1.2
3	0.001500	0.00020	5.7	1.2
4	0.001183	0.00016	4.5	1.0
5	0.050358	0.00671	191.4	41.5
6	0.050220	0.00670	190.8	41.4
7	0.049901	0.00665	189.6	41.1
8	0.049616	0.00662	188.5	40.9

Table 30. Post-tensioning force and percent loss for each strand.

VWG	Initial Force (kip)	Final Force (kip)	Force Lost (kip)	Percent Loss (%)
1	41.7	40.9	0.9	0.02
2	41.3	40.3	1.0	0.02
3	41.7	40.0	1.6	0.04
4	41.4	40.6	0.8	0.02
5	41.5	40.8	0.6	0.02
6	41.4	41.4	0.1	0.00
7	41.5	40.9	0.6	0.01

According to the bridge plans, each strand was to be stressed to 41 kip, however, tolerances specified that strand force should be between 38.95 kip and 43.05 kip. The initial and final forces in all the strands monitored are well within the limits previously noted, as can be seen in Table 30. The force in the strands initially stressed was expected to decrease as the final strands were post-tensioned. As may be seen in Table 30, the tendons lost an average force of 0.80 kip or less than 0.02 percent of the initial force. Figure 89 compares the force loss between the tendons, from when each tendon was initially stressed until after all of the tendons were stressed.

For Gages 1 through 5, located in the south half of the bridge, noticeable losses occurred during the first three stages. Minimal losses occurred for stages four through seven which were when the north half of the bridge was post-tensioned. Since the two halves of the bridge were not connected, as previously discussed, Gages 1 through 5 were not expected to have any significant elastic shortening losses during these stages. Additional losses occurred after the south half of the bridge was completely post-tensioned.

Due to the construction error mentioned earlier, neither of the strands to which Gages 6 and 7 were attached were stressed during the fourth stage (while two other strands in the north half of the bridge were stressed) which provided an opportunity to examine the effects

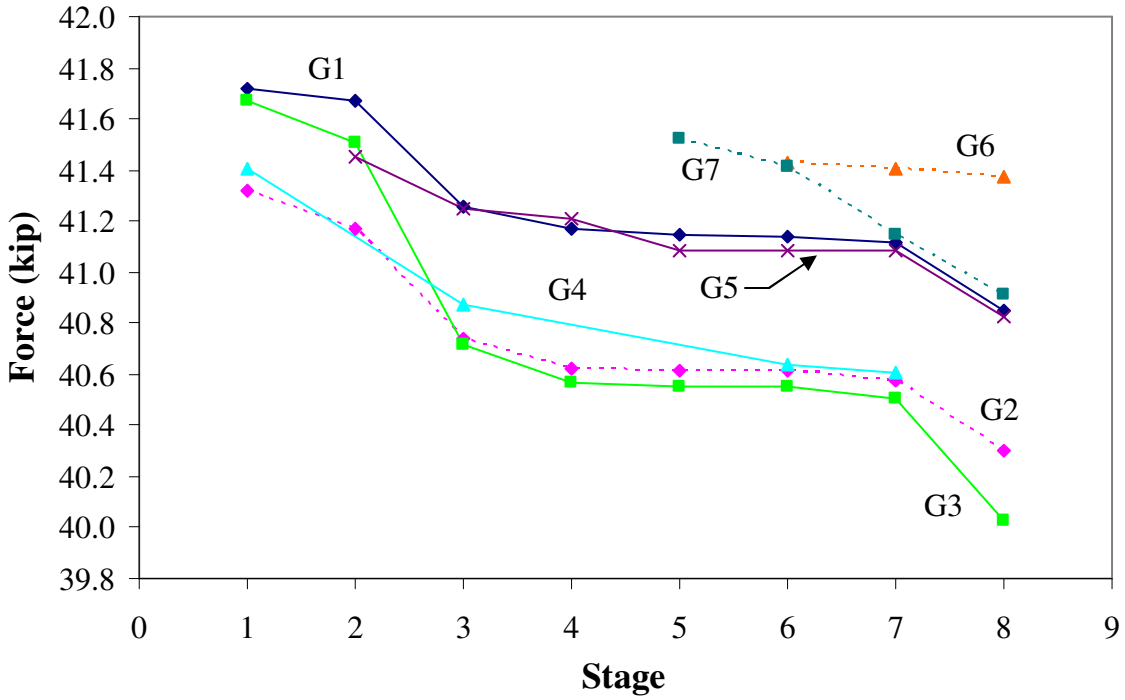

Figure 89. Force loss during the post-tensioning operation.

of elastic shortening in the tendons. Before the jacking operation was moved to the north half of the bridge, the readings from both Gage 6 and 7 indicated slight tensile force in each strand. After the first two strand in the north half of the bridge were stressed, the reading from Gages 6 and 7 showed a reduction in stress (strain); Gage 6 even showed negative tensile stress, as can be seen in Figure 90, which is a direct result of elastic shortening. Difference in stress reduction due to elastic shortening between Gages 6 and 7 could be due to friction points along each strand, which would cause the strands to behave differently.

Forces measured using the VWGs were compared to those provided by the contractor, who reported that every strand was stressed to 41 kip. After the post-tensioning was complete, the contractor verified the force in two of the strands by jacking from the 'dead' end of the strands. The force the contractor reported was the force in the strand outside the anchorage zone, which is higher than the force in the interior portion of the strand

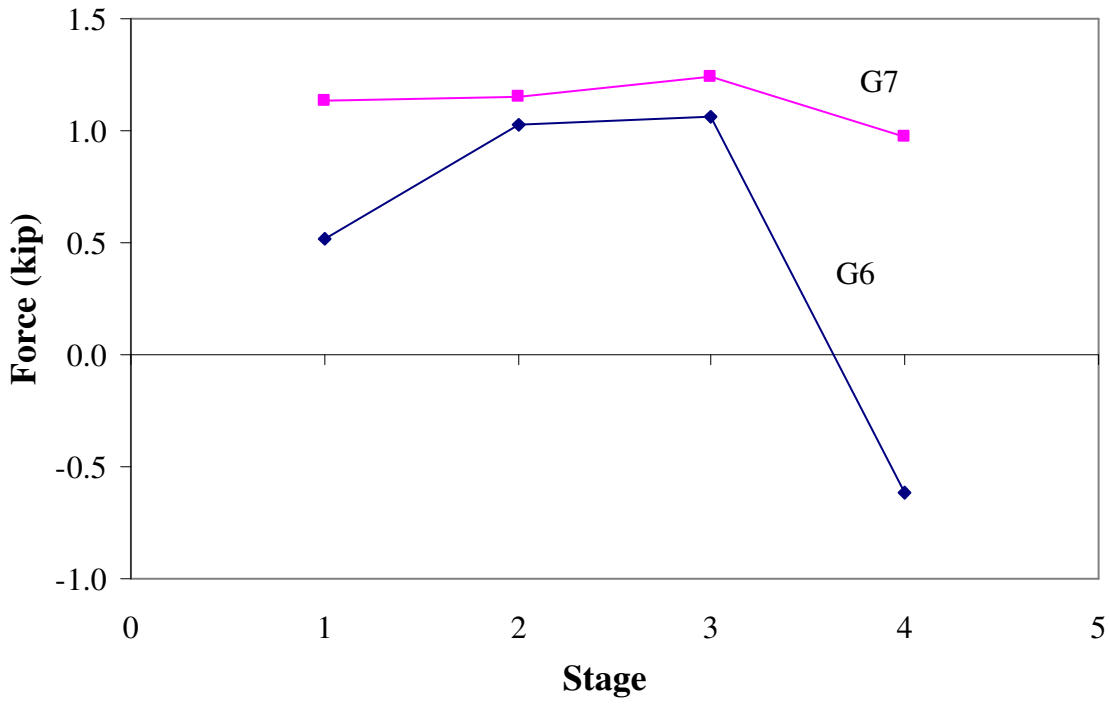

Figure 90. Elastic shortening losses in Gage 6 and Gage 7.

due to anchorage zone seating and some friction losses. According to the contractor, a force of 41 kip outside the anchorage zone corresponded to a force of 39.4 kip in the interior portion of the strand due to anchorage zone losses calculated by Dywidag, the supplier of the hydraulic jack and anchorage hardware. The contractor reported every strand was stressed to a force of 41 kip; worksheets with the gage values, final force in each strand, and elongation for each strand are presented in Appendix II.

Gage 1, as previously noted, was located one foot inside the first interior deck panel and thus the force measured by this gage should correspond to the 39.4 kip calculated by the contractor. As can be seen in Table 30, the final force measured by Gage 1 was 40.1 kip, 0.7 kip greater than the force calculated by the contractor, however, well within tolerance. Forces measured along the strand in Channel 1 are presented in Figure 91. As shown in the figure, there is a slight difference in the force measured along the length of the strand. The

greatest force occurred adjacent to the post-tensioning operation; loss of force along the tendon was most likely due to friction between the strands or friction between the strand and the leveling devices.

There are two reasons why the force calculated by the contractor does not correspond exactly to the force measured using the VWGs. The first reason is the accuracy of the pressure gage on the hydraulic jack (see Figure 92) the contractor was using. With this gage, getting a precise reading within 100 psi (which corresponds to a force of approximately 0.77 kip) would be difficult. Another reason for the difference is the complexity of calculating the anchor zone and friction losses. Post-tensioning losses are affected by several different factors including initial stress level, type of steel, curvature, and exposure conditions. Several different types of losses can occur and it is common to determine losses as a lump sum value (ACI 318-05, 2005). Since it is difficult to separate losses due to elastic shortening, relaxation, seating, and friction immediately after stressing, it is very possible

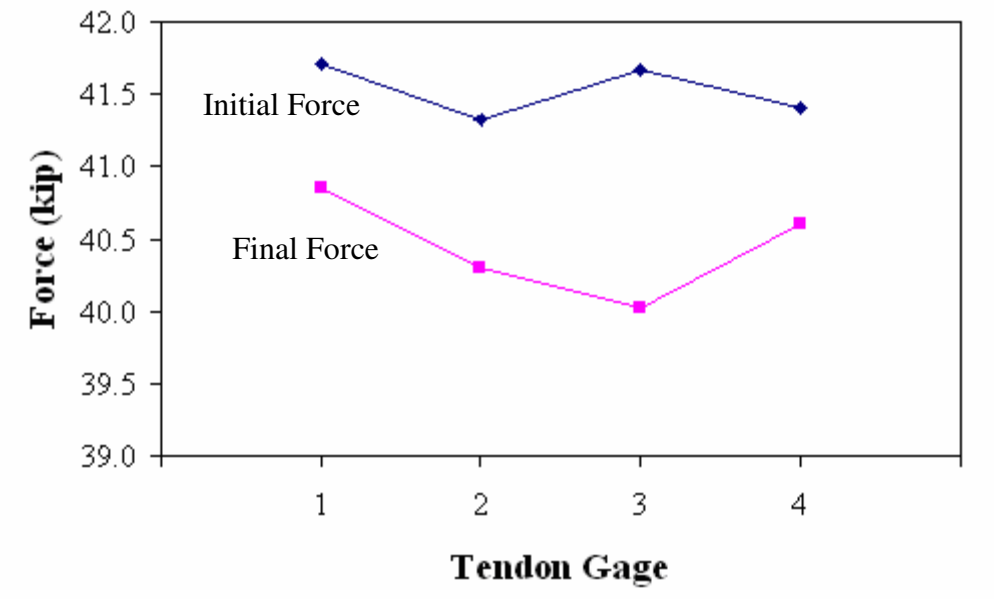

Figure 91. Initial and final force along the instrumented strand in Channel 1.

Figure 92. Hydraulic mono-jack gage.

that the contractor's calculated losses for the anchor zone seating and friction have minor errors. It should be noted the difference between the force calculated by the contractor and the force measure by the VWGs is 1.7 percent and while the values don't correspond exactly, the difference is small enough to confirm the forces reported by the contractor.

5.2.2 Post-Tensioning Strand Summary

To summarize the post-tensioning strand test results, the forces reported by the contractor have been verified. All of the tendons were stressed within tolerance and the final stresses also meet tolerance requirements set by the Iowa DOT. On average, the tendons lost 0.8 kip of force, or about 0.02 percent of the initial stressing force, primarily due to elastic shortening. The largest force lost was 1.6 kip, measured at the midspan of the tendon in Channel 1, which is still less than 0.05 percent of the initial force.

5.2.3 Post-Tensioning Deck Panel Results

The reason for using instrumentation in the deck panels during the post-tensioning operation was to determine how the stresses from post-tensioning were distributed. In order

to see how the stresses were distributed, twelve gages as shown in Figure 79, were placed in four deck panels located in the south half of the bridge. Strain data recorded directly with the hand-held data collector were obtained for each of the VWGs and were converted to stresses using the modulus of elasticity of the concrete deck panels. To determine the modulus of elasticity, the average compressive strength of the deck panels prior to delivery was used. The modulus of elasticity, calculated using a concrete strength of 6,800 psi and the relationship provided in Section 5.4.2.4 of the AASHTO LRFD Bridge Design Specification (1996), used for all of the stress calculations was 4,700 ksi.

On the morning of testing, problems were noticed in Gage B1. The connections were checked between the spliced wires, between the gage wires and the switch-and-balance unit, and between the switch-and-balance and the data collector; no connection problems were found. Most likely, Gage B1 was damaged prior to the field testing; thus, there are no results for Gage B1.

The gages used were very sensitive to loads and movements. When people were walking or moving equipment on the instrumented deck panels, there was a ‘spike’ in the strain reading. Readings stabilized when people moved off the instrumented panels and/or stopped working. Since the reading were taken during the post-tensioning operation, it was impossible to clear the entire bridge while recording data. Besides the post-tensioning operation, the contractor was working on preparing the deck for the longitudinal joint closure pour. These two operations resulted in some inconsistent strain readings and is most likely the reason for higher stresses recorded in nine of the eleven working gages.

Strain readings taken during the post-tensioning of the deck are listed in Table 31. These results were then converted into stresses, which are presented in Table 32, using the

modulus of elasticity; highlighted values represent inconsistent gage readings which occurred when the reading for a particular gage was not stable; often the unstable readings varied between 300 and 1200 micro-strains. As previously noted, the unstable readings were often the result of movement on the deck panels.

One gage in particular, Gage A2 produce variable readings on all but two of the data points. There are two possible reasons for the large number of variable readings for this gage. Although there were no problems with the connection to the switch-and-balance unit, there could have been wiring problems embedded in the deck panel. Secondly, Gage A2 may have been picking up the movement from the post-tensioning operation since Panel A was located adjacent to the end panel where the stressing took place and Gage A2 was located in between the two post-tensioning channels. Most of the movement from the post-tensioning was between Channel 1 and Channel 2 in the south half of the bridge. This could explain why the readings from Gage A2 were much more variable than Gage A1, which was located on the outside of Channel 1.

Stresses in the deck ranged from 1,670 psi to 1,775 psi for stable gage readings, below the allowable compressive stress of 4,080 psi (60% of the concrete strength) as specified by the AASHTO LRFD Bridge Design Specifications (1996). Even the highest variable gage reading produced a maximum deck panel stress of 3,545 psi, still below the allowable compressive stress due to post-tensioning. The original stress data for the deck panels, as can be seen in Figure 93, show a trend among ten of the eleven gages, disregarding Gage A2 and the higher stresses measured due to work on the bridge. Note the individual data points are ‘spikes’ in the data due to the contractor’s operations on the bridge deck.

Table 31. Deck post-tensioning strains.

Stage	Strain (μ-strain)										
	A1	A2	B2	B3	C1	C2	C3	C4	D1	D2	D3
0	369	448	361	363	362	358	368	357	371	365	358
1	370	390	753	363	362	358	406	358	371	365	355
2	370	478	361	364	362	359	369	358	371	366	355
3	373	472	370	367	364	362	371	360	374	368	358
4	374	754	365	368	366	362	372	372	375	369	358
5	374	478	366	368	366	600	372	361	375	369	359
6	422	467	365	368	366	362	372	361	375	369	359
7	374	433	365	368	366	362	372	361	375	369	359
8	377	378	368	370	368	365	375	363	378	372	361

Highlighted cells had inconsistent readings

Table 32. Deck post-tensioning stresses.

Stage	Stress (psi)										
	A1	A2	B2	B3	C1	C2	C3	C4	D1	D2	D3
0	1735	2105	1695	1705	1700	1685	1730	1675	1740	1715	1680
1	1735	1835	3540	1705	1700	1685	1905	1680	1740	1720	1670
2	1740	2245	1700	1710	1700	1690	1735	1680	1745	1720	1670
3	1750	2220	1740	1720	1715	1700	1745	1690	1755	1730	1680
4	1755	3545	1715	1730	1720	1705	1750	1750	1760	1735	1685
5	1755	2245	1720	1725	1720	2820	1750	1700	1760	1735	1685
6	1980	2195	1715	1725	1720	1705	1750	1700	1760	1735	1685
7	1755	2030	1715	1730	1720	1705	1750	1700	1760	1735	1685
8	1770	1775	1730	1740	1730	1715	1765	1710	1775	1750	1700

Highlighted cells had inconsistent readings

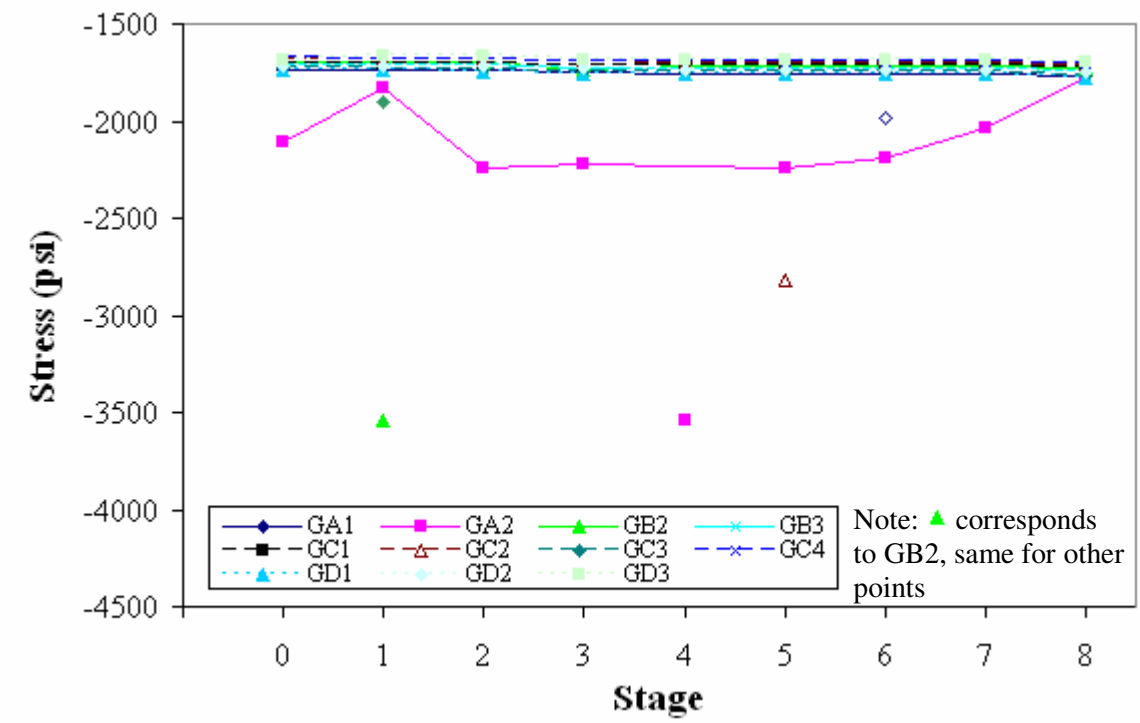

Figure 93. Complete stress results for the bridge deck post-tensioning.

After the higher stresses and inconsistent readings from Gage A2 were eliminated, a clear trend for panel stresses can be seen in Figure 94; note Figure 93 and Figure 94 display the same data at different scales. The stresses in the panels indicate as the deck was post-tensioned, the stresses in the panels increased, shown in Stages 1 through 4. At Stage 4, the stresses start to stabilize and for Stage 5 through 8, there was no appreciable stress gain. These stages correspond to when post-tensioning was moved to the north half of the bridge deck; the instrumented panels were not subjected to any additional force.

The final stage of post-tensioning results in the largest respective stresses in all of the deck panels, due to the fact all of the strands in the deck were post-tensioned at this point. Actual stresses appear to be somewhat random, and not associated with the location of the panel in the bridge. Stresses in Panel D were the greatest, which was at the dead end of the bridge. Stresses at each gage location were compared to see if the deck panel stresses were

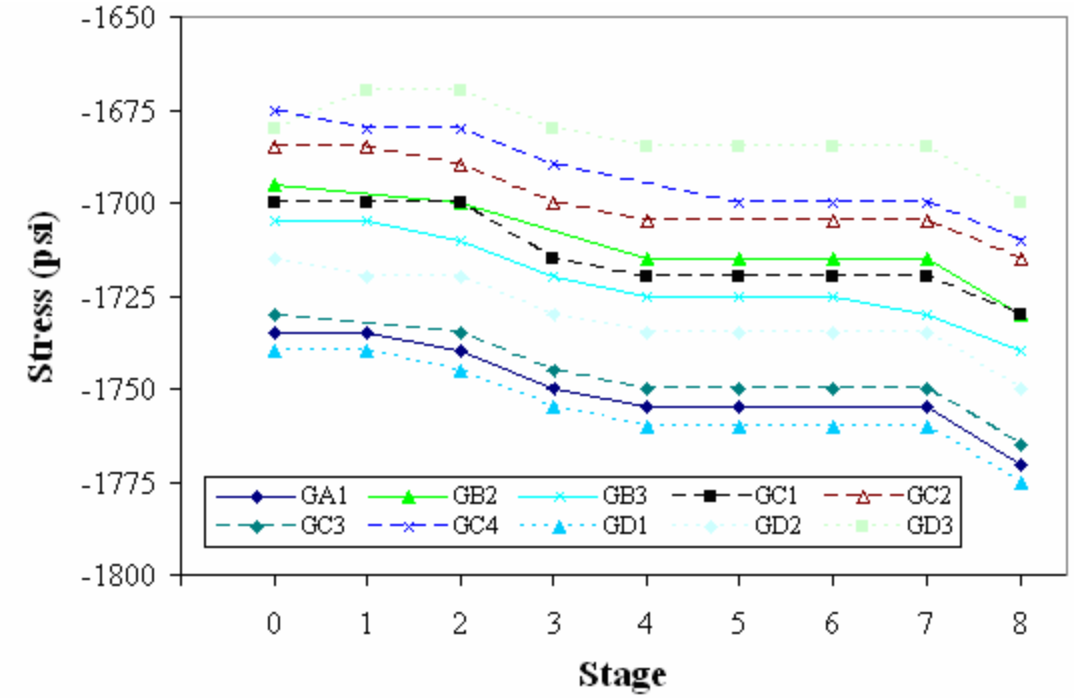

Figure 94. Deck panel stress results.

highest in the panel closest to the post-tensioning operation. To compare the stress distribution between the instrumented panels, Gage locations 1, 2 and 3 (see Figure 80) were compared; since there was only one gage at Location 4, no comparison was made.

Deck panel stresses at Location 1 (on the outside of Channel 1 in the cantilevered section of the panel) in Panel A, Panel C and Panel D are shown in Figure 95. Note deck Panel B is not shown because as previously noted, Gage B1 was not working.

The greatest stress levels at Location 1 was expected to be in deck Panel A, which was the closest to the post-tensioning operation and the lowest stress levels were expected to be in Panel D, at the dead end of the bridge. However, as shown in Figure 95, the highest stresses actually occurred in Panel D, at the dead end of the deck. Lowest stress levels were measured in Panel C, although the difference in final stress in Panels C and D was less than three percent. The difference in final stress between Panel A and Panel C was 0.3 percent.

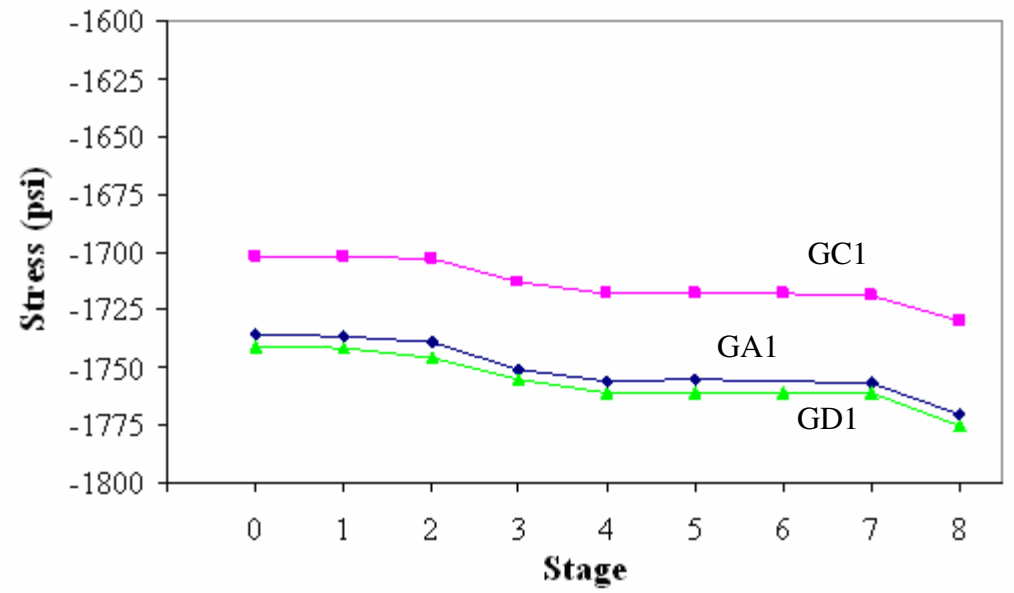

Figure 95. Comparison of deck stresses at Location 1.

Stresses recorded at Location 1 do not seem to suggest there is a significant difference in stresses in the deck panels along the length of the bridge.

Stresses measured at Location 2 were compared next, without Gage A2. The gages at Location 2 were located between Channel 1 and Channel 2, on the reinforcing steel adjacent to Channel 1. Deck panel stresses at Location 2, shown in Figure 96, were expected to be the same as those at Location 1 - highest in the panel closest to the post-tensioning operation and decreasing along the length of the deck.

According to the data in Figure 96, the highest stress levels were again in Panel D and the lowest stress levels were in Panel C with Panel B approximately in between, however, there is not significant differences in stresses along the length of the bridge. The difference in final stress between Panel C and Panel D is less than two percent at Location 2.

The stresses measured at Location 3 were also compared; the gages at Location 3 were located between Channel 1 and Channel 2, approximately two feet farther away from the Channel 1 than Location 2. Deck panel stresses at Location 3 are shown in Figure 97;

the highest stresses occurred in Panel C and the lowest stresses in Panel D. The difference in the final stress between Panel C and Panel D was 3.7 percent, which again suggests there is no significant difference in the stresses measured along the length of the bridge. When comparing the stress data from all three of the gage locations, the maximum and minimum

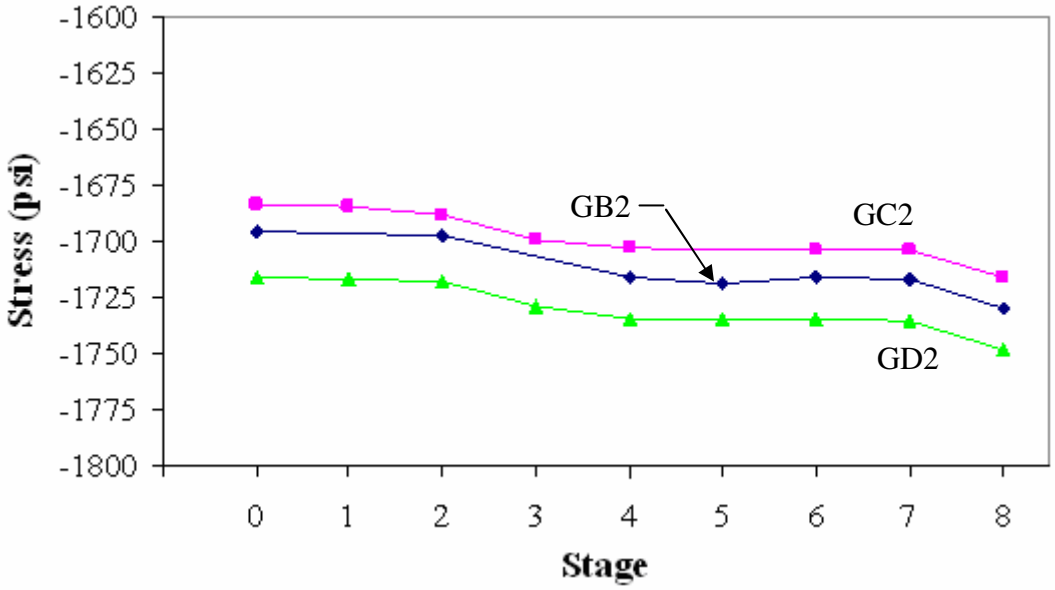

Figure 96. Comparison of deck stresses at Location 2.

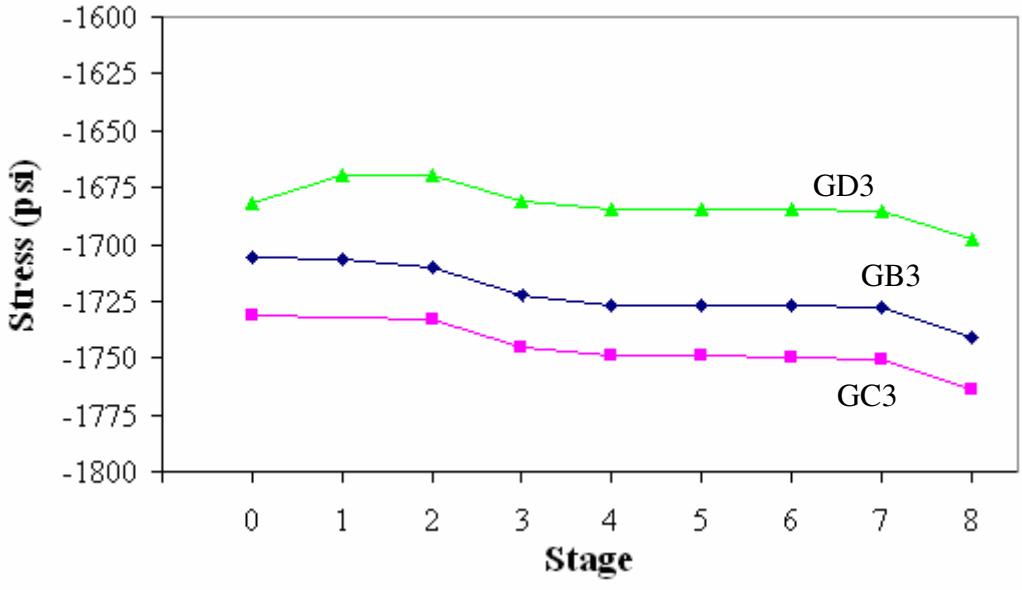

Figure 97. Comparison of deck stresses at Location 3.

stresses do not occur in the predicted panels and the maximum and minimum stresses at each location did not occur in the same panels. At each respective location, the final stresses were all within four percent, showing no significant difference between the stresses measured in the panels. The locations of the highest and lowest stresses do not show a trend; the locations for the highest and lowest stresses are different at Location 3 than at Locations 1 and 2. Based on these results, stress distribution from the post-tensioning operation does not appear to decrease along the length of the bridge, as was expected.

Stresses within each panel were also compared. Highest stresses were expected at locations adjacent to Channel 1; as the distance from the and channel increased, stresses were expected to decrease. The stresses were also expected to be higher between Channel 1 and Channel 2 than in the cantilever section of the panels.

The stresses within Panel A were not compared due to the fact that Gage A1 was the only gage working properly during the post-tensioning. The stresses in Panel B were compared first and are presented in Figure 98; only two gages are shown because as previously mentioned, Gage B1 was not working.

The stresses in Panel B did not follow the expected behavior. As illustrated in Figure 98, the higher stresses were measured at Location B3, which was farther away from Channel 1 than Location B2. However, the difference in stress between the two locations was 11 psi, or less than one percent difference.

The stresses in Panel C, the panel with the most instrumentation, were compared next. Comparison of stresses in Panel C is shown in Figure 99; the highest stresses were expected at Location C2 and the lowest at Location C4. While lowest measured stresses did occur at Location C4, the stresses measured were only 9 psi less than the stresses at Location C2,

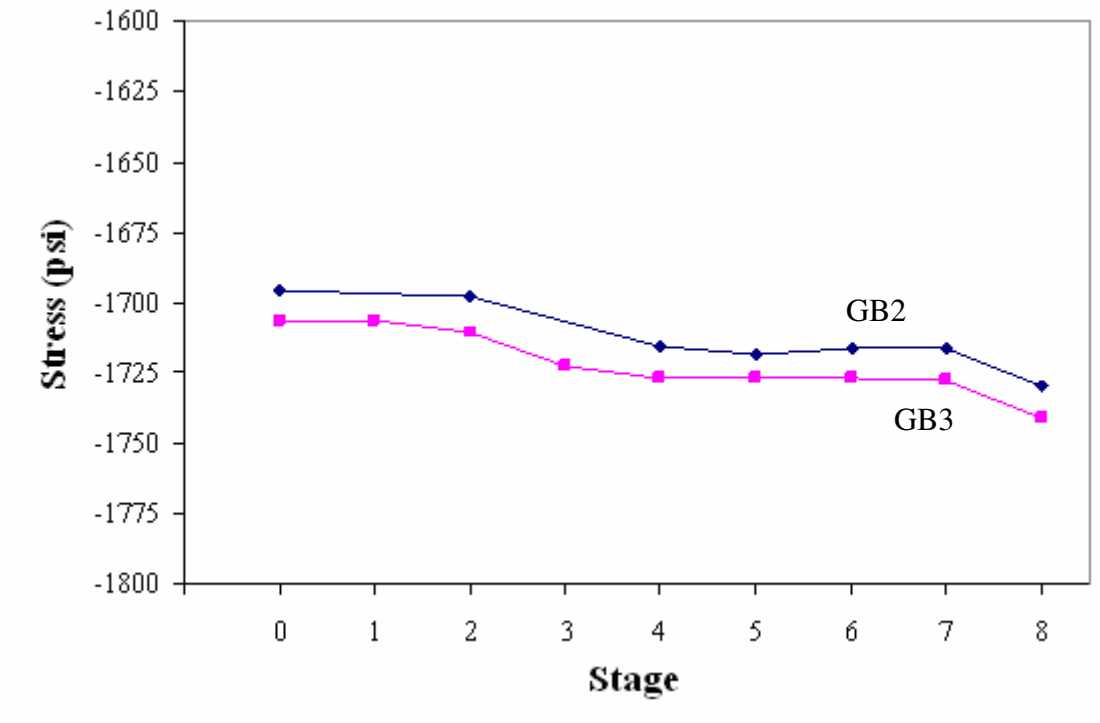

Figure 98. Comparison of deck stresses in Panel B.

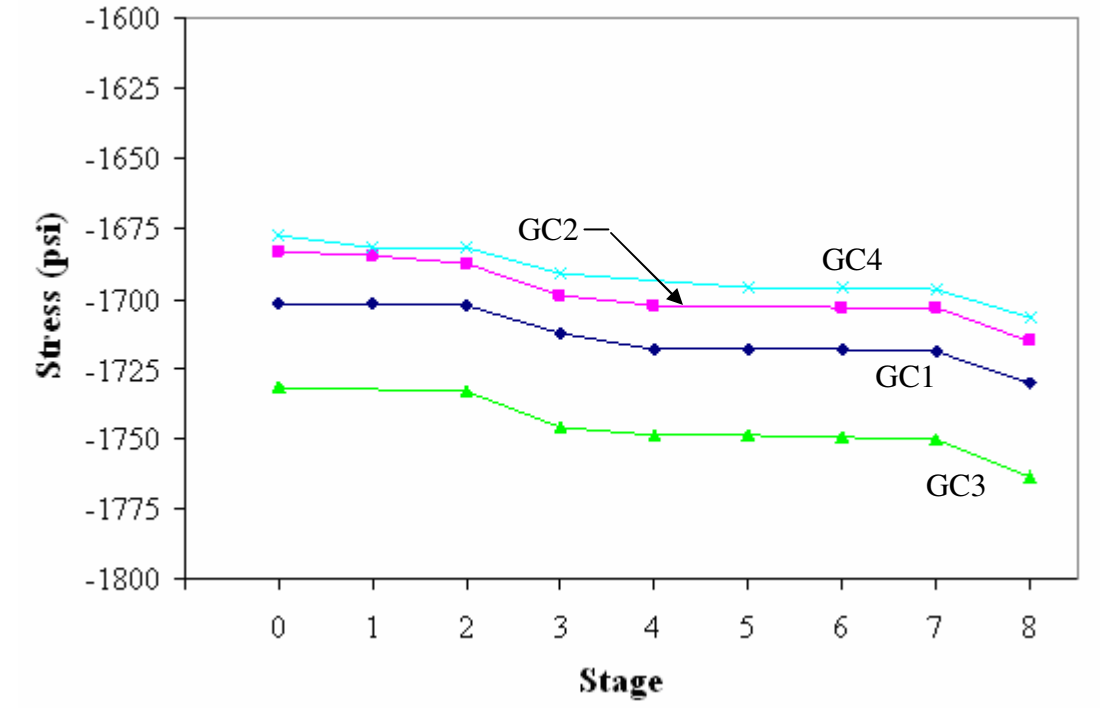

Figure 99. Comparison of deck stresses in Panel C.

which is adjacent to Channel 1. The highest stresses were at Location C3, which was the farthest from Channel 1. The largest difference in stresses measured in Panel C was between Locations C3 and C4; the difference in final stress between these two gages was 56 psi, or 3.2 percent. Measured stresses in Panel C did not follow the expected behavior, however, based on the final stress difference of 3.2 percent, the deck panel stresses do not change significantly within the deck panel.

To better represent the stresses in the panel, the stresses were compared for each instrumented location. This stress comparison is presented in Figure 100. As shown in the figure, the stresses at each location increase as the post-tensioning operation progresses. The magnitudes of the stresses within the panel are relatively similar, as previously discussed. As shown in Figure 100, the stresses are the greatest at Location 3. This is because Location 3 was the closest to Channel 2 and was most likely measuring stresses from the force in Channels 1 and 2.

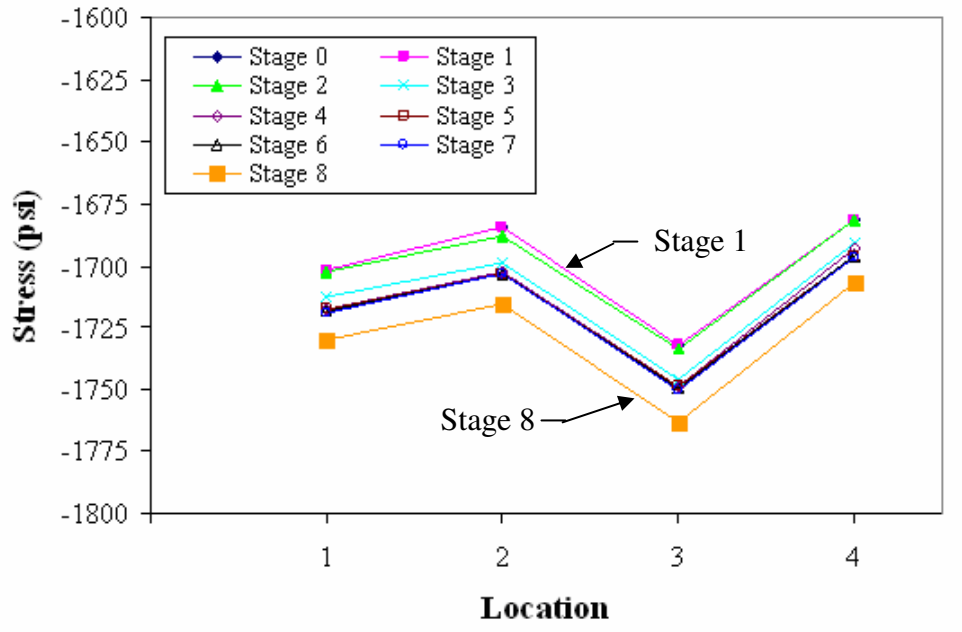

Figure 100. Comparison of deck stresses by location in Panel C.

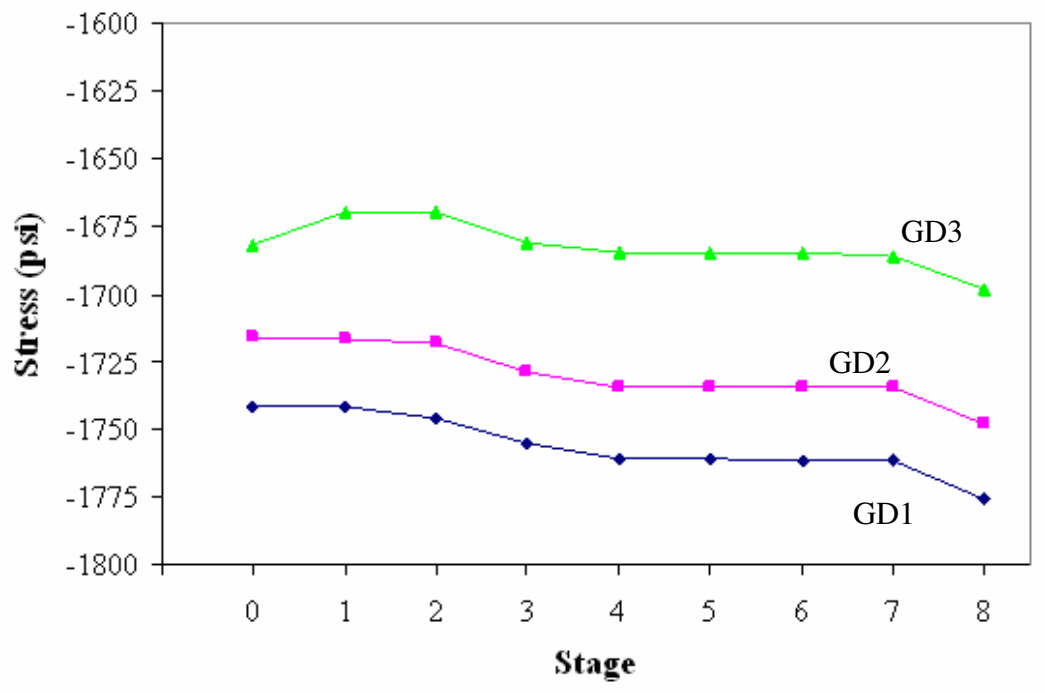

Figure 101. Comparison in deck stresses in Panel D.

Stress levels in Panel D were compared last and are presented in Figure 101. Stresses in Panel D follow the expected behavior closer than the previous panels examined. The lowest stresses were measured at Location D3, the location farthest from Channel 1. However, the highest stress was measured at Location D1, which was located in the cantilevered section of the deck panel; the highest stress was expected to occur at Location D2. The final stress difference in Panel D between Locations D1 and D3 was 78 psi, or about 4.4 percent. This small percent difference indicates there is no significant difference in stresses within a given deck panel.

5.2.4 Post-Tensioning Deck Panel Summary

When considering all of the instrumented deck panels, there was minimal correlation between the deck stresses within a given panel. The stresses do not necessarily decrease with distance from the post-tensioning channel, and the stresses are not necessarily less in the

cantilevered section of the deck panel than in the deck panel section between the two post-tensioning channels.

The location of the panel along the bridge deck also did not appear to correlate with a decrease in measured stresses; deck panel stresses did not necessarily decrease as the distance between the post-tensioning operation and the deck panel increased. After comparing all of the final stresses measured in the deck panels, the largest difference in stresses was 4.4 percent. Since the stresses measured at the locations in the panels were within five percent, it can be concluded that the stresses induced by the post-tensioning operation are essentially distributed uniformly throughout the deck, regardless of the proximity to the post-tensioning operation or to the post-tensioning channel. Finally, the measured stresses were below the allowable compressive deck panel stress of 4,080 psi, as previously described.

5.3 Post-Tensioning Testing and Verification Summary

Overall, the testing and verification of the post-tensioning operation was a success. Strand monitoring results have shown a loss of force in each strand between the initial stressing and after post-tensioning was completed. The strands exhibited a loss of force while that respective half of the bridge was being post-tensioned. When the opposite half of the bridge was being stresses, the strands showed no significant response.

The largest loss of force between the initial stress of each strand and the final stress was less than 0.05 percent of the initial force. Results from the strand monitoring also verified the strand forces provided by the contractor and verified that the strands with instrumentation were initially stressed within tolerance and remained in tolerance after the

post-tensioning was complete. An unexpected result from the strand monitoring was the evidence of elastic shortening of the deck panels in the north half of the bridge.

Deck panel monitoring was performed to measure how the force from the post-tensioning operation was distributed through the deck panels. Results from the deck panels have shown the forces measured were evenly distributed through the deck, regardless of the location of the deck panel. Stress results also showed the stresses measured in the panels were below the allowable compressive stress in the panels, as specified by AASHTO LRFD Bridge Design Specifications (1996).

CHAPTER 6. CONSTRUCTION DOCUMENTATION

6.1 Construction Sequence

This chapter presents the documentation of the demolition of the previous Boone County bridge over 120th Street, and the construction of the replacement bridge. A summary of feedback from the Boone County Engineer's Office, the prime contractor, the precast fabricator, and from the Iowa State University research team is presented at the end of the chapter.

The previous bridge was a single-span concrete Marsh Arch, shown in Figure 102, which was replaced due to width problems and weight restrictions on the bridge. Clear distance between the reinforced concrete arches was 19 feet and the bridge was 77 feet, 6 inches in length. The previous and existing road alignment can be seen in Figure 103; the bridge location remained the same while the intersecting road to the west of the bridge was moved further west to allow room for the larger replacement bridge.

Figure 102. Previous bridge on 120th Street, July 19.

Construction began on July 17, 2006 with the contractor focused on earthwork and grading. An access road south of the bridge was initially installed by the contractor before

demolition began; this causeway allowed access between the east and west banks after the original bridge was removed. Demolition of the bridge began the morning of July 24. The contractor used a back hoe with a hammer attachment, shown in Figure 104, to break apart the bridge deck and then used the back hoe to pull apart the bridge reinforcement.

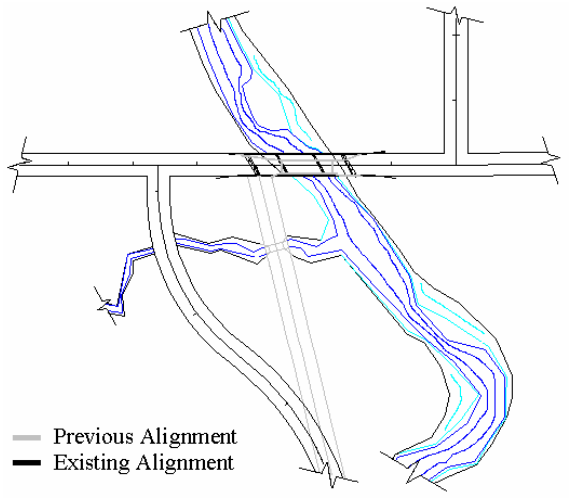

Figure 103. Previous and existing road alignment.

Figure 104. Breaking apart the Marsh Arch bridge deck with a back hoe, July 24.

In less than one day, the bridge was demolished and the abutment backwalls and wingwalls were removed. Footings from the abutments were left in place and buried under the creek bed since the location of the footings did not interfere with the substructure for the

replacement bridge. Over the next several weeks, the contractor was clearing debris from the bridge and grading, due to the elevation change for the replacement bridge. Since the profile was raised over ten feet from the previous bridge, a large amount of earth fill was required. The graded bridge site and access road can be seen on August 7, 2006 in Figure 105.

During the week of August 7, the Boone and Ames area received approximately one-half inch of precipitation, which caused the access road constructed to wash out. Several working days were lost because the site conditions were too wet to use heavy equipment and the access road had to be reconstructed. Precipitation data for July, August, and September in the Boone/Ames area is presented in Appendix II. Rain damage to the site, along with the washed out access road can be seen in Figure 106.

Figure 105. Cleared bridge site, August 7.

When the access road was replaced, the contractor removed the original sixteen-inch culvert pipe that was placed under the access road and replaced it with large rock overlaid by sand and gravel. Grading and earth work continued until the bridge abutment locations were properly prepared for pile driving; the bridge site on September 5, 2006 with the west end of the bridge site graded and leveled for pile driving is shown in Figure 107.

Figure 106. Access road and bridge site, August 11.

Figure 107. West bridge abutment site prepped for pile driving, September 5.

Pile driving began on the west end the bridge on September 14. For the abutments, five HP 10 x 57 steel piles were used. Between September 5 and September 15, over three inches of rain fell in the vicinity of the construction site. Rain and runoff caused the access road to wash for the second time. Even though there was no access to the east side of the bridge, pile driving was finished on the west side; the bridge site after the effects of the additional rain is shown in Figure 108.

After driving piles was complete, 5/8-inch diameter studs were welded to the pile webs. The contractor used steel channels welded to the sides of the H-piles to provide a level

surface for placement of the precast abutments. To ensure the channels were welded at the correct elevation, survey equipment was used. One of the piles on the west bank was driven incorrectly; the pile (which will be shown later) was rotated 90° from what the plans specified. Steel channels on the west end of the bridge before being blocked up to the correct elevation are shown in Figure 109.

Between September 15 and 20, the bridge site received an additional one and a half inches of rain. Although the access road hadn't been reconstructed, the additional rain washed away much of the material that had been used in the road. Because of the large

Figure 108. Washed out access road, September 15.

Figure 109. West abutment piles, driven and channels being blocked, September 15.

amount of rain and wet condition of the bridge site, construction progress slowed. The state of the bridge site on September 20 can be seen in Figure 110.

The rain between the dates of September 15 and 20 caused more damage to the bridge site than the previous storms. The grading on both banks of the creek were damaged after the last storm and had to be repaired; damage to the west bank of the bridge site is shown in Figure 111.

The contractor continued work on the west bank when possible, however, most of the site was too wet to work on anything other than the west abutment piles. After the channels

Figure 110. Bridge site on September 20.

Figure 111. Damage to the west bank caused by the rain, September 20.

were welded in place, the wooden blocking was removed (see Figure 112). Note in Figure 112 the north-most pile, as previously noted, was driven incorrectly; this error required the channels to be positioned parallel to the longitudinal axis of the abutment, instead of perpendicular.

The pipe piling for the west pier was driven on September 27 and 28. Each of the piers had nine, 16-inch diameter, closed-end steel pipe piles which were fitted with a pile point (shown in Figure 113) to make driving the piles easier and to prevent damage to the pile.

The two outside pier piles were batter driven at an angle of 4.8 degrees. After all of the piles in the west pier were driven, the piles were connected with steel beams and channels

Figure 112. West abutment piles after wood blocking was removed, September 20.

Figure 113. Steel pipe pile driving point, September 28.

to provide a support for the precast pier cap, until it was installed and permanently grouted in place. The west pier as well as the west abutment piles can be seen in Figure 114.

After the pipe piling was in place and secured with steel falsework, the piles were filled with concrete and the reinforcement connections were embedded in the pier cap as the concrete was placed. Pipe piles with the embedded reinforcement can be seen in Figure 115, after concrete was placed inside the pipe piles. The H-piles for the east abutment were driven, cut to length, and had the studs and channels welded in place on October 10 and 11. H-piles for the east abutment can be seen in the background in Figure 115.

Figure 114. West pier and west abutment piling, September 28.

Figure 115. Pipe pile reinforcement for pier cap connection, October 4.

On October 4, the precast abutment and pier cap for the west side of the bridge were transported to the site and placed; the abutment was delivered and set into place first. Unloading and setting the abutment in place, shown in Figure 116, took the contractor approximately fifteen minutes. There were no clearance issues with the H-piles, thus the operation went smoothly. To connect the precast portion of the abutment with the CIP portion, mechanical splicers were embedded in the precast portion to connect No. 5 reinforcing bars. In Figure 117a, the west abutment can be seen in place as well as the No. 5 reinforcing bars; in Figure 117b, one of the H-piles in the abutment is shown.

Next, the west pier cap was delivered, unloaded, and lowered into place on the falsework in approximately fifteen minutes as well. As shown in Figure 118, the pier cap

Figure 116. West abutment being lowered in place, October 4.

a) abutment in final position

b) H-pile in the abutment

Figure 117. West precast abutment in place, October 4.

was set on the falsework without any clearance issues with the pipe piles; the west pier cap is shown in place (Figure 119a) along with one of the pipe piles in the pier cap (Figure 119b).

The east abutment was delivered, unloaded, and set in place on October 4, in the same manner as the west abutment. Both abutments and the west pier cap were placed in approximately fifteen minutes each, and all were placed in the same day (October 4); the only delay in setting each element was waiting for the delivery truck. The east pier cap was the only precast substructure member that was not placed that day, due to the fact the site was still too wet to move the crane into place to drive the east pier piles. Shown in Figure 120 are the two abutments and the west pier cap on October 4, after all three were in place; the external reinforcement attached to the west abutment can be seen in this figure as well.

The following day, the contractor grouted the nineteen piles into place (five in the east abutment, five in the west abutment, and nine in the west pier cap). There were difficulties with the special concrete mix meeting the slump and entrained air requirements and the first mix was rejected. The mix was corrected in the second truck and the contractor used a concrete bucket and crane to place the concrete in the CMP; the concrete was vibrated and finished by hand. Concrete being placed in the east abutment is shown in Figure 121; the finished concrete can be seen in Figure 122.

Figure 118. West pier cap being lowered into place, October 4.

a) pier cap in place

b) pipe pile in the pier cap

Figure 119. West pier cap in place, in the field, October 4.

Figure 120. Precast abutments and pier cap in place, October 4.

Figure 121. Concrete being placed in the east abutment, October 5.

Figure 122. Finished specialty concrete in the east abutment, October 5.

By this time (October 5), the construction site had dried sufficiently for the contractor to rebuild the access road to the east side of the bridge. This time, the contractor used one sixteen-inch culvert pipe, one twelve-inch culvert pipe, and two twenty-four-inch culvert pipes, under the access road to increase the flow under the road to hopefully prevent another wash out. Once the road was finished, the crane was moved onto the access road (as shown in Figure 123) and pile driving for the east pier began on October 10.

After the east pier piles were driven and cutoff to the desired length, the piles were secured with steel falsework and filled with concrete. Reinforcement for the connection between the pipe piles and the pier cap was embedded in the concrete as it was being placed in the pipe piles. The exterior piles were driven at the same batter as previously noted for the

Figure 123. East pier pipe piles being driven, October 10.

west pier. The east pier cap pipe piles are shown in Figure 124, after being filled with concrete. Later that same day (October 12), as shown in Figure 125, the east pier cap was delivered, unloaded, and set in place without difficulty.

On October 19, the contractor primed the exposed steel pipe piles and painted the piles on October 23 to prevent corrosion. After the concrete connecting the piles and substructure had reached strength, the contractor was able to set the prestressed concrete girders on the piers and abutment caps. The girders were delivered, three per truck, unloaded and set in place October 24. Center span girders were delivered and placed on the substructure first, followed by the west span girders, and finally the east span girders. Each

Figure 124. East pier pipe piles filled with concrete, October 12.

Figure 125. East pier cap being set, October 12.

girder was unloaded and set in place in approximately ten minutes; the first girder of the center span is shown being lifted into place in Figure 126.

All of the bridge girders were set in place on October 24. Small steel beams, shown in Figure 127, supported the girders on top of the pier caps and abutments to keep the girders at the correct elevation until the pier cap diaphragms and the CIP portion of the abutment caps were placed. A view of all of the erected bridge girders (looking east) is presented in Figure 128.

Figure 126. The first bridge girder being lifted into place, October 24.

The first of the interior deck panels were delivered on October 25, four panels per truck, and erection thereof began that morning. The first two deck panels set were the panels at middle of the center span of the bridge. However, the panels were not set in the correct location; this error was not noticed until after eight panels had been set. Since the panels had to be set from midspan outwards, the contractor had to remove all eight panels and reset the first two panels. After the initial two panels were correctly positioned, the rest of the panels were then reset. One of the deck panels can be seen being lifted and placed on the girders in Figure 129.

Figure 127. Steel beams used to support the girders, October 24.

Figure 128. Erected bridge girders, October 24.

Figure 129. Deck panel being reset on the bridge girders, October 25.

Over half of the bridge deck panels, sixteen in total, were set on October 25. The remaining panels were delivered and set the next day, with the exception of the four end panels. Four sets steel plates and screws, one of which is shown in Figure 130, were used by the contractor to level the interior deck panels.

Figure 130. Deck panel leveling screw, October 26.

Once all of the deck panels were leveled to the correct elevation, the panels located over the piers were removed so the pier diaphragms could be cast. All of the panels had to be at final elevation so the contractor could form the diaphragms under the panels to the correct height. The diaphragms for both east and west piers were placed on November 3, as shown in Figure 131. After the concrete was placed, the diaphragms were covered in wet burlap and plastic for curing; the west pier diaphragm can be seen in Figure 132, a day after the concrete was placed.

The panels over the piers were replaced after the pier diaphragm concrete had gained sufficient strength and the diaphragm formwork had been 'stripped'. While waiting for the diaphragm concrete to cure, the contractor formed the transverse joints between the deck panels, as shown in Figure 133. On November 8, all four of the end panels were delivered to the site and placed on the bridge; one of the east end panels being lowered into place is shown in Figure 134.

Figure 131. Pier diaphragm before concrete placement was complete, November 3.

Figure 132. West pier diaphragm covered with burlap and plastic, November 4.

Figure 133. Transverse joint formwork, November 5.

The transverse joints between the end panels and the adjacent panels were not formed and cast with the rest of the transverse joints, since the end panels had not reached the required 28-day strength. On November 8 the remaining transverse joints were placed. Several transverse joints can be seen in Figure 135, before being finished; a finished transverse joint is shown in Figure 136.

Post-tensioning strands were 'threaded' through the end panels and the four post-tensioning channels on November 13. End panels reached the required 28-day strength on November 16, after which concrete was placed in the transverse joints between the end panels and the adjacent interior panels.

Figure 134. End panel being placed at the east end of the bridge, November 8.

Figure 135. Several transverse joints before finishing, November 8.

Figure 136. Finished transverse joint, November 8.

Post-tensioning the bridge deck could not take place until the end panel transverse joints had reached a minimum strength of 3,500 psi. Since the temperature was dropping, the contractor used heating coils and thermal blankets to heat the joints and decrease the amount of time needed for the concrete in the joints to cure and reach strength. The Iowa DOT placed thermal couples in the transverse joint concrete, shown in Figure 137, so the internal temperature of the concrete could be monitored. Temperature data from the transverse joints are presented in Appendix II. One of the finished end transverse joints can be seen in Figure 138 covered with burlap and heating coils, before the thermal blankets were put in place.

Figure 137. Thermal couple being inserted into end panel joint, November 16.

Figure 138. Burlap and heating coils on the west end panel joint, November 16.

The contractor was originally going to post-tension the bridge deck on November 21; the VWGs for monitoring some of the post-tensioning forces were attached to four of the tendons and calibrated that morning. One of the gages is shown being calibrated in Figure 139. However, there were problems keeping the joints sufficiently warm; around 2:00 a.m. on November 18, the generator for the heating coils lost power. Power was not restored until around 7:00 a.m. later that morning. Since the strength of the concrete in the end panel transverse joints was not at the required strength, post-tensioning had to be delayed one week for the concrete to cure sufficiently to meet the minimum strength requirements.

Figure 139. Calibration of one of the vibrating wire gages, November 21.

The following week, the concrete in the joints had gained sufficient strength and the post-tensioning operation, shown in Figure 140, began approximately at 8:00 a.m. on November 28. The order of post-tensioning the various tendons was presented earlier in Section 5.1 of Chapter 5. The entire post-tensioning operation took less than four hours, including the time post-tensioning had to stop for data collection.

During the time spent waiting for the transverse joint concrete to reach the required strength, the contractor formed the longitudinal joint between the north and south half of the bridge and put up formwork for the four post-tensioning channels. Longitudinal joint formwork can be seen in Figure 141 from below the bridge deck. Formwork was attached to the deck using U-bolts.

After post-tensioning was completed, concrete was cast in the post-tensioning channels and longitudinal joint. The deck leveling plates and screws were left in place until the concrete in the joints had reached the desired strength; the screws were then removed

Figure 140. Post-tensioning in progress, November 28.

from the deck and the holes were filled with grout in accordance with the Iowa DOT Materials Instructional Memoranda 491.13 Hydraulic Cement Grouts criteria. A finished post-tensioning channel, the finished center longitudinal joint, and an unfinished post-tensioning channel can all be seen in Figure 142; note the leveling screws in the post-tensioning channels.

Concrete in the longitudinal center joint and the post-tensioning channels were covered with burlap, heating coils and thermal blankets to ensure the concrete cured with the

Figure 141. Longitudinal joint formwork, November 28.

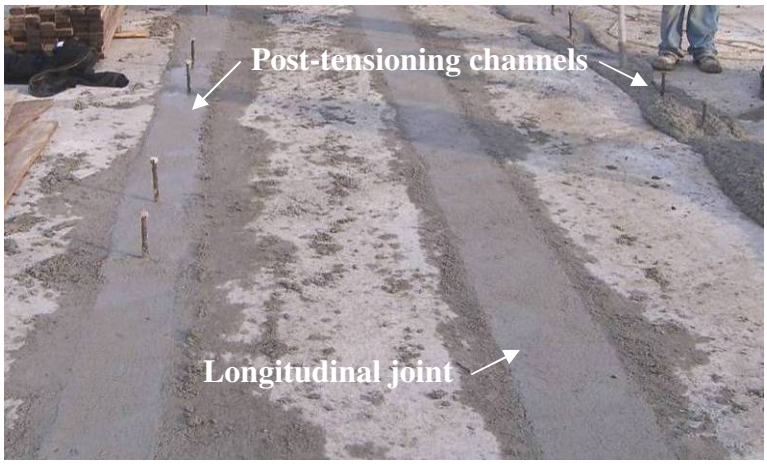

Figure 142. Longitudinal joint and one channel finished, November 28.

cold temperatures. The next day, November 29, the contractor fabricated the formwork for the abutment cap and wing walls and placed the reinforcement in the formwork; both sets of abutment caps and wing walls were placed on November 29. Next, external reinforcement for the barrier rail was added to the deck panels using embedded mechanical splicers. The reinforcement for the CIP portion of the abutment can be seen in Figure 143 and the finished abutment cap is shown in Figure 144. Note the No. 5 reinforcing bars for the guard rail system attached to the deck panels can also be seen in Figure 144.

Next, the contractor fabricated the formwork for the CIP barrier rails, (shown in Figure 145), tied the reinforcement cages to be placed in the formwork, and connected the

Figure 143. Reinforcement in the west abutment cap, November 29.

Figure 144. West abutment and wingwall, placed and finished, November 29.

external reinforcement to the deck panels using the embedded mechanical splicers. The reinforcement cage for the barrier rail in the formwork is shown in Figure 146. Both barrier rails were placed and finished on December 8; the barrier rail can be seen after being placed, before final finishing in Figure 147. After finishing, the barrier rails were covered with wet burlap and plastic for curing.

On December 11, the contractor began to 'strip' the formwork from the abutment caps and wing walls, and from the bottom of the post-tensioning channels and longitudinal

Figure 145. Barrier rail formwork, December 8.

Figure 146. Barrier rail reinforcement, December 8.

Figure 147. Barrier rail before final finishing, December 8.

joint. After the formwork was removed, the contractor was able to compact granular fill material behind the abutments and grade the road to the bridge deck. Forms for the barrier rails were stripped on December 12.

The last construction task for the bridge was to grind the surface of the bridge deck. On December 27, the surface of the deck was ground, however, due to equipment breakdown, grinding wasn't completed until December 28. Due to clearance issues with the grinding equipment, shown in Figure 148, the three feet adjacent to the barrier rails were not ground. Figure 149 shows the surface of the bridge deck after the surface was ground.

There were some difficulties encountered with the deck grinding process. Several areas of the transverse joints were not finished high enough, causing low and uneven areas on the deck. Even after grinding, there were several areas where the transverse and longitudinal joints had noticeable low areas. One such area between the transverse joint and the precast panels can be seen in Figure 150. After the bridge deck was ground, the completed bridge shown in Figure 151 was officially opened.

Figure 148. Bridge deck grinding equipment on site, December 27.

Figure 149. Bridge deck after the surface was ground, December 27.

Figure 150. Low area in one transverse joint after deck grinding, December 27.

Figure 151. Completed bridge, December 27.

6.2 Construction Feedback

The Boone County engineering staff, along with the prime contractor and the precast manufacturer, were interviewed to obtain feedback on the bridge replacement project. Information obtained can be categorized into three main areas: project positives, project negatives, and suggestions to possibly improve the construction of such bridges.

6.2.1 Feedback from the Boone County Engineering Staff

Boone County was the owner of the bridge and responsible for the construction inspection throughout the project. Bob Kieffer, Boone County Engineer, and Scott Kruse, Assistant to the Engineer, were both interviewed after the bridge was completed for feedback from the owner. During construction of the bridge, Dave Anthony was the Boone County Engineer, however, Mr. Kieffer, as Assistant Engineer, was intimately involved with the project. Mr. Kruse was the field engineer responsible for the construction inspection and was at the bridge site on a daily basis. A summary of the feedback from the Boone County engineering staff follows.

Positive aspects of the project:

- The precast substructure caps were all set in a short amount of time and without difficulty.
- The deck panels were all set in a short amount of time and without difficulty. The delivery of the panels caused most of the delay while setting the panels, not the actual process of setting the panels.

Negative aspects of the project:

- The county did not save any time or money with this project. While the county was aware the project would be slightly more expensive than traditional construction, the engineers were under the impression there would be a time-savings involved.
- The Boone County engineers are not familiar with pipe piling. Concrete encased piles would have been preferred over the steel pipe piles. Repainting the piles will be more maintenance for the county.
- Boone County felt the design calculations for the piles were not conservative. Several piles had to be tapped the day after initial driving to meet bearing requirements.
- The quality of the panel finish was poor.
- Construction progress had to wait on the precast elements. The substructure could have been set earlier but the abutments had not been fabricated. Panel placement was also delayed because the panels were not on site.
- The precast abutment and pier caps cracked during transportation.
- The Iowa State Ready Mix representative was never present on the construction site when concrete was being placed. There were difficulties with the specialty concrete mix and having someone present from the concrete supplier would have been helpful.

Suggestions for improvement:

- The backer rod used in the transverse joints did not work well. Instead of the backer rod, expansive spray foam might work better in the transverse joints.
- Better workmanship on all of the joints could have prevented the need for grinding the bridge deck. If grinding is absolutely necessary, joints should be finished one-fourth of an inch high to ensure the joints are ground smooth and prevent low spots.
- The panels did not need a roughened finish since the deck was to be ground. The joints would be easier to finish if the panels were not roughened.

6.2.2 Feedback from Petersen Contractors, Inc.

Petersen Contractors, Inc. (PCI) was the prime contractor for the Boone County bridge replacement project. Justin Clausen, project manager, and John Benjamin, foreman for the project, were both given a chance to offer feedback. Mr. Clausen compiled his feedback in a document which can be found in Appendix II. Mr. Benjamin was interviewed over the phone. A summary of the feedback from PCI follows.

Positive aspects of the project:

- Deck panel sizes worked out well.
- Precast pier caps worked well.
- Precast abutments worked well.
- Post-tensioning worked very well.

Negative aspects of the project:

- There were difficulties with the specialty concrete. The designer should have a better handle on the mix design of that concrete and the admixtures being specified.

- The formwork for grouting the post-tensioning channels and under the deck panels was time consuming (putting up the formwork took at least 100 man-hours, not including the time to strip the formwork).
- The deck grinding was poor. The ends of the deck couldn't be properly ground because of the gravel approaches.

Suggestions for improvement:

- Use a beam with a wider top flange to allow more room for the post-tensioning channel.
- Modify the pier diaphragm pour so that none of the deck panels have to be removed.
- Coordinate letting, shop drawings, fabrication, and construction so that cold weather does not become an issue. If the project was let in the fall, the winter could have been used for shop drawing submissions and approval and fabrication of precast elements and construction could begin immediately in the spring.. This way, construction would not have to wait for the fabrication and delivery of precast elements and construction would be finished before cold weather.
- Review the end panel anchorages to make tendon placement easier.
- An overlay on the bridge would eliminate problems associated with grinding the bridge deck.
- A precast barrier rail would be much faster than the CIP barrier rail used.
- Use precast wing walls instead of CIP. The formwork for the wing walls was also time-consuming.

6.2.3 Feedback from Andrews Prestressed Concrete

Andrews Prestressed Concrete fabricated all of the precast elements associated with this project. Teresa Nelson, project manager, compiled feedback in a document, which can be found in Appendix II. A summary of the feedback from Andrews Prestressed Concrete follows.

Positive aspects of the project:

- ISU and PCI were easy to work with.
- It was easy to resolve fabrication issues or mistakes and oversights in the plans.

Negative aspects of the project:

- The anchor plate was not quite the full depth of the panel. This made it very difficult to assure that the plate was suspended off of the casting bed.

Suggestions for improvement:

- Look into a larger size mesh in end panels to allow for larger openings to aid in placement and consolidation of concrete.
- Change the design of the anchor plate in the end panels.
- Use larger diameter holes for the post-tensioning tendon to allow pipe sleeves to pass thru in lieu of butting against the anchor plate.

6.2.4 Feedback from Iowa State University

Researchers at Iowa State University provided feedback based on the fabrication and construction of the substructure elements tested in the laboratory. T.J. Wipf and F.W. Klaiber, as Co-Principal Investigators for the laboratory testing provided some feedback, a summary of which follows.

Positive aspects of the project:

- Reinforcement and the connection between the pile and CMP were easy to fabricate.

Negative aspects of the project:

- CMP was not a standard size; had to be special ordered.
- Pipe piling was hard to find and not a common size used in Iowa; pipe was obtained out of state.

Suggestions for improvement:

- Use standard CMP sizes to reduce cost and eliminate special orders.
- Use piles that are standard in Iowa. This will make the piles easier to obtain and ensure owners and contractors are familiar with the product (see comments from Boone County Engineers Office).

6.3 Construction Summary

Construction for the replacement bridge over 120th Street began on July 19, 2006 and took 108 working days to complete (see Table 33 at the end of this section for important events, delays and corresponding dates). Demolition of the previous bridge was completed in one day. Rain delayed the construction progress at the end of August and through most of September; in total, 21 working days were lost due to rain or wet site conditions. The piles were driven in late September and the precast substructure was set in early October; the girders and deck panels were set in late October after the substructure was complete. Transverse concrete joints were placed in late October and early November, during which time the post-tensioning tendons were placed and formwork for the post-tensioning channels and longitudinal center joint was installed.

Construction was delayed again due to cold weather effects on the concrete joints, therefore, the joints had to be heated to ensure the concrete reached the required strength. The deck was post-tensioned in late November and the post-tensioning channels and longitudinal joint were cast with concrete. In December, the CIP abutment caps, wing walls and barrier rails were placed. In late December, the excavated area behind the abutments and wingwalls were backfilled and compacted, the road was graded to the bridge deck elevation, and the bridge deck was ground smooth. After the bridge deck was ground, the completed bridge was opened to the public (December 28, 2006).

Feedback was received from the Boone County engineering staff, PCI contractors, and Andrews Prestressed Concrete on positive and negative aspects of the project and possible ways to improve the construction process. Some of the common comments include:

- The precast elements were all set without difficulty.
- There were difficulties with the specialty concrete mix.
- The deck grinding operation needs to be improved.

Table 33. Construction events, dates, and durations.

Event	Date	Days
Construction begins	07/19/06	1
Previous bridge demolition and removal	07/24/06	5
Rain delay	08/02/06	9
Excavation and structure removal	08/03/06	15
Rain delay and repairing access road	09/11/06	6
Set up, pile driving, cutting and stud welding (abutments and west pier)	09/14/06	11
Setting precast abutments and west pier cap	10/04/06	1
Grouting piles in precast elements	10/05/06	1
Set up, pile driving, cutting, and stud welding (east pier)	10/09/06	3
Setting east pier cap	10/12/06	1
Grouting piles in east pier cap	10/13/06	1
Painted primer on pipe piles	10/16/06	2
Rain delay	10/17/06	3
Setting precast girders	10/24/06	1
Setting precast deck panels	10/25/06	2
Rain delay	10/26/06	1
Fabrication and placing pier diaphragms	10/30/06	5
Leveling deck panels	11/06/06	3
Rain/snow delay	11/10/06	1
Threading post-tensioning tendons	11/13/06	3
Forming CIP abutment diaphragms and longitudinal joints	11/13/06	8
Delay from cold weather/transverse joint strength	11/22/06	3
Post-tensioning the bridge deck and placing longitudinal joints	11/28/06	1
Placing CIP abutment diaphragms and wingwalls	11/29/06	2
Cold weather delay	11/30/06	1
Fabrication of barrier rails	12/04/06	3
Cold weather delay	12/07/06	1
Placing barrier rails and end sections	12/08/06	2
Stripping formwork and backfilling abutments	12/12/06	2
Cleaning site and shaping bridge approaches	12/14/06	2
Placing rip rap, stone, and guardrail	12/18/06	2
Delay waiting for the grinding operation	12/20/06	4
Grinding the bridge deck	12/27/06	2
Total Days	**108**	

CHAPTER 7. SUMMARY AND CONCLUSIONS

7.1 Summary

This chapter presents a summary of the laboratory testing results, the post-tensioning results for the tendons and deck panels, and a summary of the construction documentation. Conclusions are also presented based on the results obtained from testing (laboratory and field) and feedback from the Boone County Engineer's Office, PCI, Andrews Prestressed Concrete, and the research team.

7.1.1 Laboratory Testing Summary

In total, eight laboratory tests were completed: five single pile abutment tests, two double pile abutment tests, and one pier cap test. Each single pile specimen resisted over four times the unfactored design load without any sign of failure. The double pile specimen supported approximately twice the unfactored design load without failure, even though the CMPs were only 70% full of concrete. Limiting the depth of the concrete was done in an attempt to actually fail the specimen. The experimental cracking moment from the double pile test agreed with the experimental cracking moment determined from the single pile tests. The pier cap resisted over five times the unfactored design load without any signs of failure. It was not possible to completely fail any of the eight laboratory specimens since their strength exceeded the capacity of the laboratory loading system.

7.1.2 Post-Tensioning Summary

Post-tensioning of the Boone County bridge took place on the morning of November 28, 2007. The entire operation took approximately four hours, including the time needed for data collection. Vibrating wire gages were used to measure the force occurring in several of

the post-tensioning strands, to measure the losses during the post-tensioning process, and to measure the distribution of the post-tensioning forces through the deck panels. The forces in the strands, calculated using data from the VWGs, were within two percent of the forces provided by the contractor. After the post-tensioning process was complete, all of the strands were within the tolerances specified by the Iowa DOT. The strains in the deck panels indicated that the post-tensioning force is distributed through the end panels to the interior deck panels almost immediately. Strains (stresses) measured in the panels were relatively constant throughout the deck, regardless of the location of the panel in the bridge, or the distance from the post-tensioning channels.

7.1.3 Construction Documentation Summary

Construction on the Boone County replacement bridge began on July 5, 2007, after demolition of the previous bridge at the site, which began on July 24. There were delays in construction due to heavy rain in August and September; a total 15 working days were lost to due rain and/or wet conditions at the site in August and September alone. In September, piles were driven and erection of the precast substructure began October 4. The pile connections in the abutments and west pier cap were grouted in place October 5 and the east pier cap connections were grouted October 13. Once the grouted concrete reached strength, erection of the superstructure began on October 24.

The bridge girders were set on October 24; on the next day, the interior deck panels were set. The panels were leveled and the CIP diaphragms over the two piers were placed on October 30. End panels were delivered and set in place on November 8, which was followed by the casting of the interior transverse joints. Due to weather conditions, the transverse joints at the end panels (which had to be placed later when the end panels reached the desired

strength) were slow to reach the required strength for post-tensioning. The post-tensioning operation was delayed until November 28, when the deck was post-tensioned and all of the longitudinal joints were placed.

Once the deck was finished, the contractor formed and cast the CIP portion of the abutments, the wingwalls, and the barrier rails. After the concrete reached the desired strength, the formwork was stripped, the approaches were backfilled and graded to the bridge deck elevation. On December 27, the bridge deck was ground and the bridge was opened to the public. The total construction time for the replacement bridge was 108 working days, with 21 days lost to rain and wet conditions throughout the project, and 9 days lost for miscellaneous reasons (78 actual working days).

7.2 Conclusions

7.2.1 Laboratory Testing Conclusions

The following conclusions are based on the eight laboratory tests of the substructure elements for the Boone County replacement bridge:

- The abutment section capacity is at least 4.5 times greater than the unfactored design load of 80 kip per pile.
- The pier cap section capacity is at least 5.3 times greater than the unfactored design load of 72 kip per pile.
- The CMP affected the behavior and crack pattern in the abutment sections, but had no influence in their capacity.
- The CMP had no apparent effect on the pier cap section.

- The measured cracking moments for the abutment and pier cap, based on observation and strain data, were approximately 264 kip-feet and 312 kip-feet, respectively.
- Essentially no differential movement was detected between the precast concrete and the concrete in the CMP in any of the abutment specimens or pier cap specimen. The movement measured was less than 0.0033 inches in every test.
- No movement was detected in the shear tests; measured movement was less than 0.0005, the LVDT precision.
- Shear failure was not detected between the H-pile in the abutment and the concrete in the CMP.

7.2.2 Post-Tensioning Tendon Forces and Deck Panel Stress Conclusions

The following conclusions are based on the verification of the post-tensioning forces and resulting strains in the precast deck panels:

- Small losses due to seating and elastic shortening of the bridge deck (less than 0.05 percent of the initial force) were measured during the post-tensioning operation.
- The forces in the strands provided by the contractor are in agreement with the forces measured in the four instrumented strands.
- The forces in all of the strands were within the required Iowa DOT tolerances and remained within these tolerances after post-tensioning was completed.
- The force from post-tensioning was distributed evenly through the deck panels, regardless of the panels' location in the bridge or distance from the post-tensioning channels.
- Stresses calculated from the measured strains in the deck were less than allowable compressive stress due to post-tensioning (AASHTO, 1996). The maximum

measured stress (1,835 psi) was 45 percent lower than the maximum allowable compressive stress (4,080 psi).

7.2.3 Conclusions from Construction Documentation

The following conclusions were based on the construction documentation of the Boone County replacement bridge and the feed back provided by the Boone County Engineer's Office, PCI, and Andrews Prestressed Concrete:

- Construction began on July 5 and was completed on December 27, 78 days of actual construction.
- Delays in construction were caused by heavy rain and wet conditions (21 days).
- Setting all of the precast elements went quickly and smoothly with no problems.
- It was difficult to meet the slump and entrained air requirements for the specialty concrete mix used in the CMPs and in the transverse and longitudinal joints of the deck. The admixture to improve the workability of the mix only lasted about twenty minutes in the field.
- The post-tensioning process went smoothly and without any major difficulties. It is important to note that the post-tensioning was performed by the prime contractor (PCI), without any prior post-tensioning experience, with the supervision of a technical expert.
- Deck grinding was difficult; the entire deck could not be ground and low spots due to poor concrete finishing of the transverse joints were left on the deck.

CHAPTER 8. RECOMMENDATIONS FOR FURTHER INVESTIGATION

8.1 Recommendations for Further Investigation

This chapter summarizes the need for additional research on the precast bridge substructure, recommendations for monitoring the post-tensioned bridge deck, and recommendations to improve the construction sequence of this replacement bridge system in the future.

8.1.1 Substructure Recommendations

The following recommendations for the bridge substructure are based on the laboratory testing of the substructure elements:

- The cross-section and reinforcement in the abutment and pier cap should be evaluated to produce more economical sections.
- Additional research is required to quantify the effects of the CMP on the abutment section.

8.1.2 Post-Tensioning Recommendations

The following recommendation is based on the verification of the post-tensioning of the Boone County bridge:

- Long-term monitoring of the bridge should be performed using the embedded instrumentation on the post-tensioning tendons and in the deck panels.

8.1.3 Construction Recommendations

The following recommendations were made based on the construction documentation of the Boone County bridge and the feedback received from the Boone County Engineer's Office, PCI, and Andrews Prestressed Concrete:

- Construction scheduling for research projects should consider the time needed for shop drawings and approvals, and the schedule should be coordinated to avoid cold weather.
- Fabrication of precast elements should begin before on-site construction so progress in the field is not delayed by the fabrication of precast elements.
- The bridge deck grinding operation should be evaluated to produce a better riding surface for the bridge.
- Research is recommended on the specialty concrete mix to determine a mix design that meets the design requirements and is easier to place in the field.
- Additional research on this deck panel system is recommended to reduce the time required to install the formwork for the post-tensioning channels and center longitudinal closure joint.
- To reduce total construction time, the use of precast abutment caps, wingwalls, and barrier rails should be investigated (i.e. eliminate the need for the CIP concrete).

APPENDIX I TEST DATA

Table 34. Slump test results.

Test Name	Slump (in.)	
	Precast Concrete	Grouted Concrete
ASC1	3	4.5
ASC2	3	4.5
ASO1	3	4.5
ASC3	3.75	3.5
ASO2	3.75	3.5
ADC1	3.5	4.0
ADC2	3.5	4.0
PSC1	3.75	3.5

ASC1 Results: Figure 152 through Figure 154

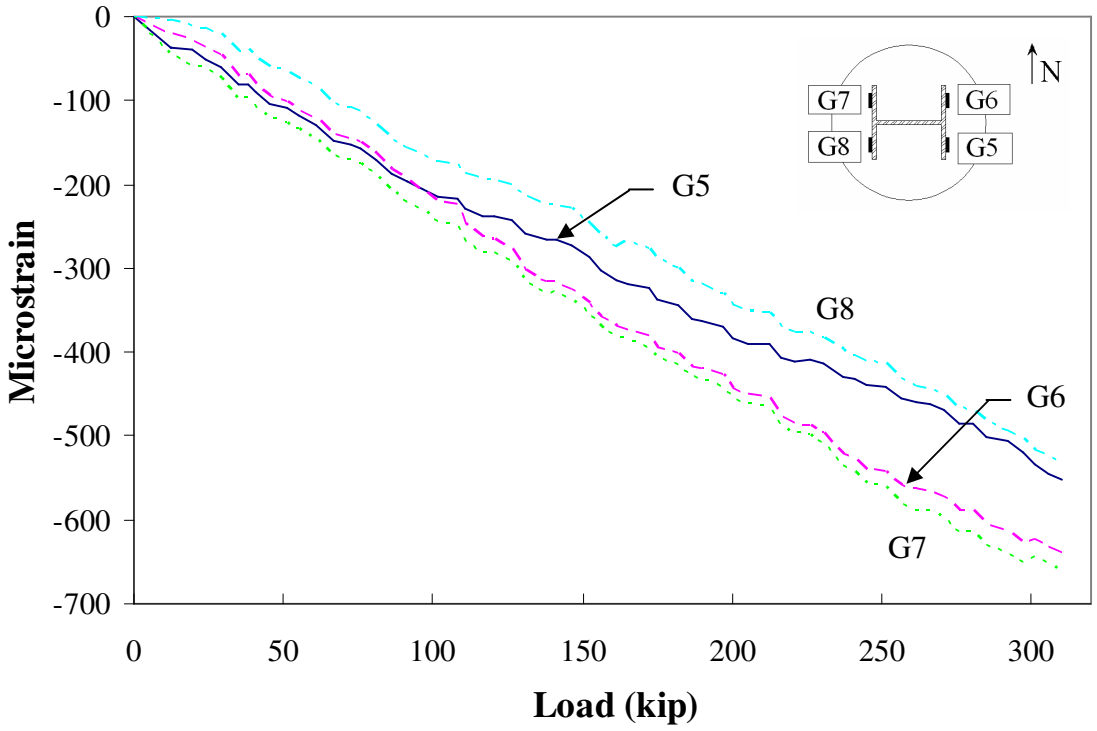

Figure 152. Steel strain for ASC1.

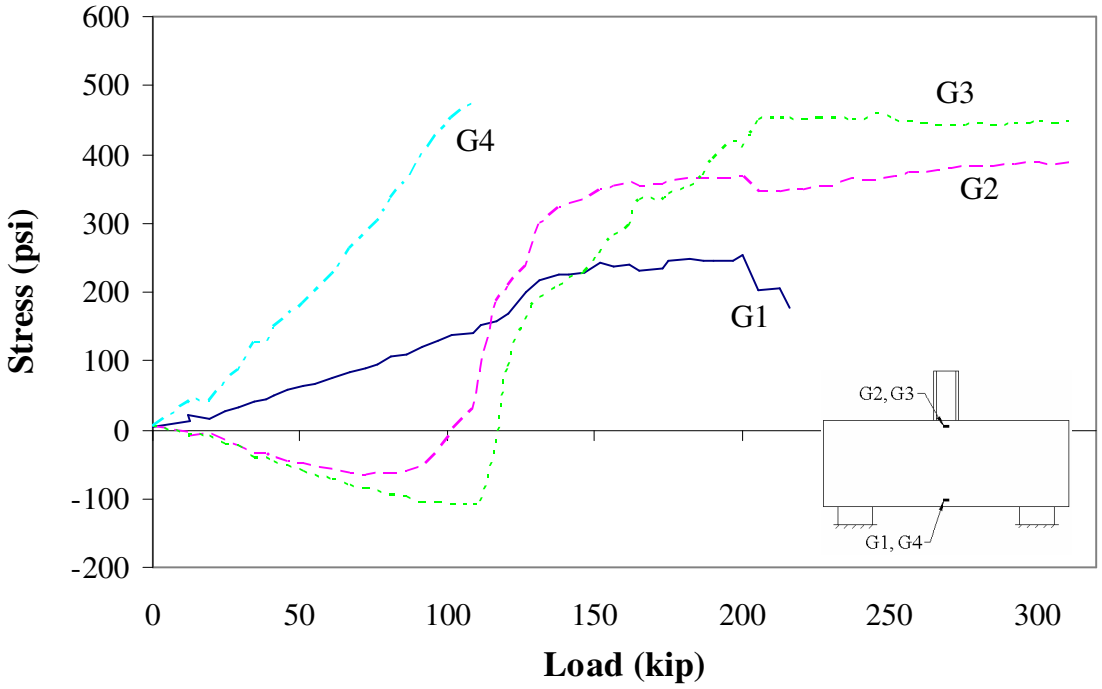

Figure 153. Concrete stress in ASC1.

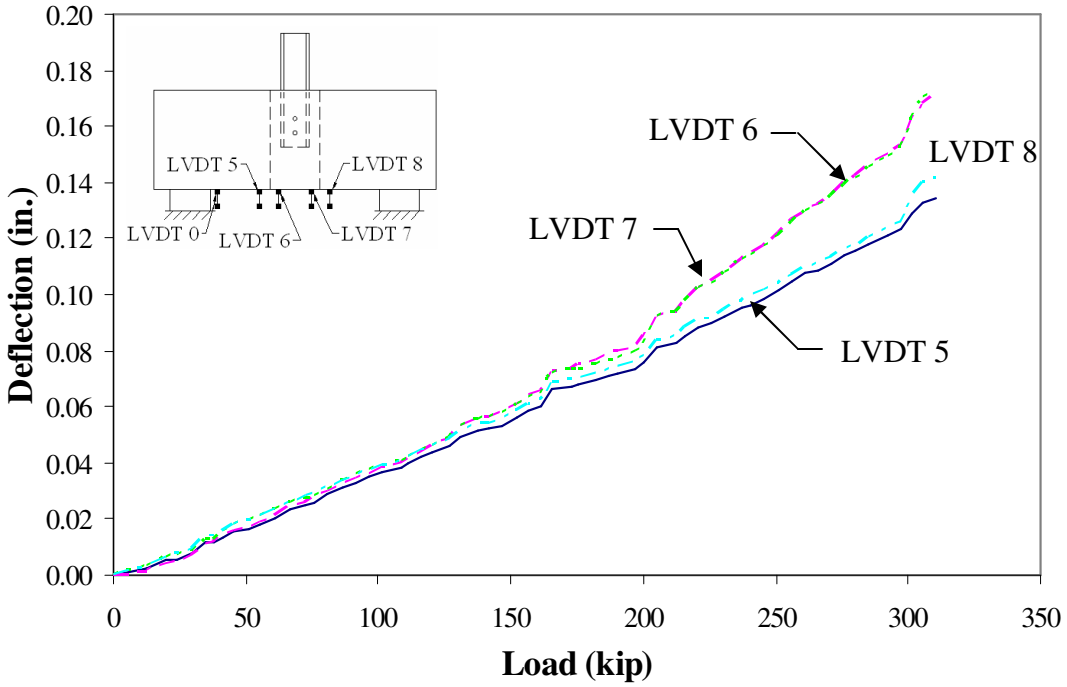

Figure 154. Total deflection for ASC1.

ASC2 Results: Figure 155 through Figure 157

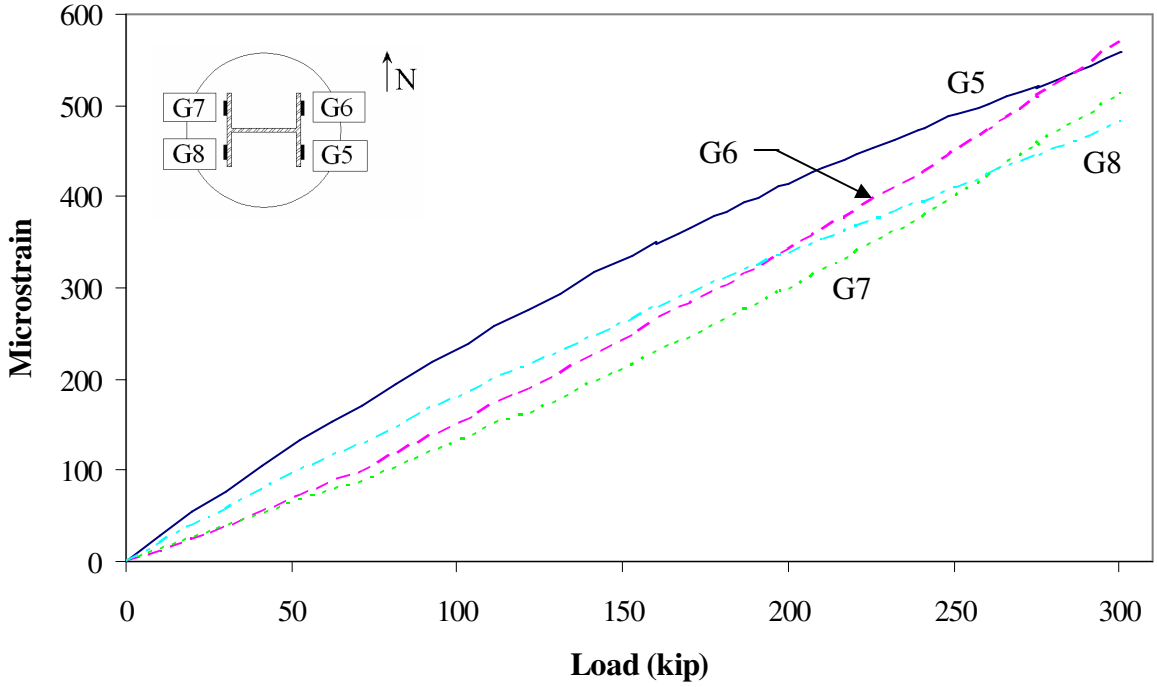

Figure 155. Steel strain for ASC2.

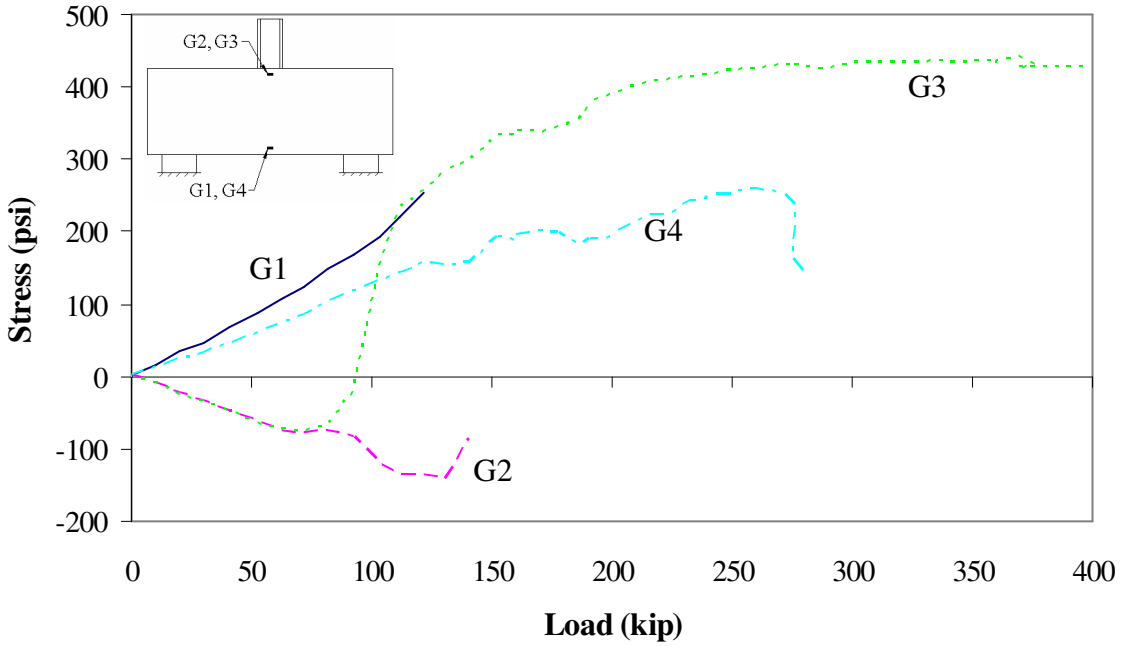

Figure 156. Concrete stress in ASC2.

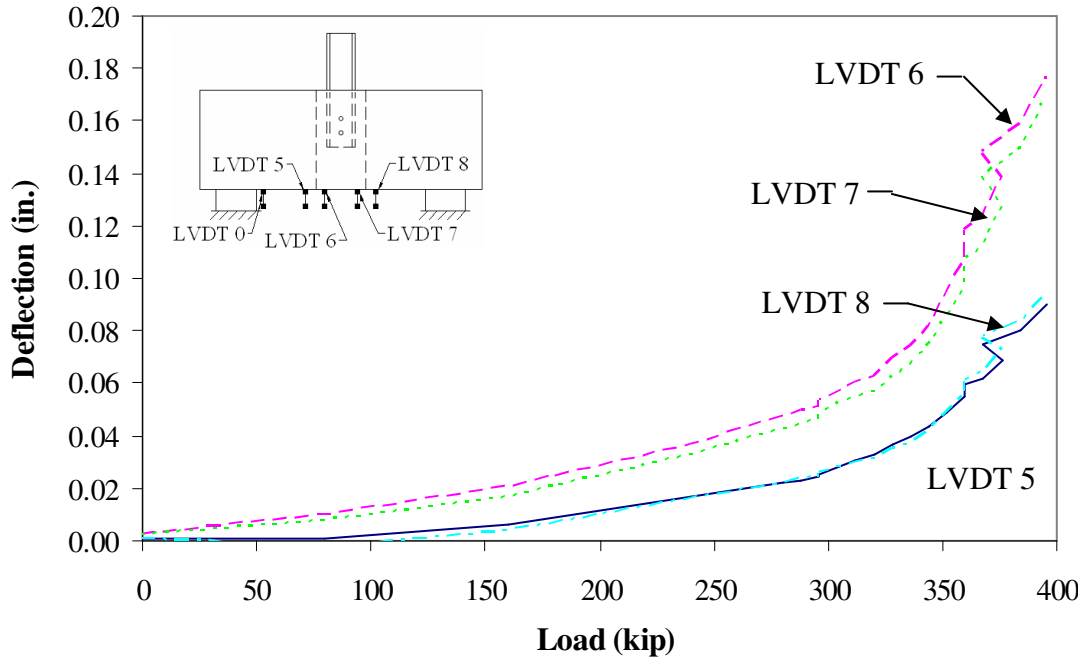

Figure 157. Total deflection for ASC2.

ASO1 Results: Figure 158 through Figure 160

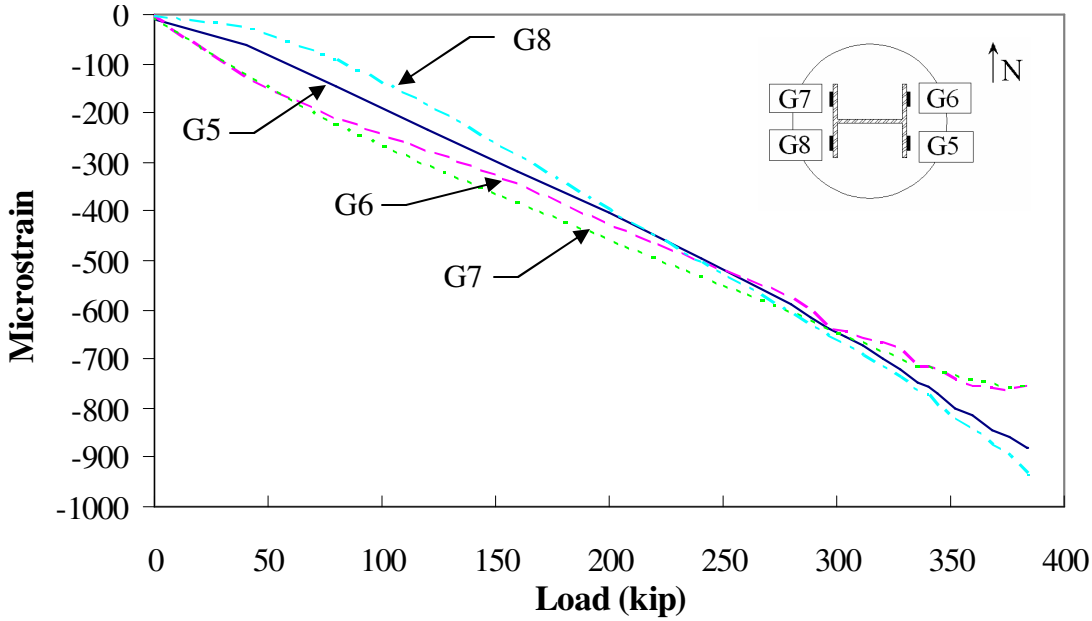

Figure 158. Steel strain for ASO1.

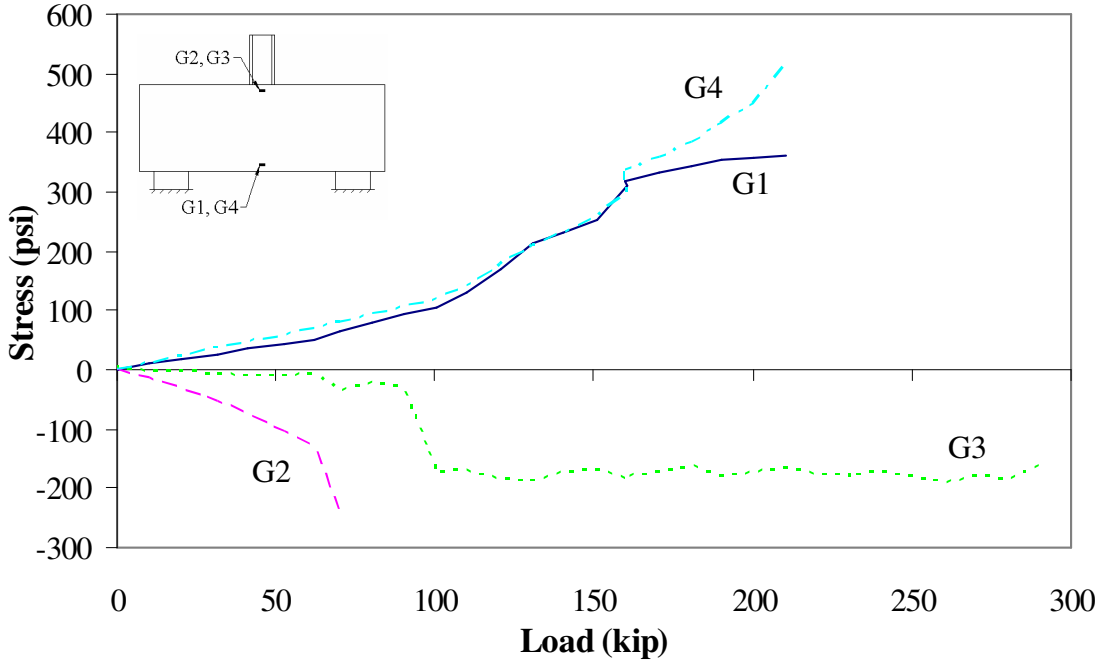

Figure 159. Concrete stress for ASO1.

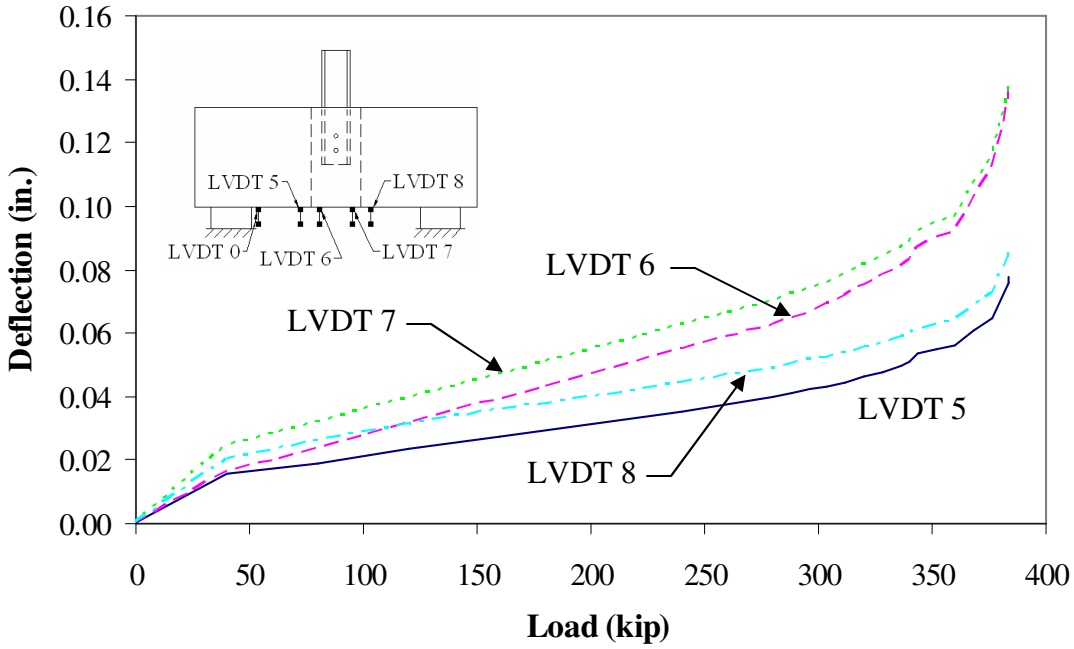

Figure 160. Total deflection for ASO1.

ADC2 Results: Figure 161 through Figure 166

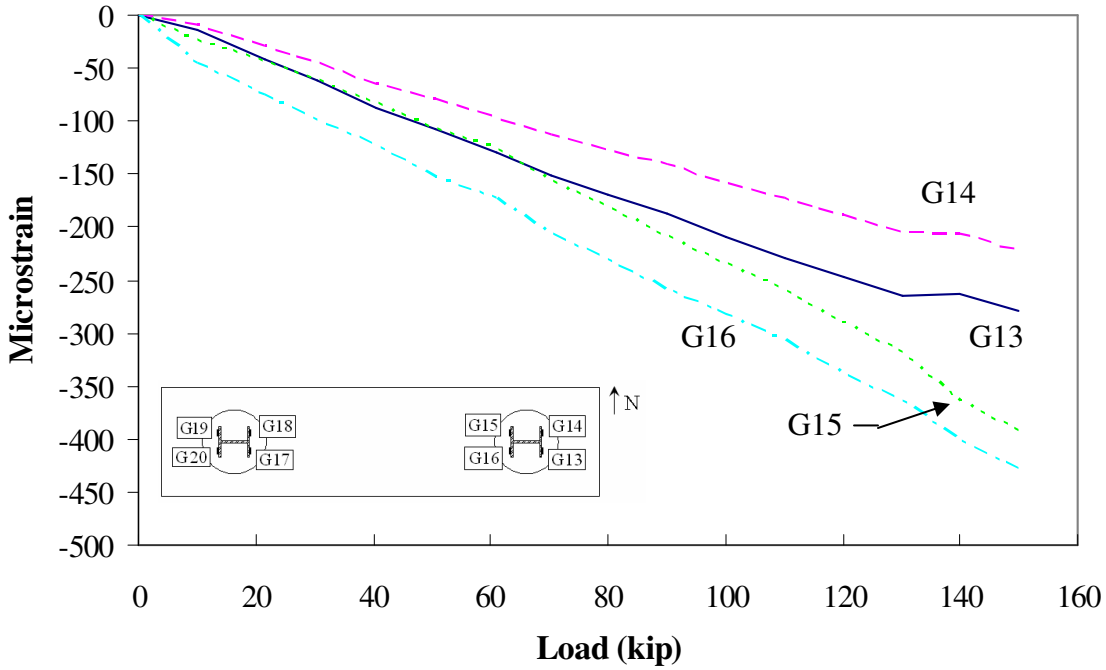

Figure 161. East pile steel strain for ADC2.

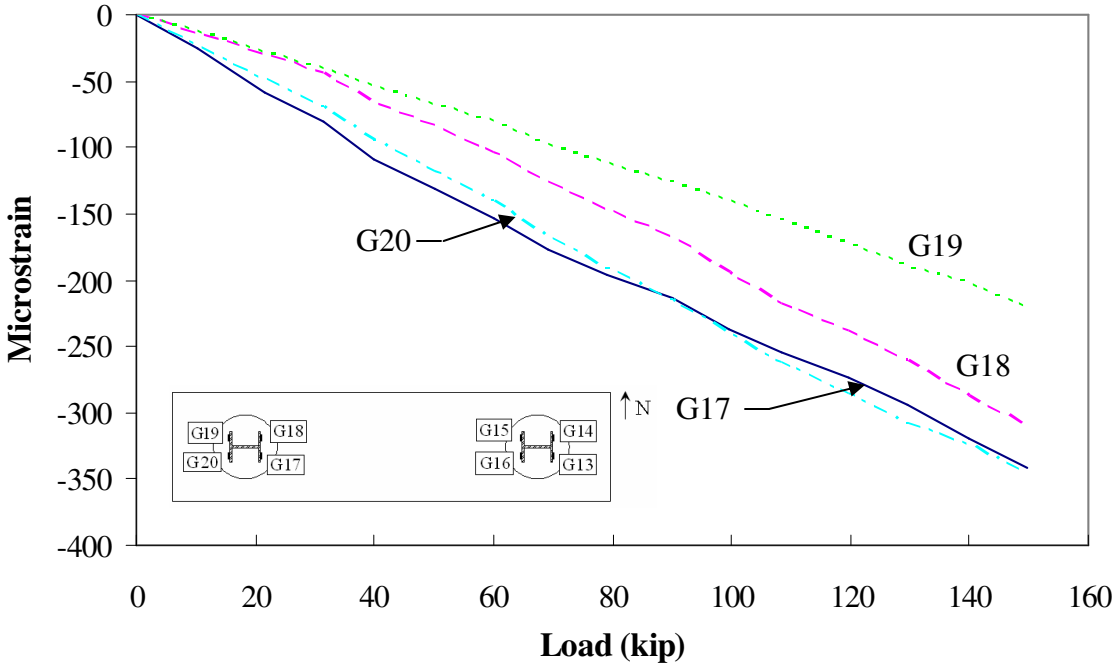

Figure 162. West pile steel strains for ADC2.

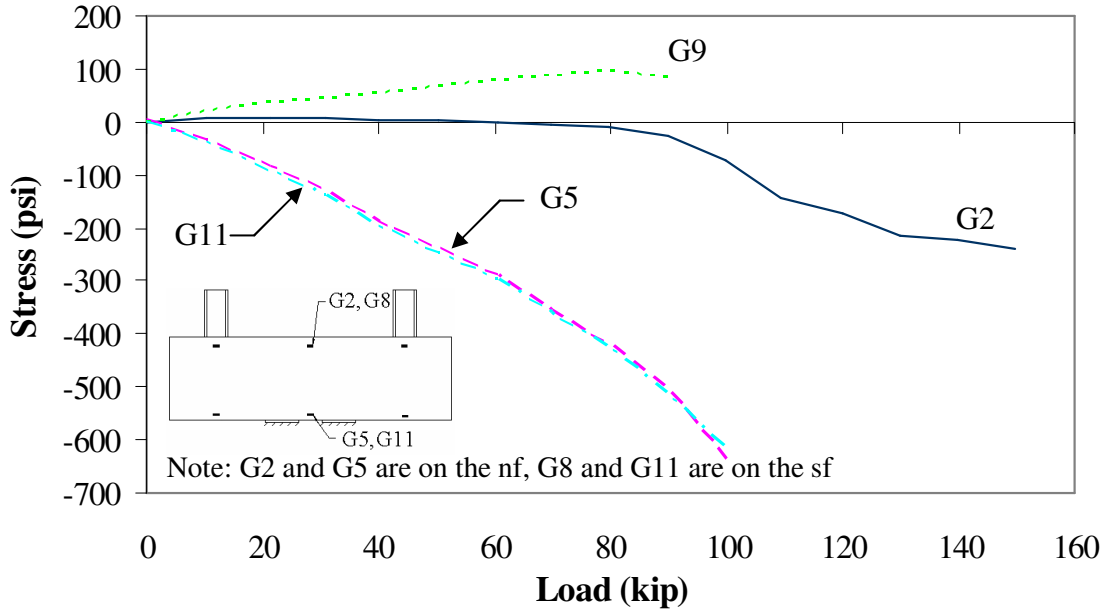

Figure 163. Concrete stresses at the center of ADC2.

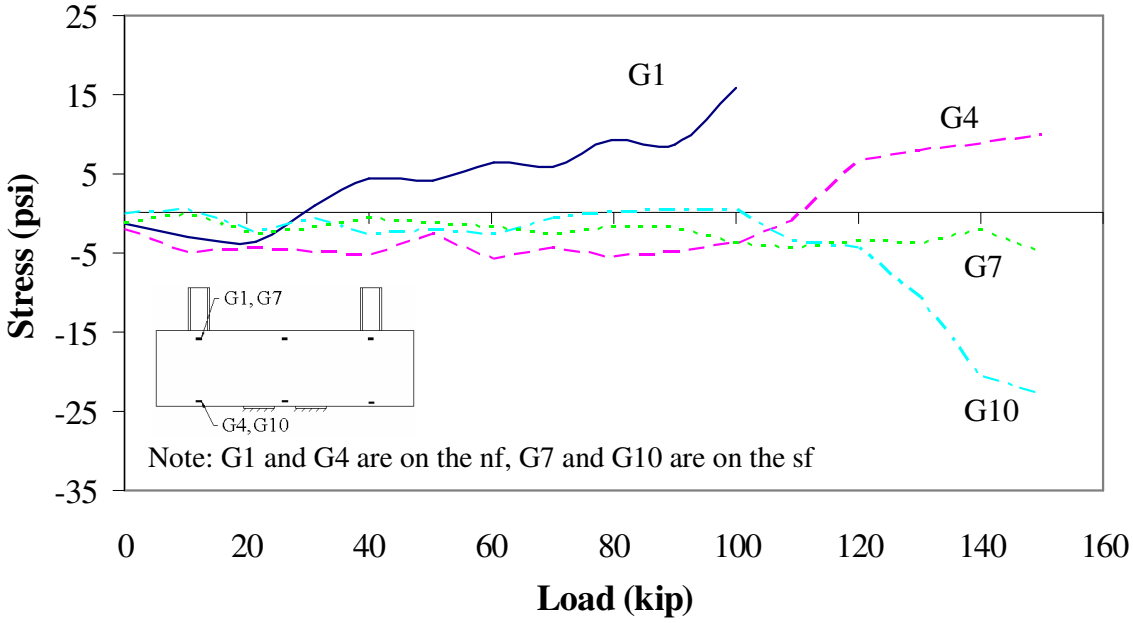

Figure 164. Concrete stresses at the east pile of ADC2.

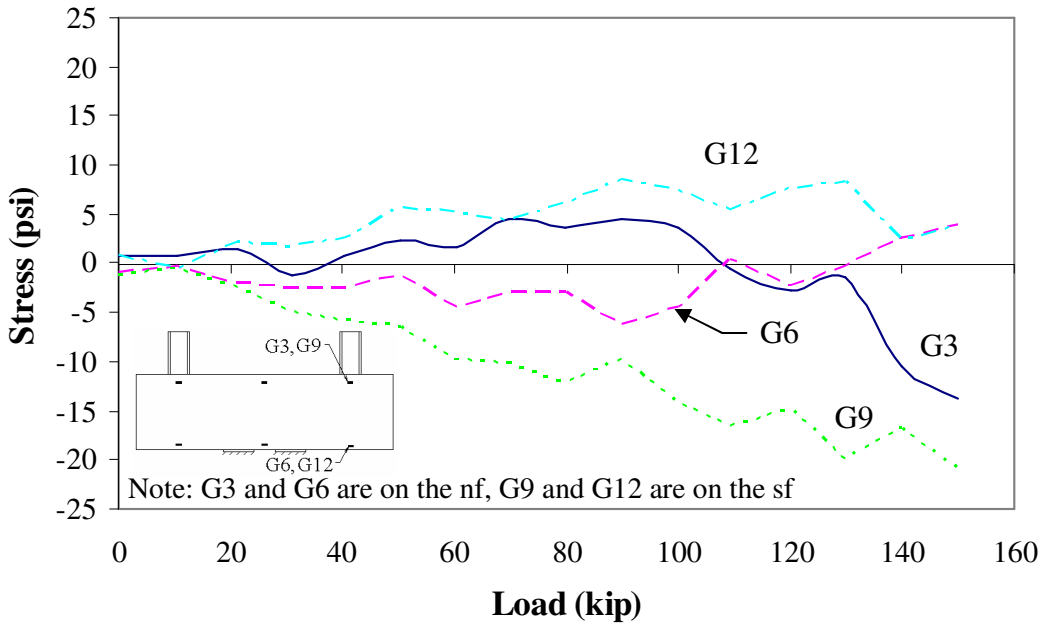

Figure 165. Concrete stresses at the west pile of ADC2.

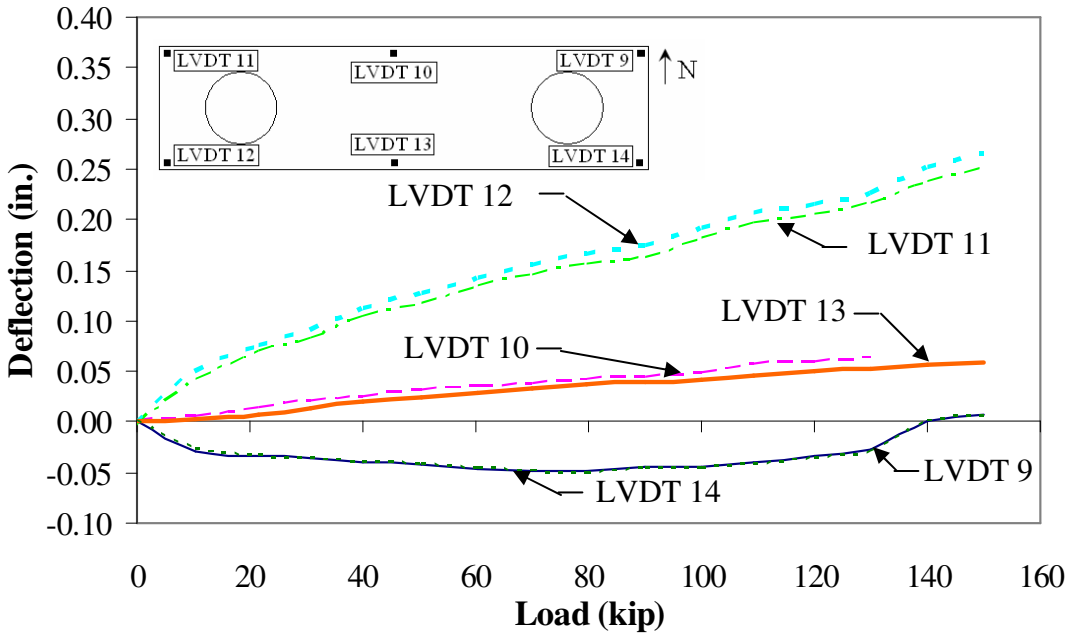

Figure 166. Total deflections for ADC2.

Shear Test 2 Results: Figure 167 through Figure 169

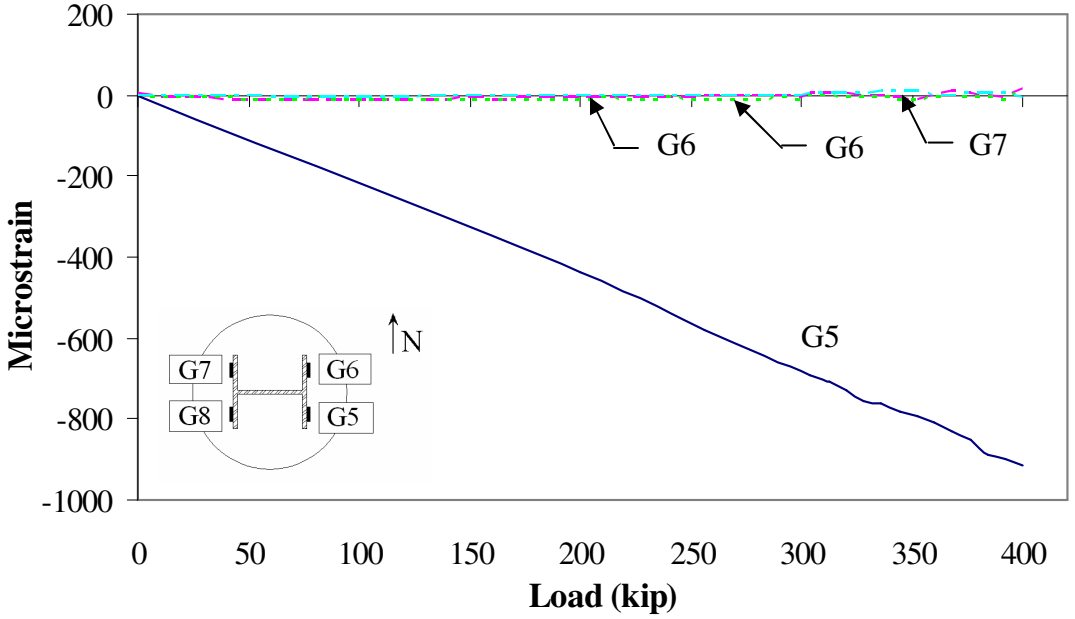

Figure 167. Steel strain for Shear Test 2.

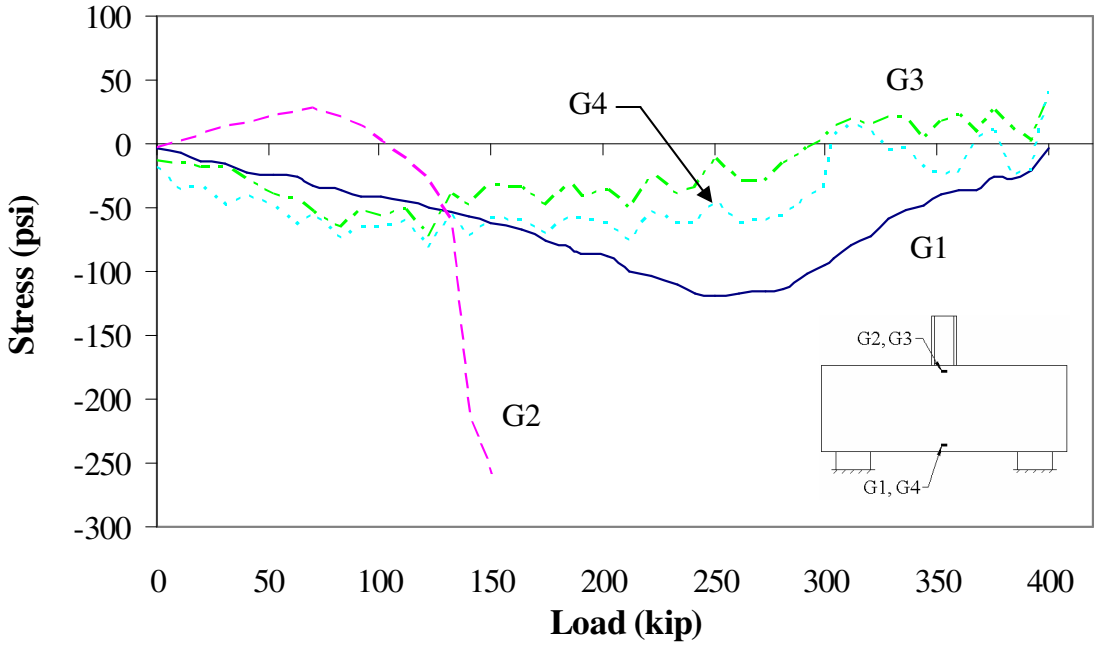

Figure 168. Concrete stress for Shear Test 2.

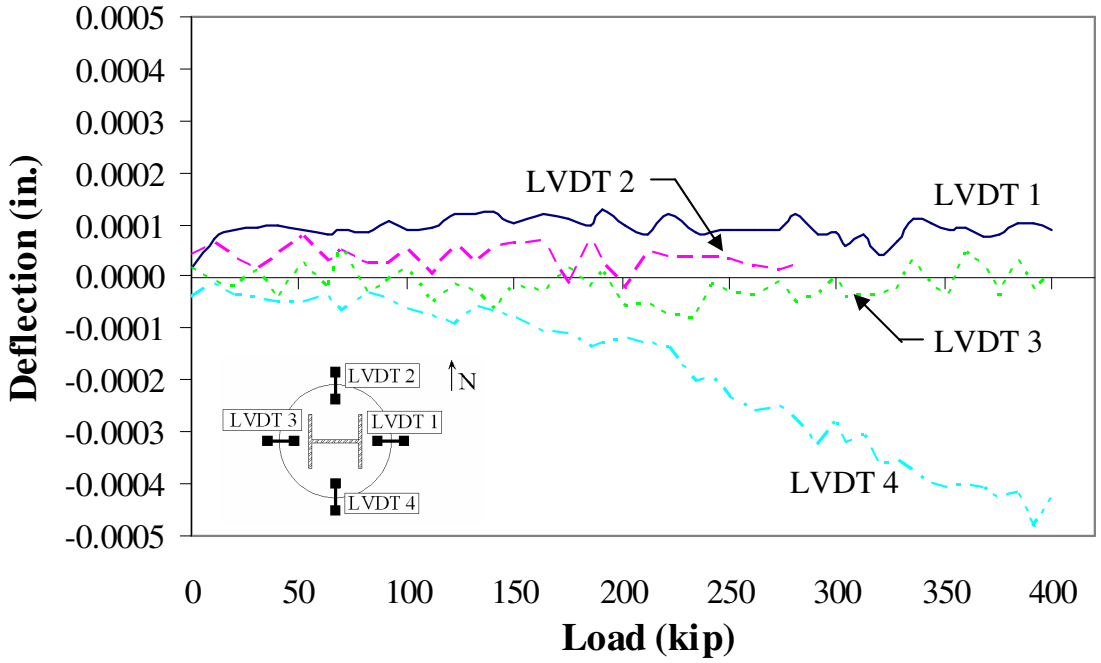

Figure 169. Top deflection for Shear Test 2.

Shear Test 3 Results: Figure 170 through Figure 172

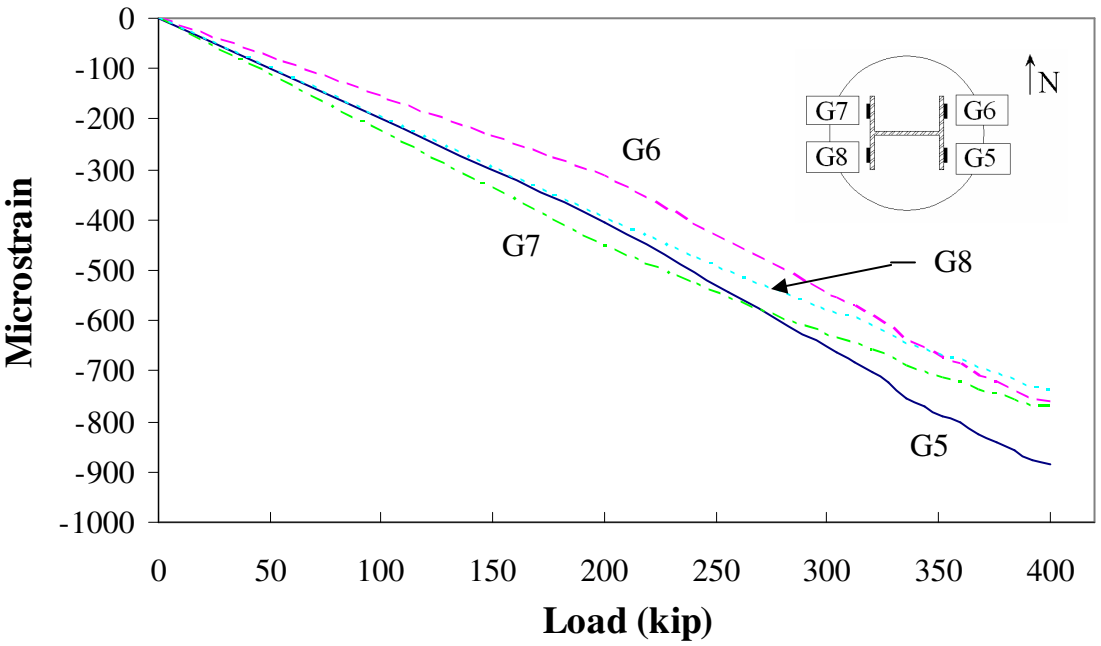

Figure 170. Steel strain for Shear Test 3.

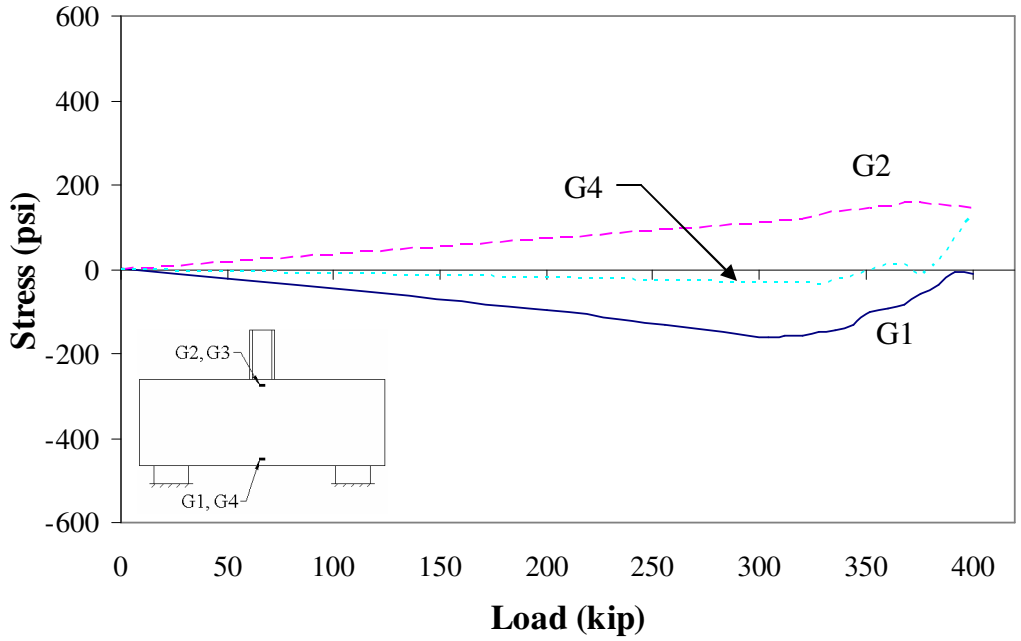

Figure 171. Concrete stress for Shear Test 3.

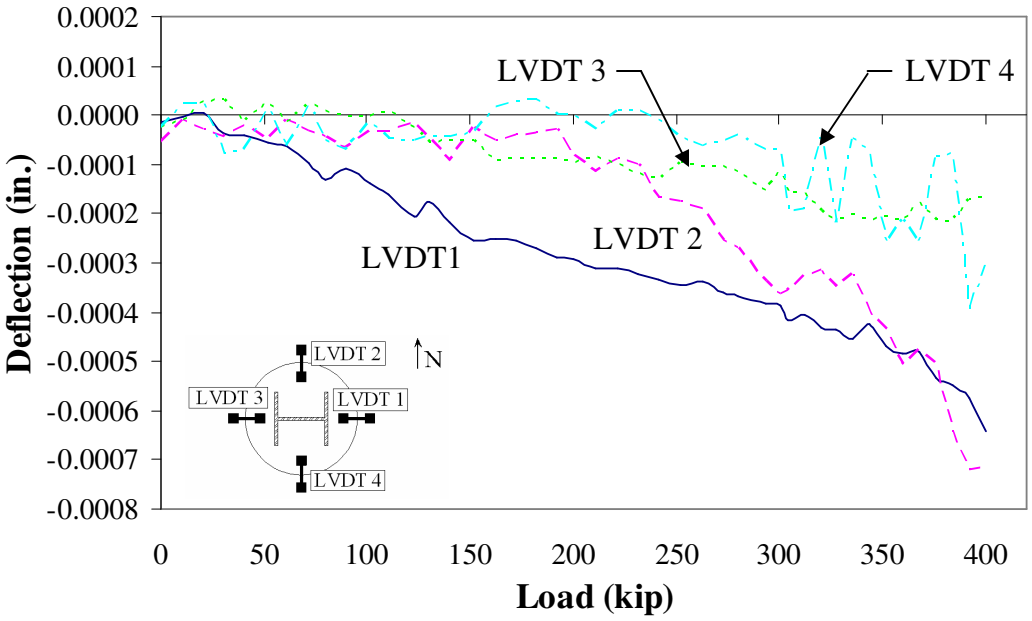

Figure 172. Top deflection for Shear Test 3.

Shear Test 4 Results: Figure 173 through Figure 175

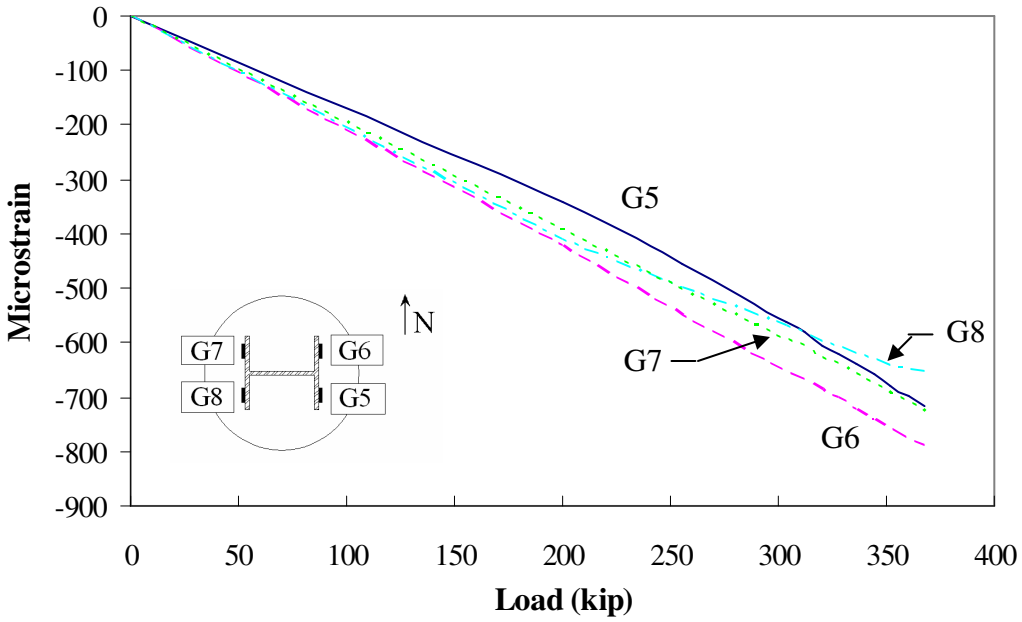

Figure 173. Steel strain for Shear Test 4.

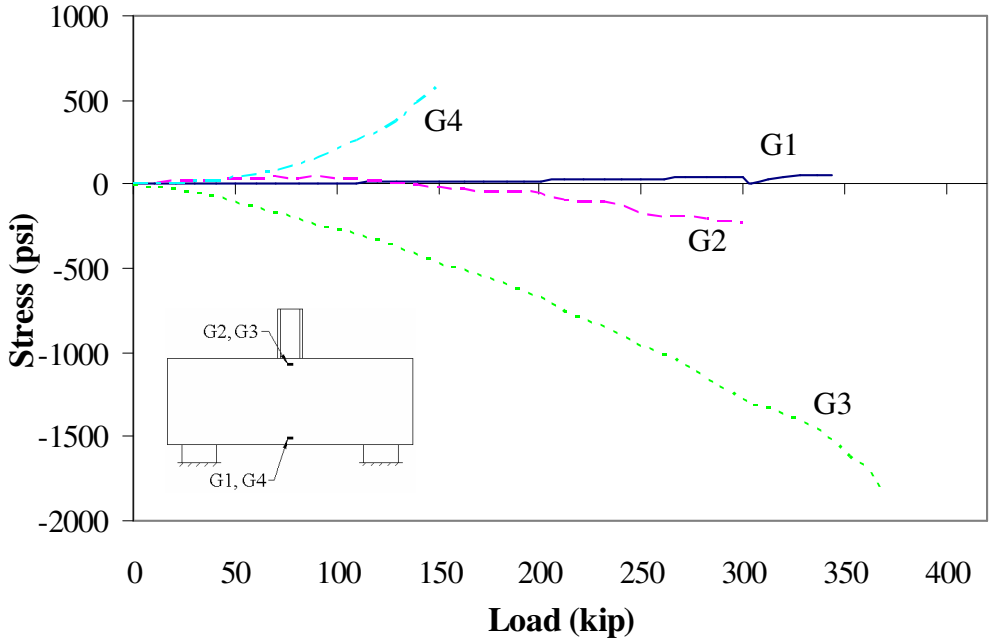

Figure 174. Concrete stress for Shear Test 4.

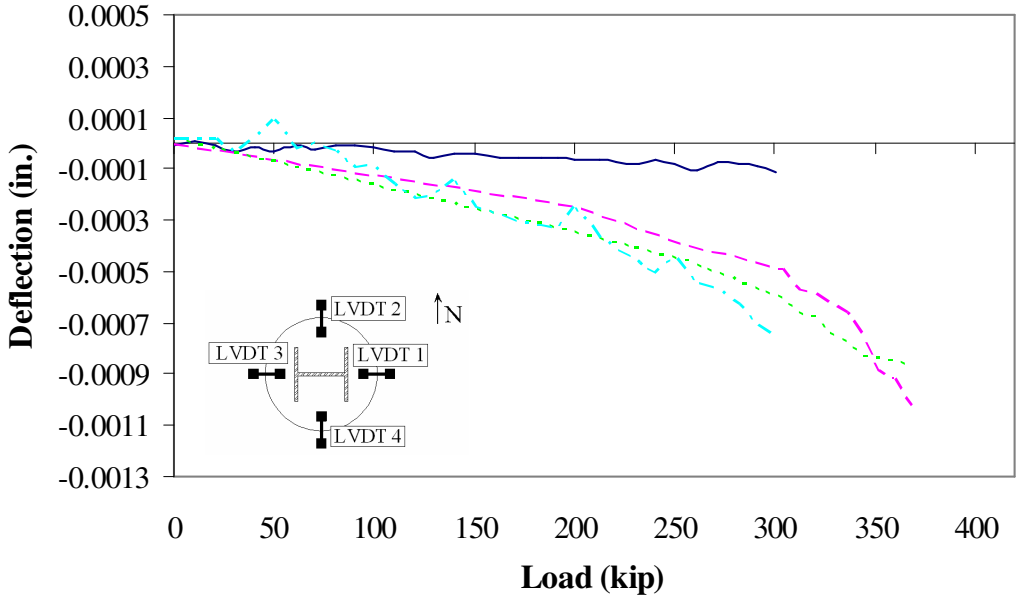

Figure 175. Top deflection for Shear Test 4.

Post-Tensioning Test Data: Table 35 through Table 44

Table 35. Post-Tensioned Strand Vibrating Wire Gage Information.

Gage Number	Correction (in/digit)	Serial Number
1	0.00002397	06-22965
2	0.00002456	06-22962
3	0.00002453	06-22964
4	0.00002468	06-22961
5	0.00002444	06-22960
6	0.00002457	06-22966
7	0.00002461	06-22959

Table 36. Gage 1 Original Post-Tensioning Data.

Reading Number	R (Digits)	K	T (ºC)
0	2573.7	-	15.6
1	4681.8	7.443E-05	16.4
2	4677.9	7.440E-05	16.9
3	4654.2	7.423E-05	17.8
4	4650.0	7.421E-05	17.8
5	4646.6	7.418E-05	18.5
6	4646.5	7.418E-05	18.3
7	4643.5	7.416E-05	19.0
8	4627.6	7.405E-05	19.8

Table 37. Gage 2 Original Post-Tensioning Data.

Reading Number	R (Digits)	K	T (ºC)
0	2581.3	-	15.4
1	4618.2	7.580E-05	16.5
2	4609.4	7.574E-05	17.0
3	4585.6	7.557E-05	17.8
4	4580.2	7.553E-05	17.7
5	4577.4	7.551E-05	18.4
6	4577.7	7.551E-05	18.3
7	4574.1	7.548E-05	18.9
8	4558.5	7.537E-05	19.6

Table 38. Gage 3 Original Post-Tensioning Data.

Reading Number	R (Digits)	K	T (ºC)
0	2408.1	-	15.5
1	4464.6	7.460E-05	16.7
2	4455.4	7.453E-05	17.1
3	4414.8	7.424E-05	17.6
4	4406.9	7.418E-05	17.7
5	4404.4	7.416E-05	18.3
6	4404.4	7.416E-05	18.3
7	4400.8	7.414E-05	18.7
8	4375.6	7.395E-05	19.3

Table 39. Gage 4 Original Post-Tensioning Data.

Reading Number	R (Digits)	K	T (ºC)
0	2533.3	-	15.6
1	4564.3	7.578E-05	16.7
2		4.255E-05	17.1
3	4533.9	7.556E-05	18.1
4		4.255E-05	18.1
5		4.255E-05	18.8
6	4520.5	7.546E-05	18.7
7	4517.2	7.544E-05	19.3
8	1500.0	5.347E-05	19.8

Table 40. Gage 5 Original Post-Tensioning Data.

Reading Number	R (Digits)	K	T (ºC)
0	2372.3	-	15.4
1	2390.7	5.937E-05	16.3
2	4425.2	7.404E-05	16.7
3	4413.3	7.395E-05	17.3
4	4410.6	7.393E-05	17.6
5	4402.3	7.387E-05	18.3
6	4402.6	7.388E-05	18.1
7	4401.1	7.387E-05	18.6
8	4385.5	7.375E-05	19.5

Table 41. Gage 6 Original Post-Tensioning Data.

Reading Number	R (Digits)	K	T (ºC)
0	2302.1	-	15.5
1	2325.3	5.921E-05	16.5
2	2349.6	5.939E-05	16.9
3	2349.7	5.939E-05	17.5
4	2266.5	5.879E-05	17.7
5	2269.4	5.881E-05	18.1
6	4339.5	7.381E-05	18.0
7	4337.1	7.379E-05	18.4
8	4333.5	7.377E-05	19.0

Table 42. Gage 7 Original Post-Tensioning Data.

Reading Number	R (Digits)	K	T (ºC)
0	2598.8	-	15.4
1	2652.1	6.168E-05	16.4
2	2652.5	6.168E-05	16.7
3	2654.5	6.170E-05	17.5
4	2641.6	6.161E-05	17.5
5	4637.0	7.609E-05	18.0
6	4631.4	7.605E-05	18.0
7	4617.2	7.595E-05	18.4
8	4604.4	7.586E-05	18.8

Table 43. Final Post-Tensioning Strand Vibrating Wire Gage Data.

Gage	Final Reading (Digits)	Final Temperature (ºC)
1	4627.6	17.3
2	4558.5	17.2
3	4375.6	16.9
4	4517.1	17.3
5	4385.5	17.0
6	4333.5	16.7
7	4604.4	16.6

Table 44. Final Post-Tensioning Deck Panel Vibrating Wire Gage Data.

Gage	Final Reading (μ-strain)
A1	377
A2	378
B2	368
B3	370
C1	368
C2	365
C3	375
C4	363
D1	378
D2	372
D3	361

APPENDIX II SUPPLEMENTAL POST-TENSIONING DATA AND CONSTRUCTION FEEDBACK

Summary of post-tensioning: Table 45 through Table 48
Document 1 through Document 3

Table 45. Channel 1 summary.

PETERSON CONTRACTORS INC

PCI Job Number: J1692

IDOT Project Number: IBRC-C008(39)--8E-08

Date: November 28, 2006

Span: Far South

Tendon Number	Initial Tension		Final Tension		Final Elongation
	Kips	Gage Reading	Kips	Gage Reading	Measurement
T1	8.2 K	1040 psi	41 K	5300 psi	9-1/4"
T2	8.2 K	1040 psi	41 K	5300 psi	9-1/4"
T3	8.2 K	1040 psi	41 K	5300 psi	9"
T4	8.2 K	1040 psi	41 K	5300 psi	9"
T5	8.2 K	1040 psi	41 K	5300 psi	8-7/8"
T6	8.2 K	1040 psi	41 K	5300 psi	9"
T7	8.2 K	1040 psi	41 K	5300 psi	8-7/8"
T8	8.2 K	1040 psi	41 K	5300 psi	8-7/8"
T9	8.2 K	1040 psi	41 K	5300 psi	9"
T10	8.2 K	1040 psi	41 K	5300 psi	9"
T11	8.2 K	1040 psi	41 K	5300 psi	8-7/8"
T12	8.2 K	1040 psi	41 K	5300 psi	8-7/8"

PCI Representative: Justin A. Clausen

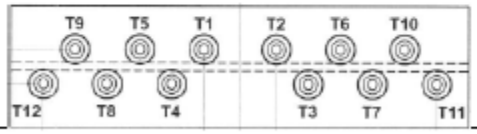

NOTES:

All Tension pulled from West End of Bridge

Tendon T1 was first tendon tensioned. Moved to East End of bridge to check tension. Jacked until 5300 psi on gage.

Measured 1/8" movement at 5300 psi.

Table 46. Channel 2 summary.

PETERSON CONTRACTORS INC

PCI Job Number: J1692

IDOT Project Number: IBRC-C008(39)--8E-08

Date: November 28, 2006

Span: Mid South

Tendon Number	Initial Tension		Final Tension		Final Elongation
	Kips	Gage Reading	Kips	Gage Reading	Measurement
T1	8.2 K	1040 psi	41 K	5300 psi	9"
T2	8.2 K	1040 psi	41 K	5300 psi	8-7/8"
T3	8.2 K	1040 psi	41 K	5300 psi	9"
T4	8.2 K	1040 psi	41 K	5300 psi	8-3/4"
T5	8.2 K	1040 psi	41 K	5300 psi	9-1/8"
T6	8.2 K	1040 psi	41 K	5300 psi	8-7/8"
T7	8.2 K	1040 psi	41 K	5300 psi	8-7/8"
T8	8.2 K	1040 psi	41 K	5300 psi	9"
T9	8.2 K	1040 psi	41 K	5300 psi	8-7/8"
T10	8.2 K	1040 psi	41 K	5300 psi	9"
T11	8.2 K	1040 psi	41 K	5300 psi	9"
T12	8.2 K	1040 psi	41 K	5300 psi	8-7/8"

PCI Representative: Justin A. Clausen

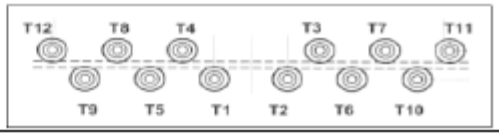

NOTES:

All Tension pulled from West End of Bridge

Table 47. Channel 3 summary.

PETERSON CONTRACTORS INC

PCI Job Number: J1692

IDOT Project Number: IBRC-C008(39)--8E-08

Date: November 28, 2006

Span: Mid North

Tendon Number	Initial Tension		Final Tension		Final Elongation
	Kips	Gage Reading	Kips	Gage Reading	Measurement
T1	8.2 K	1040 psi	41 K	5300 psi	8-7/8"
T2	8.2 K	1040 psi	41 K	5300 psi	9-1/4"
T3	8.2 K	1040 psi	41 K	5300 psi	9-1/8"
T4	8.2 K	1040 psi	41 K	5300 psi	8-7/8"
T5	8.2 K	1040 psi	41 K	5300 psi	8-7/8"
T6	8.2 K	1040 psi	41 K	5300 psi	9"
T7	8.2 K	1040 psi	41 K	5300 psi	8-7/8"
T8	8.2 K	1040 psi	41 K	5300 psi	9"
T9	8.2 K	1040 psi	41 K	5300 psi	8-7/8"
T10	8.2 K	1040 psi	41 K	5300 psi	8-3/4"
T11	8.2 K	1040 psi	41 K	5300 psi	8-3/4"
T12	8.2 K	1040 psi	41 K	5300 psi	9"

PCI Representative: Justin A. Clausen

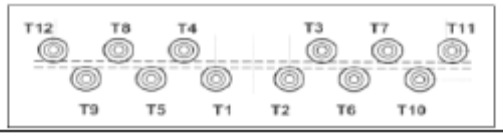

NOTES:

All Tension pulled from West End of Bridge

Table 48. Channel 4 summary.

PETERSON CONTRACTORS INC

PCI Job Number: J1692

IDOT Project Number: IBRC-C008(39)--8E-08

Date: November 28, 2006

Span: Far North

Tendon Number	Initial Tension		Final Tension		Final Elongation
	Kips	Gage Reading	Kips	Gage Reading	Measurement
T1	8.2 K	1040 psi	41 K	5300 psi	9-1/8"
T2	8.2 K	1040 psi	41 K	5300 psi	9-1/8"
T3	8.2 K	1040 psi	41 K	5300 psi	9-1/8"
T4	8.2 K	1040 psi	41 K	5300 psi	9"
T5	8.2 K	1040 psi	41 K	5300 psi	8-7/8"
T6	8.2 K	1040 psi	41 K	5300 psi	9"
T7	8.2 K	1040 psi	41 K	5300 psi	8-3/4"
T8	8.2 K	1040 psi	41 K	5300 psi	8-3/4"
T9	8.2 K	1040 psi	41 K	5300 psi	8-7/8"
T10	8.2 K	1040 psi	41 K	5300 psi	9"
T11	8.2 K	1040 psi	41 K	5300 psi	8-3/4"
T12	8.2 K	1040 psi	41 K	5300 psi	8-1/8" + 5/8" = 8-3/4"

PCI Representative: Justin A. Clausen

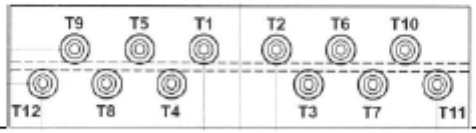

NOTES:

All Tension pulled from West End of Bridge

Tendon T12 same pulled from West end to required capacity 5300 psi = 41 kips, but only read 8-1/8" elongation.

Moved to East end of bridge and checked tension. Gage read 5300 psi. Increased tension to 5500 psi and tension cable "popped". Gage pressures fell but reading was not recorded. Gage pressure was brought back up to required tension (5300 psi) and elongation increased by 5/8", bringing overall elongation to 8-3/4".

Document 1. Mono-jack and post-tensioning force certification.

The Pro-Firm, L.C.
Repairing the earth and the structures on it.

11-30-06

Peterson Contractors Inc.
104 Blackhawk Street
Reinbeck, Iowa 50669

Re: Bridge Deck Handling and Erection
Boone County Bridge and Approaches –PPCB
On 120th Street over Squaw Creek
IBRC-C008(39)—8E-08
Boone County, Iowa

Attn: Justin Clausen

Dear Justin:

This letter is to certify that I personally supervised the stressing of 48 - .6" diameter 270 ksi cable for the above referenced project. The cable run longitudinal with the bridge with 12 cable in each of 4 pour strips. All cables with stressed to 41000 lbs based on a gage pressure of 5300 psi. The elongations were recorded to verify strain in each cable. All recorded elongation were within the +/- 5% allowable by code. Jack calibrations dated 11-17-06 were presented to me certifying the load to pressure corralation.

In conclusion, all 48 cable were stressed to 41000 lbs +/- 1000 lbs

Sincerely;

Greg J. Gear P.E.
Structural Engineer
Iowa Registration No. 9377

Post-it® Fax Note 7671	Date 11-30-06	# of pages ▶ 1
[redacted]	From [redacted]	
Co./Dept.	Co.	
Phone #	Phone #	
Fax #	Fax #	

☐ Henry D. Feeken, Manager
1449 NW 122nd St., Clive, IA 50325
Ph. (515) 223-9326
Fax (515) 225-4483

☑ Greg J. Gear, P.E., Manager
5020 Grand Ave., W Des Moines, IA 50265
Ph. (515) 221-9291
Fax (515) 221-9683

☐ Tammy Gear, Sales Consultant
529 4th St.,W Des Moines, IA 50265
Ph. (515) 255-2514
Fax (515) 277-8552

Document 2. Construction feedback from PCI.

PETERSON CONTRACTORS, INC.

ADDRESS REPLY TO:
104 BLACKHAWK STREET
P.O. BOX A
REINBECK, IOWA 50669

HEAVY & HIGHWAY CONTRACTORS

PHONE: (319) 345-2713
FAX: (319) 345-2658

January 15, 2007

Boone County Bridge and Approaches on 120th St. over Squaw Creek.
IBRC-C008(39)—8E(08)

THINGS TO CHANGE:

- Better handle on mix design including any admixtures for small grout joints.
- Use a beam with a wider top flange so that the post-tensioning channel can be wider.
- Modify pier diaphragm pour so that all panels can be set and not have to be removed.
- Let the project earlier to allow all shop drawings to be approved and thus panels to be manufactured in time to take advantage of fast tracked construction. Do not rely strictly on quoted time frames to make panels and typically shop drawing turn around time frame. PCI made this point to DOT contracts office prior to the letting of the project. Because this is such a new system, the shop drawing/review/fabrication will take longer than anyone anticipates. It does not hurt to let the project early and allow the fabrication to happen so that the time needed to erect the few bridge will be more appealing to utilize this type of structure in the future.
- Plan the letting, fabrication, and erection schedule so that the colder weather is not a problem. The cold weather was a huge problem for this project. Let the project in the fall, use the winter to perform shop drawings/review, make panels in late winter/early spring, and construct late spring/early winter. This sort of time frame will miss the cold weather concreting of the small joints, allow the existing roadway to remain open longer prior to bridge replacement, and utilize the fast tracked progress of construction to its full potential.
- Review the end panel anchorage zones. I believe that shop drawings modified the zones to all the strands to bend easier.
- Possibly think about an overlay layer on bridge.

THINGS TO KEEP THE SAME:

- Panel sizes worked out well.
- Precast pier caps worked well.
- Precast abutments worked well.
- Post tensioning worked very well.
- Let the contractor choose how to level the panels. We went through a lot of different scenarios, but ultimately, everyone will choose a different way.

Please feel free to contact me should you have any questions or wish for more information regarding details of the project.

Respectfully,

[redacted]

Justin A. Clausen
Project Manager
Peterson Contractors Inc.

Document 3. Construction feedback from Andrews Prestressed Concrete.

WebMAIL

From the desk of...
Samantha Hockerman

From: "Teresa Nelson" <tnelson@andrewsprestressedconcrete.com>
Wed, 7 Feb 2007 09:16:28 -0600
Boone Feedback

Positive
ISU and Contractor were easy to work with.
Resolving such matters as clearance issues due to mistakes or oversights in plans, i.e. placement of D14 wires fabric, placement of holes in end panels for tensioned strand and quantity and placement of inspection holes in end panels.

Negative

Would possibly look into a larger size mesh in end panels to allow for larger openings to aid in placement and consolidation of concrete.
Would suggest a different design on Jacking/tensioning plate on end panels.
Possibly larger diameter holes to allow pipe sleeves to pass thru in lieu of butting against the plate.
The plate was not quite full depth of the panel. This made it very difficult to assure that it was suspended off of the bed.

Teresa Nelson
Estimator/Project Manager
Andrews Prestressed Concrete, Inc
Ph. 641-357-5217
Cell-641-529-0026
Fax-641-357-8044

Boone/Ames Weather Data: Table 49 through Table 51

Note: Weather data is for the Ames weather station, approximately 20 miles south east of the construction site.
Site Name: AMES
Site ID: A130209

Table 49. July rain totals.

Date	Daily Precip (in.)
7/1/2006 0:00	0.08
7/2/2006 0:00	0.43
7/3/2006 0:00	0.13
7/4/2006 0:00	0
7/5/2006 0:00	0
7/6/2006 0:00	0
7/7/2006 0:00	0
7/8/2006 0:00	0
7/9/2006 0:00	0
7/10/2006 0:00	0.13
7/11/2006 0:00	0.75
7/12/2006 0:00	0.28
7/13/2006 0:00	0.13
7/14/2006 0:00	0.1
7/15/2006 0:00	0.07
7/16/2006 0:00	0.03
7/17/2006 0:00	0.02
7/18/2006 0:00	0
7/19/2006 0:00	0
7/20/2006 0:00	0
7/21/2006 0:00	0.07
7/22/2006 0:00	0
7/23/2006 0:00	0
7/24/2006 0:00	0.14
7/25/2006 0:00	0.08
7/26/2006 0:00	0.47
7/27/2006 0:00	0.12
7/28/2006 0:00	0.06
7/29/2006 0:00	0.04
7/30/2006 0:00	0.01
7/31/2006 0:00	0
Sum:	3.14

Table 50. August rain totals.

Date	Daily Precip (in.)
8/1/2006 0:00	0.18
8/2/2006 0:00	0.04
8/3/2006 0:00	0
8/4/2006 0:00	0
8/5/2006 0:00	0.14
8/6/2006 0:00	0.16
8/7/2006 0:00	0
8/8/2006 0:00	0
8/9/2006 0:00	0.19
8/10/2006 0:00	0.05
8/11/2006 0:00	0.05
8/12/2006 0:00	0.04
8/13/2006 0:00	0.05
8/14/2006 0:00	0.04
8/15/2006 0:00	0.04
8/16/2006 0:00	0.04
8/17/2006 0:00	0.05
8/18/2006 0:00	0.05
8/19/2006 0:00	0.05
8/20/2006 0:00	0.04
8/21/2006 0:00	0.06
8/22/2006 0:00	0.02
8/23/2006 0:00	0
8/24/2006 0:00	0
8/25/2006 0:00	0
8/26/2006 0:00	0
8/27/2006 0:00	0.23
8/28/2006 0:00	0.61
8/29/2006 0:00	0.1
8/30/2006 0:00	0.04
8/31/2006 0:00	0.04
Sum:	2.31

Table 51. September rain totals.

Date	Daily Precip (in.)
9/1/2006 0:00	0.04
9/2/2006 0:00	0.06
9/3/2006 0:00	0.05
9/4/2006 0:00	0.05
9/5/2006 0:00	0.06*
9/6/2006 0:00	0.07*
9/7/2006 0:00	0.08*
9/8/2006 0:00	0.04*
9/9/2006 0:00	0*
9/10/2006 0:00	1*
9/11/2006 0:00	0.22*
9/12/2006 0:00	0*
9/13/2006 0:00	0*
9/14/2006 0:00	0*
9/15/2006 0:00	0*
9/16/2006 0:00	0.72
9/17/2006 0:00	0.65
9/18/2006 0:00	0
9/19/2006 0:00	0
9/20/2006 0:00	0
9/21/2006 0:00	0.45
9/22/2006 0:00	0.02
9/23/2006 thru 9/28/2006 0:00	0
	0
9/29/2006 0:00	0.01
9/30/2006 0:00	0.01
Sum:	3.53

*Note: The construction inspector noted the bridge site received over three inches of rain during the time period indicated.

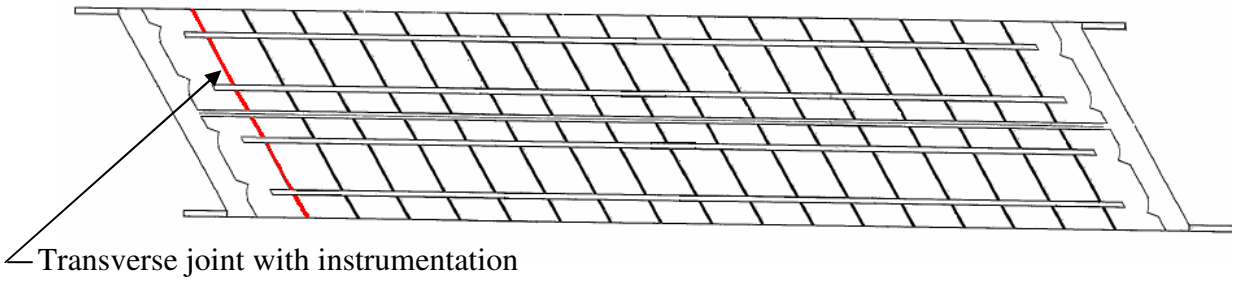

Figure 176. Location of west transverse joint with temperature instrumentation.

Table 52. West end panel transverse joint temperature data.

Reading Number	Time	Ambient Temp. (°C)	Cylinder Temp. (°C)	Joint Temp. (°C)	Ambient Temp. (°F)	Cylinder Temp. (°F)	Joint Temp. (°F)	Temp. Diff. Between Cylinder & Joint (°F)
1	11/16/06 2:30 PM	13.6	5.87	5.06	56.5	42.6	41.1	1.5
2	11/16/06 3:00 PM	12.6	6.65	6.34	54.7	44.0	43.4	0.6
3	11/16/06 3:30 PM	6.8	13.77	13.53	44.2	56.8	56.4	0.4
4	11/16/06 4:00 PM	7.6	15.83	12.31	45.7	60.5	54.2	6.3
5	11/16/06 4:30 PM	8	18.03	12.4	46.4	64.5	54.3	10.1
6	11/16/06 5:00 PM	7.8	19.34	12.51	46.0	66.8	54.5	12.3
7	11/16/06 5:30 PM	7.2	20.15	12.55	45.0	68.3	54.6	13.7
8	11/16/06 6:00 PM	6.7	20.39	12.56	44.1	68.7	54.6	14.1
9	11/16/06 6:30 PM	6.2	20.21	12.56	43.2	68.4	54.6	13.8
10	11/16/06 7:00 PM	5.7	20.48	12.69	42.3	68.9	54.8	14.0
11	11/16/06 7:30 PM	5.4	20.67	12.47	41.7	69.2	54.4	14.8
12	11/16/06 8:00 PM	5.2	20.5	12.39	41.4	68.9	54.3	14.6
13	11/16/06 8:30 PM	5	20.54	12.38	41.0	69.0	54.3	14.7
14	11/16/06 9:00 PM	5	20.79	12.26	41.0	69.4	54.1	15.4
15	11/16/06 9:30 PM	4.8	20.78	12.37	40.6	69.4	54.3	15.1
16	11/16/06 10:00 PM	4.8	20.9	12.12	40.6	69.6	53.8	15.8
17	11/16/06 10:30 PM	4.9	21.06	12.22	40.8	69.9	54.0	15.9
18	11/16/06 11:00 PM	5	21.16	11.93	41.0	70.1	53.5	16.6
19	11/16/06 11:30 PM	5.1	21.61	12.23	41.2	70.9	54.0	16.9
20	11/17/06 12:00 AM	5.1	21.92	12.03	41.2	71.5	53.7	17.8
21	11/17/06 12:30 AM	4.9	23.11	11.97	40.8	73.6	53.5	20.1
22	11/17/06 1:00 AM	4.2	24.13	11.71	39.6	75.4	53.1	22.4

Reading Number	Time	Ambient Temp. (°C)	Cylinder Temp. (°C)	Joint Temp. (°C)	Ambient Temp. (°F)	Cylinder Temp. (°F)	Joint Temp. (°F)	Temp. Diff. Between Cylinder & Joint (°F)
23	11/17/06 1:30 AM	3.9	23.82	11.79	39.0	74.9	53.2	21.7
24	11/17/06 2:00 AM	4.4	23.53	11.66	39.9	74.4	53.0	21.4
25	11/17/06 2:30 AM	4.4	22.83	12.1	39.9	73.1	53.8	19.3
26	11/17/06 3:00 AM	4.2	22.42	11.9	39.6	72.4	53.4	18.9
27	11/17/06 3:30 AM	4.1	21.87	11.93	39.4	71.4	53.5	17.9
28	11/17/06 4:00 AM	3.7	21.35	12.09	38.7	70.4	53.8	16.7
29	11/17/06 4:30 AM	3.3	20.78	12.27	37.9	69.4	54.1	15.3
30	11/17/06 5:00 AM	3.6	20.35	12.49	38.5	68.6	54.5	14.1
31	11/17/06 5:30 AM	3.8	19.92	12.63	38.8	67.9	54.7	13.1
32	11/17/06 6:00 AM	3.8	19.38	12.44	38.8	66.9	54.4	12.5
33	11/17/06 6:30 AM	3.2	18.94	12.1	37.8	66.1	53.8	12.3
34	11/17/06 7:00 AM	3.2	19.14	11.85	37.8	66.5	53.3	13.1
35	11/17/06 7:30 AM	3.8	18.75	11.44	38.8	65.8	52.6	13.2
36	11/17/06 8:00 AM	3.7	18.65	11.34	38.7	65.6	52.4	13.2
37	11/17/06 8:30 AM	3.3	18.44	11.01	37.9	65.2	51.8	13.4
38	11/17/06 9:00 AM	3.7	17.99	10.91	38.7	64.4	51.6	12.7
39	11/17/06 9:30 AM	3	16.97	10.71	37.4	62.5	51.3	11.3
40	11/17/06 10:00 AM	4.4	16.05	10.34	39.9	60.9	50.6	10.3
41	11/17/06 10:30 AM	6.4	16.15	10.25	43.5	61.1	50.5	10.6
42	11/17/06 11:00 AM	8.6	16.62	10.36	47.5	61.9	50.6	11.3
43	11/17/06 11:30 AM	9.1	16.81	10.48	48.4	62.3	50.9	11.4
44	11/17/06 12:00 PM	9.1	17.38	10.22	48.4	63.3	50.4	12.9
46	11/17/06 1:00 PM	9.2	17.45	10.7	48.6	63.4	51.3	12.2
47	11/17/06 1:30 PM	9.6	17.56	10.91	49.3	63.6	51.6	12.0

Reading Number	Time	Ambient Temp. (°C)	Cylinder Temp. (°C)	Joint Temp. (°C)	Ambient Temp. (°F)	Cylinder Temp. (°F)	Joint Temp. (°F)	Temp. Diff. Between Cylinder & Joint (°F)
48	11/17/06 2:00 PM	10	17.56	10.99	50.0	63.6	51.8	11.8
49	11/17/06 2:30 PM	10.4	17.92	11.26	50.7	64.3	52.3	12.0
50	11/17/06 3:00 PM	10.5	18.23	11.42	50.9	64.8	52.6	12.3
51	11/17/06 3:30 PM	9.9	18.31	11.65	49.8	65.0	53.0	12.0
52	11/17/06 4:00 PM	9.7	18.35	11.82	49.5	65.0	53.3	11.8
53	11/17/06 4:30 PM	9.5	18.37	12.12	49.1	65.1	53.8	11.3
54	11/17/06 5:00 PM	9.1	18.47	12.23	48.4	65.2	54.0	11.2
55	11/17/06 5:30 PM	9.3	18.2	12.17	48.7	64.8	53.9	10.9
56	11/17/06 6:00 PM	9.6	18.31	12.35	49.3	65.0	54.2	10.7
57	11/17/06 6:30 PM	9.7	17.98	12.26	49.5	64.4	54.1	10.3
58	11/17/06 7:00 PM	9.9	18.08	12.64	49.8	64.5	54.8	9.8
59	11/17/06 7:30 PM	9.4	18.31	12.72	48.9	65.0	54.9	10.1
60	11/17/06 8:00 PM	9.1	18.11	12.8	48.4	64.6	55.0	9.6
61	11/17/06 8:30 PM	8.8	18	12.75	47.8	64.4	55.0	9.5
62	11/17/06 9:00 PM	8.7	17.96	12.78	47.7	64.3	55.0	9.3
63	11/17/06 9:30 PM	8.6	17.8	12.49	47.5	64.0	54.5	9.6
64	11/17/06 10:00 PM	8.4	18.03	12.61	47.1	64.5	54.7	9.8
65	11/17/06 10:30 PM	8.2	17.83	12.47	46.8	64.1	54.4	9.6
66	11/17/06 11:00 PM	8.2	17.66	12.53	46.8	63.8	54.6	9.2
67	11/17/06 11:30 PM	8.2	17.66	12.35	46.8	63.8	54.2	9.6
68	11/18/06 12:00 AM	8.2	17.89	12.35	46.8	64.2	54.2	10.0
69	11/18/06 12:30 AM	8.2	17.56	12.22	46.8	63.6	54.0	9.6
70	11/18/06 1:00 AM	8.2	17.53	12.1	46.8	63.6	53.8	9.8
71	11/18/06 1:30 AM	8.2	17.68	11.97	46.8	63.8	53.5	10.3

Reading Number	Time	Ambient Temp. (°C)	Cylinder Temp. (°C)	Joint Temp. (°C)	Ambient Temp. (°F)	Cylinder Temp. (°F)	Joint Temp. (°F)	Temp. Diff. Between Cylinder & Joint (°F)
72	11/18/06 2:00 AM	8.1	17.58	11.87	46.6	63.6	53.4	10.3
73	11/18/06 2:30 AM	8	17.52	11.9	46.4	63.5	53.4	10.1
74	11/18/06 3:00 AM	7.9	17.48	11.67	46.2	63.5	53.0	10.5
75	11/18/06 3:30 AM	7.9	17.5	11.74	46.2	63.5	53.1	10.4
76	11/18/06 4:00 AM	7.8	17.22	11.76	46.0	63.0	53.2	9.8
77	11/18/06 4:30 AM	7.8	17.52	11.58	46.0	63.5	52.8	10.7
78	11/18/06 5:00 AM	7.7	17.49	11.6	45.9	63.5	52.9	10.6
79	11/18/06 5:30 AM	7.6	17.42	11.63	45.7	63.4	52.9	10.4
80	11/18/06 6:00 AM	7.6	17.2	11.38	45.7	63.0	52.5	10.5
81	11/18/06 6:30 AM	7.5	17.23	11.47	45.5	63.0	52.6	10.4
82	11/18/06 7:00 AM	7.4	17.25	11.05	45.3	63.1	51.9	11.2
83	11/18/06 7:30 AM	7.3	17.28	11.02	45.1	63.1	51.8	11.3
84	11/18/06 8:00 AM	7.2	17.18	11.04	45.0	62.9	51.9	11.1
85	11/18/06 8:30 AM	7.1	17.42	10.76	44.8	63.4	51.4	12.0
86	11/18/06 9:00 AM	7.1	17.37	10.7	44.8	63.3	51.3	12.0
87	11/18/06 9:30 AM	7.2	17.24	10.67	45.0	63.0	51.2	11.8
88	11/18/06 10:00 AM	7.1	17.37	10.57	44.8	63.3	51.0	12.2
89	11/18/06 10:30 AM	7.1	17.24	10.51	44.8	63.0	50.9	12.1
90	11/18/06 11:00 AM	7.1	17.3	10.38	44.8	63.1	50.7	12.5
91	11/18/06 11:30 AM	7.3	17.28	10.26	45.1	63.1	50.5	12.6
92	11/18/06 12:00 PM	7.5	17.41	10.27	45.5	63.3	50.5	12.9
93	11/18/06 12:30 PM	7.6	17.33	10.18	45.7	63.2	50.3	12.9
94	11/18/06 1:00 PM	7.6	17.26	10.18	45.7	63.1	50.3	12.7
95	11/18/06 1:30 PM	7.8	17.46	10.19	46.0	63.4	50.3	13.1

Reading Number	Time	Ambient Temp. (°C)	Cylinder Temp. (°C)	Joint Temp. (°C)	Ambient Temp. (°F)	Cylinder Temp. (°F)	Joint Temp. (°F)	Temp. Diff. Between Cylinder & Joint (°F)
96	11/18/06 2:00 PM	7.9	17.52	10.29	46.2	63.5	50.5	13.0
97	11/18/06 2:30 PM	8	17.66	10.33	46.4	63.8	50.6	13.2
98	11/18/06 3:00 PM	8	17.6	10.39	46.4	63.7	50.7	13.0
99	11/18/06 3:30 PM	8.1	17.66	10.3	46.6	63.8	50.5	13.2
100	11/18/06 4:00 PM	8.2	17.82	10.46	46.8	64.1	50.8	13.2
101	11/18/06 4:30 PM	8.1	17.97	10.49	46.6	64.3	50.9	13.5
102	11/18/06 5:00 PM	7.9	17.75	10.41	46.2	64.0	50.7	13.2
103	11/18/06 5:30 PM	7.8	17.86	10.75	46.0	64.1	51.4	12.8
104	11/18/06 6:00 PM	7.6	17.76	10.62	45.7	64.0	51.1	12.9
105	11/18/06 6:30 PM	7.6	17.94	10.43	45.7	64.3	50.8	13.5
106	11/18/06 7:00 PM	7.7	17.81	10.65	45.9	64.1	51.2	12.9
107	11/18/06 7:30 PM	7.5	17.84	10.58	45.5	64.1	51.0	13.1
108	11/18/06 8:00 PM	7.3	17.58	10.52	45.1	63.6	50.9	12.7
109	11/18/06 8:30 PM	7.5	17.83	10.64	45.5	64.1	51.2	12.9
110	11/18/06 9:00 PM	7.7	17.45	10.4	45.9	63.4	50.7	12.7
111	11/18/06 9:30 PM	7.8	17.33	10.57	46.0	63.2	51.0	12.2
112	11/18/06 10:00 PM	7.9	17.3	10.6	46.2	63.1	51.1	12.1
113	11/18/06 10:30 PM	7.8	17.36	10.44	46.0	63.2	50.8	12.5
114	11/18/06 11:00 PM	7.7	17.23	10.53	45.9	63.0	51.0	12.1
115	11/18/06 11:30 PM	7.6	17.41	10.49	45.7	63.3	50.9	12.5
116	11/19/06 12:00 AM	7.5	17.22	10.46	45.5	63.0	50.8	12.2
117	11/19/06 12:30 AM	7.3	17.18	10.32	45.1	62.9	50.6	12.3
118	11/19/06 1:00 AM	7.3	17.02	10.38	45.1	62.6	50.7	12.0
119	11/19/06 1:30 AM	7.1	16.86	10.12	44.8	62.3	50.2	12.1

Reading Number	Time	Ambient Temp. (°C)	Cylinder Temp. (°C)	Joint Temp. (°C)	Ambient Temp. (°F)	Cylinder Temp. (°F)	Joint Temp. (°F)	Temp. Diff. Between Cylinder & Joint (°F)
120	11/19/06 2:00 AM	7	16.94	10.22	44.6	62.5	50.4	12.1
121	11/19/06 2:30 AM	6.9	17.14	10.19	44.4	62.9	50.3	12.5
122	11/19/06 3:00 AM	6.8	17.01	10.09	44.2	62.6	50.2	12.5
123	11/19/06 3:30 AM	6.7	16.77	10.17	44.1	62.2	50.3	11.9
124	11/19/06 4:00 AM	6.6	16.55	10.01	43.9	61.8	50.0	11.8
125	11/19/06 4:30 AM	6.4	16.41	9.94	43.5	61.5	49.9	11.6
126	11/19/06 5:00 AM	6.3	16.61	9.78	43.3	61.9	49.6	12.3
127	11/19/06 5:30 AM	6.2	16.33	9.93	43.2	61.4	49.9	11.5
128	11/19/06 6:00 AM	6.1	16.48	9.51	43.0	61.7	49.1	12.5
129	11/19/06 6:30 AM	6	16.38	9.48	42.8	61.5	49.1	12.4
130	11/19/06 7:00 AM	5.9	15.86	9.38	42.6	60.5	48.9	11.7
131	11/19/06 7:30 AM	5.9	15.98	9.38	42.6	60.8	48.9	11.9
132	11/19/06 8:00 AM	5.9	15.98	9.19	42.6	60.8	48.5	12.2
133	11/19/06 8:30 AM	6.1	15.64	9	43.0	60.2	48.2	12.0
134	11/19/06 9:00 AM	6.4	15.58	8.98	43.5	60.0	48.2	11.9
135	11/19/06 9:30 AM	6.9	15.69	8.92	44.4	60.2	48.1	12.2
136	11/19/06 10:00 AM	7.4	16	8.85	45.3	60.8	47.9	12.9
137	11/19/06 10:30 AM	8	16.07	8.74	46.4	60.9	47.7	13.2
138	11/19/06 11:00 AM	8.3	16.33	8.79	46.9	61.4	47.8	13.6
139	11/19/06 11:30 AM	8.4	16.49	9.02	47.1	61.7	48.2	13.4
140	11/19/06 12:00 PM	8.2	16.79	8.88	46.8	62.2	48.0	14.2
141	11/19/06 12:30 PM	8.4	17.05	8.83	47.1	62.7	47.9	14.8
142	11/19/06 1:00 PM	8.7	17.01	9	47.7	62.6	48.2	14.4
143	11/19/06 1:30 PM	9.1	17.22	9.21	48.4	63.0	48.6	14.4

Reading Number	Time	Ambient Temp. (°C)	Cylinder Temp. (°C)	Joint Temp. (°C)	Ambient Temp. (°F)	Cylinder Temp. (°F)	Joint Temp. (°F)	Temp. Diff. Between Cylinder & Joint (°F)
144	11/19/06 2:00 PM	9.5	17.61	9.24	49.1	63.7	48.6	15.1
145	11/19/06 2:30 PM	9.9	17.85	9.51	49.8	64.1	49.1	15.0
146	11/19/06 3:00 PM	9.9	18.25	9.57	49.8	64.9	49.2	15.6
147	11/19/06 3:30 PM	9.7	18.49	9.75	49.5	65.3	49.6	15.7
148	11/19/06 4:00 PM	9.9	18.5	9.89	49.8	65.3	49.8	15.5
149	11/19/06 4:30 PM	9.9	18.66	10.26	49.8	65.6	50.5	15.1
150	11/19/06 5:00 PM	9.7	18.71	10.38	49.5	65.7	50.7	15.0
151	11/19/06 5:30 PM	9.3	18.84	10.48	48.7	65.9	50.9	15.0
152	11/19/06 6:00 PM	9	18.73	10.63	48.2	65.7	51.1	14.6
153	11/19/06 6:30 PM	8.8	18.53	10.56	47.8	65.4	51.0	14.3
154	11/19/06 7:00 PM	8.6	18.73	10.86	47.5	65.7	51.5	14.2
155	11/19/06 7:30 PM	8.5	18.36	10.95	47.3	65.0	51.7	13.3
156	11/19/06 8:00 PM	8.2	18.21	10.71	46.8	64.8	51.3	13.5
157	11/19/06 8:30 PM	8.1	18.36	10.68	46.6	65.0	51.2	13.8
158	11/19/06 9:00 PM	8	18.07	10.83	46.4	64.5	51.5	13.0
159	11/19/06 9:30 PM	7.9	18.16	10.73	46.2	64.7	51.3	13.4
160	11/19/06 10:00 PM	7.8	18	10.63	46.0	64.4	51.1	13.3
161	11/19/06 10:30 PM	7.7	17.9	10.84	45.9	64.2	51.5	12.7
162	11/19/06 11:00 PM	7.5	17.8	10.58	45.5	64.0	51.0	13.0
163	11/19/06 11:30 PM	7.4	17.89	10.62	45.3	64.2	51.1	13.1
164	11/20/06 12:00 AM	7.3	17.85	10.58	45.1	64.1	51.0	13.1
165	11/20/06 12:30 AM	7.1	17.34	10.57	44.8	63.2	51.0	12.2
166	11/20/06 1:00 AM	7.1	17.24	10.38	44.8	63.0	50.7	12.3
167	11/20/06 1:30 AM	7	17.33	10.28	44.6	63.2	50.5	12.7

Reading Number	Time	Ambient Temp. (°C)	Cylinder Temp. (°C)	Joint Temp. (°C)	Ambient Temp. (°F)	Cylinder Temp. (°F)	Joint Temp. (°F)	Temp. Diff. Between Cylinder & Joint (°F)
168	11/20/06 2:00 AM	6.8	17.23	10.4	44.2	63.0	50.7	12.3
169	11/20/06 2:30 AM	6.8	17.07	10.27	44.2	62.7	50.5	12.2
170	11/20/06 3:00 AM	6.7	17.16	9.99	44.1	62.9	50.0	12.9
171	11/20/06 3:30 AM	6.6	17.03	9.82	43.9	62.7	49.7	13.0
172	11/20/06 4:00 AM	6.5	16.9	9.79	43.7	62.4	49.6	12.8
173	11/20/06 4:30 AM	6.4	16.9	9.42	43.5	62.4	49.0	13.5
174	11/20/06 5:00 AM	6.3	16.76	9.71	43.3	62.2	49.5	12.7
175	11/20/06 5:30 AM	6.2	16.51	9.42	43.2	61.7	49.0	12.8
176	11/20/06 6:00 AM	6.1	16.29	9.39	43.0	61.3	48.9	12.4
177	11/20/06 6:30 AM	6.1	16.29	9.19	43.0	61.3	48.5	12.8
178	11/20/06 7:00 AM	6	16.34	9.15	42.8	61.4	48.5	12.9
179	11/20/06 7:30 AM	5.9	16.34	9.12	42.6	61.4	48.4	13.0
180	11/20/06 8:00 AM	6	16.15	9.15	42.8	61.1	48.5	12.6
181	11/20/06 8:30 AM	6.3	16.21	8.82	43.3	61.2	47.9	13.3
182	11/20/06 9:00 AM	6.8	16.36	8.63	44.2	61.4	47.5	13.9
183	11/20/06 9:30 AM	7.3	16.08	8.62	45.1	60.9	47.5	13.4
184	11/20/06 10:00 AM	7.8	16.42	8.73	46.0	61.6	47.7	13.8
185	11/20/06 10:30 AM	8	16.43	8.81	46.4	61.6	47.9	13.7
186	11/20/06 11:00 AM	8.4	16.66	8.95	47.1	62.0	48.1	13.9
187	11/20/06 11:30 AM	8.5	16.62	9.05	47.3	61.9	48.3	13.6
188	11/20/06 12:00 PM	8.6	17.06	9.03	47.5	62.7	48.3	14.5
189	11/20/06 12:30 PM	8.8	16.99	9.29	47.8	62.6	48.7	13.9
190	11/20/06 1:00 PM	8.9	17.13	9.8	48.0	62.8	49.6	13.2
191	11/20/06 1:30 PM	8.9	16.82	9.94	48.0	62.3	49.9	12.4

Reading Number	Time	Ambient Temp. (°C)	Cylinder Temp. (°C)	Joint Temp. (°C)	Ambient Temp. (°F)	Cylinder Temp. (°F)	Joint Temp. (°F)	Temp. Diff. Between Cylinder & Joint (°F)
192	11/20/06 2:00 PM	9.3	16.73	10.05	48.7	62.1	50.1	12.0
193	11/20/06 2:30 PM	9.6	16.84	10.47	49.3	62.3	50.8	11.5
194	11/20/06 3:00 PM	9.7	16.93	10.79	49.5	62.5	51.4	11.1
195	11/20/06 3:30 PM	9.6	17.02	10.85	49.3	62.6	51.5	11.1
196	11/20/06 4:00 PM	9.4	17	10.97	48.9	62.6	51.7	10.9
197	11/20/06 4:30 PM	9.4	16.95	11.28	48.9	62.5	52.3	10.2
198	11/20/06 5:00 PM	9.6	17.57	11.64	49.3	63.6	53.0	10.7
199	11/20/06 5:30 PM	10.7	18.79	12.21	51.3	65.8	54.0	11.8
200	11/20/06 6:00 PM	11.1	19.74	12.73	52.0	67.5	54.9	12.6
201	11/20/06 6:30 PM	11.3	20.73	13.24	52.3	69.3	55.8	13.5
202	11/20/06 7:00 PM	11.5	21.16	13.75	52.7	70.1	56.8	13.3
203	11/20/06 7:30 PM	11.4	21.79	14	52.5	71.2	57.2	14.0
204	11/20/06 8:00 PM	11.4	21.62	14.36	52.5	70.9	57.8	13.1
205	11/20/06 8:30 PM	11	21.4	14.84	51.8	70.5	58.7	11.8
206	11/20/06 9:00 PM	10.5	21.21	15.08	50.9	70.2	59.1	11.0
207	11/20/06 9:30 PM	9.9	20.91	15.31	49.8	69.6	59.6	10.1
208	11/20/06 10:00 PM	8.6	19.57	15.26	47.5	67.2	59.5	7.8
209	11/20/06 10:30 PM	7.6	18.16	15.03	45.7	64.7	59.1	5.6
210	11/20/06 11:00 PM	7	16.89	14.48	44.6	62.4	58.1	4.3
211	11/20/06 11:30 PM	6.4	15.33	13.76	43.5	59.6	56.8	2.8
212	11/21/06 12:00 AM	5.9	14.1	13.24	42.6	57.4	55.8	1.5
213	11/21/06 12:30 AM	5.4	12.55	12.62	41.7	54.6	54.7	-0.1
214	11/21/06 1:00 AM	4.8	11.35	12	40.6	52.4	53.6	-1.2
215	11/21/06 1:30 AM	4.7	10.58	11.6	40.5	51.0	52.9	-1.8

Reading Number	Time	Ambient Temp. (°C)	Cylinder Temp. (°C)	Joint Temp. (°C)	Ambient Temp. (°F)	Cylinder Temp. (°F)	Joint Temp. (°F)	Temp. Diff. Between Cylinder & Joint (°F)
216	11/21/06 2:00 AM	4.5	9.76	11.15	40.1	49.6	52.1	-2.5
217	11/21/06 2:30 AM	4.3	9.2	10.8	39.7	48.6	51.4	-2.9
218	11/21/06 3:00 AM	4.2	8.91	10.29	39.6	48.0	50.5	-2.5
219	11/21/06 3:30 AM	4	8.58	9.97	39.2	47.4	49.9	-2.5
220	11/21/06 4:00 AM	3.8	8.2	9.52	38.8	46.8	49.1	-2.4
221	11/21/06 4:30 AM	3.8	7.64	9.08	38.8	45.8	48.3	-2.6
222	11/21/06 5:00 AM	3.9	7.49	8.76	39.0	45.5	47.8	-2.3
223	11/21/06 5:30 AM	3.9	7.62	8.57	39.0	45.7	47.4	-1.7
224	11/21/06 6:00 AM	3.9	7.44	8.45	39.0	45.4	47.2	-1.8
225	11/21/06 6:30 AM	3.7	7.18	8.25	38.7	44.9	46.9	-1.9
226	11/21/06 7:00 AM	3.5	7.22	7.73	38.3	45.0	45.9	-0.9
227	11/21/06 7:30 AM	3.3	6.71	7.62	37.9	44.1	45.7	-1.6
228	11/21/06 8:00 AM	3.1	6.64	7.36	37.6	44.0	45.2	-1.3
229	11/21/06 8:30 AM	3.2	6.55	7.14	37.8	43.8	44.9	-1.1
230	11/21/06 9:00 AM	3.7	6.56	6.89	38.7	43.8	44.4	-0.6
231	11/21/06 9:30 AM	5.5	7.11	6.73	41.9	44.8	44.1	0.7
232	11/21/06 10:00 AM	7.4	7.9	6.63	45.3	46.2	43.9	2.3
233	11/21/06 10:30 AM	8.8	9.37	6.69	47.8	48.9	44.0	4.8
234	11/21/06 11:00 AM	9.8	10.72	7.21	49.6	51.3	45.0	6.3
235	11/21/06 11:30 AM	10.8	11.97	8	51.4	53.5	46.4	7.1
236	11/21/06 12:00 PM	9.8	14.04	8.63	49.6	57.3	47.5	9.7
237	11/21/06 12:30 PM	10.8	16.1	9.35	51.4	61.0	48.8	12.2
238	11/21/06 1:00 PM	11.4	17.44	10.17	52.5	63.4	50.3	13.1
239	11/21/06 1:30 PM	12.3	18.11	11.48	54.1	64.6	52.7	11.9

Reading Number	Time	Ambient Temp. (°C)	Cylinder Temp. (°C)	Joint Temp. (°C)	Ambient Temp. (°F)	Cylinder Temp. (°F)	Joint Temp. (°F)	Temp. Diff. Between Cylinder & Joint (°F)
240	11/21/06 2:00 PM	13.7	18.85	12.27	56.7	65.9	54.1	11.8
241	11/21/06 2:30 PM	13.7	19.4	13.19	56.7	66.9	55.7	11.2
242	11/21/06 3:00 PM	14	19.44	13.71	57.2	67.0	56.7	10.3
243	11/21/06 3:30 PM	14	19.4	13.99	57.2	66.9	57.2	9.7
244	11/21/06 4:00 PM	13.8	18.84	14.21	56.8	65.9	57.6	8.3
245	11/21/06 4:30 PM	13.7	18.55	14.38	56.7	65.4	57.9	7.5
246	11/21/06 5:00 PM	13.2	18.59	14.53	55.8	65.5	58.2	7.3
247	11/21/06 5:30 PM	12.3	20.99	15.1	54.1	69.8	59.2	10.6
248	11/21/06 6:00 PM	10.5	24.99	16.05	50.9	77.0	60.9	16.1
249	11/21/06 6:30 PM	8.3	28.52	17.45	46.9	83.3	63.4	19.9
250	11/21/06 7:00 PM	7	31.2	18.62	44.6	88.2	65.5	22.6
251	11/21/06 7:30 PM	6.1	33.94	19.73	43.0	93.1	67.5	25.6
252	11/21/06 8:00 PM	5	36.13	20.62	41.0	97.0	69.1	27.9
253	11/21/06 8:30 PM	4.3	37.3	21.41	39.7	99.1	70.5	28.6
254	11/21/06 9:00 PM	3.9	39.05	22.12	39.0	102.3	71.8	30.5
255	11/21/06 9:30 PM	3.5	39.97	22.9	38.3	103.9	73.2	30.7
256	11/21/06 10:00 PM	3.5	41.18	23.43	38.3	106.1	74.2	32.0
257	11/21/06 10:30 PM	2.6	42.05	24.05	36.7	107.7	75.3	32.4
258	11/21/06 11:00 PM	2.3	43.01	24.59	36.1	109.4	76.3	33.2
259	11/21/06 11:30 PM	2.1	43.53	24.87	35.8	110.4	76.8	33.6
260	11/22/06 12:00 AM	1.6	44.04	25.24	34.9	111.3	77.4	33.8
261	11/22/06 12:30 AM	1.4	44.38	25.53	34.5	111.9	78.0	33.9
262	11/22/06 1:00 AM	1.8	44.64	25.67	35.2	112.4	78.2	34.1
263	11/22/06 1:30 AM	2.6	44.95	25.97	36.7	112.9	78.7	34.2

Reading Number	Time	Ambient Temp. (°C)	Cylinder Temp. (°C)	Joint Temp. (°C)	Ambient Temp. (°F)	Cylinder Temp. (°F)	Joint Temp. (°F)	Temp. Diff. Between Cylinder & Joint (°F)
264	11/22/06 2:00 AM	3.1	45.36	26.38	37.6	113.6	79.5	34.2
265	11/22/06 2:30 AM	3	45.35	26.4	37.4	113.6	79.5	34.1
266	11/22/06 3:00 AM	2	45.48	26.44	35.6	113.9	79.6	34.3
267	11/22/06 3:30 AM	2.6	45.62	26.57	36.7	114.1	79.8	34.3
268	11/22/06 4:00 AM	2.8	45.71	26.7	37.0	114.3	80.1	34.2
269	11/22/06 4:30 AM	1.4	45.67	26.92	34.5	114.2	80.5	33.8
270	11/22/06 5:00 AM	1	45.75	27.15	33.8	114.4	80.9	33.5
271	11/22/06 5:30 AM	0.4	45.98	27.18	32.7	114.8	80.9	33.8
272	11/22/06 6:00 AM	0.3	46.07	27.23	32.5	114.9	81.0	33.9
273	11/22/06 6:30 AM	0.3	45.91	27.16	32.5	114.6	80.9	33.8
274	11/22/06 7:00 AM	0.5	46.05	27.19	32.9	114.9	80.9	33.9
275	11/22/06 7:30 AM	0.9	45.79	27.24	33.6	114.4	81.0	33.4
276	11/22/06 8:00 AM	1.1	46.06	27.11	34.0	114.9	80.8	34.1
277	11/22/06 8:30 AM	1.4	46.49	26.85	34.5	115.7	80.3	35.4
278	11/22/06 9:00 AM	2.1	46.37	27.13	35.8	115.5	80.8	34.6
279	11/22/06 9:30 AM	3.1	45.53	26.74	37.6	114.0	80.1	33.8
280	11/22/06 10:00 AM	4.1	42.31	26.82	39.4	108.2	80.3	27.9
281	11/22/06 10:30 AM	6	42.12	26.57	42.8	107.8	79.8	28.0
282	11/22/06 11:00 AM	6.7	38.78	26.2	44.1	101.8	79.2	22.6
283	11/22/06 11:30 AM	8.1	35.76	25.23	46.6	96.4	77.4	19.0
284	11/22/06 12:00 PM	10.4	36.4	24.55	50.7	97.5	76.2	21.3
285	11/22/06 12:30 PM	12.4	37.32	23.99	54.3	99.2	75.2	24.0
286	11/22/06 1:00 PM	13.6	38.09	23.83	56.5	100.6	74.9	25.7
287	11/22/06 1:30 PM	14.6	38.69	23.99	58.3	101.6	75.2	26.5

Reading Number	Time	Ambient Temp. (°C)	Cylinder Temp. (°C)	Joint Temp. (°C)	Ambient Temp. (°F)	Cylinder Temp. (°F)	Joint Temp. (°F)	Temp. Diff. Between Cylinder & Joint (°F)
288	11/22/06 2:00 PM	15.7	39.42	23.81	60.3	103.0	74.9	28.1
289	11/22/06 2:30 PM	16	40.35	24.07	60.8	104.6	75.3	29.3
290	11/22/06 3:00 PM	16.8	39.45	24.04	62.2	103.0	75.3	27.7
291	11/22/06 3:30 PM	16.9	38.27	23.54	62.4	100.9	74.4	26.5
292	11/22/06 4:00 PM	16.1	36.82	23.2	61.0	98.3	73.8	24.5
293	11/22/06 4:30 PM	15.5	35.34	22.47	59.9	95.6	72.4	23.2
294	11/22/06 5:00 PM	14.4	33.93	22.02	57.9	93.1	71.6	21.4
295	11/22/06 5:30 PM	13.5	32.23	21.67	56.3	90.0	71.0	19.0
296	11/22/06 6:00 PM	12	30.74	21	53.6	87.3	69.8	17.5
297	11/22/06 6:30 PM	10.2	29.11	20.32	50.4	84.4	68.6	15.8
298	11/22/06 7:00 PM	8.8	27.63	19.87	47.8	81.7	67.8	14.0
299	11/22/06 7:30 PM	8.3	26.41	19.32	46.9	79.5	66.8	12.8
300	11/22/06 8:00 PM	8.4	25.43	18.79	47.1	77.8	65.8	12.0
301	11/22/06 8:30 PM	7.9	24.25	18.46	46.2	75.7	65.2	10.4
302	11/22/06 9:00 PM	7.2	23.31	18.04	45.0	74.0	64.5	9.5
303	11/22/06 9:30 PM	6.8	22.37	17.68	44.2	72.3	63.8	8.4
304	11/22/06 10:00 PM	6.1	21.57	17.25	43.0	70.8	63.1	7.8
305	11/22/06 10:30 PM	5.2	20.36	16.54	41.4	68.6	61.8	6.9
306	11/22/06 11:00 PM	3.7	19.52	16.24	38.7	67.1	61.2	5.9
307	11/22/06 11:30 PM	3.7	18.96	15.66	38.7	66.1	60.2	5.9
308	11/23/06 12:00 AM	3.1	18.27	15.11	37.6	64.9	59.2	5.7
309	11/23/06 12:30 AM	2.9	17.18	14.77	37.2	62.9	58.6	4.3
310	11/23/06 1:00 AM	2.4	16.77	14.31	36.3	62.2	57.8	4.4
311	11/23/06 1:30 AM	2.1	16.16	13.98	35.8	61.1	57.2	3.9

Reading Number	Time	Ambient Temp. (°C)	Cylinder Temp. (°C)	Joint Temp. (°C)	Ambient Temp. (°F)	Cylinder Temp. (°F)	Joint Temp. (°F)	Temp. Diff. Between Cylinder & Joint (°F)
312	11/23/06 2:00 AM	1.8	15.28	13.33	35.2	59.5	56.0	3.5
313	11/23/06 2:30 AM	1.5	14.96	12.85	34.7	58.9	55.1	3.8
314	11/23/06 3:00 AM	1.1	14.27	12.79	34.0	57.7	55.0	2.7
315	11/23/06 3:30 AM	0.9	13.86	11.99	33.6	56.9	53.6	3.4
316	11/23/06 4:00 AM	0.7	12.99	11.93	33.3	55.4	53.5	1.9
317	11/23/06 4:30 AM	0.6	12.92	11.42	33.1	55.3	52.6	2.7
318	11/23/06 5:00 AM	0.4	12.27	11.13	32.7	54.1	52.0	2.1
319	11/23/06 5:30 AM	0.2	11.76	10.61	32.4	53.2	51.1	2.1
320	11/23/06 6:00 AM	0.1	11.71	10.3	32.2	53.1	50.5	2.5
321	11/23/06 6:30 AM	-0.1	11.31	10.2	31.8	52.4	50.4	2.0
322	11/23/06 7:00 AM	-0.6	10.72	9.84	30.9	51.3	49.7	1.6
323	11/23/06 7:30 AM	-0.5	10.47	9.39	31.1	50.8	48.9	1.9
324	11/23/06 8:00 AM	-0.6	9.93	9.2	30.9	49.9	48.6	1.3
325	11/23/06 8:30 AM	-0.6	9.94	8.73	30.9	49.9	47.7	2.2
326	11/23/06 9:00 AM	-0.1	9.77	8.55	31.8	49.6	47.4	2.2
327	11/23/06 9:30 AM	1.4	9.72	8.55	34.5	49.5	47.4	2.1
328	11/23/06 10:00 AM	3.7	9.91	8.59	38.7	49.8	47.5	2.4
329	11/23/06 10:30 AM	5.2	10.38	8.91	41.4	50.7	48.0	2.6
330	11/23/06 11:00 AM	6.5	10.94	8.88	43.7	51.7	48.0	3.7
331	11/23/06 11:30 AM	7.9	11.77	9.15	46.2	53.2	48.5	4.7
332	11/23/06 12:00 PM	9.4	12.1	9.55	48.9	53.8	49.2	4.6
333	11/23/06 12:30 PM	10.6	12.77	9.69	51.1	55.0	49.4	5.5
334	11/23/06 1:00 PM	11.3	13.56	10.2	52.3	56.4	50.4	6.0
335	11/23/06 1:30 PM	12.7	14.03	10.71	54.9	57.3	51.3	6.0

Reading Number	Time	Ambient Temp. (°C)	Cylinder Temp. (°C)	Joint Temp. (°C)	Ambient Temp. (°F)	Cylinder Temp. (°F)	Joint Temp. (°F)	Temp. Diff. Between Cylinder & Joint (°F)
336	11/23/06 2:00 PM	13.8	14.86	11.45	56.8	58.7	52.6	6.1
337	11/23/06 2:30 PM	15.3	14.85	12.03	59.5	58.7	53.7	5.1
338	11/23/06 3:00 PM	15.1	15.07	12.43	59.2	59.1	54.4	4.8
339	11/23/06 3:30 PM	14.9	15.27	13.03	58.8	59.5	55.5	4.0
340	11/23/06 4:00 PM	14.7	15.34	13.34	58.5	59.6	56.0	3.6
341	11/23/06 4:30 PM	13.8	15.18	13.55	56.8	59.3	56.4	2.9
342	11/23/06 5:00 PM	13.2	14.79	13.55	55.8	58.6	56.4	2.2
343	11/23/06 5:30 PM	11.8	14.59	13.52	53.2	58.3	56.3	1.9
344	11/23/06 6:00 PM	10.5	14.16	13.68	50.9	57.5	56.6	0.9
345	11/23/06 6:30 PM	9.8	13.81	13.42	49.6	56.9	56.2	0.7
346	11/23/06 7:00 PM	9.3	13.64	13.28	48.7	56.6	55.9	0.6
347	11/23/06 7:30 PM	8.4	13.24	13.29	47.1	55.8	55.9	-0.1
348	11/23/06 8:00 PM	8.1	13.03	12.96	46.6	55.5	55.3	0.1
349	11/23/06 8:30 PM	8.2	12.51	12.53	46.8	54.5	54.6	0.0
350	11/23/06 9:00 PM	7.8	12.53	12.48	46.0	54.6	54.5	0.1
351	11/23/06 9:30 PM	7.4	12.49	12.32	45.3	54.5	54.2	0.3
352	11/23/06 10:00 PM	7.1	12.21	12.16	44.8	54.0	53.9	0.1
353	11/23/06 10:30 PM	7	11.79	11.81	44.6	53.2	53.3	0.0
354	11/23/06 11:00 PM	6.9	11.94	11.45	44.4	53.5	52.6	0.9
355	11/23/06 11:30 PM	6.8	11.71	11.47	44.2	53.1	52.6	0.4
356	11/24/06 12:00 AM	6.7	11.45	11.46	44.1	52.6	52.6	0.0
357	11/24/06 12:30 AM	6.4	11.23	11.14	43.5	52.2	52.1	0.2
358	11/24/06 1:00 AM	6.2	11.19	10.85	43.2	52.1	51.5	0.6
359	11/24/06 1:30 AM	6.1	11.13	10.57	43.0	52.0	51.0	1.0

Reading Number	Time	Ambient Temp. (°C)	Cylinder Temp. (°C)	Joint Temp. (°C)	Ambient Temp. (°F)	Cylinder Temp. (°F)	Joint Temp. (°F)	Temp. Diff. Between Cylinder & Joint (°F)
360	11/24/06 2:00 AM	6	10.94	10.38	42.8	51.7	50.7	1.0
361	11/24/06 2:30 AM	6	10.95	10.3	42.8	51.7	50.5	1.2
362	11/24/06 3:00 AM	6	10.58	10.23	42.8	51.0	50.4	0.6
363	11/24/06 3:30 AM	5.7	10.65	9.87	42.3	51.2	49.8	1.4
364	11/24/06 4:00 AM	4.7	10.31	9.69	40.5	50.6	49.4	1.1
365	11/24/06 4:30 AM	4.4	10.04	9.51	39.9	50.1	49.1	1.0
366	11/24/06 5:00 AM	4	10.32	9.14	39.2	50.6	48.5	2.1
367	11/24/06 5:30 AM	3.1	9.77	9.05	37.6	49.6	48.3	1.3
368	11/24/06 6:00 AM	2.4	9.78	8.89	36.3	49.6	48.0	1.6
369	11/24/06 6:30 AM	2.1	9.65	8.74	35.8	49.4	47.7	1.6
370	11/24/06 7:00 AM	1.8	9.4	8.48	35.2	48.9	47.3	1.7
371	11/24/06 7:30 AM	1.3	9.07	8.18	34.3	48.3	46.7	1.6
372	11/24/06 8:00 AM	1.1	8.96	8.03	34.0	48.1	46.5	1.7
373	11/24/06 8:30 AM	0.9	8.67	7.67	33.6	47.6	45.8	1.8
374	11/24/06 9:00 AM	1.4	8.48	7.5	34.5	47.3	45.5	1.8
375	11/24/06 9:30 AM	2.3	8.78	7.79	36.1	47.8	46.0	1.8
376	11/24/06 10:00 AM	6	9.14	7.99	42.8	48.5	46.4	2.1
377	11/24/06 10:30 AM	8.4	9.84	8.25	47.1	49.7	46.9	2.9
378	11/24/06 11:00 AM	10	10.47	8.57	50.0	50.8	47.4	3.4
379	11/24/06 11:30 AM	11.3	11.33	9.44	52.3	52.4	49.0	3.4
380	11/24/06 12:00 PM	12.6	12.13	9.64	54.7	53.8	49.4	4.5
381	11/24/06 12:30 PM	13.4	12.79	10.46	56.1	55.0	50.8	4.2
382	11/24/06 1:00 PM	13.9	13.7	11.03	57.0	56.7	51.9	4.8
383	11/24/06 1:30 PM	14.5	13.98	11.42	58.1	57.2	52.6	4.6

Reading Number	Time	Ambient Temp. (°C)	Cylinder Temp. (°C)	Joint Temp. (°C)	Ambient Temp. (°F)	Cylinder Temp. (°F)	Joint Temp. (°F)	Temp. Diff. Between Cylinder & Joint (°F)
384	11/24/06 2:00 PM	15.1	14.41	11.91	59.2	57.9	53.4	4.5
385	11/24/06 2:30 PM	15.2	14.7	12.43	59.4	58.5	54.4	4.1
386	11/24/06 3:00 PM	14.9	14.79	12.75	58.8	58.6	55.0	3.7
387	11/24/06 3:30 PM	15	15.11	13.34	59.0	59.2	56.0	3.2
388	11/24/06 4:00 PM	14.6	15.02	13.36	58.3	59.0	56.0	3.0
389	11/24/06 4:30 PM	13.2	14.55	13.27	55.8	58.2	55.9	2.3
390	11/24/06 5:00 PM	12.5	14.28	13.63	54.5	57.7	56.5	1.2
391	11/24/06 5:30 PM	11.3	13.98	13.49	52.3	57.2	56.3	0.9
392	11/24/06 6:00 PM	9.8	13.52	13.38	49.6	56.3	56.1	0.3
393	11/24/06 6:30 PM	8.2	13.22	13.36	46.8	55.8	56.0	-0.3
394	11/24/06 7:00 PM	7.3	12.91	13.21	45.1	55.2	55.8	-0.5
395	11/24/06 7:30 PM	6.2	12.35	13.02	43.2	54.2	55.4	-1.2
396	11/24/06 8:00 PM	5.7	11.92	12.73	42.3	53.5	54.9	-1.5
397	11/24/06 8:30 PM	4.7	11.56	12.62	40.5	52.8	54.7	-1.9
398	11/24/06 9:00 PM	3.7	11.5	12.34	38.7	52.7	54.2	-1.5
399	11/24/06 9:30 PM	3.4	10.76	11.9	38.1	51.4	53.4	-2.1
400	11/24/06 10:00 PM	2.6	10.46	11.62	36.7	50.8	52.9	-2.1
401	11/24/06 10:30 PM	2.1	10.25	11.51	35.8	50.5	52.7	-2.3
402	11/24/06 11:00 PM	1.8	9.92	11.36	35.2	49.9	52.4	-2.6
403	11/24/06 11:30 PM	1.1	9.92	11.11	34.0	49.9	52.0	-2.1
404	11/25/06 12:00 AM	0.7	9.46	10.84	33.3	49.0	51.5	-2.5
405	11/25/06 12:30 AM	0.7	9.18	10.55	33.3	48.5	51.0	-2.5
406	11/25/06 1:00 AM	0.8	9.29	10.37	33.4	48.7	50.7	-1.9
407	11/25/06 1:30 AM	1.2	9.37	10.11	34.2	48.9	50.2	-1.3

Reading Number	Time	Ambient Temp. (°C)	Cylinder Temp. (°C)	Joint Temp. (°C)	Ambient Temp. (°F)	Cylinder Temp. (°F)	Joint Temp. (°F)	Temp. Diff. Between Cylinder & Joint (°F)
408	11/25/06 2:00 AM	1.8	8.99	9.88	35.2	48.2	49.8	-1.6
409	11/25/06 2:30 AM	2	8.84	9.71	35.6	47.9	49.5	-1.6
410	11/25/06 3:00 AM	2	9.09	9.42	35.6	48.4	49.0	-0.6
411	11/25/06 3:30 AM	1.6	8.78	9.17	34.9	47.8	48.5	-0.7
412	11/25/06 4:00 AM	1.6	8.35	9.28	34.9	47.0	48.7	-1.7
413	11/25/06 4:30 AM	1.6	8.59	8.86	34.9	47.5	47.9	-0.5
414	11/25/06 5:00 AM	1.3	8.02	8.85	34.3	46.4	47.9	-1.5
415	11/25/06 5:30 AM	1.1	8.19	8.58	34.0	46.7	47.4	-0.7
416	11/25/06 6:00 AM	0.9	8.06	8.28	33.6	46.5	46.9	-0.4
417	11/25/06 6:30 AM	0.7	7.6	8.02	33.3	45.7	46.4	-0.8
418	11/25/06 7:00 AM	0.5	7.57	7.96	32.9	45.6	46.3	-0.7
419	11/25/06 7:30 AM	0.3	7.4	7.88	32.5	45.3	46.2	-0.9
420	11/25/06 8:00 AM	0.2	7.34	7.55	32.4	45.2	45.6	-0.4
421	11/25/06 8:30 AM	0.1	7.24	7.44	32.2	45.0	45.4	-0.4
422	11/25/06 9:00 AM	0.4	7.27	7.01	32.7	45.1	44.6	0.5
423	11/25/06 9:30 AM	0.8	7.42	6.88	33.4	45.4	44.4	1.0
424	11/25/06 10:00 AM	2.5	7.56	6.89	36.5	45.6	44.4	1.2
425	11/25/06 10:30 AM	3.7	8.14	6.95	38.7	46.7	44.5	2.1
426	11/25/06 11:00 AM	5.2	8.36	6.82	41.4	47.0	44.3	2.8
427	11/25/06 11:30 AM	6.7	8.92	7.04	44.1	48.1	44.7	3.4
428	11/25/06 12:00 PM	8.6	9.43	6.88	47.5	49.0	44.4	4.6
429	11/25/06 12:30 PM	9.1	9.75	7.24	48.4	49.6	45.0	4.5
430	11/25/06 1:00 PM	10.1	10.42	7.47	50.2	50.8	45.4	5.3
431	11/25/06 1:30 PM	11.4	10.89	7.74	52.5	51.6	45.9	5.7

Reading Number	Time	Ambient Temp. (°C)	Cylinder Temp. (°C)	Joint Temp. (°C)	Ambient Temp. (°F)	Cylinder Temp. (°F)	Joint Temp. (°F)	Temp. Diff. Between Cylinder & Joint (°F)
432	11/25/06 2:00 PM	12	11.34	8.1	53.6	52.4	46.6	5.8
433	11/25/06 2:30 PM	12.9	11.75	8.71	55.2	53.2	47.7	5.5
434	11/25/06 3:00 PM	12.8	11.95	8.82	55.0	53.5	47.9	5.6
435	11/25/06 3:30 PM	12.3	11.97	9.02	54.1	53.5	48.2	5.3
436	11/25/06 4:00 PM	12	11.75	9.7	53.6	53.2	49.5	3.7
437	11/25/06 4:30 PM	10.8	11.74	9.92	51.4	53.1	49.9	3.3
438	11/25/06 5:00 PM	9.9	11.37	9.76	49.8	52.5	49.6	2.9
439	11/25/06 5:30 PM	8.9	11.36	9.49	48.0	52.4	49.1	3.4
440	11/25/06 6:00 PM	8.1	11.25	9.97	46.6	52.3	49.9	2.3
441	11/25/06 6:30 PM	7.6	10.95	9.96	45.7	51.7	49.9	1.8
442	11/25/06 7:00 PM	8.4	10.8	10.02	47.1	51.4	50.0	1.4
443	11/25/06 7:30 PM	8.1	10.8	9.86	46.6	51.4	49.7	1.7
444	11/25/06 8:00 PM	7.4	10.54	9.69	45.3	51.0	49.4	1.5
445	11/25/06 8:30 PM	7.4	10.45	9.97	45.3	50.8	49.9	0.9
446	11/25/06 9:00 PM	7.2	10.32	9.81	45.0	50.6	49.7	0.9
447	11/25/06 9:30 PM	7.1	10.41	9.71	44.8	50.7	49.5	1.3
448	11/25/06 10:00 PM	7.1	10.37	9.96	44.8	50.7	49.9	0.7
449	11/25/06 10:30 PM	7	10.45	9.82	44.6	50.8	49.7	1.1
450	11/25/06 11:00 PM	6.9	10.19	9.85	44.4	50.3	49.7	0.6
451	11/25/06 11:30 PM	6.8	10.17	9.7	44.2	50.3	49.5	0.8
452	11/26/06 12:00 AM	6.6	10.09	9.62	43.9	50.2	49.3	0.8
453	11/26/06 12:30 AM	6.7	9.97	9.65	44.1	49.9	49.4	0.6
454	11/26/06 1:00 AM	6.5	9.93	9.59	43.7	49.9	49.3	0.6
455	11/26/06 1:30 AM	5.7	9.76	9.6	42.3	49.6	49.3	0.3

Reading Number	Time	Ambient Temp. (°C)	Cylinder Temp. (°C)	Joint Temp. (°C)	Ambient Temp. (°F)	Cylinder Temp. (°F)	Joint Temp. (°F)	Temp. Diff. Between Cylinder & Joint (°F)
456	11/26/06 2:00 AM	4.6	9.28	9.46	40.3	48.7	49.0	-0.3
457	11/26/06 2:30 AM	4	9.23	9.32	39.2	48.6	48.8	-0.2
458	11/26/06 3:00 AM	3.7	9.13	9.01	38.7	48.4	48.2	0.2
459	11/26/06 3:30 AM	3.1	8.67	8.92	37.6	47.6	48.1	-0.4
460	11/26/06 4:00 AM	3	8.66	8.76	37.4	47.6	47.8	-0.2
461	11/26/06 4:30 AM	2.6	8.36	8.8	36.7	47.0	47.8	-0.8
462	11/26/06 5:00 AM	2.9	8.57	8.51	37.2	47.4	47.3	0.1
463	11/26/06 5:30 AM	3.1	8.9	8.48	37.6	48.0	47.3	0.8
464	11/26/06 6:00 AM	4.3	8.62	8.33	39.7	47.5	47.0	0.5
465	11/26/06 6:30 AM	5	8.61	8.13	41.0	47.5	46.6	0.9
466	11/26/06 7:00 AM	5.4	8.87	8.23	41.7	48.0	46.8	1.2
467	11/26/06 7:30 AM	5.7	8.86	8.22	42.3	47.9	46.8	1.2
468	11/26/06 8:00 AM	5.9	9.16	8.16	42.6	48.5	46.7	1.8
469	11/26/06 8:30 AM	6	8.99	8.34	42.8	48.2	47.0	1.2
470	11/26/06 9:00 AM	6.3	9.38	8.29	43.3	48.9	46.9	2.0
471	11/26/06 9:30 AM	6.7	9.33	8.35	44.1	48.8	47.0	1.8
472	11/26/06 10:00 AM	6.9	9.62	8.29	44.4	49.3	46.9	2.4
473	11/26/06 10:30 AM	7.1	9.77	8.34	44.8	49.6	47.0	2.6
474	11/26/06 11:00 AM	7.2	9.7	8.27	45.0	49.5	46.9	2.6
475	11/26/06 11:30 AM	7.6	10.05	8.61	45.7	50.1	47.5	2.6
476	11/26/06 12:00 PM	7.9	10.28	8.61	46.2	50.5	47.5	3.0
477	11/26/06 12:30 PM	8.5	10.52	8.93	47.3	50.9	48.1	2.9
478	11/26/06 1:00 PM	9.1	10.9	8.73	48.4	51.6	47.7	3.9
479	11/26/06 1:30 PM	9.9	11.43	9.01	49.8	52.6	48.2	4.4

Reading Number	Time	Ambient Temp. (°C)	Cylinder Temp. (°C)	Joint Temp. (°C)	Ambient Temp. (°F)	Cylinder Temp. (°F)	Joint Temp. (°F)	Temp. Diff. Between Cylinder & Joint (°F)
480	11/26/06 2:00 PM	11.5	12.04	9.25	52.7	53.7	48.7	5.0
481	11/26/06 2:30 PM	12.7	12.39	9.63	54.9	54.3	49.3	5.0
482	11/26/06 3:00 PM	12.4	12.7	9.9	54.3	54.9	49.8	5.0
483	11/26/06 3:30 PM	12.2	12.62	10.18	54.0	54.7	50.3	4.4
484	11/26/06 4:00 PM	11.9	12.76	10.38	53.4	55.0	50.7	4.3
485	11/26/06 4:30 PM	11.7	12.73	10.45	53.1	54.9	50.8	4.1
486	11/26/06 5:00 PM	11.4	12.58	10.91	52.5	54.6	51.6	3.0
487	11/26/06 5:30 PM	11.2	12.45	10.84	52.2	54.4	51.5	2.9
488	11/26/06 6:00 PM	10.8	12.53	10.92	51.4	54.6	51.7	2.9
489	11/26/06 6:30 PM	10.6	12.59	11.2	51.1	54.7	52.2	2.5
490	11/26/06 7:00 PM	10.5	12.37	11.14	50.9	54.3	52.1	2.2
491	11/26/06 7:30 PM	10.5	12.33	11.2	50.9	54.2	52.2	2.0
492	11/26/06 8:00 PM	10.4	12.34	11.31	50.7	54.2	52.4	1.9
493	11/26/06 8:30 PM	10.3	12.31	11.43	50.5	54.2	52.6	1.6
494	11/26/06 9:00 PM	10.2	12.26	11.43	50.4	54.1	52.6	1.5
495	11/26/06 9:30 PM	10.1	12.3	11.55	50.2	54.1	52.8	1.3
496	11/26/06 10:00 PM	9.8	12.27	11.46	49.6	54.1	52.6	1.5
497	11/26/06 10:30 PM	9.1	12.13	11.33	48.4	53.8	52.4	1.4
498	11/26/06 11:00 PM	7.9	11.77	11.2	46.2	53.2	52.2	1.0
499	11/26/06 11:30 PM	7.2	11.2	11.04	45.0	52.2	51.9	0.3
500	11/27/06 12:00 AM	6.4	11.2	10.63	43.5	52.2	51.1	1.0
501	11/27/06 12:30 AM	5.7	10.83	10.67	42.3	51.5	51.2	0.3
502	11/27/06 1:00 AM	5.2	10.25	10.23	41.4	50.5	50.4	0.0
503	11/27/06 1:30 AM	4.7	10.61	9.85	40.5	51.1	49.7	1.4

Reading Number	Time	Ambient Temp. (°C)	Cylinder Temp. (°C)	Joint Temp. (°C)	Ambient Temp. (°F)	Cylinder Temp. (°F)	Joint Temp. (°F)	Temp. Diff. Between Cylinder & Joint (°F)
504	11/27/06 2:00 AM	4.5	10.11	9.81	40.1	50.2	49.7	0.5
505	11/27/06 2:30 AM	4.8	9.92	9.29	40.6	49.9	48.7	1.1
506	11/27/06 3:00 AM	5.1	10.03	9.24	41.2	50.1	48.6	1.4
507	11/27/06 3:30 AM	5.4	9.77	9.14	41.7	49.6	48.5	1.1
508	11/27/06 4:00 AM	5.7	9.83	9.05	42.3	49.7	48.3	1.4
509	11/27/06 4:30 AM	5.5	9.85	8.99	41.9	49.7	48.2	1.5
510	11/27/06 5:00 AM	5.5	9.47	8.97	41.9	49.0	48.1	0.9
511	11/27/06 5:30 AM	5.2	9.4	8.78	41.4	48.9	47.8	1.1
512	11/27/06 6:00 AM	4.7	9.05	8.62	40.5	48.3	47.5	0.8
513	11/27/06 6:30 AM	4.2	9.21	8.47	39.6	48.6	47.2	1.3
514	11/27/06 7:00 AM	4.1	9.24	8.35	39.4	48.6	47.0	1.6
515	11/27/06 7:30 AM	4.2	9.34	8.26	39.6	48.8	46.9	1.9
516	11/27/06 8:00 AM	4.4	8.96	8.26	39.9	48.1	46.9	1.3
517	11/27/06 8:30 AM	4.5	8.97	8.15	40.1	48.1	46.7	1.5
518	11/27/06 9:00 AM	4.5	9.09	8.15	40.1	48.4	46.7	1.7
519	11/27/06 9:30 AM	4.7	9.18	8.07	40.5	48.5	46.5	2.0
520	11/27/06 10:00 AM	5	8.84	7.82	41.0	47.9	46.1	1.8
521	11/27/06 10:30 AM	5.4	9.05	8.17	41.7	48.3	46.7	1.6
522	11/27/06 11:00 AM	5.3	9.05	7.9	41.5	48.3	46.2	2.1
523	11/27/06 11:30 AM	5.4	9.11	8.03	41.7	48.4	46.5	1.9
524	11/27/06 12:00 PM	5.7	9.43	7.99	42.3	49.0	46.4	2.6
525	11/27/06 12:30 PM	6.2	9.37	7.84	43.2	48.9	46.1	2.8
526	11/27/06 1:00 PM	6.7	9.62	7.84	44.1	49.3	46.1	3.2
527	11/27/06 1:30 PM	7.2	9.43	7.94	45.0	49.0	46.3	2.7

Reading Number	Time	Ambient Temp. (°C)	Cylinder Temp. (°C)	Joint Temp. (°C)	Ambient Temp. (°F)	Cylinder Temp. (°F)	Joint Temp. (°F)	Temp. Diff. Between Cylinder & Joint (°F)
528	11/27/06 2:00 PM	7.2	9.66	7.92	45.0	49.4	46.3	3.1
529	11/27/06 2:30 PM	7.2	9.53	8.14	45.0	49.2	46.7	2.5
530	11/27/06 3:00 PM	7.3	9.52	8.24	45.1	49.1	46.8	2.3
531	11/27/06 3:30 PM	7.3	9.83	8.32	45.1	49.7	47.0	2.7
532	11/27/06 4:00 PM	7.4	9.73	8.28	45.3	49.5	46.9	2.6

REFERENCES

American Association of State Highway and Transportation Officials. *AASHTO LRFD Bridge Design Specifications*, American Association of State Highway and Transportation Officials. Second Edition, 1998, pp 9-14.

American Association of State Highway and Transportation Officials. *AASHTO Standard Specifications for Highway Bridges*, American Association of State Highway and Transportation Officials. 16th Edition, 1996.

American Concrete Institute. *ACI 318-05 Building Code Requirements for Structural Concrete*, American Concrete Institute, 2005, pp 99.

Arditi, David, Uluc Ergin, and Suat Gunhan. *Factors Affecting the Use of Precast Concrete Systems*, Journal of Architectural Engineering. Vol. 6, No. 3, September 2000, pp. 79-86.

Badie, Sameh S., Baishya, Mantu C., Tadros, Maher K. *NUDECK – An Efficient and Economical Precast Prestressed Bridge Deck System*, PCI Journal. Vol.43, No.5, September/October 1998, pp 56-71.

Bonded Strand Post-Tensioning System, http://www.dywidag-systems.com/. 2007. http://www.dywidag-systems.com/products/Bonded_Strand_PT_System _Anchorages.html, Accessed January 31, 2007.

Billington, S.L., R.W. Barnes, J.E. Breen. *Alternate Substructure Systems for Standard Highway Bridges*, Journal of Bridge Engineering. Vol.6, No.2, March/April 2001, pp 87-94.

Billington, S.L., R.W. Barnes, J.E. Breen. *A Precast Segmental Substructure System for Standard Bridges,* PCI Journal. Vol. 44 No. 4, July/August 1999, pp56-72.

Cooper, Thomas and Pearson-Kirk, Donald. *Improving the Durability of Post-Tensioned Bridges,* Transportation Research Board 2006 Annual Meeting CD-ROM. pp 1-8.

Fallaha, Sam, Chuanbing Sun, Mark D. Lafferty, Maher K. Tadros. *High Performance Precast Concrete NUDECK Panel System for Nebraska's Skyline Bridge***,** PCI Journal. Vol. 49, No. 5, September/October 2004, pp 40-50.

Hale, W. Micah and Russell, Bruce W. *Effects of Allowable Compressive Stress at Release on Prestress Losses and on the Performance of Precast, Prestressed Concrete Bridge Girders,* PCI Journal. Vol. 51, No. 2, March/April 2006, pp 14-25.

Hamilton III, H.R., Wheat, H.G., Breen, J.E., and Frank, K.H. *Corrosion Testing of Grout for Posttensioning Ducts and Stay Cables,* Journal of Structural Engineering. Vol. 126, No. 2, February 2000, pp 163-170.

Haroon, Saif, Yazdani, Nur and Tawfiq, Kamal. *Posttensioned Anchorage Zone Enhancement with Fiber-Reinforced Concrete*, Journal of Bridge Engineering. Vol.11, No. 5, September/October 2006, pp 566-572.

Harrison, Alex and LeBlanc, N, David. *Design and Construction of a Full-Width, Full-Depth Precast Concrete Deck Slab on Steel Girder Bridge,* Transportation Research Record: Journal of the Transportation Research Board. No.1907, 2005, pp. 55-66.

Hieber, DG., JM. Wacker, MO Eberhard, and JF Stanton. *State-of-the-Art Report on Precast Concrete Systems for Rapid Construction of Bridges***,** Final Technical Report, Washington State Transportation and the Federal Highway Administration. March 2005, pp 1-85.

Issa, Moshen, Cyro L. Ribeiro do Valle, Hiba A. Abdalla, Shahid Islam, Mahmoud A. Issa. *Performance of Transverse Joint Grout Materials in Full-Depth Precast Concrete Bridge Deck Systems*, PCI Journal. Vol. 48, No. 4, July/August 2003, pp 92-103.

Issa, Moshen, Yousif, Alfred, Issa, Mahmoud, Kaspar, Iraj, and Khayyat, Salah. *Analysis of Full Depth Precast Concrete Bridge Deck Panels,* PCI Journal. Vol. 43, No.1, January/February 1998, pp 74-85.

Khayat, K.H., Yahina, A., and Duffy, P. *High-Performance Cement Grout for Post-Tensioning Application,* ACI Materials Journal. Vol. 96, No. 4, July-August 1999, pp 471-477.

Lounis, Z, Mirza M.S, and M. Z. Cohn, *Segmental and Conventional Precast Prestressed Concrete I-Bridge Girders,* Journal of Bridge Engineering. Vol. 2 No. 3, August 1997, pp 73-82.

Naaman, Antione. *Prestressed Concrete Analysis and Design Fundamentals*, Techno Press 3000. 2nd Edition, 2004.

NCHRP Project 20-58(1) *Detailed Planning for Research on Accelerating the Renewal of America's Highways (Renewal), Preliminary Draft Final Report*. February 28, 2003.

PCI Industry Handbook Committee. *PCI Design Handbook Precast and Prestressed Concrete,* Precast/Prestressed Concrete Institute, Sixth Edition, 2004, pp 2-1 – 2-10.

Russell, Henry G., Ralls, Mary Lou, Tang, Benjamin. *Prefabricated Bridge Elements and Systems in Japan and Europe,* Transportation Research Record: Journal of the Transportation Research Board. No.1928, 2005, pp 103-109.

Salas, R.M., Schokker, A.J., West, J.S., Breen, J.E. and Kreger, M.E. *Conclusions, Recommendations and Design Guidelines for Corrosion Protection of Post-Tensioned Bridges,* Texas Department of Transportation. Research Report 0-1405-9, February 2004, pp 1-73.

Schokker, A. J., Koester, B.D., Breen, J.E., and Kreger, M.E. *Development of High Performance Grouts for Bonded Post-Tensioned Structures,* Texas Department of Transportation. Research Report 1405-2, October 1999, 1-56.

Stamnas, Peter E. P.E. and Whittemore, Mark D. P.E. *All-Precast Substructure Accelerates Construction of Prestressed Concrete Bridge in New Hampshire ,* PCI Journal. Vol. 50 No. 3, May/June 2005, pp 26-39.

Tokerud, Roy. *Precast Prestressed Concrete Bridges for Low-Volume Roads,* PCI Journal. Vol. 24 No. 4, July/August 1979, pp 42-55.

VanGeem, Martha. *Achieving Sustainability with Precast Concrete,* PCI Journal. Vol. 51 No 1, January/February 2006, pp 42-55.

VSL Post-Tensioning Systems, http://www.vsl.net/. 2006. http://www.vsl.net/construction_systems/post_tensioning.html, Accessed January 31, 2007.

Yamane, Takashi, Tadros, Maher, Badie, Sameh, and Baishya, Mantu. *Full Depth Precast, Prestressed Concrete Bridge Deck System,* PCI Journal. Vol. 42, No. 3, May/June 1998, pp 50-66.